

The Identification and Analysis of Molecular Biomarkers in the p53 Tumour Suppressor Pathway that Affect Cancer Progression in Humans

Anna Maria Grawenda

A thesis submitted in fulfilment of the requirements for the degree of

Doctor of Philosophy

Trinity Term 2013

Wolfson College

Ludwig Institute for Cancer Research

Nuffield Department of Clinical Medicine

University of Oxford

The Identification and Analysis of Molecular Biomarkers in the p53 Tumour Suppressor Pathway that Affect Cancer Progression in Humans

Anna Maria Grawenda, Ludwig Institute for Cancer Research, Nuffield Department of Medicine, University of Oxford, Wolfson College, DPhil in Clinical Medicine, Trinity 2013

The tumour suppressor p53 is at the centre of the signalling pathway that controls cellular processes crucial in tumourogenesis, cancer progression and tumour clearance. Alterations in the p53 pathway that lead to cancer progression can be good candidates for molecular biomarkers that would assist in the identification of patients with different prognoses, but also serve as good predictors of appropriate targeted therapies.

Patient cohorts and cancer cell panels are utilised to seek associations with the attenuation of the p53 pathway and cancer progression. Firstly, the alternatively spliced transcript of the p53 inhibitor HDMX, which is frequently found in tumours with poor prognosis, is studied. The high ratio of the alternatively spliced *HDMX-S* transcript over the full-length *HDMX-FL* transcript (HDMX-S/FL) is demonstrated to associate with p53 pathway attenuation in cancer cells and breast carcinomas, and with faster metastatic progression of osteosarcoma and breast cancer patients. Secondly, inherited polymorphism in the *HDMX* gene is investigated and demonstrated as a unique and highly reproducible eQTL, which identifies patients with different prognoses for metastatic disease in breast cancer and melanoma cohorts. Lastly, a screening approach to identify novel inherited polymorphisms in the p53 pathway genes that associate with metastatic progression of melanoma is developed and implemented, and subsequently *in silico* and *in vitro* functional analyses are performed to investigate a mechanism behind the FOXO3 SNP, identified as the strongest candidate, whereby the experimental evidence demonstrate that the causal SNP in the *FOXO3* haplotype is controlled by the GATA3 transcription factor.

Together, the work presented in this thesis provides strong support for the role of the p53 pathway in the metastatic progression of cancer, and suggests that molecular biomarkers that can detect changes in the activity of p53 pathway genes could offer a robust set of biomarkers for cancer progression applicable to different types of cancer.

"Not all battles can be won. Not all lives can be saved. And no matter how we wish it, not all songs end in joy."
— C.L. Wilson, *Queen of Song and Souls*

In loving memory of my mother

I would like to thank everyone who has contributed to the successful completion of my DPhil Thesis:

- My supervisors Gareth Bond and Colin Goding, for invaluable support and guidance.
- Aart Jochemsen, Pancras C. W. Hogendoorn and Kristiaan Lenos from Leiden University, the Netherlands, for a productive collaboration on the work presented in Chapter 3.
- Peter Würl from the Diakonie-Hospital Halle, Germany, and Helge Taubert from University Clinic of Urology, Erlangen, Germany, for the contribution of the German soft-tissue sarcoma cohort.
- Vessela N. Kristensen, Hege Edvardsen and Elen Møller from Oslo University Hospital, Norway, for the contribution of the MicMa and ULL breast cancer cohorts.
- Douglas Bell and Xuting Wang from The National Institute of Environmental Health Sciences and Francesc Castro-Giner from the University of Oxford, for their contributions to the eQTL/cancer GWAS screen presented in Chapter 5.
- Mark Middleton from the University of Oxford for the contribution of the melanoma cohort.
- Emmanouela Repapi and Lukasz F. Grochola from the University of Oxford, for their contribution to the melanoma metastasis screen presented in Chapter 6.
- Claire Beveridge for professional proofreading and editing of the manuscript.

I would also like to express my sincere gratitude to my family and friends for all of the much needed support and compassion that I have received over the past few years, which has made my DPhil journey a lot more manageable.

The work presented in Chapter 3 has been published in a journal, in the form of a paper on which I have shared first authorship (Lenos, K., Grawenda, A.M., *et al.*, 2012, Cancer Research *72*, 4074-4084). Permission has been granted from the co-authors of this publication for the inclusion of the material in my Thesis.

Some of the data and analyses (including my own work) presented in Chapter 3 have been accepted as a part of the thesis for the degree of Doctor of Philosophy of Kristiaan Lenos at the University of Leiden.

Some of the work presented in Chapter 6 was conducted in collaboration with a fellow group member and DPhil student, Emmanouela Repapi. Some of the data presented in this chapter is, therefore, also being submitted as a part of the thesis for the degree of Doctor of Philosophy of Emmanouela Repapi at the University of Oxford.

All of the data in this thesis that is not my own work is clearly indicated and referenced in the manuscript.

Word count:

43,200

1 GENERAL INTRODUCTION 1

1.1 Genetic basis of tumourogenesis 2

1.2 Biomarkers in cancer 3

1.3 Metastasis: a prognostic challenge 5

1.4 The p53 tumour suppressor 7

1.4.1 p53 and its role in cancer progression 10

1.4.2 The p53 inhibitors: HDM2 and HDMX 13

1.5 Genetic alterations of p53 and its inhibitors 17

1.5.1 TP53 mutations 17

1.5.1.1 Somatic mutations 17

1.5.1.2 Germline mutations 20

1.5.2 Germline polymorphisms 21

1.5.3 Amplification and overexpression of p53 inhibitors 25

1.6 p53 in the clinic 28

1.6.1 TP53 gene mutation as a prognostic and predictive biomarker 28

1.6.2 Reactivation of the p53 pathway 30

1.6.3 Gene expression signatures for TP53 mutational status 33

1.7 Objectives of the study 36

2 MATERIALS AND METHODS 39

2.1 Materials 41

2.1.1 Reagents 41

2.1.2 Antibodies, gene specific TaqMan assays and oligonucleotides 47

2.2 Patients cohorts 49

2.2.1 The Osteosarcoma cohort *49*

2.2.2 The Soft Tissue Sarcoma cohort *50*

2.2.3 The Norwegian breast cancer cohorts *52*

2.2.4 The Melanoma cohort *54*

2.3 Cell lines **55**

2.3.1 NCI60 human cancer cell lines *55*

2.3.2 Osteosarcoma and breast cancer cell lines *55*

2.3.3 Cancer cell lines grown in the cell culture. *58*

2.4 Methods **59**

2.4.1 Cell culture *59*

2.4.2 Plasmid preparation *59*

2.4.3 Cell transfection assays *60*

2.4.3.1 siRNA transfections 60

2.4.3.2 Transient plasmid transfections 61

2.4.4 Luciferase bioluminescence detection *61*

2.4.5 DNA extraction *62*

2.4.6 RNA extraction and cDNA synthesis *62*

2.4.7 Genotyping *63*

2.4.8 Polymerase chain reaction (qRT-PCR and semiQ-PCR) *64*

2.4.8.1 Gene expression qRT-PCR. 64

2.4.8.2 Allele-specific qRT-PCR 66

2.4.8.3 Semi-Quantitative PCR 67

2.4.9 Analysis of DNA-protein interactions *67*

2.4.9.1 Electromobility Shift Assay (EMSA) 67

2.4.9.2 Chromatin Immunoprecipitation (ChIP) 69

2.4.10 Protein analysis by Western blotting 71

2.4.11 Data analyses 72

3 ALTERNATIVE SPLICING OF THE P53 INHIBITOR HDMX OFFERS A PROGNOSTIC BIOMARKER THAT IS SUPERIOR TO *TP53* MUTATION IN SARCOMAS 75

3.1 Introduction 76

3.2 Results 78

3.2.1 The HDMX-S/FL ratio in osteosarcoma 78

3.2.2 The HDMX-S/FL ratio in breast cancer and NCI60 cells 88

3.2.3 The HDMX-S/FL ratio and TP53 mutation as prognostic markers 92

3.3 Discussion 97

4 THE *HDMX-S/FL* BIOMARKER INTERACTS WITH p53 GENE MUTATIONS TO PREDICT THE METASTATIC PROGRESSION OF BREAST CANCER PATIENTS.. 100

4.1 Introduction 101

4.2 Results 103

4.2.1 High HDMX-S/FL ratios associate with p53 inhibition in breast cancer 103

4.2.2 The HDMX-S/FL ratio interacts with TP53 mutational status to further define individuals in their survival of breast cancer. 109

4.2.3 The HDMX-S/FL ratio and TP53 mutational status predict breast cancer survival better than BC molecular subtypes 113

4.2.4 The HDMX-S/FL ratio interacts with TP53 mutational status to further define metastasis-free survival. *116*

4.2.5 The HDMX-S/FL ratio associates with HDMX P2 promoter activity *118*

4.3 Discussion **124**

5 SINGLE NUCLEOTIDE POLYMORPHISMS IN THE *HDMX* GENE ASSOCIATE WITH DIFFERENTIAL BREAST CANCER RISK AND PROGRESSION **133**

5.1 Introduction **134**

5.2 Results **135**

5.2.1 The HDMX haplotype block is the most reproducible eQTL, and associates with differential cancer risk of the most types of cancer *135*

5.2.2 The HDMX haplotype block associates with breast cancer survival *139*

5.2.3 The HDMX SNP and HDMX-S/FL ratio *142*

5.2.4 The HDMX SNP interacts with TP53 mutation and Estrogen Receptor status to define metastasis-free and overall survival of breast cancer patients *144*

5.3 Discussion **150**

6 IDENTIFICATION AND ANALYSIS OF FUNCTIONAL SINGLE NUCLEOTIDE POLYMORPHISMS THAT AFFECT MELANOMA PROGRESSION **156**

6.1 Introduction **157**

6.2 Results **160**

6.2.1 The HDMX SNP associates with the progression of melanoma patients *160*

6.2.2 A screen for SNPs in p53 network genes identifies a SNP in the FOXO3 gene that affects melanoma progression *162*

6.2.3 The analysis of the FOXO3 rs2802292 SNP haplotype block identifies three functional SNP candidates that could affect FOXO3 gene transcription..... 170

6.2.4 The rs2802292 SNP associates with the strongest evidence for regulatory potential affecting FOXO3 gene transcription..... 174

6.2.5 The GATA3 transcription factor binds to the causal SNP candidate rs2802292 in vitro and in vivo..... 180

6.2.6 Endogenous GATA3 regulates transcription of the FOXO3 gene..... 188

6.3 Discussion..... 190

7 GENERAL DISCUSSION..... 196

8 REFERENCES..... 211

- ABL- Abelson murine leukemia viral oncogene homologue 1 protein
- Ad- Adenovirus
- ADR - Adrenocortical carcinomas
- AJCC- American Joint Committee on Cancer
- AKT- Protein kinase B
- APS- Ammonium persulfate
- ARF- Alternate reading frame product of the CDKN2A locus
- Arg- Arginine
- ATM- Ataxia telangiectasia mutated protein
- ATR- Ataxia telangiectasia and Rad3-related protein

- BARD1- BRCA1 associated RING domain 1
- BAX- Bcl-2-associated X protein
- BC- Breast cancer
- BCL-2- B-cell lymphoma 2 protein
- BCS- Breast cancer survival
- Bis-Tris- Bis(2-hydroxyethyl) aminotris (hydroxymethyl) methane
- Bp- Base pair
- BRAF- v-raf murine sarcoma viral oncogene homolog B
- BRCA1- Breast cancer type 1 susceptibility protein
- BSA- Bovine serum albumin

- Cdc42- Cell division control protein 42 homologue
- CDK- Cyclin dependent kinase
- CDKN2A- cyclin-dependent kinase inhibitor 2A
- cDNA- Complementary DNA

- CEU- Individuals from the Centre d'Etude du Polymorphisme Humaincollected in Utah, USA, with ancestry from northern and western Europe
- ChIP- Chromatin immunoprecipitation
- CLL- Chronic lymphocytic leukaemia
- CMF- Cyclophosphamide-Methotrexate-Fluorouracil
- CNS- Central nervous system
- CSE1L- Cellular apoptosis susceptibility protein
- ct- Cycle threshold

- dd- Double-distilled
- deltaCT- delta Cycle-threshold
- dATP- Deoxyadenosine triphosphate
- dCTP- Deoxycytidine triphosphate
- ddH2O- Double-distilled water
- DEPC- Diethylpyrocarbonate
- dGTP- Deoxyguanosine triphosphate
- di-dC- Poly(deoxyinosinic-deoxycytidylic) acid sodium salt
- DMEM- Dulbecco's Modified Eagle's Medium
- DMSO- Dimethyl sulfoxide
- DNA- Deoxyribonucleic acid
- DNA-PK- DNA-dependent protein kinase
- dNTP- Deoxyribonucleotide
- DTT- Dithiothreitol
- dTTP- Deoxythymidine triphosphate

- ECL- Enhanced Chemical Luminescence
- ECM- Extracellular matrix

- EDTA- Ethylene diamine tetraacetic acid
- EGFR- Epidermal growth factor receptor
- EGTA- Ethylene glycol tetraacetic acid
- EMSA- Eloctromobility Shift Assay
- EMT- Epithelial to mesenchymal transition
- ENCODE- Encyclopedia of DNA Elements
- EpCAM- Epithelial cell adhesion molecule
- eQTL- Expression quantitative trait loci
- ER- Estrogen receptor
- ERB2- Human Epidermal Growth Factor Receptor 2
- ESR1- Estrogen receptor 1
- E2F1- E2F transcription factor 1 (retinoblastoma-associated protein 1)
- E4F1- E4F transcription factor 1

- FAM- Fluorescein
- FBS- Foetal Bovine Serum
- FOXO3- Forkhead box O3 transcription factor
- FL- Full-length

- GAPDH- Glyceraldehyde 3-phosphate dehydrogenase
- GATA- GATA-binding factor
- GTPase- Hydrolase enzyme that can bind and hydrolyze guanosine triphosphate
- GWAS- Genome-wide association study

- HAc- Acetic acid
- HCC- Hepatocellular carcinoma

- HDAC- Histone deacetylase
- HDM2- Human double minute 2 homologue
- HDMX- Human double minute X (4) homologue
- HEPES- 4-(2-hydroxyethyl)-1-piperazineethanesulfonic acid
- HRP- Horseradish peroxidase
- H3K4Me1- Mono-methylation of histone 3 in lysine 4
- H3K4Me3- Tri-methylation of histone 3 in lysine 4
- H3K27Ac- Acetylation of histone 3 in lysine 27

- iASPP- Inhibitor of Apoptosis Stimulating Protein of p53
- Ig- Immunoglobulin
- IGF1R- Insulin-like growth factor 1 receptor
- IHC- Immunohistochemistry
- inc- Inconclusive
- IP- Immunoprecipitate

- Kb- Kilo base pairs
- KM- Kaplan-Meier

- L- Litre
- L-15- Leibovitz l-glutamine medium
- LASSO- Least Absolute Shrinkage and Selection Operator
- LB- Luria Broth
- LCL- Lymphoblastoid cell line
- LD- Linkage disequilibrium
- LFS- Li-Fraumeni syndrome

- MAPK- Mitogen activated kinase-like protein

- MAP4- Microtubule-associated protein 4
- MC1R- Melanocortin 1 receptor
- MFH- Malignant fibrous histiocytoma
- MicMa- MicroMetastasis Project
- min- Minutes
- miR- MicroRNA
- MOPS- 3-morpholinopropane-1-sulfonic acid
- mRNA- Messenger RNA
- mut/mt- Mutant
- Myc- V-myc avian myelocytomatosis viral oncogene homolog

- NaOV- Sodium orthovanadate
- NaPPi- Sodium pyrophosphate
- NCI- National Cancer Institute
- neg- Negative
- NIH- National Institutes of Health
- NP40- Nonyl phenoxypolyethoxylethanol
- NSCLC- Non-small lung carcinoma
- NT- Non-targeting

- O/N- Overnight
- Opti-MEM- Reduced serum modified Eagle's Minimum Essential Medium
- OR- Odds ratio

- PAM50- Prediction Analysis of Microarray 50-gene classifier
- PBS- Phosphate buffered saline
- PCR- Polymerase chain reaction

- pCR- Pathological complete response
- PI- Protease inhibitors
- PIK3R3- Phosphoinositide-3-kinase, regulatory subunit 3
- PLX4032- Vemurafenib
- Pol2- RNA polymerase II
- PP1D- Protein Phosphatase 1-Delta
- PRIMA-1- p53-dependent reactivation of massive apoptosis small molecule drug
- PRMT5- Protein arginine N-methyltransferase 5
- Pro- Proline
- PTEN- Phosphatase and tensin homologue
- PVDF- Polyvinylidene fluoride
- P2RY5- Lysophosphatidic acid receptor 6

- qRT-PCR- Quantitative real-time PCR
- Quant.- Quantification

- Rac- Ras-related C3 botulinum toxin substrate
- RAS- Rat sarcoma protein
- RASSF1- RAS association domain-containing protein 1
- Rb- Retinoblastoma protein
- RCC- Renal cell carcinoma
- RE- Response element
- Rel.- Relative
- RhoA- Ras homologue gene family, member A
- RNA- Ribonucleic acid
- rpm- Revolutions per minute

- RPMI- Roswell Park Memorial Institute medium
- RSF- Random survival forest
- RT- Room temperature
- RTK- Receptor tyrosine kinase

- S- Synthesis phase
- SDS- Sodium dodecyl sulphate
- siRNA- Small interfering RNA
- SLUG- Snail family zinc finger 2
- SNP- Single Nucleotide Polymorphism
- STS- Soft tissue sarcoma
- SV40- Simian virus 40

- TAE- Tris-acetate-EDTA buffer
- TAL-1- T-cell acute lymphocytic leukemia 1 protein
- TBE- Tris/Borate/EDTA buffer
- TBST- Tris-Buffered Saline with Tween 20
- TCF7L2- Transcription factor 7-like 2
- TEMED- Tetramethylethylenediamine
- TF- Transcription factor
- TGF-β- Transforming growth factor beta
- TP- Tumour Protein
- TP53BP2- Tumor protein p53 binding protein 2
- TRANSFAC- TRANScription FACtor database
- Tris- 2-Amino-2-hydroxymethyl-propane-1,3-diol

- U- Unit

- ULL- Ullevål University Hospital
- UTR- Untranslated region
- v/v- Volume/volume
- WB- Western Blotting
- Wt- Wild-type
- YY1- Yin Yang 1 protein
- ZEB- Zinc finger E-box-binding homeobox protein
- 5-FU- Fluorouracil
- -ve- Negative
- +ve- Positive

1 GENERAL INTRODUCTION

1.1 Genetic basis of tumourogenesis

1.2 Biomarkers in cancer

1.3 Metastasis: a prognostic challenge

1.4 The p53 tumour suppressor

1.4.1 p53 and its role in cancer progression

1.4.2 The p53 inhibitors: HDM2 and HDMX

1.5 Genetic alterations of p53 and its inhibitors

1.5.1 TP53 mutations

1.5.1.1 Somatic mutations

1.5.1.2 Germline mutations

1.5.2 Germline polymorphisms

1.5.3 Amplification and overexpression of p53 inhibitors

1.6 p53 in the clinic

1.6.1 TP53 gene mutation as a prognostic and predictive biomarker

1.6.2 Reactivation of the p53 pathway

1.6.3 Gene expression signatures for TP53 mutational status

1.7 Objectives of the study

1.1 Genetic basis of tumourogenesis

Malignant tumours arise as an effect of an accumulation of somatic mutations and inherited alterations in the genome over time. Tumourogenesis requires an acquisition of the 'driver' mutations that, directly or indirectly, confer the selective growth advantage over the surrounding cells of the given tissue, which are then followed by mutations that allow the clonal expansion. Throughout the selection process, beside the driver mutations, a number of neutral passenger mutations, which do not confer any direct on indirect growth or invasion advantage, are accumulated (Vogelstein, Papadopoulos *et al.*, 2013). Development of robust sequencing technologies and statistical methods has led to identification of an ever increasing number of driver mutations. However, it is often problematic to distinguish driver mutations from the neutral alterations, particularly in the case of low frequency mutations (Haber and Settleman, 2007; Simpson, 2009). Driver mutations largely associate with the driver genes, however in cases of changes in gene expression patterns, which lead to over- or under-expression, and epigenetic modifications, some driver genes do not carry any driver mutations (Vogelstein, Papadopoulos *et al.*, 2013).

Tumourogenesis is a multistep process of a clonal selection that resembles Darwinian natural selection of the species, where the cancer clones are asexually reproducing 'species' and the tumour microenvironment is a habitat, which through its constraints provides a selective pressure on the cancer clones to accumulate driver mutations that will allow uncontrolled growth and invasion to distant organs. (Greaves and Maley, 2012). Decades of research lead to validation of cancer as an adaptive, evolutionary system, where both clonal

expansion and genetic heterogeneity were observed in a number of different tumours (Merlo, Pepper *et al.*, 2006). Mutations that render clones the fittest can be fixed in the cell population by the selective sweep. However, tumour evolution is a dynamic process, and as tumour cells divide, increased genomic instability and changes in the microenvironment, throughout a disease progression, but also triggered by drug treatment, lead to heterogeneous, genetically distinct subclonal cell populations. Together, this complex system creates heterogeneity within the primary tumours and metastatic lesions, as well as tumours arising between different individuals, and at different tissue and cell types (Burrell, McGranahan *et al.*, 2013; Merlo, Pepper *et al.*, 2006).

1.2 Biomarkers in cancer

Cancer is a heterogeneous disease that associates with different clinical outcomes. Adequate biomarkers that define the molecular complexity of cancer could improve both diagnosis and treatment, and effectively lead to significant advances in the cancer patient care. Development of numerous technologies that allow detecting of changes in tumours at the DNA, RNA and protein level could help to determine disease progression as well as the effectiveness of targeted therapies. Amid the rapid development of different technologies a fundamental definition of the biomarker was introduced by the Biomarkers Definitions Working Group. It states that a biomarker is: "a characteristic that is objectively measured and evaluated as an indicator of normal biological processes, pathogenic processes, or pharmacologic responses to a therapeutic intervention" (Biomarkers Definitions Working Group, 2001). Three main categories of biomarkers are recognised, (i) prognostic, which allows it to

determine the outcome of the individual cancer and guide the decisions regarding the treatment and its intensity based on the aggressiveness of the assessed tumour (ii) predictive, which indicate a benefit and probability of the response to a particular treatment, and (iii) pharmacodynamic, which indicate the most effective dose of the drug (Sawyers, 2008).

In the past decade a plethora of potential cancer biomarkers have been described in the scientific literature, however it is estimated that less than 1% of these biomarker candidates will ever find its use in the oncology clinics (Kern, 2012). The inefficient study design together with the inconsistent methodologies can significantly affect the validation and implementation process of the candidate biomarkers. As careful consideration of each step of a biomarker development process is needed for a successful introduction of the new biomarkers into the clinical use, specific guidelines for a design and conduct of biomarkers studies have been introduced (Cesario, Marcus *et al.*, 2011). Detailed road maps for prognostic, predictive and pharmacological biomarkers have been recommended by the Cancer Research UK Biomarkers and Imaging Discovery and Development Committee (BIDD), which stipulate the rationale for the appropriate biomarker, and specify critical stages in the biomarker discovery, assay development and biomarker quantification (www.cancerresearchuk.org). In brief, any prospective biomarker needs to address an unmet clinical need, to begin with. Further to that, both clinical retrospective sample collection and an accurate and reproducible assay need to be available to determine biomarker clinical utility in the target population and subsequently to assess associations with clinical outcome, in the case of a

prognostic/predictive biomarker or to compare with gold standard diagnostic tests, in the case of a pharmacological biomarker. Subsequently, after the assay has been developed to appropriate clinical standards, the prospective study is performed. At this stage, if a pharmacological biomarker demonstrates improved diagnostic accuracy, it is then ready to be transferred to a routine clinical practice, whereas in case of a prognostic/predictive biomarker for which correlation with a clinical outcome is statistically robust, an additional quantification stage, which includes a randomised clinical trial, is required before a final transfer to clinical practice.

1.3 Metastasis: a prognostic challenge

Metastasis, a progression of cancer to distant organs, is a primary cause of death in around 90% of cancer patients (Mehlen and Puisieux, 2006). Despite much progress in understanding the molecular characteristics of invasive tumours, current prognostic assessment of tumours is still mainly based on histopathological TNM classification, which includes tumour size, lymph node status and the presence of distant metastases (Bidard, Pierga *et al.*, 2013). Because of a lack of effective classification, around 60% of early stage breast cancer patients receive adjuvant chemotherapy, but it is estimated that only 2-15% of these patients ultimately derive a benefit from the treatment (Reis-Filho and Pusztai, 2011). At the same time, patients at high risk of metastatic disease that do not fulfil the current criteria of aggressive tumours might be misclassified and, consequently, not receive a life-saving or life-prolonging treatment. One of the greatest challenges facing modern oncology today is, therefore, the improvement of tumour classification and the development of

biomarkers that will improve indications for the use of targeted therapies. This will help distinguish between indolent and aggressive cancers which, in an advent of improved cancer screening, will become increasingly important as a number of low-grade tumours that might be clinically insignificant and not require treatment are detected.

Over a decade ago, Bernards and Weinberg challenged a widely accepted model of cancer progression, where metastases arise from rare populations of progenitor cells that, during a process of clonal selectivity, accumulate new mutations that enable them to metastasise to distant organs. They proposed a new concept: that the metastatic potential of tumour cells is determined by the mutations that arise in the early stages of tumourigenesis, and that tumour suppressor genes and oncogenes are likely to play an important role in the processes that lead to the metastatic progression of a tumour (Bernards and Weinberg, 2002). Indeed, support for this hypothesis comes from gene expression studies in primary and metastatic tumours. Extensive gene expression profiling of primary breast carcinomas has demonstrated that tumours that develop metastases can be distinguished from those that do not metastasise by their gene expression profiles (Weigelt, Peterse *et al.*, 2005). Gene expression profiling of matched samples from primary and metastatic colorectal carcinomas has demonstrated similar overall results (Steeg and Theodorescu, 2008). Together, these data suggest that molecular biomarkers that enable the sensing of functional changes in the core pathways that play pivotal roles in tumourigenesis will have strong potential as prognostic

biomarkers for the metastatic potential of primary tumours, and could lead to improvements to management strategies for cancer patients.

1.4 The p53 tumour suppressor

The tumour suppressor p53 is one of the most extensively studied proteins and genes, with over 66,000 publications about it listed in a PubMed search since its discovery in 1979. p53 is a central node of the cellular stress response pathway that regulates transcriptional programmes important in suppressing tumour formation (Kruse and Gu, 2009; Vogelstein, Lane *et al.*, 2000). p53 acts as a transcription factor, that binds as a tetramer to p53 response elements (REs) within the DNA sequences of its target genes, in a sequence-specific manner. The REs include consensus half-sites, often separated by a spacer, comprising of 5'-RRRCWWGYYY-3', where R is a purine, C is cytosine, W is either adenine or thymidine, G is guanine and Y is a pyrimidine (el-Deiry, Kern *et al.*, 1992; Funk, Pak *et al.*, 1992). p53 can both activate and repress the transcription of its target genes. Transcriptional activation by p53 is direct and mediated through p53's binding to REs. It may often include the recruitment of general transcription proteins to the promoter-enhancer region. p53-dependent gene repression, on the other hand, can either be direct or indirect. p53 can repress its target gene either by binding to its RE which overlaps with the binding element of another transactivating protein and, in turn, competes with such factors. Alternatively, it binds to other transcription factors through protein-protein interactions and acts on sites that don't include REs (Riley, Sontag *et al.*, 2008). Out of the several hundred p53-responsive genes that have been identified to date, over a hundred have been demonstrated

to be directly controlled by p53 (Whibley, Pharoah *et al.*, 2009). It is currently estimated that p53 activates most of its target genes. However, around 15% of the p53 target REs that have been described and validated are repressed by p53, and the exact mechanism underlying the p53-dependent repression is not well understood (Rinn and Huarte, 2011).

Under normal conditions, the activity of p53 is kept at low levels, predominantly by protein degradation mediated by the p53 inhibitor HDM2. p53 is able to activate the transcription of the *HDM2* gene which, in turn, creates a negative feedback loop to keep the levels of both p53 and HDM2 in check (Momand, Wu *et al.*, 2000). In response to diverse stress signals such as hypoxia, oncogene activation, mitotic spindle damage, telomere erosion or nutrient deprivation, p53 is stabilised and activated as the result of the self-degradation of HDM2 and post-translational modifications that are exerted by a number of different mediators of the stress response pathway, enabling a rapid stress response, in contrast to what would be a much slower response through the transcriptional activation of the p53 gene (Riley, Sontag *et al.*, 2008). The protein modifications of p53 are required for its full activation, and range from phosphorylation, through to acetylation, methylation and sumoylation (Vogelstein, Lane *et al.*, 2000). The conformational changes triggered by modifications at the N-terminal end of p53 lead to the inhibition of its interaction with HDM2. However, most of the post-translational modifications occur near p53's C-terminal end, including the core domain responsible for its DNA binding, which in turn modify p53's binding activity and specificity as well as its recruitment of transcriptional co-factors (Kruse and Gu, 2009).

Nonetheless, the notion that p53 can present some cellular activity in unstressed cells, without the above-mentioned modifications, has emerged in recent years, underscoring the fact that the roles of some of these modifications in regulating p53's activity are still unknown (Kruse and Gu, 2009; Riley, Sontag *et al.*, 2008).

Once activated, p53 can protect the organism from the potential threats of cancerous mutations that arise in stressed cells by initiating the cellular programmes of apoptosis, cell cycle arrest and senescence, which are fundamental in tumour suppression as they prevent damaged cells from propagating (Lane and Levine, 2010; Vogelstein, Lane *et al.*, 2000; Vousden and Lu, 2002). In an attempt to stop the cell from replicating DNA that has undergone stress-induced damage, p53 activates the transcription of p21 which, through the inhibition of cyclin dependent kinases (CDKs), activates cell cycle checkpoints and arrests cell division at the gap phases of G1 and G2, therefore preventing the cell from going into DNA replication phase (S) or mitotic division (Vogelstein, Lane *et al.*, 2000). In contrast to reversible cell cycle arrest, which is often activated in the event of transient stress causing repairable damage to DNA, when cells sustain high levels of stress associated with substantial, irreparable damage, p53 can co-operate with retinoblastoma protein (Rb) to lead to terminal replication arrest through the activation of cell senescence (Courtois-Cox, Jones *et al.*, 2008; Vousden and Prives, 2005). In many cases, however, as a safeguard against tumourigenesis in stressed cells, p53 induces programmed cell death via apoptosis through a vast number of different effectors. Although, p53 can mediate the extrinsic programme of apoptosis that

is activated by death receptors, its principal role has been indicated to be the control of the BCL-2 family, leading to intrinsic apoptosis associated with the mitochondrial response and the release of cytochrome c (Cotter, 2009; Vousden and Lu, 2002). Given the vital roles of these cellular stress response processes in helping the organism contain induced damage within affected cell, which in turn protect the organism from the consequences of replicating potentially cancer-generating mutations, it is evident that p53 functions as a guardian of the genome's stability.

1.4.1 p53 and its role in cancer progression

A growing body of evidence suggests that, beside p53's pivotal role in the processes of apoptosis and cell cycle arrest that protect the cell from neoplastic transformation, p53 is also involved in processes that lead to cancer progression (Roger, Gadea *et al.*, 2006). The ability of a cancer cell to migrate and invade depends on differences in extracellular protease activities, cell-matrix adhesion, cell-cell adhesion, cell polarity, and cytoskeletal arrangement (Yilmaz and Christofori, 2010). In order to metastasise, tumour cells must first disseminate from the primary tumour. The epithelial to mesenchymal transition (EMT), a crucial event in morphogenesis, is associated with the gain of invasive and migratory attributes by epithelial cells. However, the same process is hijacked by tumour cells of epithelial origin in a move to gain an invasive phenotype, leading to the loosening of cell-cell junctions, dissociation from the primary tumour and the eventual formation of distant metastases (Nieto, 2011). Wild-type (wt) p53 has been demonstrated to up-regulate E-cadherin, the key cell adhesion mediator and suppressor of EMT-dependent cancer cell invasion,

through the facilitation of HDM2-mediated ubiquitination and the subsequent degradation of pro-invasive Zinc-finger transcription factor SLUG, a transcriptional suppressor of E-cadherin (Wang, Wang *et al.*, 2009). Further to this, wt p53 has been shown to transcriptionally repress the epithelial cell adhesion molecule (EpCAM), another negative regulator of E-cadherin (Sankpal, Willman *et al.*, 2009). In a similar fashion, wt p53 also negatively regulates SNAIL, another E-cadherin suppressor from the same family of transcription factors as are involved in the EMT (Lim, Kim *et al.*, 2010). However, it has been demonstrated that p53 acts indirectly on the expression of the *SNAIL* gene, through the transactivation of microRNA miR-34, that in turn antagonises *SNAIL*'s expression by binding to the 3'-UTR of the *SNAIL* transcript (Kim, Kim *et al.*, 2011). In a similar manner, p53 transactivates microRNA miR-200, a repressor of yet another family of EMT activators the ZEB transcription factors (De Craene and Berx, 2013). In contrast, mutant p53 promotes the invasiveness of tumour cells via the activation of SLUG or the prevention of wt p53 from binding to its miR targets (De Craene and Berx, 2013; Muller, Vousden *et al.*, 2011).

Following their dissemination from a tumour, cells invade the extracellular matrix (ECM) in a move to reach blood or lymph vessels. The interactions of these cells with the ECM, the formation of invadopodia, cell polarity and cell spreading are all important features of migrating cells that are influenced by p53 (Roger, Gadea *et al.*, 2006). p53 prevents invasion of the ECM by inducing the expression of the actin binding protein Caldesmon, as well as regulating miRNA (miR) 142, which inhibits the formation of cell invadopodia

(podosomes) that contribute to the degradation of the ECM a consequently allows cells to enter the stroma. Concurrently, p53 suppresses the expression of fibronectin and collagens, ECM proteins that contribute to the cell's elongated mesenchymal migratory phenotype (Muller, Vousden *et al.*, 2011). Reorganisation of the actin cytoskeleton, which results in polarisation of the cell and enables it to migrate, is mediated by Rho-GTPases, CDC42, RAC and RHOA. CDC42 is a major component of cell polarity control, but also stimulates cell spreading through the formation of migratory protrusions called filopodia. p53 acts downstream of CDC42 to inhibit the formation of filopodia and effectively prevents cell spreading, but also prevents the reformation of the Golgi apparatus in the direction of movement, effectively preventing the polarisation of the cell (Gadea, Lapasset *et al.*, 2002; Roger, Gadea *et al.*, 2006).

Yet another association of p53 with metastatic progression is mediated by mutant p53, where mutant p53's oncogenic gain of function leads to its interaction with, and the subsequent inactivation of, the p53 family member p63. The loss of p63 expression associates with a metastatic phenotype in a number of tumours, and p63 serves as a marker for non-invasive epithelial tumours (Melino, 2011). The loss of p63's activity can be driven by mutant p53 through direct interaction with p63, leading to the inhibition of p63-mediated anti-metastatic genes that include the miRNA regulator DICER, as well as SHARP1 and cyclin G2, which oppose TGF-β-mediated metastasis (Adorno, Cordenonsi *et al.*, 2009; Neilsen, Noll *et al.*, 2011; Su, Chakravarti *et al.*, 2010). All of this evidence underscores the importance of wt and mutant p53 in controlling the invasive phenotype of cancer cells.

1.4.2 The p53 inhibitors: HDM2 and HDMX

The activity of p53 is tightly controlled by the balance between cell death and survival signals. The average half-life of p53 varies between 6 and 20 minutes in unstressed conditions, whereas it increases from minutes to hours under stress (Riley, Sontag *et al.*, 2008). This tight control of p53 levels is secured by a negative-regulatory feedback loop with two critical p53 inhibitors, HDM2 and its homolog HDMX. *HDM2*, also known as *MDM2*, was first described as a gene amplified on the murine double minute chromosome (hence its name) that confers a tumourigenic phenotype, and its role as inhibitor of p53-dependent transactivation was discovered only a year later. Five years after HDM2's discovery, the highly homologous protein HDMX, also known as MDMX or MDM4, was discovered in a screen for p53-interacting proteins (Perry, 2010).

HDM2 and HDMX are structurally similar (Figure 1.1A). However, evidence from mouse studies suggests that the function of either of HDM2 or HDMX is clearly non-redundant, whereby the deletion of either *mdm2* or *mdmx* leads to p53-dependent embryonic lethality that can be rescued by the simultaneous deletion of *TP53*. These studies also suggest that HDM2 and HDMX control different p53 pathways: HDM2 controls apoptosis, whereas HDMX regulates cell proliferation. Indeed, *mdm2*-deficient mouse embryos die before implantation as a result of accelerated apoptosis and can be rescued by the deletion of the pro-apoptotic protein BAX. In contrast, *mdmx* deficiency leads to both apoptosis and growth arrest resulting in embryonic death post-implantation and can be rescued, although not fully, by the deletion of the cell cycle regulator and p53 target p21 (Jones, Roe *et al.*, 1995; Montes de Oca Luna,

Wagner *et al.*, 1995; Parant, Chavez-Reyes *et al.*, 2001; Perry, 2010). Nevertheless, a different hypothesis whereby HDM2 controls p53 levels whilst HDMX contributes to the regulation of its activity is supported by other mouse models (Toledo and Wahl, 2006).

Both HDM2 and HDMX contain a p53-binding domain at their N-terminus. The p53 domain facilitates the inhibition of p53's transactivation by binding to the p53 transactivation domain and preventing the binding of p53 transcriptional co-factors and transcription machinery (Figure 1.1B) (Toledo and Wahl, 2006). Both *HDM2* and *HDMX* are transcriptional targets of p53. Under basal conditions, *HDM2* and *HDMX* are transcribed from a constitutive promoter named P1, whereas in the presence of p53 transcription from alternative p53-responsive promoter P2 is activated (Phillips, Teunisse *et al.*, 2010; Zauberman, Flusberg *et al.*, 1995). The transcription of the *HDM2* and *HDMX* genes is also activated in response to mitogens like RAS and MYC (Wade, Li *et al.*, 2013).

At their C-termini, both HDM2 and HDMX contain RING domains that confer ubiquitin ligase activity. However, despite the high sequence homology in their domains, only that of HDM2 appears to exert the E3 ligase activity that leads to a rapid degradation of p53, driven by either mono-ubiquitination of p53 leading to its nuclear exclusion or poly-ubiquitination leading to proteasome degradation (Figure 1.1B) (Badciong and Haas, 2002; Haupt, Maya *et al.*, 1997; Wade, Li *et al.*, 2013; Wang and Jiang, 2012). The RING domains of both proteins also enable their dimerisation. HDM2 can form homodimers, as well as heterodimers with the HDMX. A large body of evidence suggest that hetero-

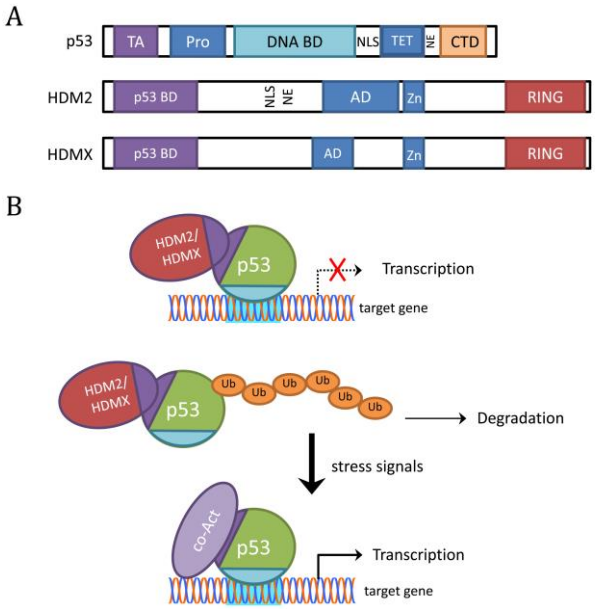


Figure 1.1 Structure and model of interactions of p53 and its inhibitors, HDM2 and HDMX.

A, Schematic representation of p53, HDM2 and HDMX protein structure. p53 is a protein consisting of 393 amino acids, with following domains: transactivation domain (TA), which is essential for transcriptional activation of p53, proline-rich domain (Pro), DNA binding domain (DNA BD), nuclear localisation signal (NLS), tetramerisation domain (TE), nuclear export signal (NE) and C-terminal regulatory domain (CTD), which is ubiquitiated at its lysine residues by HDM2's ubiquitin-ligase located within the ring domain of the HDM2. HDM2 and its homologue are proteins consisting of 491 and 490 amino acids accordingly. They both contain p53 binding domain (p53 BD), acidic domain (AD), Zinc domain (Zn) and ring domain, which is required for homo- and hetero-dimerization of HDM2 with HDMX. HDM2 additionally contains nuclear NLS and NE residues. **B**, Schematic model depicting the regulation of p53 by HDM2 and HDMX. HDM2/HDMX represents HDM2/HDM2 or HDM2/HDMX dimers. In unstressed cells HDM2/HDMX binds to p53's transactivation domain, which prevents the recruitment of transcriptional co-activators. HDM2 also mediates degradation of p53 through its ubiquitin-ligase activity. Upon stress signals, p53 is modified by stress-induced kinases and phosphorylation of serine and threonine residues within TA domain, as well as threonine residues within Pro domain, which reduce the binding of the HDM2/HDMX and effectively allow binding of transcription co-activators (co-Act) and stabilises p53 (Lenos and Jochemsen, 2011; Toledo and Wahl, 2006).

dimerisation of HDM2 with HDMX stimulates the degradation of p53 and leads to accelerated p53 ubiquitination (Linares, Hengstermann *et al.*, 2003; Okamoto, Taya *et al.*, 2009). Nevertheless, HDMX is also a target of HDM2 E3 ligase, thus the role of HDMX in HDM2-mediated p53 degradation is complex and depends on the basal levels of HDMX in the cell. Under normal conditions in unstimulated cells, HDM2 targets HDMX for polyubiquitination, which contributes to the stabilisation of HDM2 and the maintenance of its basal levels by preventing its auto-degradation. Consequently, upon p53 activation excess HDMX can compete with p53 for HDM2-dependent ubiquitination and, in turn, lead to the stabilisation of p53 (Wang and Jiang, 2012; Wang, Wade *et al.*, 2007). Interestingly, removal of the RING domain of either *HDM2* or *HDMX* in mouse models leads to p53-dependent embryonic lethality in a manner similar to complete mutants (Huang, Yan *et al.*, 2011; Itahana, Mao *et al.*, 2007; Pant, Xiong *et al.*, 2011).

HDM2 and p53 are further regulated by protein interactions and post-translational modifications. p53 can be stabilised as the result of HDM2's interaction with the tumour suppressors ARF or RASSF1A. ARF binds directly to HDM2, which results in inhibition of HDM2's E3 ligase activity and its sequestration in the nucleolus, whereas RASSF1A stimulates HDM2's ubiquitination by disrupting the complex formed by HDM2 and the de-ubiquitinase machinery. In contrast, the transcription factor YY1 promotes the HDM2-dependent degradation of p53 by strengthening the binding of HDM2 and p53 (Kruse and Gu, 2009). Post-translational modifications affect the activity of both HDM2 and HDMX. ATM and ATR, protein kinases that are

activated in response to DNA damage, both directly and indirectly, phosphorylate HDM2 and HDMX at various sites. HDM2 is similarly phosphorylated following genotoxic stress by the DNA-dependent protein kinase (DNA-PK), whereas HDMX is phosphorylated by the tyrosine kinase ABL. Consequently, these phosphorylations lead to the disruption of the HDM-p53 complexes and lead to p53's stabilisation (Meulmeester, Pereg *et al.*, 2005; Wade, Li *et al.*, 2013). Conversely, de-phosphorylation of the sites phosphorylated by stress response kinases by protein phosphatases like PP1D, as well as the phosphorylation of HDM2 and HDMX by AKT, a kinase frequently activated in cancer, leads to the stabilisation of HDM2 and HDMX and the inhibition of p53 (Wade, Li *et al.*, 2013).

1.5 Genetic alterations of p53 and its inhibitors

1.5.1 *TP53* mutations

1.5.1.1 Somatic mutations

Given p53's role in controlling the key cellular processes associated with the prevention of malignant transformation, it is not surprising that a loss of p53's function is common in many cancers. In approximately 50% of all tumours, p53 is lost by mutation in the *TP53* gene (Hainaut and Hollstein, 2000; Hollstein, Sidransky *et al.*, 1991). Somatic mutations can be a consequence of unrepaired DNA damage or may arise spontaneously. The prevalence of somatic mutations in *TP53* ranges from less than 15% in bone malignancies to more than 40% in oesophagus, head and neck and colorectal tumours. More than 70% of all reported p53 genic mutations are missense substitutions that lead to the

expression of mutant protein. Other mutations with a frequency of over 5% are frame-shift mutations (9%) and nonsense mutations (8%). The current count of all *TP53* mutations reported to date in more than 2,000 publications stands at just under 30,000 (Petitjean, Mathe *et al.*, 2007) (R16, November 2012).

In many cases, mutant p53 proteins exhibit a loss of wild-type function, however, they also may gain (i) a dominant-negative effect over any remaining wt p53 and (ii) an oncogenic function independent of wt p53 (Muller and Vousden, 2013). A single amino acid substitution in a protein that comprises a total of 393 amino acids might seem like a very modest alteration. However, most of the mutations are critical to the p53 protein's structure and function. This is underscored by the fact that 90% of all p53 mutations are located in exons five, six, seven and eight, which encode the DNA binding domain, a pivotal element for p53's transcriptional activity. Furthermore, 26% of all exonic mutations cluster in only 6 codons (Petitjean, Mathe *et al.*, 2007) (R16, November 2012) (Muller and Vousden, 2013; Vousden and Lu, 2002; Whibley, Pharoah *et al.*, 2009). The substitution of a single amino acid yields mutant forms of p53 protein that can be categorised either as DNA-contact mutants, in cases where the substituted amino acid was critical for DNA binding, or structural mutants where the substituted amino acid dramatically changes the folding of the mutant protein (Sigal and Rotter, 2000). However, due to the intrinsically unstable structure of p53, most DNA contact mutants that result in the substitution of an amino acid residue also result in the unfolding of the p53 protein to some extent (Muller and Vousden, 2013). Although DNA-contact and structural mutations have been shown to associate with different clinical

outcomes of breast cancer patients, as well as those of non-small cell lung cancer patients (Powell, Soong *et al.*, 2000; Skaug, Ryberg *et al.*, 2000), the body of evidence suggests that these mutations, through different mechanisms, lead to similar outcomes (Muller and Vousden, 2013).

As mentioned above, most p53 mutants have a dominant negative effect over the remaining wt p53 molecules and this inhibition, the efficiency of which may vary depending on the type of mutation, arises from the hetero-oligomerisation of mutant p53 with wt p53 to form a tetramer with impaired transcriptional activity (Goh, Coffill *et al.*, 2011; Vousden and Lu, 2002). The most compelling attribute of mutant p53 is, however, the acquisition of the new oncogenic activities, whereby mutant p53 can: (i) bind to new targets and alter their expression; (ii) bind to transcription factors to enhance or inhibit their function; or (iii) bind to proteins to directly alter their function (Muller and Vousden, 2013). Indeed, studies on genetically engineered mice have demonstrated that both structural and contact mutant p53 mice develop tumours with more aggressive phenotypes that lead to more metastases, unlike p53-null mice (Lang, Iwakuma *et al.*, 2004; Olive, Tuveson *et al.*, 2004).

Just as wt p53 is rapidly degraded under normal cellular conditions and stabilised in response to stress stimuli, mutant p53 is also regulated by protein degradation. HDM2 mediates the degradation of mutant p53, whereas heat shock proteins, activated RAS and PTEN have been demonstrated to stabilise it. While targeting pathways that lead to the stabilisation of mutant p53 could offer a new therapeutic window with which to treat tumours with mutant p53, other targeted therapies that lead to its stabilisation by affecting the HDM2-p53

interaction have to be used with caution in the context of mutant p53 (Muller and Vousden, 2013).

1.5.1.2 Germline mutations

The genetically engineered mutant *TP53* mice mentioned above were a model of a Li-Fraumeni syndrome (LFS), a rare genetic syndrome that associates with a range of germline mutations across the *TP53* gene. The vast majority (73%) of these mutations are located within a hot spot for somatic mutations, a coding sequence of exons 5 to 8 (Varley, 2003). Li-Fraumeni syndrome is highly penetrant and associates with a 50% risk of developing cancer before the age of 40, compared to just 1% within the general population (Palmero, Achatz *et al.*, 2010).

Unlike other familial syndromes, LFS predisposes mutation carriers to a vast spectrum of different tumours ranging from soft tissue sarcomas and adrenocortical carcinomas (ADR), through breast, pancreatic and prostate cancers to brain tumours and melanomas (Varley, 2003). The classic definition of LFS, formulated by Li *et al.* (Li, Fraumeni *et al.*, 1988) and subsequently modified by Birch *et al.* (Birch, Hartley *et al.*, 1994), states that LFS is defined as any proband with any childhood tumour, or any sarcoma, brain tumour, or adrenocortical tumour when aged under 45 years, plus a first- or second-degree relative in the same lineage with a typical LFS tumour at any age, and an additional first- or second-degree relative in the same lineage with any cancer under the age of 60 years. Over 500 hundred families have been diagnosed with Li-Fraumeni syndrome and fulfil these classic criteria. However, the description of new tumour types, often with early ages of onset and different familial

histories, has prompted numerous changes to this definition and families that do not conform to the classic criteria are termed as Li-Fraumeni-like (LFS-L) (Malkin, 2011).

The phenomenon of such a wide cancer spectrum is associated with the diverse effects that each mutation can have on p53 protein's function or structure, as discussed above in section 1.3.1.1. Mice with different point mutations in the *TP53* gene engineered by the Jack lab (Olive, Tuveson *et al.*, 2004) have demonstrated that distinct *TP53* missense mutations not only associate with different outcomes to *TP53*-null mice, but each mutation can also lead to a distinct tumour spectrum. They demonstrated that DNA contact mutant $p53^{R270H/+}$ mice developed carcinomas as well as B cell lymphomas, whereas the most common tumours in structural mutant $p53^{R172H/+}$ mice were osteosarcomas. Indeed, a pattern of differential tumour spectra depending on the type of *TP53* missense mutation has been found in *TP53* germline mutation carriers, whereby brain tumours are associated with DNA contact mutants, and ADRs are common in the carriers of mutations found outside of the DNA binding region (Palmero, Achatz *et al.*, 2010).

1.5.2 Germline polymorphisms

Single nucleotide polymorphisms (SNPs) are the most common type of inherited genetic variation with a minimum frequency of 1% in a given population. However, around 80% of all SNPs have a minor allele frequency higher than 10% (Chakravarti, 2001). In contrast to the highly penetrant germline *TP53* mutations associated with LFS, the vast majority of SNPs are thought to have little or no effect on human phenotypic variation. However,

functional SNPs, like other genetic variations, could contribute to a wide spectrum of differences observed between individuals including susceptibility to cancer and differential responses to treatments. Indeed, a growing body of evidence supports the idea that functional SNPs in the p53 network can lead to altered cancer risk, progression and survival.

One of the most well studied functional SNPs in the p53 pathway is HDM2 SNP309 (G/T). HDM2 SNP309 resides in the transcriptional enhancer region in the first intron of the *HDM2* gene, and alters the binding affinity of the SP1 transcription factor. Specifically, the G-allele recruits more SP1 resulting in increased *HDM2* transcription in cells with a G/G-genotype, resulting in attenuation of the p53 stress response pathway and, in turn, tumour suppression (Bond, Hu *et al.*, 2004). *In vitro* experiments have demonstrated that cancer cell lines harbouring the G-allele of SNP309 have significantly higher levels of HDM2, which correlates with the attenuation of p53's apoptotic response after exposure to DNA damaging therapies (Vazquez, Bond *et al.*, 2008). Additionally, Post *et al.* generated mice that carried polymorphic *mdm2*^{SNP309G} and *mdm2*^{SNP309T} alleles and demonstrated that cells harbouring the G-allele had elevated HDM2 levels, reduced p53 levels and decreased apoptosis, while mice harbouring the G-allele had shorter latency to tumour formation and decreased survival (Post, Quintas-Cardama *et al.*, 2010). Indeed, a number of studies in different types of cancer have demonstrated that SNP309G associates with cancer risk and poor prognosis. The earlier age of onset of the G-allele carriers has been associated with cancers like soft-tissue sarcomas, lymphoma, leukaemia, head, neck and oral squamous cell carcinomas,

colon, breast, bladder, ovary, brain and liver (Firoz, Warycha *et al.*, 2009; Grochola, Zeron-Medina *et al.*, 2010). Interestingly, it has also been demonstrated that the effect of SNP309 is modified by gender and the estrogen signalling pathway (Bond and Levine, 2007). Indeed, Hue *et al.* demonstrated that estrogen stimulates the transcription of the *HDM2* gene and preferentially binds to the G-allele of SNP309 (Hu, Feng *et al.*, 2007). Furthermore, as indicated in the SNP309 mouse model, the G-allele of SNP309 also associates with poor prognosis. For example, an analysis of 176 renal cell carcinoma (RCC) patients revealed that SNP309 is an independent prognostic factor in RCC, with the G-allele associating with worse prognosis and shorter survival (Hirata, Hinoda *et al.*, 2007). Similarly, studies on patients with advanced non-small cell lung carcinoma (NSCLC) (Han, Lee *et al.*, 2008), pancreatic adenocarcinoma (Asomaning, Reid *et al.*, 2008), sporadic gastric carcinoma (Ohmiya, Taguchi *et al.*, 2006), B-cell chronic lymphocytic leukaemia (B-CLL) (Gryshchenko, Hofbauer *et al.*, 2008), and advanced neuroblastoma (Perfumo, Parodi *et al.*, 2008) have demonstrated that the G-allele of SNP309 associates with shorter survival.

Another frequently studied SNP in the p53 pathway resides in the coding region of the *TP53* gene. The alleles of p53-codon72 SNP encode for either a proline (Pro) or an arginine (Arg) residue, which is part of the proline-rich region located between p53's transactivation and DNA binding domains that has been demonstrated to be important in the induction of apoptosis (Sakamuro, Sabbatini *et al.*, 1997). *In vitro* studies have demonstrated that the p53-codon72-Arg variant associates with the elevated transcription of apoptotic

effectors, and is more efficient in inducing apoptosis than the p53-codon72-Pro variant in a context of wt *TP53*. Conversely, in a context of mutant *TP53*, the more efficient induction of apoptosis associates with the p53-codon72-Pro variant (Grochola, Zeron-Medina *et al.*, 2010). These *in vitro* associations are supported by the clinical reports of advanced head and neck squamous cell carcinoma patients treated with radio-chemotherapy, where patients with wtp53-codon72-Arg associated with the best response to treatment and longest overall and progression-free survival. In contrast, better clinical outcome amongst mutant p53 patients was associated with p53-codon72-Pro (Vazquez, Bond *et al.*, 2008). Additionally, resistance to chemotherapy and shorter progression-free survival associated with p53-codon72-Pro was demonstrated in NSCLC (Han, Lee *et al.*, 2008), breast cancer (Toyama, Zhang *et al.*, 2007; Xu, Yao *et al.*, 2005) and neuroblastoma (Cattelani, Ferrari-Amorotti *et al.*, 2012) patients.

Together, these studies suggest that functional polymorphisms in the p53 pathway genes can alter patients' responses to adjuvant therapy and disease progression, and could serve as predictive as well as prognostic biomarkers in some types of cancer. Additionally, the SNP309 and p53-codon72-Arg/Pro polymorphisms have also been described as genetic modifiers of *TP53* germline mutations in a number of different studies, underscoring the role of this p53 pathway functional polymorphism in altering cancer risk, alongside the importance of understanding how the interactions of these distinct genetic alterations can alter cancer risk and outcome (Bougeard, Baert-Desurmont *et al.*, 2006; Marcel, Palmero *et al.*, 2009; Ruijs, Schmidt *et al.*, 2007).

1.5.3 Amplification and overexpression of p53 inhibitors

The function of p53 in a number of tumours that retain wt p53 is compromised through the mutation or overexpression of other p53 pathway genes, upstream and downstream of p53 (Toledo and Wahl, 2006; Vousden and Lu, 2002). For instance, the activity of p53 can be affected by a mutation in the *ARF* tumour suppressor gene, which interferes with the p53-HDM2 complex and stabilises p53 in response to oncogenic stress (Kruse and Gu, 2009). Similarly, the mutation of *PTEN* further upstream or other alterations that lead to the up-regulation of AKT, which activates HDM2 through phosphorylation, result in the attenuation of p53-regulated processes (Georgescu, 2010). Nonetheless, the *HDM2* and *HDMX* genes are frequently upregulated in human tumours by either amplification of the gene, overexpression or enhanced translation.

The oncogenic properties of HDM2 and HDMX were first confirmed in *in vitro* experiments, where the overexpression of *mdm2* in immortalised mouse NIH3T3 cells lead to neoplastic transformation, and the overexpression of *mdmx* led to the immortalisation and neoplastic transformation of primary mouse embryonic fibroblasts and accelerated proliferation in primary human fibroblasts (Danovi, Meulmeester *et al.*, 2004; Wade, Li *et al.*, 2013). Further to that, the oncogenic potential of mdm2 was studied in a transgenic mouse model, where deregulated expression of *mdm2* resulted in the formation of mammary gland tumours in 16% of mice by 14 to 18 months of age (Lundgren, Montes de Oca Luna *et al.*, 1997). In addition, 26% of transgenic *mdmx*-overexpressing mice developed tumours within the 18 months observation period, with

sarcomas and lymphomas being the most prevalent tumour types (Xiong, Pant *et al.*, 2010).

The first comprehensive analysis of *HDM2* gene amplification by Momand *et al.*, which studied 3889 samples from either tumours or xenografts from 28 different tumour types, demonstrated that the *HDM2* gene was amplified in 7% of all samples with 19 tumour types harbouring the *HDM2* gene amplification. Soft tissue tumours, osteosarcomas and oesophageal carcinomas demonstrated the highest frequencies of *HDM2* gene amplification of up to 19% (Momand, Jung *et al.*, 1998). Another study in 130 osteosarcomas found *HDM2* gene amplification in 12% of the samples, however, no significant associations were found with the progression of osteosarcoma (Onel and Cordon-Cardo, 2004). Sarcomas also had a high frequency of *HDMX* gene amplification of up to 17%. The frequency of *HDMX* amplification in benign samples was relatively high, however, at 5%. Nonetheless, *HDMX* amplification in Ewing's sarcomas was 50%, suggesting that HDMX can associate with the malignant phenotype in some, but not all, subtypes of sarcoma (Ito, Barys *et al.*, 2011).

Comprehensive genomic analysis of 206 glioblastomas, the most common brain tumour in adults, identified the p53 pathway as one of the three core pathways in glioblastomas, alongside the Rb and RTK signalling pathways. Sixty six percent of the 206 samples analysed had copy number variations in p53 pathway genes, and the sequence analysis of 91 samples increased the number of somatic mutations in the p53 pathway to 87%. In addition to the mutation or deletion of the *TP53* gene found in 35% of the samples, the p53 pathway was altered by the deletion of *ARF* in 55% of the samples, mutually exclusive

amplifications of *HDM2* in 14% of the samples and *HDMX* in 7% of the samples (McLendon, Friedman *et al.*, 2008). While a number of studies have found significant associations between the amplification of *HDM2* in gliomas and poor prognosis, this is not consistent across all association studies and, furthermore, there is no significant difference in the frequency of *HDM2* amplification in primary and recurrent tumours, casting doubt on the role of this lesion in tumour progression in this type of cancer (Onel and Cordon-Cardo, 2004).

The gene amplification of either *HDM2* or *HDMX* has also been found in breast tumours (Danovi, Meulmeester *et al.*, 2004; Toledo and Wahl, 2006). Amplification of *HDM2* has also been reported in tumours like ovarian, endometrial, salivary gland, liver, small intestine, bladder and lung, as well as in Hodgkin's lymphoma (Toledo and Wahl, 2006). Interestingly, the amplifications of both *HDM2* and *HDMX* are frequently mutually exclusive with *TP53* mutation (Danovi, Meulmeester *et al.*, 2004; Ito, Barys *et al.*, 2011; Shibagaki, Tanaka *et al.*, 1995; Toledo and Wahl, 2006).

Another, less common mechanism that leads to up-regulation of p53's inhibitors is overexpression. In contrast to gene amplification, overexpression is mostly associated with the *HDMX* gene, where it has been implicated in as many as 40% of cancer cell lines, most of which had retained wt p53 (Ramos, Stad *et al.*, 2001). The analyses of Danovi *et al.* in hundreds of primary tumour samples demonstrated that 19% of primary breast, 19% of colon and 18% of lung tumours had high levels of *HDMX* mRNA. Other tumour types like stomach, testis, larynx, uterus and melanoma, although represented by a relatively small number of samples, also demonstrated higher frequencies of *HDMX*

overexpression (Danovi, Meulmeester *et al.*, 2004). Recent analysis of 54 cutaneous and metastatic melanoma samples by Gembarska *et al.* demonstrated that a staggering 68.5% of malignant melanomas had significantly increased expression of *HDMX* compared to normal melanocytes. Interestingly, the frequency of *HDMX* overexpression was higher in metastatic samples, where 83.3% of stage III and IV melanomas demonstrated *HDMX* overexpression, while the frequency of *HDMX* overexpression in stage I and II tumours was 56.7% (Gembarska, Luciani *et al.*, 2012).

1.6 p53 in the clinic

1.6.1 *TP53* gene mutation as a prognostic and predictive biomarker

Mutation of *TP53* associates with poor prognosis of a number of different cancers. The IARC *TP53* database, which compiles all *TP53* mutation studies that have been conducted on a minimum of 50 cases, reveals that *TP53* mutation is most frequently studied in breast cancer and that the association of *TP53* mutation with the poor prognosis of breast cancer is very consistent. The latest version of the database (R16, November 2012) states that *TP53* mutation relates to the poor prognosis of breast cancer in 28 out of a total of 34 different studies. The poor prognoses of other malignancies like colorectal cancer, leukaemias, lung, ovary and head and neck cancers are also related to *TP53* mutation in at least 7 different reports (Petitjean, Mathe *et al.*, 2007). Despite the large number of studies linking *TP53* mutation with poor outcome, the prognostic value of *TP53* mutation has been reported in only a relatively small number of breast cancer cohorts (Petitjean, Mathe *et al.*, 2007). Factors like

TP53 mutation detection and classification methods, the type of *TP53* mutation concerned, clinicopathologic status of the tumours, and study size all contribute to the inconclusive assessment of mutant *TP53*'s prognostic value. Indeed, the meta-analysis of 1,794 woman with primary breast cancer with long follow-up times, whose tumours were screened for *TP53* mutations within exons 5 to 8 using sequencing methods performed by Olivier *et al.,* demonstrated that *TP53* mutations within exons 5 to 8 associated with over a 2-fold higher risk of tumour-related death ($p<0.0001$) compared to patients lacking these mutations, proving that the detection of *TP53* mutations by sequencing methods can be used as a prognostic biomarker in clinical practice (Olivier, Langerod *et al.*, 2006). Moreover, this analysis also underscores the importance of effective and accurate assessment of *TP53* mutation status for clinical use. Nonetheless, *TP53* mutation status is already used to assist the management of chronic lymphocytic leukaemia (CLL) patients, whereby the loss of *TP53* associated with the deletion on chromosome 17p is an effective predictor of resistance to standard chemotherapy (Boyd and Vlatkovic, 2008).

Several specific *TP53* mutations have been associated with exposure to environmental carcinogens. Codon 249 mutation is prevalent in individuals exposed to aflatoxin B1 and associates with hepatocellular carcinomas (HCC), thus is used as a biomarker for aflotoxin exposure and early detection of HCC. Other mutations that are used as a biomarkers of carcinogen exposure are pyrimidine dimers associated with UV exposure and the risk of skin cancer, and G to T transversions associated with cigarette smoke and lung cancer (Robles and Harris, 2010). Although these associations need experimental support, such

mutations could potentially be used as biomarkers for the early detection of cancer.

The activation of apoptosis is the mode of action of many anti-cancer drugs. The activation of senescence has also recently been proposed as another cellular programme that might lead to cancer treatment response (Brown and Attardi, 2005). These two cellular programmes are largely mediated by p53. Consequently, any disruption of the p53 pathway can affect a patient's response to DNA damage-inducing cancer therapies. Indeed, p53 status has been demonstrated to affect the response to chemotherapeutics in cellular systems and mouse models. However, despite extensive research, the predictive significance of p53 status is extremely variable, mostly because assessments have been conducted in different tumour types with different drug regimens. Methodological issues like the methods used to detect p53 status and clinical assessment of response also contribute to this variability (Bertheau, Espie *et al.*, 2008).

1.6.2 Reactivation of the p53 pathway

Further to the role of p53 in the cell's response to DNA-damaging therapies, studies in mice suggest that restoration of p53's function alone can lead to tumour clearance. Ventura *et al.* demonstrated that restoration of endogenous p53 lead to the regression of autochthonous lymphomas and sarcomas in mice by a tumour-specific mechanism, whereby the p53-dependent regression of lymphomas was caused by widespread apoptosis, while the regression of sarcomas was due to cellular senescence (Ventura, Kirsch *et al.*, 2007). Similarly, Xue *et al.* demonstrated that reactivation of p53 in a mosaic

mouse model of carcinoma led to complete tumour regression, facilitated by the cellular senescence programme (Xue, Zender *et al.*, 2007).

Three different strategies to reactivate the p53 pathway are currently under development and at the preclinical or clinical stage. Two of these strategies, the first based on recombinant viruses that encode wt *TP53* and the second on small molecule drugs that target mutant p53, aim to restore wt p53 function. The third strategy focuses on small molecule inhibitors that target the p53-HDM2 interaction, resulting in the stabilisation of p53.

Thus far, the p53 reactivating therapies based on recombinant viruses have been the most successful in terms of progress made in the development of a usable treatment. The recombinant Ad-p53 gene therapy, Gendicine, is a drug that has been licensed to treat head and neck squamous cell carcinoma in China (Pearson, Jia *et al.*, 2004), and is undergoing or has already completed a number of Phase I through Phase IV clinical trials to treat tumours like NSCLC, ovarian and advanced head and neck tumours (ClinicalTrials.gov, ClinicalTrials.gov). Another two recombinant adenovirus therapies, Advexin and SCH 50500, are undergoing or have undergone Phase I through Phase III clinical trials to treat head and neck, NSCLC, bronchoaveolar, glioblastoma, breast, oesophageal, bladder, prostate and ovarian tumours (ClinicalTrials.gov, ClinicalTrials.gov; Vazquez, Bond *et al.*, 2008). The potential of this type of therapy is supported by the clinical report of Senzer *et al.*, that demonstrated the complete and durable remission of an injected lesion after Advexin treatment in a patient with refractory, progressive LFS (Senzer, Nemunaitis *et al.*, 2007).

The small molecule drug PRIMA-1 (p53-dependent reactivation of massive apoptosis), also known as APR246, is the first small molecule drug targeting mutant p53 that has successfully gone through Phase I clinical trials to test its efficacy in 22 patients with haematological malignancies and prostate cancer (Lehmann, Bykov *et al.*, 2012). Treatment with PRIMA-1 leads to limited cell growth and the activation of p53 target genes *in vitro*, and the reduction of tumour size *in vivo*, by re-folding structural p53 mutants into the wt conformation. However, its mechanism of action is not yet fully understood (Olivier, Petitjean *et al.*, 2009; Zandi, Selivanova *et al.*, 2011).

JNJ-26854165, a tryptamine derivative, was the first small molecule that targets the p53-HDM2 interaction to enter clinical trials in 2006, to determine its safety and dose efficacy in patients with advanced stage or refractory solid tumours (ClinicalTrials.gov, ClinicalTrials.gov). JNJ-26854165 increases p53 levels by binding to the RING domain of HDM2 to prevent proteasomal degradation. However, it has also been shown to have some p53-independent apoptotic and anti-proliferative activity in tumour models such as breast cancer, multiple myeloma and leukaemia (Yuan, Liao *et al.*, 2011).

Nutlin-3, also known as or RG7112, is another small molecule that targets the p53-HDM2 interaction, and Phase I clinical trials to determine the maximum tolerated dose in advanced solid tumour patients and patients with haematological neoplasms have been already completed (ClinicalTrials.gov, ClinicalTrials.gov). Nutlin-3 is a selective small molecule antagonist of HDM2 from the Nutlin family, first described by Vasilev *et al.*, the most thoroughly studied small molecule inhibitors of HDM2. Nutlins bind to the p53-binding

pocket of HDM2 and activate p53 (Vassilev, Vu *et al.*, 2004). Nutlin-3 has been reported to have anti-tumour activity across a wide range of cancers with wt p53, such as breast, colon, neuroblastoma, mantle cell lymphoma and osteosarcoma. However, *in vitro* experiments using cancer-derived cell lines and *in vivo* xenograft models have demonstrated that Nutlin-3 has the best response and anti-tumour activity in osteosarcomas harbouring the amplification of *HDM2* (Tovar, Graves *et al.*, 2013; Yuan, Liao *et al.*, 2011). A proof of mechanism study on 20 patients with liposarcoma demonstrated that Nutlin-3 activated the p53 pathway and decreased cell proliferation in liposarcomas with wt *TP53* and amplified *HDM2* (Ray-Coquard, Blay *et al.*, 2012). A body of evidence from *in vitro* experiments with null and mutant p53 cells suggests that Nutlin-3 can directly, or indirectly through E2F1, activate the pro-apoptotic homolog of p53, p73, and induce apoptosis independently of p53 (Ambrosini, Sambol *et al.*, 2007; Lau, Nugent *et al.*, 2008). It is therefore possible that the Nutlin family of drugs may prove to have uses beyond wt p53 tumours. However, a study by Terzian *et al.* on mice with codon172 mutant p53 that lacked *mdm2* demonstrated that HDM2 inhibition strategies need to be used with caution, as a lack of HDM2 clearly stabilised mutant p53 in a same way as wt p53, and the activation of mutant p53 led to faster metastatic progression (Terzian, Suh *et al.*, 2008).

1.6.3 Gene expression signatures for *TP53* mutational status

Microarray-based gene expression profiling for the classification of breast cancer was developed over a decade ago, when it was demonstrated that mutant *TP53* clusters with subtypes that associate with the worst prognosis,

whereby 71% of ERB2+ and 82% of basal-like subtypes contained mutant *TP53* in contrast to only 13% of the luminal A subtype having *TP53* mutation (Perou, Sorlie *et al.*, 2000; Sorlie, Perou *et al.*, 2001). However, a subsequent study demonstrated that even though *TP53* mutation status is a strong predictor of breast cancer outcome, gene expression profiles are better predictors of the outcome of breast cancer (Langerod, Zhao *et al.*, 2007). Nonetheless, Miller *et al.* identified a clinically embedded 32-gene expression signature, using *TP53*-sequenced primary tumours, that enables the recognition of wt and mutant *TP53* and could serve as an independent prognostic biomarker for breast cancer survival and progression, which out-performs sequence-based assessment of p53 in predicting prognosis as well as response to adjuvant therapy (Miller, Smeds *et al.*, 2005). Moreover, the authors demonstrated that the identified gene expression signature facilitated the better classification of misclassified wt *TP53* tumours that have impaired p53 function downstream of the *TP53* gene. Specifically, when the gene expression classifier was tested on a subset of women with wt *TP53* (by sequence) tumours, it was observed that the women with wt *TP53* genes but mutant-like *TP53* gene expression signatures were at significantly higher risk of tumour-related death. Notably, the prediction of p53 inactivation by this gene signature was also validated in liver cancer.

Another p53-specific gene expression signature was described by Takahashi *et al.* (Takahashi, Moriya *et al.*, 2008). Specifically, it was demonstrated that a mutant p53-like group, identified by a 33-gene expression classifier, associates with a significantly higher risk of progression in early stage breast cancer, which could not be predicted by p53 IHC. The prognostic value of

this new gene expression profile was validated in two independent breast cancer patient cohorts, including the cohort used by Miller *et. al.*, however none of the 33 genes overlapped with those of the 32-gene signature described by Miller *et al*.. Yet another gene expression pattern associated with p53 status was identified by Troester *et al.* using an experimental isogenic system in breast cancer cell lines, that allowed correction for gene expression patterns specific to tumour subtype and the exclusion of genes that were not downstream of p53 (Troester, Herschkowitz *et al.*, 2006). As in the studies described above, a 52-gene classifier allowed the identification of tumours with a p53-loss signature that associated with highly significant differences in disease specific survival in 3 independent patient datasets, including the dataset of Miller *et al*., as well as progression-free survival in 2 datasets for which the data was available.

Interestingly, a study by Oshima *et al*. (Oshima, Naoi *et al.*, 2011) demonstrated that a p53-specific gene expression signature could also serve as a predictive biomarker for response to chemotherapy in breast cancer. Specifically, it was demonstrated that the p53 gene expression signature described by Takakeshi *et al.* could predict the response to sequential paclitaxel and 5-FU/epirubicin/cyclophosphamide treatment (P-FEC), whereby mutant-like p53 tumours were more likely to achieve pathological complete response (pCR) after P-FEC treatment than wt-like p53 tumours. No differences in the rate of pCR were observed in wt and mutant p53 groups assessed by either sequencing or IHC. Another study by Coutant *et al*. (Coutant, Rouzier *et al.*, 2011) demonstrated that a *TP53* gene expression profile could not only define a group of breast cancer patients with a higher risk of metastatic progression, but

could also be predictive of response to chemotherapy, where a mutant-like p53 signature associated with worse metastasis-free survival but higher sensitivity to chemotherapy. However, the 39-gene signature defined in this study was specific to estrogen receptor (ER) tumours and was only predictive in this group, whereas the p53 gene expression signature identified based on ER-negative tumours had no predictive value. Altogether, these studies suggest that molecular signatures that identify tumours with active and inactive p53 pathways better than *TP53* sequencing or IHC strategies could serve as independent prognostic and predictive biomarkers.

1.7 Objectives of the study

Metastasis is the primary cause of death of most cancer patients. However, the current predictors of invasive phenotype that guide treatment decisions in the clinic are grossly inefficient. A growing body of evidence suggests that the metastatic potential of primary tumour cells is determined by genetic lesions arising early in tumourigenesis. Therefore, the identification of molecular biomarkers that could detect these lesions in primary tumours may potentially prove more effective for the management of cancer patients.

The tumour suppressor p53 is at the centre of the one of the core signalling pathways that controls cellular processes crucial in the prevention of cancer, while also determining the cell's response to DNA-damaging cancer therapies. p53 is also involved in processes that determine the ability of primary tumour cells to exert an invasive phenotype and subsequently metastasise to distant organs. *TP53* gene mutation is the most frequent genetic lesion that leads to attenuation of the p53 pathway, and has been demonstrated

to have substantial potential as an independent prognostic biomarker in many cancer types. However, the function of p53 in a number of tumours that retain wt p53 is compromised by other mechanisms. Indeed, alterations in the genes and gene expression patterns of *HDM2* and *HDMX*, critical inhibitors of p53, are frequently found in tumours. The loss of p53 function through genetic alterations in the *TP53*, *HDM2* and *HDMX* genes associates with both cancer risk and poor clinical outcome. Additionally, high frequency single nucleotide polymorphisms in the *TP53* and *HDM2* genes have been demonstrated to alter the function of both genes and could, therefore, influence clinical outcome. While this adds further complexity, it also suggests that other SNPs in p53 pathway genes could alter p53's function.

The aim of this thesis is, therefore, to contribute to the understanding of the effects that alterations in the p53 pathway can have on cancer progression, and identify candidates for molecular biomarkers that would assist in the identification of patients with different prognoses. To do so, associations of potential biomarker candidates with metastasis-free and overall survival are sought here in multiple cohorts of cancer patients. Additionally, *in silico* and *in vitro* analyses are performed to further characterise prospective biomarkers and investigate the potential molecular mechanisms behind them.

- In Chapter 3 and 4, the associations with (i) HDMX-FL protein levels, (i) common p53 pathway alterations, namely TP53 mutation and HDM2 overexpression and (iii) overall and metastasis-free survival of sarcoma and breast cancer patients are sought for the alternatively spliced transcript of HDMX-S, which is frequently found in tumours with poor prognosis.

- In Chapter 5, an inherited polymorphism in the HDMX gene, which associates with cancer risk and differences in the transcript levels of the HDMX gene is investigated in relation to the allelic differences in the metastasis-free prognoses of breast cancer patients whose tumours had different TP53 mutation and estrogen receptor status.
- In Chapter 6, a HDMX SNP is investigated in relation to different prognoses of melanoma patients and a screening approach to identify novel inherited polymorphisms in the p53 pathway genes that associate with metastatic progression of melanoma is developed and implemented. Subsequently, functional experimental analyses are undertaken to study the mechanism behind the observed phenotype associated with the strongest candidate identified in the screen.

2 MATERIALS AND METHODS

2.1 Materials

2.1.1 Reagents

2.1.2 Antibodies, gene specific TaqMan assays and oligonucleotides

2.2 Patients cohorts

2.2.1 The Osteosarcoma cohort

2.2.2 The Soft Tissue Sarcoma cohort

2.2.3 The Norwegian breast cancer cohorts

2.2.4 The Melanoma cohort

2.3 Cell lines

2.3.1 NCI60 human cancer cell lines

2.3.2 Osteosarcoma and breast cancer cell lines

2.3.3 Cancer cell lines grown in the cell culture.

2.4 Methods

2.4.1 Cell culture

2.4.2 Plasmid preparation

2.4.3 Cell transfection assays

2.4.3.1 siRNA transfections

2.4.3.2 Transient plasmid transfections

2.4.4 Luciferase bioluminescence detection

2.4.5 DNA extraction

2.4.6 RNA extraction and cDNA synthesis

2.4.7 Genotyping

2.4.8 Polymerase chain reaction (qRT-PCR and semiQ-PCR)

2.4.8.1 Gene expression qRT-PCR.

2.4.8.2 Allele-specific qRT-PCR

2.4.8.3 Semi-Quantitative PCR

2.4.9 Analysis of DNA-protein interactions

2.4.9.1 Electromobility Shift Assay (EMSA)

2.4.9.2 Chromatin Immunoprecipitation (ChIP)

2.4.10 Protein analysis by Western blotting

2.4.11 Data analyses

2.1 Materials

2.1.1 Reagents

All chemicals, unless otherwise stated, were obtained from Sigma-Aldrich (UK), Fisher-Scientific (UK), Severn Biotech Ltd. or BDH Chemicals (UK).

10% (w/v) Ammonium Persulfate (APS) (500 ml)

50 g Ammonium persulfate

ddH_2O

Stored at -20°C in 500µl aliquots.

2x anneal buffer (1ml)

10µl 1M Tris pH 7.6

10µl 1M DTT

20µl 1M $MgCl_2$

20µ 100mM Spermidine

ddH_2O

Ampicillin stock

0.5g of the antibiotic was dissolved in 10ml of sterile distilled water, creating a 50mg/ml solution, and stored at -20°C in single-use aliquots.

Black buffer 10x

400mM KCl

150mM HEPES (pH 7.9)

10mM EDTA

5mM DTT

50% glycerol

ddH_2O

Blocking solution

5% Bovine Serum Albumin (BSA; Sigma, Cat. No. A7906-100G) in 1X Tris Buffered Saline (TBS) / 0.1% Tween.

Buffer 2 (100ml)

2ml 0.5M HEPES pH 7.9

150µl 1M $MgCl_2$

1ml 1M KCl

100µl 0.5M DTT

ddH_2O

Buffer 3 (100ml)

4ml 0.5M HEPES pH 7.9

8.4ml 5M NaCl

150µl 1M $MgCl_2$

100µl 0.2M EDTA

25ml Glycerol

100µl 0.5M DTT

ddH_2O

DNA markers

100bp was purchased from Promega, USA (Cat. No. G210A, G571A).

Hyperladder I (Cat. No. BIO-33025) and Hyperladder IV (Cat. No. BIO-33029) were purchased from Bio Line and were used as a size standard for agarose gel electrophoresis.

Elution Buffer for EMSA

40mM KCl in ddH_2O

Freezing medium

20% (v/v) FBS

10% (v/v) DMSO

DMEM or RPMI

MOPS SDS Running Buffer 20x (500ml)

104.6g MOPS

60.6g Tris Base

10g SDS

3.0g EDTA

ddH_2O

LDS 4X sample buffer

The NuPAGE LDS sample buffer was purchased from Life, Technologies, Invitrogen (Cat. No.NP0007)

Nutlin-3

Nutlin-3 was purchased from Sigma, UK (Cat. No. SML0580), dissolved in DMSO to 10mM concentration and stored in single-use aliquots at -20°C.

Polyacrylamide and Agarose Gel Solutions

1% TAE Agarose Gel (100ml)

100ml 1X TAE

1g Agarose

Microwave to melt

20µg/ml Ethidium Bromide

6% Non-denaturing Polyacrylamide Gel (40 ml)

8ml 30% Acrylamide/Bis, 37.5:1

4ml 5x TBE

450µl 10% APS

26µl TEMED

ddH_2O

10% Non-denaturing Polyacrylamide Gel (40 ml)

10ml 40% Acrylamide/Bis, 19:1

4ml 5x TBE

500µl 10% APS

25µl TEMED

ddH_2O

10% (w/v) SDS (500ml)

50g SDS

ddH_2O

SDS-Polyacrylamide gels

4-12% gradient gels were purchased from Life, Technologies, Invitrogen, UK (Cat. No. NP0321).

Stripping solution

Re-blot Plus Strong Solution 10x was purchased from Millipore, US (Cat.No. 2504).

50x TAE (1L)

242g Tris base

57ml glacial HAc

100ml 0.5M EDTA pH 8.0

ddH_2O

5x TBE (1L)

54g Tris base

27.5g Boric Acid

20ml 0.5M EDTA pH 8.0

ddH_2O

TE buffer (1L)

10ml 1M Tris pH 7.4

2ml 0.5M EDTA 8.0

ddH_2O

10x Transfer Buffer (1L)

145g Glycine

29g Tris base

ddH_2O

Tris stock solution

Tris base was dissolved in water to provide a 1M solution, which was adjusted with concentrated HCl to the desired pH.

Whole cell lysis buffer (10ml)

500µl 1M Tris pH 7.6

375µl 4M NaCl

50µl 1M $MgCl_2$

200µl 0.25M EGTA

100µl Igepal

100mg Na deoxycholate

100µl SDS (10%)

100µl 0.5M NaF

20mg NaOV

500µl 0.1M NaPPi

ddH_2O

Water

DEPC-treated, nuclease-free water was purchased from Severn Biotech Ltd, UK (Cat.No. 20-9000-01) and used for PCR applications. Nano-pure generated by the MilliQ water system was used for all other procedures.

2.1.2 Antibodies, gene specific TaqMan assays and oligonucleotides

Table 2.1 Primary antibodies.

name	antigen	host	type	Source (catalog number)	application	working condition
C-4	β-actin	mouse	monoclonal	Santa Cruz (sc-47778)	WB	1:1000
75D8	FOXO3	rabbit	monoclonal	Cell Signaling (2497)	WB	1:1000
CG2-96	GATA2	mouse	monoclonal	Santa Cruz (sc-267)	EMSA	5µg
B-10	GATA3	mouse	monoclonal	Santa Cruz (sc-137152)	ChIP	5µg
HG-35	GATA3	mouse	monoclonal	Santa Cruz (sc-269)	ChIP/EMSA	5µg
					WB	1:200
SMP14	HDM2	mouse	monoclonal	Santa Cruz (sc-965)	WB	na[1]
anti-HDMX	HDMX	rabbit	polyclonal	Bethyl (A300-287A)	WB	na[1]
DO-1	p53	mouse	monoclonal	Santa Cruz (sc-126)	WB	na[1]
anti-USP7	USP7	rabbit	polyclonal	Bethyl (A300-033A)	WB	na[1]

Table 2.2 Secondary antibodies.

name	source (catalog number)	application	working dilution
rabbit anti-mouse HRP	Dako (P0260)	WB	1:1000
goat anti-rabbit	Bethyl (A120-101P)	WB	1:10 000

Table 2.3 TaqMan gene expression and genotyping assays.

gene	assay ID	
CDKN1A (p21)	Hs00355782_m1	
ESR1	Hs01046818_m1	
FOXO3	Hs00921424_m1	
GAPDH	4326317E	
GATA3	Hs00231122_m1	
HDMX-FL	Hs00967241_m1	
HDMX-S	custom made	HDMX-S_F: 5'-GCCCTCTCTATGATATGCTAAGAAAGAATC-3'
		HDMX-S_R: 5'-TTCTGTAGTTCTTTTTCTGGAAGTGGAA-3'
		HDMX-S_M FAM: 5'-CTGCACTTTGCTGTAGTAGC-3'
HDMX-P1	custom made	HDMX-P1_F: 5'-GAGGCCCTAGGATCTGTGACT-3'
		HDMX-P1_R: 5'-TGAAGAAACTGCAGTCTGTTGGTAA-3'
		HDMX-P1_M FAM: 5'-CAGCTCCATGAGTCGCT-3'
HDMX-P2	custom made	HDMX-P2_F: 5'-TCAGAACTAGAAAGTAGTCAGAAGATATGCA-3'
		HDMX-P2_R: 5'-GTAGTGAAGAAACTGCAGTCTGTTG-3'
		HDMX-P2_M FAM: 5'-CCTCAGCAAGGTTTTAC-3'
HDM2-P1	custom made	HDM2-P1_F: 5'-GACTCCAAGCGCGAAAACC-3'
		HDM2-P1_R: 5'-CACCATCAGTAGGTACAGACATGTT-3'
		HDM2-P1_M FAM: 5'-CACATTTGCCTGCTCCTC-3'
HDM2-P2	custom made	HDM2-P2_F:5'-GGACGCACGCCACTTTT-3'
		HDM2-P2_R: 5'-CACCATCAGTAGGTACAGACATGTT-3'
		HDM2-P2_M FAM: 5'-CTGATCCAGGCAAATGT-3'
FOXO3 rs2802292	C_16097219_10	
HDMX rs1563828	C_9493064_10	

Table 2.4 Oligonucleotides and PCR primers.

name	application		5'-3' sequence
FOXO3-ChIP-rs2802292	ChIP	forward	AACCCAGCCTGCTCACTCCA
		reverse	TCCCTTGAGCAATTTGGGACCGA
FOXO3-ChIP-rs2802288	ChIP	forward	GATAAACGTGAGCAGGCAGC
		reverse	GTCCTCCTTACACTTCAGGCT
FOXO3-ChIP-rs2764261	ChIP	forward	CACAGCCTTGCCAGACTATGAT
		reverse	GTCCTGTCACTAAACTCTTGGT
FOXO3-EMSA-rs2802292-G	EMSA	sense	CTAGATCAGGGCTGGGA[G]AAGCCTCTGTGTT
		antisense	TACACAGAGGCTT[C]TCCCAGCCCTGAAGATC
FOXO3-EMSA-rs2802292-T	EMSA	sense	CTAGATCAGGGCTGGGA[T]AAGCCTCTGTGTT
		antisense	TACACAGAGGCTT[A]TCCCAGCCCTGAAGATC
FOXO3-EMSA-rs2802288-A	EMSA	sense	CTAGAGGAGGCAGCTGC[A]GTAGAAGTTGGCT
		antisense	TGCCAACTTCTAC[T]GCAGCTGCCTCCAGATC
FOXO3-EMSA-rs2802288-G	EMSA	sense	CTAGAGGAGGCAGCTGC[G]GTAGAAGTTGGCT
		antisense	TGCCAACTTCTAC[C]GCAGCTGCCTCCAGATC
FOXO3-EMSA-rs2764261-A	EMSA	sense	CTAGAACAAGCAGGTTC[A]GAAAGCCAGGAAT
		antisense	TTTCCTGGCTTTC[T]GAACCTGCTTGTAGATC
FOXO3-EMSA-rs2764261-G	EMSA	sense	CTAGAACAAGCAGGTTC[G]GAAAGCCAGGAAT
		antisense	TTTCCTGGCTTTC[C]GAACCTGCTTGTAGATC
FOXO3-LUCIF-rs2802292-G	LUCIFERASE	sense	GATCCTTGCTCACAAGAGCTCAGGGCTGGGA[G]AAGCCTCTGTGTGACAGATGAAGGGGTA
		antisense	GATCTACCCCTTCATCTGTCACACAGAGGCTT[C]TCCCAGCCCTGAGCTCTTGTGAGCAAG
FOXO3-LUCIF-rs2802292-T	LUCIFERASE	sense	GATCCTTGCTCACAAGAGCTCAGGGCTGGGA[T]AAGCCTCTGTGTGACAGATGAAGGGGTA
		antisense	GATCTACCCCTTCATCTGTCACACAGAGGCTT[A]TCCCAGCCCTGAGCTCTTGTGAGCAAG
FOXO3-LUCIF-rs2802288-A	LUCIFERASE	sense	GATCCGAGGACTGTGTGGCTGGAGGCAGCTGC[A]GTAGAAGTTGGCAGTGCCACTGTGGAA
		antisense	GATCTTCCACAGTGGCACTGCCAACTTCTAC[T]GCAGCTGCCTCCAGCCACACAGTCCTCG
FOXO3-LUCIF-rs2802288-G	LUCIFERASE	sense	GATCCGAGGACTGTGTGGCTGGAGGCAGCTGC[G]GTAGAAGTTGGCAGTGCCACTGTGGAA
		antisense	GATCTTCCACAGTGGCACTGCCAACTTCTAC[C]GCAGCTGCCTCCAGCCACACAGTCCTCG
FOXO3-LUCIF-rs2764261-A	LUCIFERASE	sense	GATCCCAAGCAGCCTTGTGAACAAGCAGGTTC[A]GAAAGCCAGGAACTGACAAACTTTTCA
		antisense	GATCTGAAAAGTTTGTCAGTTCCTGGCTTTC[T]GAACCTGCTTGTTCACAAGGCTGCTTGG
FOXO3-LUCIF-rs2764261-G	LUCIFERASE	sense	GATCCCAAGCAGCCTTGTGAACAAGCAGGTTC[G]GAAAGCCAGGAACTGACAAACTTTTCA
		antisense	GATCTGAAAAGTTTGTCAGTTCCTGGCTTTC[C]GAACCTGCTTGTTCACAAGGCTGCTTGG
HDMX	qRT-PCR	forward	CAGCAGGTGCGCAAGGTGAA
HDMX-FL		reverse	CTGTGCGAGAGCGAGAGTCTG
HDMX-S		reverse	GCACTTTGCTGTAGTAGCAGTG
HDMX ex-3 Fw	semiQ-PCR	forward	TGCATGCAGCAGGTGCG
HDMX ex-8 Rev		reverse	CATTACTTCTAGGTGTAT
GAPDH		forward	AATCCCATCACCATCTTCC
		reverse	ATGAGTCCTTCCACGATACC

2.2 Patients cohorts

2.2.1 The Osteosarcoma cohort[1]

The cohort consists of 51 osteosarcoma patients from Germany, Holland and Italy (32 males, 19 females; age at diagnosis 3-58 years; mean 17.5 years) (Table 2.5). Part of the samples was previously described (Buddingh, Anninga *et al.*, 2010). Biopsies were taken before pre-operative chemotherapeutics were administered. The differences in response to chemotherapy were classified as good or poor, using the Huvos criteria. All tissue samples were handled

[1] Aart Jochemsen and Pancras C. W. Hogendoorn, Leiden University, the Netherlands

Table 2.5 Clinical and histopathological characteristics of the osteosarcoma patients.

	Number of Patients (%)
Huvos*	
I	14 (28.6%)
II	19 (38.8%)
III	11 (22.4%)
IV	5 (10.2%)
Tumor localization	
femur	26 (51%)
fibula	3 (5.9%)
humerus	7 (13.7%)
tibia	15 (29.4%)
Tumor type	
Anaplastic	2 (3.9%)
Chondroblastic	3 (5.9%)
Chondromyxoid fibroma like	1 (1.9%)
Fibroblastic	6 (11.8%)
Giant cell rich	1 (1.9%)
Osteoblastic	34 (66.7%)
Sclerosing	1 (1.9%)
Telangiectatic	3 (5.9%)
*The tumor Huvos status of 2 patients was not known	

according to the National Ethical Guidelines ('Code for Proper Secondary Use of Human Tissue in The Netherlands', Dutch Federation of Medical Scientific Societies).

2.2.2 The Soft Tissue Sarcoma cohort[1]

The Soft Tissue sarcoma cohort comprises 130 patients (57 males, 73 females; ages 14-87 years; mean 56.3 years) diagnosed with soft-tissue sarcomas (STS) between the years 1991 to 2001 at Surgical Clinic 1, University

[1] Peter Würl, the Diakonie-Hospital Halle and Helge Taubert, University Clinic of Urology, Erlangen, Germany

Table 2.6 Clinical and histopathological characteristics of the soft tissue sarcoma patients.

	Number of Patients (%)
Stage	
I	23 (9.6%)
II	68 (43.3%)
III	51 (32.5%)
IV	15 (9.6%)
Tumor resection*	
Radical	110 (70%)
Non-radical	47 (30%)
Tumor localization**	
Extremities	102 (65.8%)
Trunk	13 (8.4%)
Head/neck	4 (2.6%)
Intraabdominal/retroperitoneum	34 (21.9%)
Multiple localizations	2 (1.3%)
Tumor type	
Liposarcoma	37 (23.6%)
Fibrosarcoma and MFH***	49 (31.2%)
Neurogenic sarcoma	22 (14.0%)
Rhabdo- and Leiomyosarcoma	34 (21.6%)
Others	15 (9.6%)
*Radical resection: primary wide excision, primary resection of compartment; non-radical resection: enucleation, palliative resection	
**The tumor localization of 2 patients was not known	
***Malignant Fibrous Histiocytoma	

of Leipzig, Germany, and the Institute of Pathology of the Martin-Luther-University Halle, Germany (Table 2.6). Tumour samples were taken before adjuvant radio- and/or chemotherapeutics were administered. The DNA of 66 patients was extracted from whole blood samples (n= 22) or from normal, pathologically confirmed tumour-free tissue, adjacent to the resection specimen (n= 44). The DNA of the remaining 64 patients was obtained from tissue within the confines of the tumour. Tumour tissue was available for 92 patients included in this study. The somatic *TP53* mutation status of the STS tissues was

determined by direct sequencing of exons 4 to 10 of the *TP53* gene, as previously described (Taubert, Meye et al. 1998; Taubert, Wurl et al. 1998). The study adhered to national regulations on ethical issues and was approved by the local ethical committee. All patients gave written and informed consent (Department of Surgery 1, University of Leipzig, Germany).

2.2.3 The Norwegian breast cancer cohorts[1]

MicMa cohort. The cohort consists of 113 women with early stage breast cancer from the Oslo MicroMetastasis Project (Table 2.7), started in 2001 to investigate disseminating tumour cell (DTC) status in relation to clinical outcome (Naume, Zhao *et al.*, 2007; Wiedswang, Borgen *et al.*, 2003). Genomic DNA was extracted from blood samples and tumour material for RNA analyses was obtained before adjuvant radio- and/or chemotherapeutics were administered. The somatic *TP53* mutation status of the breast cancer tissues was determined by direct sequencing of exons 4 to 10 using an ABI PRISM™ 377 DNA Sequencer (Applied Biosystems). Some patients received adjuvant treatment by tamoxifen, CMF chemotherapy, radiation and/or hormone therapy. All patients were treated according to Norwegian national guidelines at the time of diagnosis.

ULL cohort. The cohort consists of 78 women with breast cancer recruited to the ULL project at Ullevål University Hospital between 1990 and 1994 (Table 2.7)(Langerod, Zhao *et al.*, 2007). Patients with stage IV tumours received neo-adjuvant treatment, and some patients received adjuvant

[1]Vessela N. Kristensen, Oslo University Hospital, Norway

Table 2.7 Clinical and histopathological characteristics of the MicMa and ULL breast cancer cohorts.

		MicMa	ULL
cohort size		113	78
age	average	61 (±15)	65 (±14)
	≤ 50	27.40%	19.20%
	50-60	17.70%	16.70%
	≥60	54.90%	64.10%
pN	-ve	39.40%	38.00%
	+ve	53.00%	43.60%
	na	7.60%	18.40%
ER	-ve	28.30%	46.10%
	+ve	69.90%	53.80%
	na	1.80%	0.10%
PR	-ve	31.80%	34.60%
	+ve	64.60%	65.40%
	na	3.60%	0.00%
HER2	-ve	77.00%	85.90%
	+ve	14.10%	14.10%
	na	8.90%	0.00%
stage	1	21.20%	11.50%
	2	44.20%	35.90%
	3	24.80%	25.60%
	4	0.00%	6.40%
	na	9.80%	20.60%

pN-pathological node status; ER-estrogen receptor status; PR-progesteron receptor status; -ve-negative; +ve-positive; na-not available

treatment in the form of CMF chemotherapy, tamoxifen and/or radiation therapy. All patients were treated according to Norwegian national guidelines at the time of diagnosis.

Genomic DNA was extracted from blood samples, and tumour material for RNA analyses was obtained before adjuvant radio- and/or chemotherapeutics were administered. The somatic *TP53* mutation status of the breast cancer

tissues was determined by direct sequencing of exons 4 to 10 using an ABI PRISM™ 377 DNA Sequencer (Applied Biosystems).

2.2.4 The Melanoma cohort[1]

The melanoma cohort comprises 105 patients from South East England (57 males, 48 females; age at primary diagnosis 17-82 years; mean 54.6 years) diagnosed with cutaneous melanoma between 1989 and 2008 (Table 2.8). Some of the patients received adjuvant treatment and/or radiation therapy. The patients' genomic DNA was extracted from whole blood cells and subsequently whole genome amplified by Source Bioscience Services. Each person gave written and informed consent and approval from the local ethics committee was obtained.

Table 2.8 Clinical and histopathological characteristics of the discovery melanoma cohort.

	Number of Patients (%)
AJCC Stage*	
I	20 (21.3%)
II	40 (42.6%)
III	29 (30.8%)
IV	5 (5.3%)
Tumor localization	
Extremities	64 (61.0%)
Head/neck	10 (9.5%)
Trunk	25 (23.8%)
Unknown	6 (5.7%)
Tumor type	
Skin	99 (94.3%)
Unknown	6 (5.7%)
*The AJCC stage of 11 patients was not known	

[1] Mark Middleton, University of Oxford

2.3 Cell lines

2.3.1 NCI60 human cancer cell lines

The National Cancer Institute 60 (NCI60) panel consists of 59 human tumour cell lines, representing 9 cancer types (Table 2.9; Table 3.6): leukaemia and lymphoma (represented by 6 cell lines), melanoma (8 cell lines), non-small-cell lung cancer cell (NSCLC, 9 lines), colon (7 cell lines), central nervous system (CNS, 6 cell lines), ovary (6 cell lines), breast (7 cell lines), prostate (2 cell lines) and renal (8 cell lines) (Shoemaker, 2006). The mutational status of p53 in these lines (Table 2.9) was obtained from the National Cancer Institute (NCI)/NIH Developmental Therapeutics Program.

2.3.2 Osteosarcoma and breast cancer cell lines[1]

Most of the osteosarcoma cell lines (Table 3.1) have been described recently, including their genotyping and detailed methods on *TP53* sequencing (Ottaviano, Schaefer *et al.*, 2010). Osteosarcoma cell lines L2531, L2635, L2792, L2826, L2857 and L2962 were recently established at the Dept. of Molecular Cell Biology, LUMC in the lab of Dr. Szuhai. p53 gene status was determined as described by Da Costa *et al.* (da Costa, Szuhai *et al.*, 2009). Tumour -, normal - and cell line DNA was typed to confirm cell line identity using the Cell ID system of Promega. Normal osteoblasts were obtained as described previously (Cleton-Jansen, Anninga *et al.*, 2009). Breast cancer cell lines (Table 2.10; Table 3.5) were a gift from Mieke Schutte (Erasmus MC, Rotterdam). The origin of all breast cancer cell lines and verification of their individual identity has been

[1] Aart Jochemsen, Leiden University, the Netherlands

described previously, including a full description of p53 gene sequencing (Elstrodt, Hollestelle *et al.*, 2006; Wasielewski, Elstrodt *et al.*, 2006).

Table 2.9 NCI60 cell lines.

Origin	Cell line	*TP53*	*HDMX-S/FL* ratio	deltaCT								HDMX SNP rs1563828	FOXO3 rs2802292
				HDMX-FL	*HDMX-S*	p21	*HDMX-P2*	*HDMX-P1*	*HDM2-P2*	*HDM2-P1*	*FOXO3*		
br	BT-549	mut	3.11	10.2	8.56	5.42	23.36	7.09	15.18	8.58	8.23	A/A	T/T
br	HS 578T	mut	5.89	11	8.44	3.59	nd	7.97	16.21	9.8	7.15	G/G	T/T
br	MCF7	wt	0.31	7.47	9.16	2.32	12.26	6.96	10.33	8.06	7.8	A/G	G/T
br	MDA-MB-231	mut	0.79	9.18	9.53	2.67	24.51	6.62	16.11	8.93	8.06	A/A	G/G
br	MDA-MB-435	mut	3.65	10.66	8.79	8.18	nd	7.51	16.73	9.78	9.15	G/G	T/T
br	NCI/ADR-RES	mut	0.42	11.21	12.48	5.88	nd	9.19	17.75	9.78	9.78	A/G	T/T
br	T-47D	mut	0.55	7.63	8.51	2.78	22.83	5.51	8.25	4.94	6.6	A/G	G/G
CNS	SF-268	mut	2.63	11.11	9.71	5.69	nd	5.28	14.84	8.76	8.27	G/G	T/T
CNS	SF-295	mut	2.34	12.82	11.59	5.99	nd	9.87	16.9	10.73	9.27	G/G	G/T
CNS	SF-539	inc	2.63	9.48	8.08	3.03	27.33	6.7	15.23	8.52	7.46	A/A	G/G
CNS	SNB-19	mut	2.37	11.83	10.58	4.1	25.08	8.79	11.97	9.3	8.25	A/G	G/G
CNS	SNB-75	mut	2.64	11.64	10.24	4.73	nd	9.34	15.77	9.48	7.34	A/G	T/T
CNS	U251	mut	0.33	10.45	12.07	5.98	nd	8.52	15.86	9.52	8.99	A/G	G/G
co	COLO 205	mut	1.55	10.69	10.06	4.92	nd	7.39	14.45	8.14	8.2	A/G	T/T
co	HCC-2998	mut	0.27	11.03	12.92	4.55	19.9	9.82	17.34	10.62	9.15	A/G	T/T
co	HCT-116	wt	0.05	7.79	12.1	2.03	15.73	6.63	10.15	7.56	7.82	A/A	G/G
co	HCT-15	inc	0.07	9.13	13.06	3.62	21.02	7.56	11.97	7.35	8.93	A/G	G/T
co	HT29	mut	1.67	9.16	8.42	4.31	nd	6.55	16.06	8.67	6.9	G/G	T/T
co	KM12	mut	0.12	10.1	13.15	5.79	nd	8.4	16.54	10.73	8.17	G/G	G/T
co	SW-620	mut	2.34	11.84	10.61	10.03	nd	8.82	14.04	9.03	9.25	G/G	G/T
lk	CCRF-CEM	mut	0.27	8.16	10.06	7.71	12.92	6.41	15.19	7.97	8.63	A/G	T/T
lk	HL-60 (TB)	mut	2.25	10.58	9.41	9.47	nd	7.1	14.61	9.77	8.86	A/G	G/T
lk	K-562	mut	5.03	10.7	8.37	2.85	17.52	8.12	17.7	10.23	7.81	A/A	G/G
lk	MOLT-4	inc	0.30	7.79	9.52	8.53	13.64	5.73	12.17	5.72	7.76	A/G	T/T
lk	RPMI-8226	mut	3.07	9.67	8.06	2.96	22.76	6.25	9.14	7.95	5.28	A/A	G/T
lk	SR	wt	0.29	9.91	11.68	2.81	24.16	8.2	8.01	7.89	11.74	A/G	T/T
mel	LOX IMVI	wt	0.13	10.81	13.71	3.84	22.09	10.68	11.55	12.35	10.61	G/G	T/T
mel	M14	mut	3.95	12.38	10.4	5.91	nd	9.98	14.35	9.74	9.54	G/G	T/T
mel	MALME-3M	wt	1.08	10.74	10.64	2.58	20.59	9.08	9.25	8.51	9.3	G/G	G/G
mel	SK-MEL-2	mut	0.14	9.31	12.11	5.57	nd	8.91	15.85	11.08	9.27	G/G	G/G
mel	SK-MEL-28	mut	7.48	13.71	10.8	6.66	nd	9.99	12.51	12.22	9.12	G/G	T/T
mel	SK-MEL-5	wt	0.23	9.51	11.62	5.7	19.51	8.62	10.88	10.43	10.32	A/G	G/T
mel	UACC-257	wt	8.82	12.94	9.8	1.18	19.77	8.9	6.14	7.56	9.67	A/G	T/T
mel	UACC-62	wt	3.12	13.58	11.93	3.81	21.25	10.49	11	10.22	10.64	G/G	T/T
NSCLC	A549	wt	0.34	11.05	12.59	2.7	15.14	9.42	8.93	8.65	10.23	A/G	G/T
NSCLC	EKVX	inc	0.27	9.67	11.55	4.36	nd	7.47	16.04	10.19	9.36	G/G	T/T
NSCLC	HOP-62	mut	1.23	12.06	11.77	5.58	nd	10.18	14.23	12.12	9.36	A/G	T/T
NSCLC	HOP-92	mut	2.94	11.48	9.92	2.18	nd	8.7	12.8	8.54	7.76	G/G	G/G
NSCLC	NCI-H226	inc	0.37	11.03	12.45	1.21	16.05	8.3	6.87	8.29	10.12	A/A	G/G
NSCLC	NCI-H23	mut	1.48	10.48	9.92	4.21	17.82	8.68	9.07	8.22	8.66	A/G	G/G
NSCLC	NCI-H322M	mut	1.24	11.51	11.2	4.28	20.08	8.5	10.01	7.1	9.14	G/G	T/T
NSCLC	NCI-H460	wt	0.11	8.65	11.81	4.75	18.39	7.97	9.8	8.15	10.46	A/G	G/T
NSCLC	NCI-H522	mut	0.96	9.43	9.49	5.03	21.49	8.85	11.91	11.69	8.21	A/G	G/G
ov	IGROV1	inc	0.03	9.23	14.25	3.79	16.14	9.04	10.14	9.64	9	G/G	T/T
ov	OVCAR-3	mut	5.95	12.63	10.06	7.34	nd	9.92	16.23	11.28	8.37	G/G	T/T
ov	OVCAR-4	inc	4.58	12.06	9.87	7.32	nd	9.49	13.53	11.63	8.36	G/G	T/T
ov	OVCAR-5	inc	0.08	8.44	12.02	4.63	nd	8.04	16.91	9.96	8.49	A/G	T/T
ov	OVCAR-8	mut	0.18	10.41	12.92	5.35	nd	9.91	15.97	11.97	9.39	A/G	T/T
ov	SK-OV-3	mut	2.61	10.98	9.6	4.61	nd	8.69	14.81	10.6	7.41	G/G	G/T
pr	DU-145	mut	2.25	11.63	10.46	5.61	nd	9.99	17.39	10.87	9.58	G/G	T/T
pr	PC-3	mut	4.36	11.72	9.6	5.49	24.57	9.28	17.38	11.11	8.25	A/G	T/T
re	786-O	inc	2.98	12.94	11.37	4.22	nd	10.34	18.1	12.42	8.86	A/A	T/T
re	A498	wt	0.27	10.21	12.1	3.36	16.94	10.48	9.76	12.12	8.64	A/G	T/T
re	ACHN	wt	0.62	10.59	11.29	2.22	19.57	10	9.46	10.25	9.28	G/G	T/T
re	CAKI-1	wt	0.34	7.43	9	0.93	17.75	7.12	8.38	9.46	7.89	G/G	T/T
re	RXF-393	mut	0.66	11.32	11.92	5.16	nd	10.48	16.68	14.01	8.06	G/G	G/T
re	SN12C	mut	0.47	9.34	10.44	7.79	nd	8.35	16.67	10.3	7.29	G/G	G/G
re	TK-10	mut	0.08	9.61	13.17	4.86	20.96	10.24	13.04	10.76	8.51	A/G	G/G
re	UO-31	wt	0.94	11.84	11.92	0.88	19.29	9.81	7.14	8.29	8.14	G/G	G/G

br-breast; co-colorectal; lk-leukemia/lymphoma; mel-melanoma; ov-ovary; pr-prostate; re-renal; nd- not detected

Table 2.10 Breast cancer cell lines.

#	Cell line	*TP53*	deltaCT		*HDMX-S/FL* ratio
			HDMX-FL	*HDMX-S*	
1	BT20	mut	11.68	12.15	0.72
2	BT474	mut	12.24	11.86	1.31
3	BT549	mut	11.55	9.80	3.38
4	CAMA-1	mut	6.20	9.15	0.13
5	DU4475	wt	8.87	10.26	0.38
6	EVSA-T	mut	7.30	6.29	2.01
7	HCC1937	mut	12.09	11.25	1.79
8	Hs578T	mut	11.25	11.57	0.80
9	MCF-7	wt	8.81	13.10	0.05
10	MDA-MB-134VI	mut	9.21	10.53	0.40
11	MDA-MB-157	mut	12.82	11.26	2.95
12	MDA-MB-175VII	wt	10.74	14.60	0.07
13	MDA-MB-231	mut	9.94	10.78	0.56
14	MDA-MB-330	mut	9.66	8.99	1.59
15	MDA-MB-361	mut	13.51	13.11	1.32
16	MDA-MB-415	mut	11.50	10.91	1.51
17	MDA-MB-436	mut	11.93	10.74	2.27
18	MDA-MB-453	mut	7.49	11.15	0.08
19	MDA-MB-468	mut	11.01	13.98	0.13
20	MPE600	wt	9.97	14.72	0.04
21	B: OCUB-F	mut	7.65	11.01	0.10
22	SK-BR-3	mut	11.73	12.57	0.56
23	SK-BR-5	mut	13.25	12.07	2.27
24	SK-BR-7	wt	10.63	14.37	0.08
25	SUM44PE	mut	10.51	12.76	0.21
26	SUM52PE	mut	12.74	11.11	3.11
27	SUM149PT	mut	10.96	10.47	1.40
28	SUM159PT	mut	10.60	12.68	0.24
29	SUM185PE	mut	11.18	12.84	0.32
30	SUM190PT	mut	13.05	15.31	0.21
31	SUM1315M02	mut	12.20	13.64	0.37
32	T47D	mut	8.17	10.78	0.16
33	UACC-812	wt	9.30	10.29	0.50
34	UACC-893	mut	11.98	11.74	1.18
35	ZR75-1	wt	11.35	10.79	1.47
36	ZR75-30	wt	8.32	16.16	0.00
wt- wild type; mut-mutant					

2.3.3 Cancer cell lines grown in the cell culture.

Table 2.11 Cell lines.

CELL LINE	0rigin	FOXO3 rs2802292	*FOXO3* deltaCT
501	melanoma	GT	8.33
1205 Lu	melanoma	TT	9.88
Colo 783	melanoma	TT	8.00
Colo 800	melanoma	GT	8.77
Colo 853	melanoma	TT	9.41
IGR 37	melanoma	TT	10.70
IGR 39	melanoma	TT	9.88
LND1	melanoma	TT	13.32
LOXIMVI	melanoma	TT	9.68
M14	melanoma	TT	10.10
MALME 3M	melanoma	GG	7.50
MDA MB 435	melanoma	TT	7.96
Me235	melanoma	GT	8.92
Me248.3	melanoma	GT	7.03
Me260	melanoma	TT	9.42
Me300	melanoma	GG	10.38
MM0117	melanoma	TT	8.95
MM031	melanoma	TT	8.62
SK MEL 14	melanoma	TT	9.34
SK MEL 17	melanoma	TT	8.07
SK MEL 19	melanoma	TT	7.05
SK MEL 2	melanoma	GG	7.34
SK MEL 21	melanoma	GG	8.50
SK MEL 23	melanoma	TT	9.48
SK MEL 26	melanoma	GT	9.03
SK MEL 28	melanoma	TT	8.20
SK MEL 37	melanoma	GT	8.53
SK MEL 5	melanoma	GT	9.18
SK MEL 7	melanoma	GT	9.56
T135 3A	melanoma	GT	6.37
T333A	melanoma	GT	7.81
UACC 257	melanoma	TT	8.90
UACC 62	melanoma	TT	9.66
WM115	melanoma	TT	9.29
WM1789	melanoma	GG	9.50
WM278	melanoma	TT	5.82
MCF7	breast cancer	GT	
ZR75-1	breast cancer		
U2OS	osteosarcoma		

2.4 Methods

2.4.1 Cell culture

Most cell lines listed in Table 2.11 were maintained in RPMI1640 (GIBCO, UK), although the WM1789 cell line was maintained in 80% (v/v) MCDM153 (Sigma, UK) and 20% (v/v) L-15 (Sigma, UK) supplemented with 5µg/ml insulin (Sigma, UK). All media were supplemented with 10% (v/v) foetal bovine serum (PAA Laboratories), 100µg/ml penicillin G and 100mg/ml streptomycin (GIBCO, UK). Cells were grown at 37°C in a humidified atmosphere of 5% CO_2, and cells in the exponential growth phase used for all analyses. For Nutlin-3 treatment, cells were grown in standard growth medium supplemented with penicillin and streptomycin to a confluency of 70-80%. Nutlin-3 diluted in DMSO was added to the cells to appropriate concentrations and dishes swirled immediately to equally distribute the drug. Cells were harvested after 6 hours for RNA analysis.

2.4.2 Plasmid preparation

The oligonucleotides with appropriate restriction enzyme sequence overhangs for each allele of the appropriate SNP were annealed by mixing 5µl of each oligonucleotide, re-suspended in water to a concentration of 1µg/µl, with 10µl of 2x anneal buffer and consequent incubation at 95°C, 65°C, 37°C and RT, for 10 minutes for each temperature step. The firefly luciferase vector pGL3-TK-Promoter (Promega) was linearised with the BglII restriction enzyme using 1µg plasmid DNA, 2.5µl 10X NEBuffer 3 (New England BioLabs, Cat. No. B7003S), 1µl BglII (New England BioLabs, Cat. No. R0144), and 16.5µl ddH2O for 2 hours at 37°C. The reaction was subsequently run on a 1% acrylamide gel. The fragment corresponding to the vector was excised and the DNA extracted using

a QIAquick Gel Extraction Kit (Qiagen, Cat No 28704) according to the manufacturer's instructions. The linearised plasmid was then re-circularised for 2-3 hours at RT in the presence of annealed allele-specific oligonucleotides (Table 2.4) at different mass ratios using 1U T4 DNA ligase (Invitrogen, Cat No 15224-041), 4 μ l 5X Ligase Reaction Buffer (Invitrogen, Cat No 15224-041) and distilled water adjusted to the final volume of 20µl. The circularised vector was transformed into chemically competent *E. coli* cells and incubated on a selective LB agar plate containing 50µg/ml ampicillin for O/N incubation. Colonies carrying the plasmid were selected and grown in 4ml of LB medium containing 50 μ g/ml ampicillin O/N at 37°C. After incubation, 2ml of the LB medium was used to isolate plasmid DNA with a QIAprep Spin Miniprep Kit (Invitrogen, Cat. No. 27106) according to the manufacturer's instructions, and all constructs subsequently verified by sequencing (Geneservice, Oxford, UK). The cells carrying the plasmid were grown in 400ml LB medium supplemented with ampicillin, and the plasmids purified using Qiagen Plasmid Maxi Kit (Qiagen, Cat No 12163) according to the manufacturer's instructions.

2.4.3 Cell transfection assays

2.4.3.1 siRNA transfections

On-Target Smart Pool siRNA for GATA3 were purchased from Dharmacon Inc. (Lafayette, USA). Transfections were performed using Dharma*FECT* 1 reagent (Cat. No. T-2001-02) as per the manufacturer's instructions. Cells were plated in 6-well culture plates the day before transfection at densities resulting in 70% confluency on the day of transfection. The siRNA for GATA3 was used at

a concentration of 80nM. Cells were harvested 24 h after transfection for RNA analysis, and after 48 h for protein analysis.

2.4.3.2 Transient plasmid transfections

Cells were grown in monolayers until they reached 50-80% confluency in complete growth medium without antibiotics. Fugene-6 transfection reagent (Promega, Cat. No. E2692) and the plasmid vector were diluted in Opti-MEM I Medium (Invitrogen, Cat. No. 31985), without serum and antibiotics, at a 6:1 ratio (i.e. 6µl Fugene-6 reagent per 1µg of plasmid DNA), the reaction then mixed and incubated for 15 minutes at RT. The transfection reagent-DNA complexes were added to the cells and the plates swirled to ensure an even distribution over the entire plate surface. The cells were then harvested after 24 or 48 hours.

2.4.4 Luciferase bioluminescence detection

Luciferase expression in plasmid-transfected cells was assayed using the Luciferase Assay System (Promega, USA, Cat. No. E1500) as per the manufacturer's instructions. In brief, 24 to 30 hours post luciferase plasmid transfection, growth medium was removed from cells cultured in either 24- or 12-well formats and the cells rinsed with ice-cold 1X PBS. Cells were lysed in either 100µl or 200µl of 1X Passive Lysis Buffer (Promega, USA; Cat. No. E1941), depending on the plate format and incubated for 15-20 minutes on a rotating table at RT. Subsequently, 20µl of the cell lysate was mixed with 100µl of the Luciferase Assay Reagent in a 96-well plate and the luciferase luminescent signal measured using the Glomax Multi Detection System (Promega).

2.4.5 DNA extraction

Genomic DNA from cultured cells, harvested using trypsin at sub-confluency, was extracted using a DNeasy Blood & Tissue Kit (QIAGEN), according to the manufacturer's instructions. In brief, 200µl cultured cells re-suspendend in PBS was lysed with 20µl proteinase K (600mAU/ml) and 4µl RNAse A (100mg/ml). Buffering conditions were adjusted by adding the provided buffers, and DNA selectively bound to the spin column membrane and eluted in water. The concentration was determined by spectrophotometry using a Nanodrop spectrophotometer (Thermo Scientific, UK).

2.4.6 RNA extraction and cDNA synthesis

Total RNA from cultured cells was extracted using a RNeasy Kit (QIAGEN). The RNAs for the NCI60 cell line panel were obtained from the National Cancer Institute (NCI)/NIH Developmental Therapeutics Program. Following RNA quantification using a Nanodrop spectrophotometer, 1µg of RNA was subjected to reverse transcription using oligo dT and random hexamers (Bio Line), and SSIII reverse transcriptase (Life Technologies) according to the manufacturer's instructions.

RNA of breast cancer and osteosarcoma cell panels and lines was isolated[1] using the SV Total RNA Isolation System (Promega) according to the manufacturer's protocol, followed by cDNA synthesis following standard protocols.

[1] Krystiaan Lenos, Leiden University, the Netherlands

The RNA of breast cancer patients was extracted[1] from primary tumours using TRIzol reagent (Invitrogen) from freshly frozen tumour material, followed by cDNA synthesis following standard protocols.

2.4.7 Genotyping

Genotyping of all cell lines and breast cancer[1] cohort samples was performed by PCR amplification of genomic DNA, and subsequent allelic discrimination using appropriate SNP genotyping assays (Table 2.3) as previously described (Vazquez, Grochola *et al.*, 2010). In brief, the allelic discrimination was performed as a multiplexed reaction in a 96-well format, using two primer/probe pairs in each reaction with a unique pair of fluorescent dye detectors to allow genotyping of the two possible variants at the SNP site in a target template sequence. Each well contained 2µl of DNA (conc. 10ng/µl), 12.5 µL of TaqMan Genotyping PCR Master Mix (Applied Biosystems, Part Nr. 4371357), 0.625 µL of the genotyping assay, and 9.875 µL distilled water. Following PCR, fluorescence was measured with an AB 7500 Real-Time PCR System (Applied Biosystems) and genotype clusters scored using Sequence Detection Software (version 1.3; Applied Biosystems).

The RT-PCR cycling conditions were as follows:

1) 10 min at 95°C
2) 40X :

   15 sec at 92°C

   1 min at 60°C

[1] Elen Møller, Oslo University Hospital, Norway

The Golden Gate platform[1] (Illumina Inc., San Diego, CA, USA) was utilised in order to determine the genotypes of 672 SNPs in a melanoma cohort in a high accuracy, medium-throughput, 96-well plate assay. In brief, a multiplexed PCR reaction, which generates allele- and SNP-specific PCR products that are then hybridised to beads, was performed. Subsequently, the fluorescence on each bead was quantified resulting in a signal associated with a particular genotype (AA/AB/BB) at each locus, and the genotype determined.

2.4.8 Polymerase chain reaction (qRT-PCR and semiQ-PCR)

2.4.8.1 Gene expression qRT-PCR.

Quantitative real-time PCR (qRT-PCR) was performed in triplicate duplex reactions as a relative quantification of synthesised cDNA using TaqMan gene expression assays on the ABI 7500 Real-Time PCR System (Applied Biosystems). For the reaction, 2-8µl of 5-fold diluted cDNA was mixed with 10µl 2X TaqMan Gene Expression Master Mix, 1µl 20X FAM TaqMan Gene Expression Assays (Table 2.3), 1 µl VIC GAPDH primer delimited TaqMan Gene Expression Assay (Table 2.3) and ddH_2O added to a final volume of 20µl when appropriate. The online real-time PCR Miner version 3.0 (Department of Biological Sciences & Program in Neuroscience, Stanford, California) (Zhao and Fernald, 2005) was used to analyse qRT-PCR raw fluorescence data to calculate cycle threshold (CT) for each sample and primer/probe set. The CT values of the gene of interest were normalised to housekeeping gene GAPDH measured in the same reaction with VIC labelled TaqMan probe (deltaCT). Relative gene expression was

[1] Lukasz F Grochola, University of Oxford

calculated using a 2(-deltadelta(CT)) method, where deltadelta(CT)= deltaCT(untreated/control)− deltaCT(treated). The relative HDMX-S/FL ratio in cell lines where the qRT-PCR was used to measure HDMX-FL and HDMX-S expression (Table 2.9 and 2.10) was calculated using the same method where deltadelta(CT)= deltaCT(HDMX-S)− deltaCT(HDMX-FL).

The qRT-PCR amplification of breast cancer patient cDNA was performed[1] using the Applied Biosystem 7900HT detector system. A Human Breast Total RNA (Ambion) was used as a reference to generate a standard curve. Sequence Detection Systems (SDS) Software v2.3 was used to calculate the amount of transcript expressed for each sample from the standard curve.

The qRT-PCR cycling conditions were as follows:

1) 2 min at 50°C
2) 10 min at 95°C
3) 45X :

   15 sec at 95°C

   1 min at 60°C

Measurements of *HDM2* transcript levels for the NCI60 panel (Table 3.6) were performed[2] by qRT-PCR using a commercially available RoboGene®-*HDM2* cDNA quantification module, with an ABI PRISM 7000 Sequence Detection System. *HDM2* measurements were normalised to GAPDH transcript levels and calculated as relative transcript levels in zeptomole per attomole GAPDH mRNA .

[1] Elen Møller, Oslo University Hospital, Norway
[2] AJ Roboscreen GmbH, Leipzig, Germany

HDMX-FL and *HDMX-S* transcript levels in STS samples were measured[1] by quantitative real-time RT-PCR as described (Bartel, Schulz *et al.*, 2005). Briefly, the reactions were carried out on a Rotor-Gene 3000 (Corbett Research, Sydney, Australia), with a common forward primer for both FL-HDMX and HDMX-Sand reverse primers specifically designed for amplification of either HDMX-FL or HDMX-S (Table 2.4). Each reaction included 1/10 of the cDNA reaction, 10 µL of 2X Quantitect SYBR Green Master Mix (Qiagen) and 20 pmol of the respective primers in a total volume of 20 µL. The PCR consisted of 50 cycles with 30 sec of denaturation at 95 °C, 30 sec of primer annealing at 58 °C, and synthesis at 72 °C for 30 sec. The HDMX-FL and HDMX-S levels were normalised against GAPDH expression levels.

2.4.8.2 Allele-specific qRT-PCR

The method was performed on input chromatin and immunoprecipitated (IP) chromatin with the appropriate antibody (Table 2.1). The input and IP chromatin were purified utilising the NucAway Spin Columns (Ambion, Cat. No. AM10070). Subsequently, a duplex real-time PCR reaction was performed in a 96-well format, with the appropriate SNP genotyping assay (Table 2.3). In the same duplex qRT-PCR reaction, using input chromatin, a standard curve of the differences in fluorescence for both alleles over varying concentrations was generated and utilised to calculate the fold-difference in fluorescence for both alleles found in the IP chromatin. Each well contained 2µl of IP chromatin, 12.5µL of TaqMan Genotyping PCR Master Mix (Applied Biosystems, Part Nr.

[1] Peter Würl, the Diakonie-Hospital Halle and Helge Taubert, University Clinic of Urology, Erlangen, Germany

4371357), 0.625µL of the genotyping assay, and 9.875µL distilled water. The AB 7500 Real-Time PCR System and Sequence Detection Software (version 1.3; Applied Biosystems) were used.

The RT-PCR cycling conditions were as follows:

1) 2 min at 50°C
2) 10 min at 95°C
3) 45X :

   15 sec at 95°C

   1 min at 60°C

2.4.8.3 Semi-Quantitative PCR

Semi-Quantitative PCR was performed[1] according to standard protocols; for detection of both *HDMX-FL* and *HDMX-S,* the *HDMX* ex3 and *HDMX* ex8 reverse primers were used (Table 2.4). For detection of *GAPDH*, the GAPDH and GAPDH reverse 5'- primers were used (Table 2.4). Band intensities were quantified using Odyssey 2.1 analysis software (LI-COR Biosciences, Lincoln, Nebraska USA).

2.4.9 Analysis of DNA-protein interactions

2.4.9.1 Electromobility Shift Assay (EMSA)

Nuclear extracts. Cells were grown in monolayers in a 15cm culture dish until they reached 70-80% confluency, and harvested by scraping in ice-cold PBS. The cells were spun down at 1000rpm for 5min using a bench-top centrifuge, washed in ice-cold PBS and pelleted again. The pellet was re-

[1] Krystiaan Lenos, Leiden University, the Netherlands

suspended in 1 volume of ice-cold Buffer 2 and incubated on ice for 10min. After the cells had swollen, a 0.1% final concentration of NP-40 was added, the cells incubated for a further 5 minutes then resolved at 4000rpm for 4 minutes using a bench-top centrifuge. Subsequently 1x the original volume of buffer 3 was added to the pellet, incubated on ice for 10 minutes and resolved at 14000rpm for 20min using a refrigerated bench-top centrifuge. Supernatant containing the nuclear extracts was stored in aliquots at -80°C.

Preparation of ^{32}P-labelled probe. The sense and antisense oligonucleotides described in Table 2.4 were annealed by mixing 5µl of each oligonucleotide, re-suspension in water to the concentration of 1µg/µl, mixing with 10µl of 2x anneal buffer and consecutive incubation at 95°C, 65°C, 37°C and RT, for 10 minutes for each temperature step. Both sense and antisense strand oligonucleotides had 5'ctaga and 3't overhangs. Double stranded oligonucleotides were labelled with ^{32}P-dCTP, to fill in the overhanging 5' ends and purified on a non-denaturing polyacrylamide TBE gel. In brief, 1µl of the annealed oligonucleotide mix was incubated at RT for 30-60 minutes with 2.5µl Buffer 2 (New England Biolabs, Cat. No. B7002S), 1µl 0.5mM dGTP, 1µl 0.5mM dATP and 1µl 0.5mM dTTP (Fisher Scientific, Cat. No BP2564-1), 0.5µl DNA Polymerase I Large Klenow Fragment (New England Biolabs, Cat. No. M0210L), 17µl ddH2O and 1µl of α-^{32}P-radioactively labelled dCTP (Perkin Elmer, Cat No. NEG513H250UC). For purification, 3µl of a 10X loading buffer was added to the EMSA probe and the mix run on a 10% non-denaturing acrylamide gel for 2 hours at 150V in 0.5X TBE buffer. Subsequently, the gel area containing the radiolabelled probe was identified on autoradiography film (GE Healthcare, UK)

by placing directly on the gel for 10-20 seconds. The film was subsequently developed and the gel area corresponding to the hot probe excised with a scalpel. The radiolabelled probe was eluted from the gel slice by incubation in 100µl of 40mM KCl O/N at 37°C.

EMSA. The radioactivity of the labelled probes was counted using 1µl of the probe suspended in 1ml liquid scintillation cocktail (Fisher Scientific; Cat No. SC/6000/17) with a 1450 Microbeta Liquid Scintillation Counter (Perkin Elmer). Binding reactions were pre-incubated at room temperature for 10 min in 10x black buffer containing 3-5µl of nuclear extract, 1µg of poly dI-dC (Fisher Scientific, UK), 1µl of competitor oligonucleotides (when indicated) and water up to a volume of 18µl. For the super-shift reaction, 0.6µg of appropriate antibody (Table 2.1) was added to the binding reaction prior to addition of binding buffer and polydI-dC, and incubated at RT for up to 10 minutes. Subsequently, 2µl of radiolabelled probe at 30,000-40,000 cpm/µl was added to the binding reaction and incubated for a further 20 min at RT. Next, 2µl of 10X DNA loading buffer was added, and the reaction loaded onto a 6% acrylamide gel and run at 150V in 0.5X TBE buffer for 2-3 hours at RT. The gel was dried at 80°C for 45-60 minutes on a gel-drier on nitrocellulose filter paper and exposed to radiography film for the appropriate time.

2.4.9.2 Chromatin Immunoprecipitation (ChIP)

Preparation of cell lysates. MCF7 cells were grown in monolayers in 20ml of appropriate medium until 80-90% confluency in a 15cm dish. Crosslinking was performed for 10 min using 37% formaldehyde (Sigma, Cat No. F8775) to a final concentration of 1%. The unreacted formaldehyde was

quenched with 2ml 10X Glycine. The cells were washed twice with ice-cold PBS and scraped from each dish in 2ml PBS containing protease inhibitors (PI), centrifuged at 4°C in a bench-top centrifuge, and re-suspended in SDS lysis buffer containing PI. 400µl of the lysate was aliquoted per tube.

Chromatin shearing. Sonication was performed in chilled Bioruptor with 20 cycles of pulses [30/30 sec on/off] at the maximum amplitude. The chromatin shearing conditions were determined empirically to acquire the cross-linked DNA of 200-1000 base pairs in length, as confirmed on an agarose gel where the maximum signal intensity was observed at 400-500 bp.

Chromatin immunoprecipitation. Chromatin immunoprecipitation was performed using the EZ-ChIP kit (Millipore, Cat. No. 17-371) and protein G Dynabeads (Invitrogen) according to the manufacturer's instructions. In brief, 30µl of protein G Dynabeads were added to 100µl of cell lysate diluted in 900µl ChIP dilution buffer containing protease inhibitors, to pre-clear the sample from non-specific proteins or DNA, and incubated at 4°C for 1h with rotation. Subsequently, after removal of the Dynabeads on a magnetic rack, 10µl of the supernatant was removed to serve as Input and stored at -20°C until the reverse cross-linking of the protein/DNA complexes. To the remaining supernatant, 5µg of appropriate antibody (Table 2.1) was added and incubated O/N at 4°C with rotation. Next, 35µl of Protein G Dynabeads was added to each immunoprecipitate (IP) and incubated for 1 hour at 4°C with rotation. The Protein G Dynabeads-antibody/chromatin complex was consecutively washed in low, high and LiCl salt immune complex wash buffers, and twice in TE buffer. Next, each IP and the Input sample were eluted in the appropriate buffers. The

eluates were subjected to reverse cross-linking, the DNA subsequently purified using a PCR Purification Kit (Qiagen) according to the manufacturer's instructions and eluted in 25µl water.

PCR. 1µl of purified genomic DNA was subjected to PCR using Kapa2G Fast polymerase (Kapa Biosystems) and *FOXO3* rs2802292 ChIP primers specified in Table 2.4 according to the manufacturer's instructions.

The PCR cycling conditions were as follows:

1) 3 min at 95°C
2) 35X :

   15 sec at 95°C

   15 sec at 54°C

   5 sec at 72°C

The products of the PCR reactions were resolved on a 1.5% agarose gel and visualised a ChemiDoc system.

2.4.10 Protein analysis by Western blotting

Cells were lysed using modified RIPA buffer containing 1x protease inhibitor cocktail (Roche), incubated at 4°C with rotation and cleared by centrifugation at 14000rpm at 4°C. Protein concentration was determined using a BSA Protein Kit (Thermo) according to the manufacturer's instructions. The absorbance was measured in duplicate for each sample at 595nm using a microplate reader (TECAN, sunrise microplate reader) and compared against a BSA standard curve. Protein lysates, at a concentration between 20-50µl of total protein, were mixed with 5x LDS loading buffer (Invitrogen), DTT at the final concentration of 20mM and an appropriate volume of water, and were heated at

70°C for 10 minutes. Subsequently, samples were subjected to SDS-PAGE on 4-12% Bis-Tris gels (Invitrogen) at 200V for 1h in MOPS buffer and transferred to a methanol-activated PVDF membrane (Hybond-P, Amersham). Membranes were blocked in 5% BSA (Sigma) in TBS 0.1% Tween (TBST) and probed with appropriate primary antibodies (Table 2.1) diluted in 5% BSA in TBS 0.1% Tween, and incubated with agitation either for 1h at RT or O/N at 4°C . Subsequently membranes were washed 3 times for 15 minutes in TBST and incubated with appropriate HRP-conjugated secondary antibodies (Table 2.2) diluted in 5% milk-TBST for 1h at RT, before washing 3 times for 15 minutes with TBST. The results were visualised by ECL detection (Enhanced Chemical Luminescence; Amersham Pharmacia Biotech, GE Healthcare, UK) using X-ray films (Amersham Pharmacia Biotech). For re-probing with another primary antibody, the membranes were stripped using Millipore-strong stripping solution according to the manufacturer's instructions. In brief, the membrane was incubated in 1x stripping solution for 20 minutes at RT with agitation, and subsequently washed/re-blocked 3 times for 10 minutes in 5% BSA-TBST.

2.4.11 Data analyses

Statistical analyses. Survival analyses were performed using the Kaplan Meier analysis with log-rank test and the Cox's multivariate proportional hazards regression model with SPSS 20.0 and 21.0 software (SPSS Inc., Chicago, IL, USA; IBM, USA). The Shapiro-Wilk test was used to assess a normal distribution of the sample. The Kruskal-Wallis test, Mann-Whitney test and unpaired t-test were applied to determine the statistical significance in the differences between the means. Fisher's exact test was used to compare the

differences in frequency distributions. Correlation analysis was carried out using the Spearman-Rho and Pearson tests.

Statistical analyses of 672 SNPs[1]. KM metastasis-free survival, Cox multivariate regression for metastasis-free survival and KM overall survival for 672 SNPs and LASSO and RSF data mining techniques were performed by Emmanouela Repapi. Minor allele homozygotes represented by less than 10 patients were grouped with the heterozygous patients for the log-rank test. LASSO and RSF algorithms were applied 100 times on sub-samples of the data (75% of the sample without replacement). In LASSO, all the SNPs were treated as penalised variables and the known independent prognostic factors as un-penalised variables. The penalisation algorithm was applied with a parameter found after each optimisation step to find the optimum tinning parameter that maximises the likelihood for the specific sub-sample based on cross validation, thereafter counts of informative predictors (with a co-efficient higher than 0) for each SNP were determined. In RSF, the top 30 variables were selected each time based on their variable importance and thereafter counts of relatively high importance were determined for each SNP.

Hap Map and 1000 genomes. Haplotype analysis was performed using publicly available data from the Hap Map Project (Hap Map Phase I, II and III, http://hapmap.ncbi.nlm.nih.gov/) (Consortium, 2003) and the 1000 Genomes Project Pilot 1 (http://www.broadinstitute.org/mpg/snap/) (Abecasis, Auton *et al.*, 2012). All SNPs in high LD [r2≥0.8; MAF≥0.2; CEU] with a tag-SNP were included in the analysis.

[1] Emmanouela Repapi, University of Oxford

Identification of functional elements in the human genome. The Encyclopedia of DNA Elements (ENCODE) project (http://genome.ucsc.edu/ENCODE/) (BirneyStamatoyannopoulos *et al.*, 2007) was used to access experimental data aiming to study chromatin accessibility, histone modification patterns and sequence-specific factors.

Transcription factor binding site analysis. Binding site analysis was performed using the computer algorithm ExPlain 3.0 and the Transfac 2009.3 database (Biobase; http://www.biobase-international.com/). A region of 25 base pairs up- and downstream of each SNP was included for each allelic variant in the analysis.

BioGPS. The publicly available microarray data available from: http://biogps.org (Wu, Macleod *et al.*, 2013) was used to determine the cancer cell line with high *GATA2* and *GATA3* gene expression levels.

Computer images. All autoradiographs and agarose gel images were scanned using an Epson perfection 1660 Photo scanner and Adobe Photoshop 8.0 software. Images were manipulated only as a whole for size, brightness and contrast. No signal was modified in relation to the whole image.

.

3 ALTERNATIVE SPLICING OF THE P53 INHIBITOR HDMX OFFERS A PROGNOSTIC BIOMARKER THAT IS SUPERIOR TO *TP53* MUTATION IN SARCOMAS

3.1 Introduction

3.2 Results

3.2.1 The HDMX-S/FL ratio in osteosarcoma

3.2.2 The HDMX-S/FL ratio in breast cancer and NCI60 cells

3.2.3 The HDMX-S/FL ratio and TP53 mutation as prognostic markers

3.3 Discussion

3.1 Introduction

Osteosarcoma is the most common primary bone malignancy in children and adolescents, occurring mostly in patients between 10 and 25 years of age and found in the rapid growth areas of the long bones (Raymond, Ayala *et al.*, 2002). The vast majority of osteosarcomas arise without a clear hereditary component, with the exception of a small subset including individuals with the Li-Fraumeni and Progeria syndromes. Overall long-term (5-year) survival for patients with non-metastatic osteosarcomas has increased from 10 to 65% over the past 20 years, due to improved surgical techniques and multidrug chemotherapy, but further improvement is needed (Lewis, Nooij *et al.*, 2007). Indeed, 25-50% of patients will relapse or metastasise, and the 5-year survival rate for metastatic osteosarcomas is only 10 to 20% (Buddingh, Anninga *et al.*, 2010; Gelderblom, Jinks *et al.*, 2011). It is clear that additional therapies are required in order to increase the survival of osteosarcoma patients.

In high-grade osteosarcoma, mutations in the *TP53* gene are found in only 20% of the tumours (Park, Jung *et al.*, 2004; Wunder, Gokgoz *et al.*, 2005; Yokoyama, Schneider-Stock *et al.*, 1998). However, the genomic region that encodes for a key negative regulator of p53, *HDM2* (Kawai, Wiederschain *et al.*, 2003; Meulmeester, Frenk *et al.*, 2003), was found to be amplified in 10-35% of osteosarcomas and these amplifications were shown to be mutually exclusive to *TP53* mutations (Ito, Barys *et al.*, 2011; Park, Jung *et al.*, 2004; Wunder, Gokgoz *et al.*, 2005; Yokoyama, Schneider-Stock *et al.*, 1998).

In many previous studies that were aimed at determining the importance of the inactivation of the p53 pathway during the progression of osteosarcoma,

only p53 mutational status was studied and the level of HDM2 protein expression was not included, resulting in the possible underestimation of the influence of p53 inactivation on prognosis. Moreover, the somatic mutation or alteration of other crucial effectors of p53 activity has also been under-studied in osteosarcoma. For example, the oncogene *HDMX* is a close homolog of *HDM2* and encodes a protein product that also clearly inhibits p53 activity (Marine and Jochemsen, 2005; Shvarts, Steegenga *et al.*, 1996). In several tumour types, overexpression and amplification of *HDMX* has been shown both in tumours (Danovi, Meulmeester *et al.*, 2004; Riemenschneider, Knobbe *et al.*, 2003) and tumour-derived cell lines and is primarily found in tumours that have retained wild-type p53 (Ramos, Stad *et al.*, 2001). Indeed, two tumour types that have a very low frequency of *TP53* gene mutation (retinoblastomas and Ewing sarcomas) have demonstrated elevated *HDMX* expression (Laurie, Donovan *et al.*, 2006; Pishas, Al-Ejeh *et al.*, 2011).

In sarcomas, amplification of the *HDMX* gene has been found in both soft tissue sarcomas (STS, 16 to 17%) and osteosarcomas (35%) (Bartel, Schulz *et al.*, 2005; Ito, Barys *et al.*, 2011). Bartel et al. demonstrated a significant association between *HDMX* amplification and poor prognosis after initial STS diagnosis (Bartel, Schulz *et al.*, 2005). Interestingly, they showed that the mRNA expression of an alternative splice variant of *HDMX*, *HDMX-S*, is up-regulated in 14% of STS, and that an increase in the ratio of the transcript levels of the splice variant over full-length (the *HDMX-S/FL* ratio) correlates with a higher tumour grade at diagnosis and decreased overall survival (Bartel, Schulz *et al.*, 2005). The *HDMX-S/FL* ratio was also found to be increased in high-grade

glioblastomas (Riemenschneider, Knobbe *et al.*, 2003) and papillary thyroid carcinomas (Prodosmo, Giglio *et al.*, 2008). The *HDMX-S* transcript results from the exclusion of exon 6 (Rallapalli, Strachan *et al.*, 2003), resulting in a truncated protein essentially consisting of the p53-binding domain which, in over-expression studies, was found to bind to and inhibit p53 more efficiently (Rallapalli, Strachan *et al.*, 2003). Although studies such as these suggest an oncogenic role for the HDMX-S protein, no conclusive evidence has been published to date to suggest that the protein is produced and active in cells (Lenos and Jochemsen, 2011). Indeed, previous work by our collaborator Aart Jochemsen suggests that an increase in the *HDMX-S/FL* ratio associates primarily with reduced levels of full-length HDMX protein (Lenos and Jochemsen, 2011).

In this chapter, further evidence regarding alterations in the *HDMX-S/FL* ratio in relation to p53 status and cancer progression is described. The results indicate that changes in the *HDMX-S/FL* ratio could serve as a more effective biomarker for p53 pathway attenuation in cancers than p53 gene mutation.

3.2 Results

3.2.1 The *HDMX-S/FL* ratio in osteosarcoma

To further explore the importance of the p53 pathway during the progression of osteosarcoma, the *HDMX-S/FL* ratio and its association with HDMX protein levels was initially analysed in 22 osteosarcoma cell lines. The levels of *HDMX-S* and *HDMX-FL* mRNA were determined in logarithmically growing cells for all 22 osteosarcoma cell lines and 1 osteoblast.

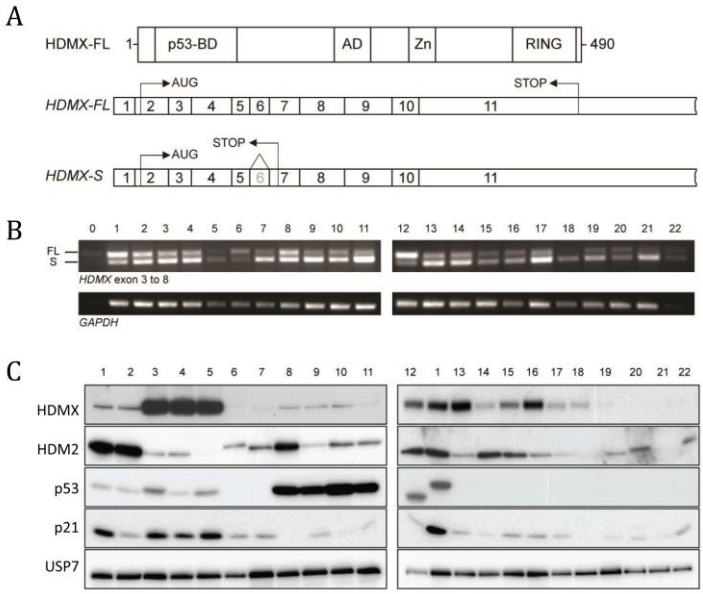


Figure 3.1 Analysis of *HDMX-S* and *HDMX-FL* in 22 osteosarcoma cell lines[1]**.**
A, schematic drawing of HDMX protein structure (upper), containing the p53 Binding Domain (p53-BD), Acidic Domain (AD), Zinc-finger (Zn) and RING Domain. Structure of *HDMX-FL* and *HDMX-S* mRNA is depicted below. Arrows indicate start and stop codons. Exon 6 is spliced out in *HDMX-S* resulting in 26 novel amino acids and a premature stop codon. **B,** 22 osteosarcoma cell lines and 1 osteoblast sample were examined for *HDMX-FL* and *HDMX-S* mRNA expression using primers for *HDMX* exon 3 (Fw) to exon 8 (Rev). *GAPDH* mRNA expression was examined as an internal control. **C**, protein levels were analysed with immunoblotting using the indicated antibodies. USP7 expression was analysed as a loading control. The lane numbers in (B) and (C) correspond to cell lines listed in Table 3.1.

Semi-quantitative PCR was performed using primers designed to amplify exons 3 to 8 (Figure 3.1A). The intensities of the bands for *HDMX-S* and *HDMX-FL* were quantified and normalized to GAPDH expression levels (Figure 3.1B), and the results are summarised in Table 3.1. The *HDMX-S/FL* ratios varied from 0.39 to 3.18 with a median of 1.5, a standard deviation of 0.7 and a normal distribution (Figure 3.2A). The protein levels of HDMX were also determined

[1] Krystiaan Lenos, Leiden University, the Netherlands

Table 3.1 Summary of p53 status, HDM2 and HDMX levels in 22 osteosarcoma cell lines[1].

#	name	Protein Levels			mRNA Levels			nutlin-3 response
		p53	HDM2	HDMX Rel. Quant.	*HDMX-S/FL*	Rel. Quant. *HDMX-FL*	Rel. Quant. *HDMX-S*	
0	Osteoblast	wt	n.a	n.a.	0.18	n.a.	n.a.	n.a.
1	U2OS	wt	+	1.89	0.71	0.8	0.57	+
2	KPD	wt	+	2.03	1.16	0.55	0.64	+
3	MHM	wt(high)	high	0.18	1.31	0.54	0.7	+
4	OSA/SJSA1	wt	high	0.22	1.4	0.55	0.77	+
5	L2792	wt	high	0.01	1.83	0.25	0.46	+
6	L2962	wt (low)	very low	0.29	0.61	0.58	0.36	+
7	OST	mt	low	0.24	2.31	0.48	1.1	-
8	HOS	mt(high)	low	0.84	1.27	0.75	0.95	-
9	HOS-143b	mt(high)	low	0.11	2.34	0.34	0.8	-
10	HOS-MNNG	mt(high)	low	0.51	1.77	0.33	0.59	-
11	IOR/OS15	mt(high)	low	0.3	2.63	0.4	1.04	-
12	HAL	mt	low	3.44	0.39	1.45	0.56	-
13	IOR/OS18	neg	+	0.93	1.56	0.7	1.09	-
14	MG-63	neg	low	3.58	1.46	0.85	1.24	-
15	ZK58	neg	low	1.6	1.51	0.41	0.62	-
16	HOS58	neg	+	0.45	1.56	0.84	1.31	-
17	IOR/OS9	neg	low	0.38	2.05	0.76	1.56	-
18	SaOS2	neg	low	0.24	2.78	0.39	1.09	-
19	L2531	neg	low	0.54	2.07	0.56	1.16	-
20	L2857	neg	low	0.74	1.31	0.48	0.62	-
21	L2826	neg	low	0	3.18	0.39	1.23	-
22	L2635	neg	low	0.65	1.32	1.5	1.97	-

from logarithmically growing cells (Figure 3.1C). The intensities of the band corresponding to HDMX were quantified and normalised to USP7 levels (Table 3.1). Interestingly, the *HDMX-S/FL* ratio significantly negatively correlated with the measured HDMX protein levels (p=0.004, Spearman's test, correlation co-efficient -0.583, Figure 3.2B). Specifically, the five cell lines with the highest *HDMX-S/FL* ratios had 9.5-fold less HDMX protein than the five cell lines with the lowest ratios (p= 0.0238 unpaired t-test, Figure 3.2C).

In order to explore the potential association of the *HDMX-S/FL* ratio with osteosarcoma progression and survival 51 high-grade osteosarcoma patients from Germany, Holland and Italy were studied (Table 3.2). The patient group

[1] Krystiaan Lenos, Leiden University, the Netherlands

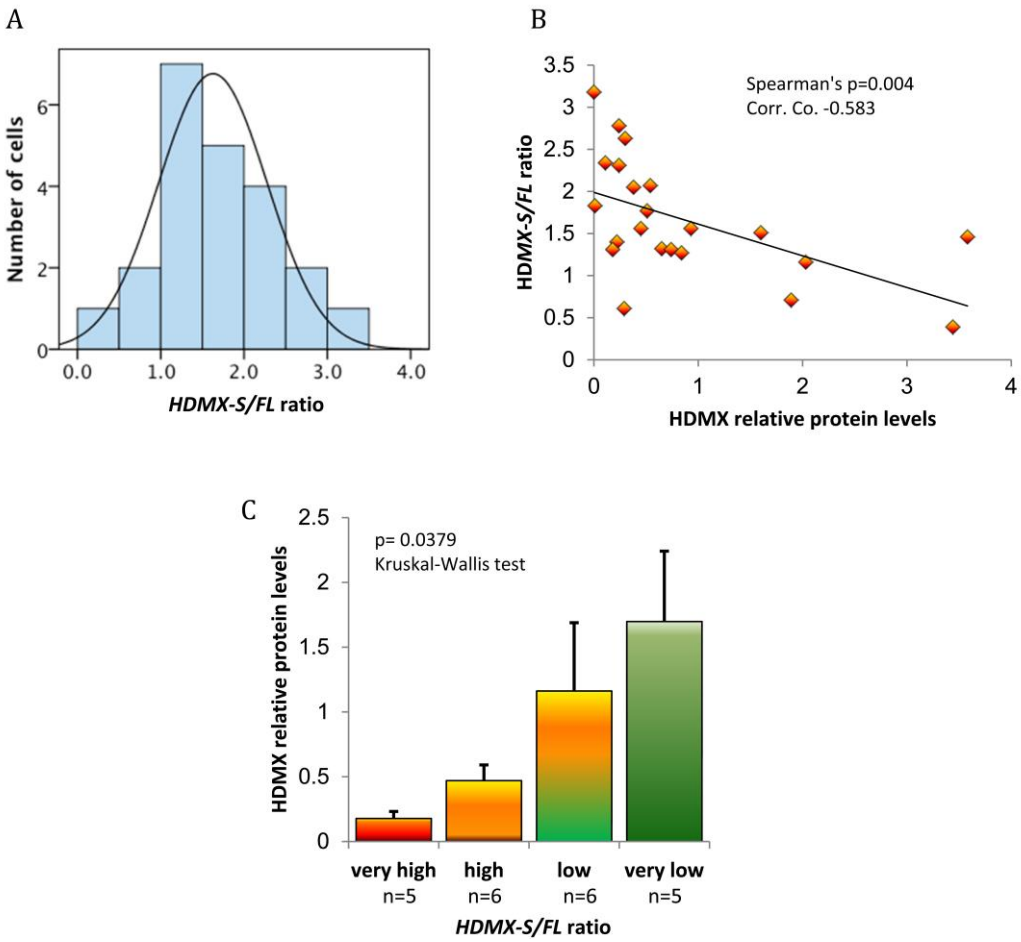


Figure 3.2 High *HDMX-S/FL* ratios in 22 osteosarcoma cell lines associate with lower HDMX protein levels.

A, column graph depicting the number of cells with a given *HDMX-S/FL* ratio, whereby a normal distribution is observed. **B**, graph depicting the negative correlation of the *HDMX-S/FL* ratio on the y-axis with HDMX protein levels on the x-axis. **C**, column graph depicting the average HDMX protein levels for the groups of cell lines with varying ratios of *HDMX-S/FL*, whereby cells with higher ratios contain less HDMX protein. Error bars depict standard errors.

consisted of 32 males and 19 females with an average age of diagnosis of 17.5 years, ranging from 3 to 58 years. The levels of *HDMX-S* and *HDMX-FL* were determined in biopsies that were taken before pre-operative chemotherapy. The level of each transcript was determined in 49 of the samples (Figure 3.3A, Table 3.3), and the intensities of the bands for *HDMX-S* and *HDMX-FL* were

Table 3.2 Clinicopathological data of 51 osteosarcoma patients[1].

Patient ID	Age	Sex	Histological subtype	Tumour Location	Huvos	ToM	ToM (2nd)	ToD	ToF	Origin
L3446	174	M	Giant cell rich	left distal femur	4	0	16	27	27	WWU
L3447	162	M	Osteoblastic	left proximal humerus	2	16		21	21	WWU
L3448	170	M	Osteoblastic	left distal femur	3	0	22		46	WWU
L3449	133	F	Fibroblastic	left distal femur	1	10			28	WWU
L3431	81	F	Osteoblastic	humerus	1	5		11	11	WWU
L3432	144	M	Chondroblastic	tibia	2	30			37	WWU
L3433	204	F	Osteoblastic	left femur	1	9		33	33	WWU
L3434	181	M	Sclerosing	right proximal tibia	1	25			25	WWU
L3435	200	M	Osteoblastic	right proximal femur	1	0	13	30	30	WWU
L3436	205	M	Chondroblastic	left distal femur	3	9		35	35	WWU
L3437	183	M	Osteoblastic	distal femur	2	0	21	27	27	WWU
L3438	220	M	Osteoblastic	right proximal tibia	4	0	18		26	WWU
L3439	385	M	Chondromyxoid fibroma like	right humerus	1	10		18	18	WWU
L3440	264	M	Osteoblastic	femur	1	10			36	IOR
L3441	228	M	Osteoblastic	femur	3	24			123	IOR
L3442	144	F	Osteoblastic	femur	3	44		110	110	IOR
L3443	204	F	Fibroblastic	humerus	2				63	IOR
L3444	264	M	Fibroblastic	humerus	1				60	IOR
L3445	696	F	Telangiectatic	tibia					60	IOR
L1386	101	M	Osteoblastic	diaphysis femur left	1				105	LUMC
L2295	487	F	Anaplastic	proximal femur left	2				97	LUMC
L2611	242	F	Osteoblastic	distal femur right	3				91	LUMC
L2281	212	M	Osteoblastic	proximal fibula left	2	36		64	64	LUMC
L2298	244	F	Anaplastic	distal femur right	3				94	LUMC
L2300	217	M	Osteoblastic	proximal fibula right	3				87	LUMC
L2297	137	F	Osteoblastic	proximal tibia left	2				77	LUMC
L2292	136	M	Osteoblastic	proximal tibia left	3				78	LUMC
L2613	181	M	Osteoblastic	proximal tibia right	3				40	LUMC
L2614	165	M	Osteoblastic	distal femur left	2	0		29	29	LUMC
L2615	261	M	Osteoblastic	proximal tibia left	3				35	LUMC
L2616	218	M	Osteoblastic	proximal fibula left	2	24			32	LUMC
L2617	181	F	Osteoblastic	proximal tibia left	4				32	LUMC
L2618	96	M	Osteoblastic	distal femur left	2	0			31	LUMC
L1368	177	M	Osteoblastic	distal femur left	4	0			95	LUMC
L1369	212	F	Osteoblastic	distal femur right	2	17		83	83	LUMC
L1370	216	M	Osteoblastic	distal femur left	3				246	LUMC
L1016	200	M	Osteoblastic	proximal tibia left	1	6		10	10	LUMC
L2619	128	F	Osteoblastic	distal femur right	1	0		25	25	LUMC
L1372	200	M	Telangiectatic	distal femur right	1	0		25	25	LUMC
L2620	217	M	Osteoblastic	distal femur left	2				219	LUMC
L428	192	F	Osteoblastic	proximal tibia right	2				193	LUMC
L436	37	F	Osteoblastic	proximal tibia left	4				194	LUMC
L1376	164	F	Telangiectatic	proximal tibia right	1	18		40	40	LUMC
L1378	197	F	Fibroblastic, MFH-like	distal femur left	2			14	14	LUMC
L2294	205	F	Osteoblastic	distal femur left	1				147	LUMC
L2289	136	M	Fibroblastic	distal femur left	2				135	LUMC
L2290	440	M	Fibroblastic	distal femur left	2	10		13	13	LUMC
L2301	304	M	Osteoblastic	proximal ibia left	2	27		47	47	LUMC
L1382	175	M	Osteoblastic	distal tibia right	2				143	LUMC
L2302	229	F	Chondroblastic	proximal humerus right	2				120	LUMC
L1385	200	M	Osteoblastic	proximal humerus left		0		11	11	LUMC

Unit of time is months; ToM: time until metastasis detection after diagnosis; ToD: time until death after diagnosis; ToF: total time of follow up after diagnosis; The Origins are WWU: Westfälische Wilhemsinversität, Münster, Germany; IOR: Instituti Ortopedici Rizzoli, Bologna, Italy; LUMC: Leiden University Medical Centre, The Netherlands.

[1] Krystiaan Lenos, Leiden University, the Netherlands

Table 3.3 *HDMX-S/FL* ratio in 51 osteosarcomas[1].

#	Sample ID	*HDMX- S/FL* ratio
1	L1368	0.9
2	L1376	2.17
3	L2290	1.13
4	L1385	0.38
5	L2295	0.72
6	L2611	1.77
7	L2300	1.17
8	L2614	4.86
9	L2617	1.19
10	L1369	1.25
11	L1370	0.85
12	L1016	3.18
13	L2619	0.84
14	L1372	1.19
15	L2620	2.77
16	L436	1.39
17	L428	0.83
18	L1378	1.12
19	L2294	1.15
20	L2289	0.44
21	L2301	1
22	L1382	0.91
23	L2302	1.88
24	L1386	0.82
25	L2281	0.68
26	L2298	0.85
27	L2297	1.3
28	L2292	1
29	L2613	0.8
30	L2615	0.69
31	L2616	1.74
32	L2618	3.42
33	L3446	3.72
34	L3447	2.24
35	L3448	2.92
36	L3449	n.d.*
37	L3431	4.07
38	L3432	1.29
39	L3433	1.56
40	L3434	3.29
41	L3435	1.89
42	L3436	2.06
43	L3437	1.44
44	L3438	2.89
45	L3439	1.2
46	L3440	2.3
47	L3441	2.02
48	L3442	2.63
49	L3443	n.d.*
50	L3444	1.8
51	L3445	2.8

* Upper band below detection limit

[1] Krystiaan Lenos, Leiden University, the Netherlands

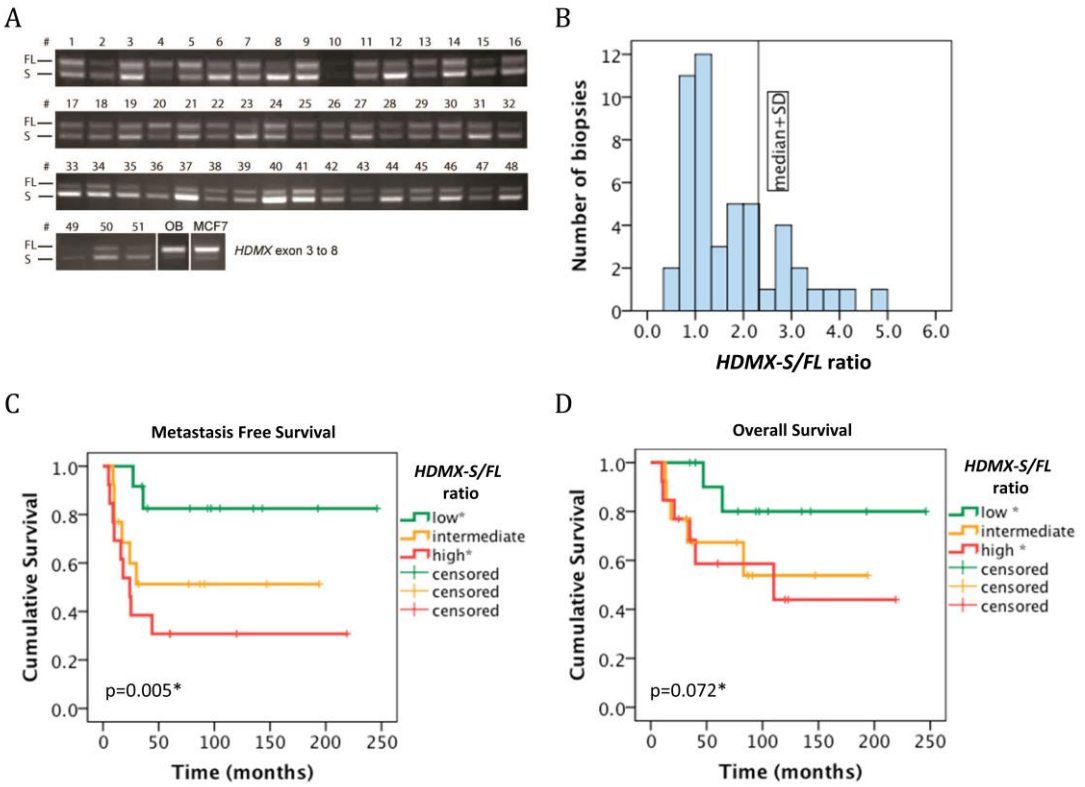


Figure 3.3 Analysis of *HDMX-S* and *HDMX-FL* mRNA expression in osteosarcoma biopsies, and its association with worse clinical outcome.

A[1], expression patterns of *HDMX-FL* and *HDMX-S* mRNA in 51 osteosarcoma biopsies, normal osteoblasts and the breast cancer cell line MCF7, analysed by semi-quantitative PCR with *HDMX* primers in exon 3 (Fw) and exon 8 (Rev). **B**, column graph depicting the number of biopsies with a given *HDMX-S/FL* ratio. **C**, **D**, Kaplan-Meier plots displaying the metastasis free survival (C) or overall survival (D) for patients whose biopsies contain high (n=13), intermediate (n=13) or low *HDMX-S/FL* ratios (n=12). The p-values are derived from a log-rank test comparing patients with high ratios to those with low ratios, as depicted by * symbol.

quantified and normalised to *GAPDH* expression levels. The *HDMX-S/FL* ratios varied from 0.38 to 4.86, with a median of 1.3 and a standard deviation of 1.0. Interestingly, the distribution of the *HDMX-S/FL* ratios was not normal (p=0.0011). In fact, 11 tumours demonstrated very high ratios, as defined by

[1] Krystiaan Lenos, Leiden University, the Netherlands

one standard deviation above the median (Figure 3.3B).

To determine whether the *HDMX-S/FL* ratios associated with progression of the high-grade osteosarcomas, we explored whether patients whose tumours had the highest *HDMX-S/FL* ratios had a shorter time to metastasis than patients with the lowest ratios. Metastasis information was available for all osteosarcoma patients. Of the 49 patients where the *HDMX-S/FL* ratios were successfully determined, 38 patients had not yet presented metastases upon inclusion in the study. Interestingly, when the patients were divided into three equal groups based on the measured *HDMX-S/FL* ratios in the tumours (12 low, 13 intermediate and 13 high), those patients whose tumours had the highest ratios had the shortest times to metastasis, while those with the lowest ratios had the longest times (p=0.005 log-rank test, Figure 3.3C). Specifically, the 13 patients whose tumours had the highest *HDMX-S/FL* ratios (average ratio of 2.55, ranging from 1.8 to 4.07) associated with a significantly shorter time of metastasis-free survival than the 12 whose tumours had the lowest ratios (average ratio of 0.8, ranging from 0.44 to 1.0). In two and a half years, 62% of those patients with the highest *HDMX-S/FL* ratios had presented with a metastasis, compared to only 8% of those with the lowest ratios. Similar, trends were seen in overall survival, whereby the 13 patients with the highest *HDMX-S/FL* ratios associated with shorter overall survival than the 12 with the lowest ratios (p= 0.072 log-rank test, Figure 3.3D).

These results show that the *HDMX-S/FL* ratio positively correlates with less HDMX protein expression, faster metastatic progression and worse overall survival of osteosarcoma. It is possible that cancer cells do not retain the

oncogenic activity of full-length HDMX because they already have inhibited p53 signalling caused by mutations of other key regulatory genes in the pathway and, therefore, are no longer under selective pressure to sustain high levels of HDMX. If this hypothesis is true, cancer cells with higher *HDMX-S/FL* ratios should associate with higher frequencies of other p53 pathway mutations. To test this possibility, the status was determined of two well characterised somatic alterations that result in p53 inhibition, *TP53* mutation and over-expression of *HDM2*, in all 22 osteosarcoma cell lines. The protein levels of HDM2 were determined in logarithmically growing cells, and normalised to USP7 levels (Figure 3.1C; Table 3.1). The *TP53* mutation status of all 22 osteosarcoma cell lines was determined using a combination of direct sequencing, *TP53* mRNA measurements and measurements of the response of each cell line to Nutlin-3, a small molecule inhibitor of the p53-HDM2 interaction that activates p53 signalling (Vassilev, Vu *et al.*, 2004). A cell line was only deemed to have functional wild-type p53 if no mutations were found in exons 3 to 11, it expressed *TP53* mRNA and responded to Nutlin-3, as measured by the determination of p53 and HDM2 levels upon Nutlin-3 treatment (data not shown). Of the 22 cell lines, only 6 lines were deemed to be wild type for p53 (Table 3.1). Interestingly, and in support of the hypothesis above, those 6 cell lines contained significantly lower *HDMX-S/FL* ratios than the remaining 16 cell lines ($p=0.0325$ Mann-Whitney test, Table 3.4). Similar trends were observed when those cells retaining wild-type p53 and low levels of HDM2 were compared to those with wild-type p53 and higher levels of HDM2 ($p=0.1$ Mann-Whitney test, Table 3.4), thereby lending further support to the

Table 3.4 The associations of the *HDMX-S/FL* ratios with p53 pathway mutations in three cell panels.

			***HDMX-S/FL* ratio**
Osteosarcoma	p53 (n=22)	wt (n=6)	1.17
		mut (n=16)	1.84
		p value	0.0325*
	wt p53 (n=6)	low HDM2 (n=3)	0.83
		high HDM2 (n=3)	1.51
		p value	0.1*
Breast cancer	p53 (n=37)	wt (n=8)	0.69
		mut (n=29)	1.76
		p value	0.0028*
	wt p53 (n=8)	low HDM2 (n=4)	0.34
		high HDM2 (n=4)	1.03
		p value	0.343*
NCI60	p53 (n=50)	wt (n=14)	1.47
		mut (n=36)	2.71
		p value	0.0227*
	wt p53 (n=14)	low HDM2 (n=7)	0.57
		high HDM2 (n=7)	2.38
		p value	0.0728* 0.0364**
All Cell Lines	p53 (n=106)	wt (n=27)	1.22
		mut (n=79)	2.24
		p value	0.0001*
	wt p53 (n=27)	low HDM2 (n=13)	0.56
		high HDM2 (n=14)	1.93
		p value	0.0116*
* Mann-Whitney test, 2-tail			
** Mann-Whitney test, 1-tail			

hypothesis that higher *HDMX-S/FL* ratios, and therefore lower HDMX protein levels, can arise in cancer cells that have already inhibited p53 signalling through alterations of other key p53 pathway genes.

3.2.2 The *HDMX-S/FL* ratio in breast cancer and NCI60 cells

To further test this hypothesis, the associations of the *HDMX-S/FL* ratio were explored in a panel of 37 cell lines derived from breast cancer, a tumour type that is clearly surveyed by the p53 pathway, and in which *TP53* mutational status of the tumour has clear prognostic value (Petitjean, Achatz *et al.*, 2007). The levels of *HDMX-S* and *HDMX-FL* were first determined (Figure 3.4A). HDMX, HDM2 and p53 protein levels and *TP53* mutational status in all of the 37 lines studied have previously been published (Lam, Lodder *et al.*, 2010; Wasielewski, Elstrodt *et al.*, 2006). The results are summarised in Table 3.5. The *HDMX-S/FL* ratios varied from 0.12 to 4.35, with a median of 1.1 and a standard deviation of 1.15. The distribution of the *HDMX-S/FL* ratios was not normal (p=0.0241). Of 37 cell lines, 9 showed very high ratios as defined by one standard deviation above the median (Figure 3.4B).

Interestingly, the *HDMX-S/FL* ratio significantly negatively correlated with measured HDMX protein levels (p=2.28E-08 Spearman's test, correlation co-efficient -0.772, Figure 3.4C). Furthermore, when the cell lines were ranked by the measured *HDMX-S/FL* ratios and subsequently divided into almost equal groups of 9, the groups with increasing ratios had significantly decreasing HDMX protein levels (p=0.0001 Kruskal-Wallis test, Figure 3.4D). Specifically, the 9 cell lines with the highest *HDMX-S/FL* ratios had 9.87-fold less HDMX protein than the 9 lines with the lowest ratios (p= 0.0002 Mann-Whitney test). The 8 breast cancer cell lines with wild-type p53 contained significantly lower *HDMX-S/FL* ratios than the remaining 29 lines (p=0.0028 Mann-Whitney test, Table 3.4). Similar differences were seen when cells retaining wt *TP53* and low

Table 3.5 Summary of *TP53* status, and the HDM2 and HDMX levels in breast cancer cell lines[1].

#	name	p53	Protein Levels		mRNA Levels		
			HDMX Rel. Quant.	HDM2 Rel. Quant.	Rel. Quant. *HDMX-FL*	Rel. Quant. *HDMX-S*	*HDMX-S/FL* ratio
1	BT20		3.36	32.09	1.03	1.14	1.11
2	BT474		12.41	96.58	0.31	0.51	1.63
3	BT549		1.7	47.74	0.78	2.07	2.67
4	CAMA-1		30.34	47.27	2.45	1.22	0.5
5	DU4475	wt	20.42	75.09	0.82	0.41	0.5
6	EVSA-T		8.35	34.6	0.94	2.09	2.22
7	HCC1937		2.02	30.12	0.63	1.43	2.25
8	Hs578T		9.32	76.26	0.51	0.67	1.32
9	MCF-7	wt	38.88	85.31	2.25	0.81	0.36
10	MDA-MB-134VI		9.21	58.12	1.4	1.4	1
11	MDA-MB-157		2.3	15.7	0.41	1.69	4.09
12	MDA-MB-175VII	wt	35.74	136.49	2.52	0.92	0.37
13	MDA-MB-231		28.81	81.52	1.37	1.35	0.99
14	MDA-MB-330		4.31	37.12	0.9	1.98	2.2
15	MDA-MB-361		0.21	18.74	0.21	0.7	3.27
16	MDA-MB-415		2.32	21.87	0.21	0.41	1.98
17	MDA-MB-436		2.16	29.48	0.47	1.55	3.33
18	MDA-MB-453		13.44	23.77	2.03	0.83	0.41
19	MDA-MB-468		11.14	49.24	1.41	0.78	0.55
20	MPE600	wt	21.4	62.36	2.06	0.69	0.34
21	OCUB-F		4.07	14.3	1.42	0.62	0.43
22	SK-BR-3		3.32	47.08	0.67	1.07	1.59
23	SK-BR-5		2.06	45.83	0.3	1.03	3.4
24	SK-BR-7	wt	24.31	61.06	1.32	0.54	0.41
25	SUM44PE		6.87	16.85	0.67	0.51	0.76
26	SUM52PE		0.85	147.33	0.3	1.3	4.35
27	SUM149PT		2.02	27.32	0.42	0.7	1.66
28	SUM159PT		10.3	34.75	0.64	0.45	0.69
29	SUM185PE		10	24.41	0.62	0.55	0.9
30	SUM190PT		3.06	11.34	0.24	0.18	0.74
31	SUM229PE		2.9	24.7	0.21	0.57	2.64
32	SUM1315M02		0.43	5.41	0.12	0.15	1.26
33	T47D		15.29	31.1	1.08	0.56	0.52
34	UACC-812	wt	45.97	98.83	1.35	1.45	1.07
35	UACC-893		1.01	71.19	0.24	0.63	2.59
36	ZR75-1	wt	13.59	135.77	0.83	1.94	2.33
37	ZR75-30	wt	75.72	63.18	2	0.23	0.12

levels of HDM2 were compared with those with wt *TP53* and high levels of HDM2 (p=0.343, Mann-Whitney test, Table 3.4). In order to test this hypothesis further in another cell line panel, the *HDMX-S/FL* ratios and *HDM2* mRNA levels were determined in the National Cancer Institute 60 (NCI60) panel (Shoemaker, 2006), which consists of 59 human cancer cell lines, representing 9 cancer types (Table 3.6). Three cell lines overlap with the above-analysed breast cancer cell

[1] Krystiaan Lenos, Leiden University, the Netherlands

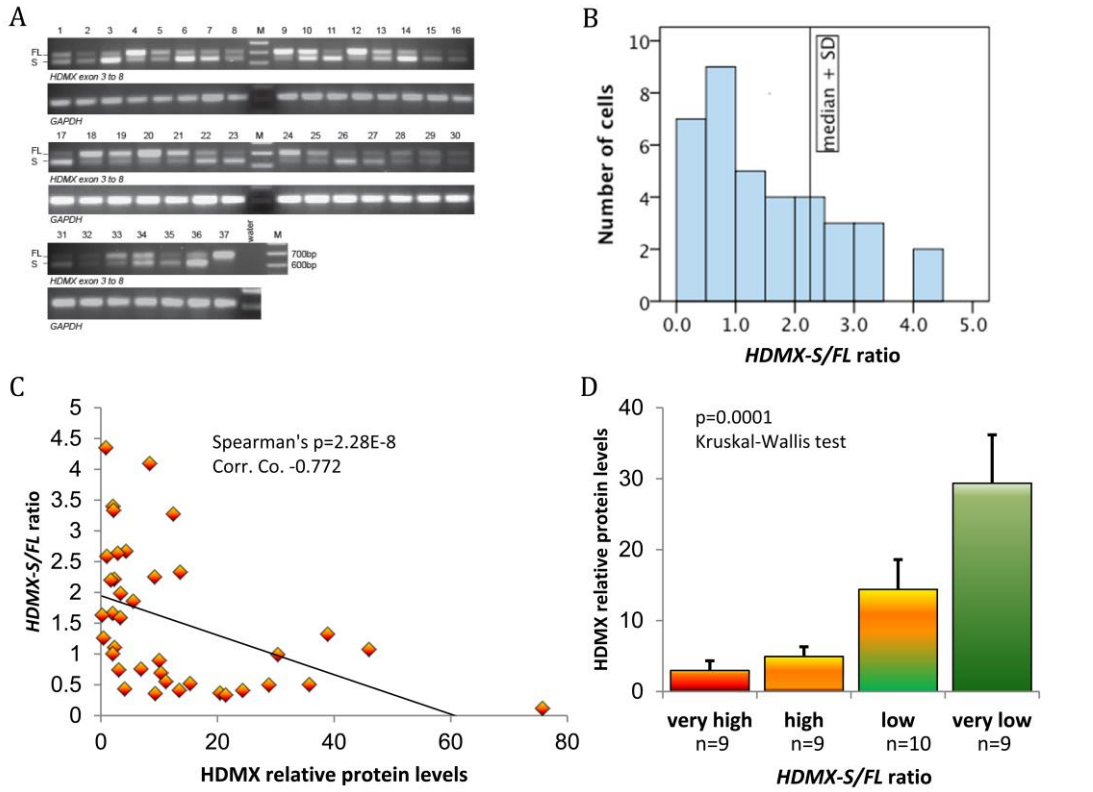


Figure 3.4 Analysis of the *HDMX-S/FL* ratio and its association with HDMX protein levels in breast cancer cell lines.

A[1], cell lines were examined for *HDMX-FL* and *HDMX-S* mRNA expression using primers for *HDMX* exon 3 (Fw) to exon 8 (Rev). **B**, column graph depicting the number of cells with a given *HDMX-S/FL* ratio. **C**, graph depicting the negative correlation of *the HDMX-S/FL* ratio on the y-axis with HDMX protein levels on the x-axis. **D**, column graph depicting the average HDMX protein levels for the groups of cell lines with varying ratios of *HDMX-S/FL*, whereby cells with higher ratios contain less HDMX protein. Error bars depict the standard error of the means.

panel. Of the 59 cell lines, 14 are known to have wt *TP53*, 36 have either mutated or deleted *TP53*, while for the remaining cell lines *TP53* mutation status is inconclusive (Caron de Fromentel and Soussi, 1992; Mejia and Larin, 2000). The levels of *HDMX-FL* and *HDMX-S* mRNA were determined using the semi-quantitative PCR (Figure 3.5A; Table 3.6) and the levels of *HDM2* mRNA

[1] Krystiaan Lenos, Leiden University, the Netherlands

were determined using qRT-PCR (Table 3.6). The levels of each transcript were determined and normalised to *GAPDH* expression levels. The *HDMX-S/FL* ratios varied from 0 to 18.65, with a median of 1.25 and a standard deviation of 3.3. The distribution of the ratios, similarly to the breast cancer cell panel and osteosarcoma patients, was not normal (Figure 3.5B). Interestingly, the 14 cell lines with wt *TP53* had significantly lower *HDMX-S/FL* ratios than the remaining 36 cell lines lacking functional p53 (p=0.0227 Mann-Whitney test, Table 3.4). Furthermore, a similar significant trend was observed when *HDMX-S/FL* ratios were compared in the wt TP53 cell lines with either high or low levels of *HDM2* mRNA. Specifically, the 7 cell lines with the lowest *HDM2* mRNA levels had significantly lower *HDMX-S/FL* ratios than the 7 cell lines with the highest levels of *HDM2* (p=0.0364, Mann-Whitney test, 1-tailed, Table 3.4).

Together these observations, made in three cell panels comprising a total of 115 different cell lines, lend support to a model that higher *HDMX-S/FL* ratios, and therefore lower HDMX protein levels, arise in cancer cells that have attenuated p53 signalling through alterations of key p53 pathway genes. Indeed, the 27 cell lines with wt *TP53* in the three cell panels had significantly lower *HDMX-S/FL* ratios than the 79 cell lines lacking functional p53 (p=0.0001 Mann-Whitney test, Table 3.4). Furthermore, in the 27 wt *TP53* cell lines, the 13 lines with the lowest HDM2 levels had significantly lower *HDMX-S/FL* ratios than the 14 with the highest levels of HDM2 (p=0.0116, Mann-Whitney test, Table 3.4). When the 106 cell lines with *TP53* mutational status were separated into almost equal numbers after ranking based on the *HDMX-S/FL* ratios, it was observed that of the 35 lines with the lowest ratios, 12 (34%) had wt *TP53* and lower

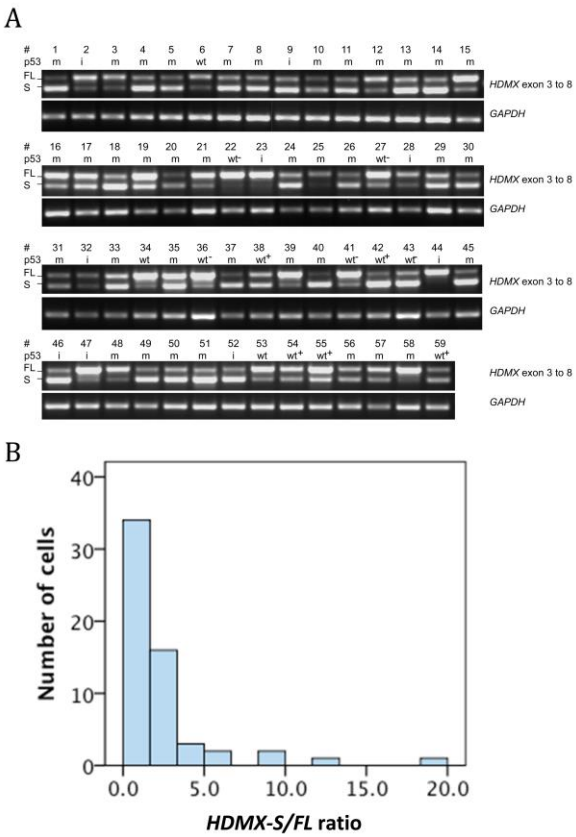


Figure 3.5 Analysis of *HDMX-S* and *HDMX-FL* mRNA expression in the NCI60 cell panel.

A[1], cell lines were examined for *HDMX-FL* and *HDMX-S* mRNA expression using primers for *HDMX* exon 3 (Fw) to exon 8 (Rev). **B**, a column graph depicting the number of cells with a given *HDMX-S/FL* ratio.

HDM2 levels. In contrast, in the 36 cell lines with the highest ratios, only 1 cell line (3%) had wt *TP53* and lower HDM2 levels (p=0.0006, Fisher's exact test,Figure 3.6), compared to 4 of the 35 cell lines with intermediate ratios (11%, p=0.001 Fisher's exact test).

3.2.3 The *HDMX-S/FL* ratio and *TP53* mutation as prognostic markers

Thus far in cells, cancer lines with higher *HDMX-S/FL* ratios had significantly higher frequencies of two common p53 pathway mutations, namely

[1] Krystiaan Lenos, Leiden University, the Netherlands

Table 3.6 Summary of the *TP53* status, and the *HDM2* and *HDMX* levels in the NCI60 cell panel[1].

#	Name	origin	*p*53	relative band intensity		*HDMX-S/FL* ratio	*HDM2* RNA
				HDMX-FL	*HDMX-S*		
1	K-562	Leukemia	mut	302.5	2788.5	9.22	149.51
2	MOLT-4	Leukemia	inc	2176.1	254.6	0.12	73.97
3	CCRF-CEM	Leukemia	mut	1769.3	366.8	0.21	46.01
4	RPMI-8226	Leukemia	mut	714.4	2189.6	3.06	88.77
5	HL-60 (TB)	Leukemia	mut	509.4	1526.8	3	35.18
6	SR	Leukemia	wt	1171	354.4	0.3	108.97
7	SF-268	CNS	mut	679.3	1542.4	2.27	36.58
8	SF-295	CNS	mut	611.1	1387.7	2.27	22.44
9	SF-539	CNS	inc	785.5	1924.1	2.45	74.54
10	SNB-19	CNS	mut	405.1	1065.9	2.63	36.73
11	SNB-75	CNS	mut	604.9	1467.3	2.43	50.21
12	U251	CNS	mut	1416.8	495.6	0.35	31.4
13	BT-549	Breast	mut	796.6	1703.8	2.14	47.37
14	HS 578T	Breast	mut	563.6	1765.4	3.13	56.01
15	MCF7	Breast	wt	2820.1	707.3	0.25	171.02
16	NCI/ADR-RES	Ovarian	mut	1253.7	425.1	0.34	36.8
17	MDA-MB-231/ATCC	Breast	mut	1517	1017.6	0.67	54.63
18	MDA-MB-435	Melanoma	mut	638.4	1489.3	2.33	25.1
19	T-47D	Breast	mut	2636.3	1367.7	0.52	440.6
20	COLO 205	Colon	mut	139.3	1303.7	9.36	36.93
21	HCC-2998	Colon	mut	1294.4	212.8	0.16	29.33
22	HCT-116	Colon	wt	2555.6	4.4	0	94.29
23	HCT-15	Colon	inc	1893.1	0.7	0	75.56
24	HT29	Colon	mut	1257.2	2434.1	1.94	56.22
25	KM12	Colon	mut	1247.3	105.7	0.08	33.69
26	SW-620	Colon	mut	469.3	1325.4	2.82	52.01
27	A549/ATCC	NSCL	wt	1904	352	0.18	64.92
28	EKVX	NSCL	inc	1527.2	427.5	0.28	34.59
29	HOP-62	NSCL	mut	644	864.8	1.34	38.35
30	HOP-92	NSCL	mut	421.8	1493.4	3.54	44.32
31	NCI-H322M	NSCL	mut	852.3	1195.9	1.4	82.82
32	NCI-H226	NSCL	inc	1141.6	598.4	0.52	343.99
33	NCI-H23	NSCL	mut	1994.7	2575.9	1.29	142.03
34	NCI-H460	NSCL	wt	2282.5	438.9	0.19	145.87
35	NCI-H522	NSCL	mut	1549.1	1396.3	0.9	91.74
36	LOX IMVI	Melanoma	wt	1423.3	518.2	0.36	79.69
37	M14	Melanoma	mut	383	2433.5	6.35	49.32
38	MALME-3M	Melanoma	wt	1310.1	1631.5	1.25	280.18
39	SK-MEL-2	Melanoma	mut	2312.4	52.1	0.02	55.74
40	SK-MEL-28	Melanoma	mut	150.8	2812.6	18.65	60.55
41	SK-MEL-5	Melanoma	wt	2293.9	216.1	0.09	82.27
42	UACC-257	Melanoma	wt	179.4	2223.9	12.4	549.69
43	UACC-62	Melanoma	wt	481.3	1383.3	2.87	81.6
44	IGROV1	Ovarian	inc	2769.9	143.4	0.05	139.75
45	OVCAR-3	Ovarian	mut	379.4	2021.8	5.33	64.05
46	OVCAR-4	Ovarian	inc	410.8	1644.2	4	57.66
47	OVCAR-5	Ovarian	inc	2010.4	151.2	0.08	69.08
48	OVCAR-8	Ovarian	mut	1896.1	134.8	0.07	42.99
49	SK-OV-3	Ovarian	mut	649.4	1999.5	3.08	53.9
50	DU-145	Prostate	mut	717.5	1519.2	2.12	41.83
51	PC-3	Prostate	mut	460	1508.5	3.28	72.64
52	786-O	Renal	inc	422.1	1427.9	3.38	27.26
53	A498	Renal	wt	1608.7	271.4	0.17	111.81
54	ACHN	Renal	wt	1274.8	644.4	0.51	179.48
55	CAKI-1	Renal	wt	1832.5	775.4	0.42	506.89
56	RXF-393	Renal	mut	1057.6	894.5	0.85	28.3
57	SN12C	Renal	mut	2178.2	898	0.41	49.42
58	TK-10	Renal	mut	1791.6	93.2	0.05	68.12
59	UO-31	Renal	wt	640.5	1041	1.63	421.72

[1] Krystiaan Lenos, Leiden University, the Netherlands; AJ Roboscreen GmbH, Leipzig, Germany (*HDM2* RNA)

TP53 gene mutation and *HDM2* overexpression (Table 3.4, Figure 3.6). Inhibition of p53 signalling through *TP53* mutation has clearly been shown to have prognostic value in multiple cancers (Petitjean, Achatz *et al.*, 2007). If the model proposed here is true, the *HDMX-S/FL* ratio could potentially serve as a more effective prognostic biomarker than *TP53* gene mutation, because alterations of other key p53 pathway genes that result in p53 pathway attenuation could be captured simultaneously. To begin to explore this possibility, the prognostic value of either *TP53* tumour mutation or the *HDMX-S/FL* ratio was compared in another tumour type that is clearly surveyed by p53 signalling, namely soft tissue sarcoma (STS), where an increase of the *HDMX-S/FL* ratio has been shown to associate with altered survival (Bartel, Schulz *et al.*, 2005).

A cohort of 157 soft tissue sarcoma patients from Germany was studied. Sufficient tumour material was obtained from 80 patients for *HDMX* transcript analysis, of which 36 were males and 44 females. The levels of *HDMX-S* and *HDMX-FL* were determined using qRT-PCR and SYBR chemistry with the appropriate primers (Table 2.3), as described in the materials and methods, in tumour samples that were taken before therapy. The levels of each transcript were determined and normalised to *GAPDH* expression levels. Sixteen tumours (20%) had no detectable *HDMX* transcript levels, 24 tumours (30%) had more *HDMX-FL* than *HDMX-S* transcripts (low *HDMX-S/FL* ratio), 24 tumours (30%) had equal amounts of *HDMX-S* and full-length transcripts (intermediate *HDMX-S/FL* ratio), while 16 tumours (20%) had more *HDMX-S* than *HDMX-FL* transcripts (high *HDMX-S/FL* ratio). *TP53* mutational status was successfully

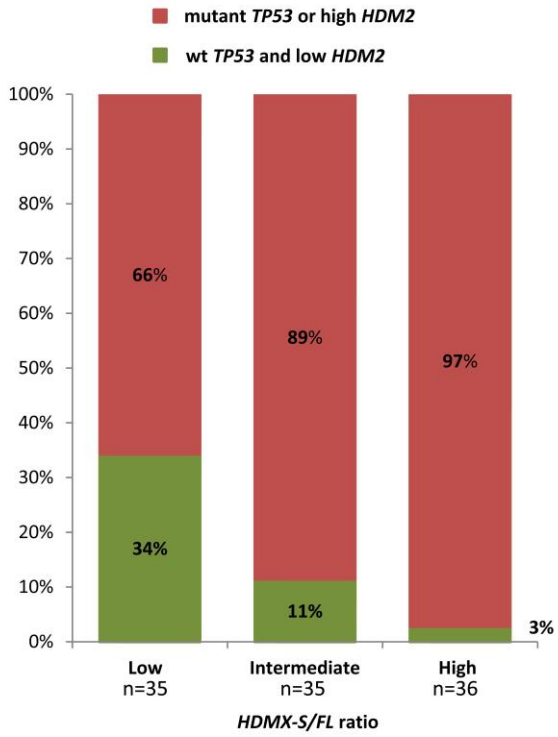


Figure 3.6 Cancer lines with high *HDMX-S/FL* ratios have significantly higher frequencies of two common p53 pathway mutations, namely *TP53* gene mutation and *HDM2* over-expression.

Column graph depicting the percentage of cell lines with wild-type *TP53* and lower HDM2 in the 106 cell lines that are divided into three groups based on low, intermediate and high expression of the *HDMX-S/FL* ratio.

determined in tumours from 104 of the 157 patients. Of the 104 tumour DNAs, 19 were found to have missense mutations in the *TP53* gene. Interestingly, similar to the observations made in the three cell panels, in the 46 tumours where both the levels of *HDMX-S* and *HDMX-FL* and *TP53* mutational status were determined, the tumours with higher *HDMX-S* transcript levels than *HDMX-FL* were enriched for *TP53* mutations (p=0.0337, Fisher's exact test, one-sided, Figure 3.7A). *TP53* mutation status alone could not effectively serve as a prognostic factor. Patients that had retained wt *TP53* in their sarcomas had longer survival times than those with mutant *TP53*, although the difference was

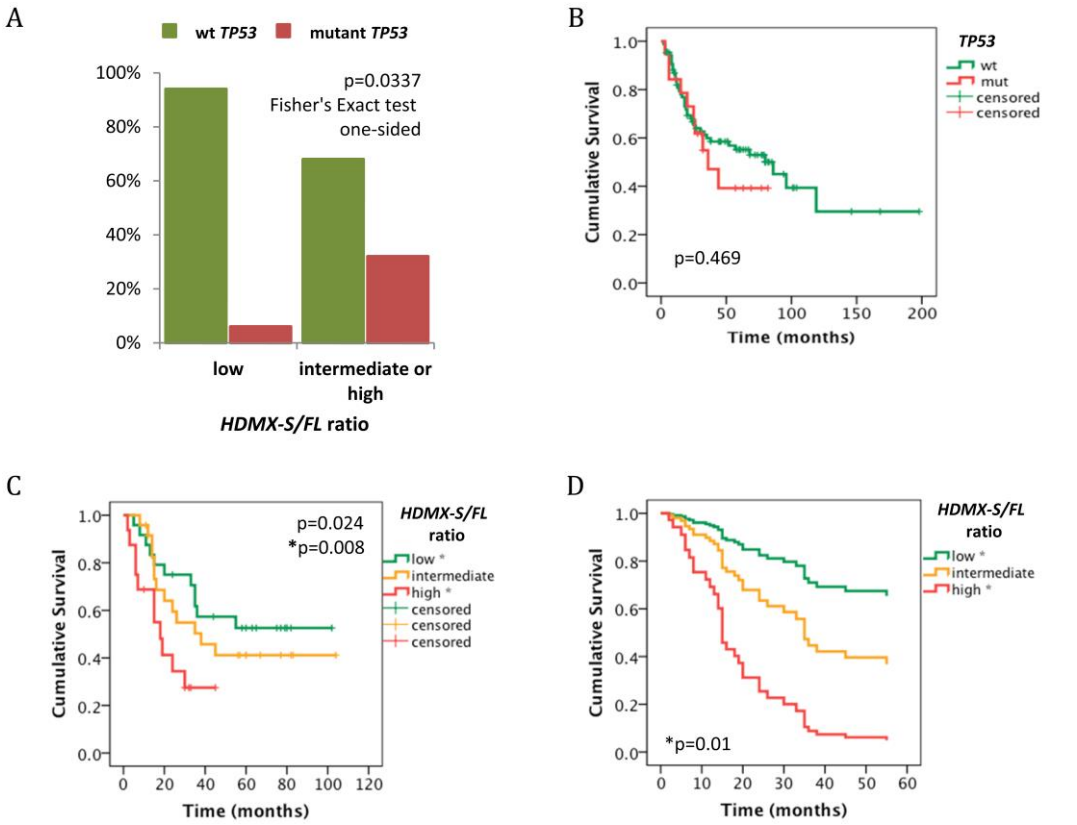


Figure 3.7 High *HDMX-S/FL* ratios, but not *TP53* gene mutation, associate with worse clinical outcome of soft tissue sarcoma patients.

A, column graph depicting the percentage of tumours with missense *TP53* mutations for tumours with either low (n=18) or higher (n=28) *HDMX-S/FL ratios*. Tumours with higher ratios contain a greater percentage of *TP53* mutations. **B**, Kaplan-Meier plot that displays overall survival for patients whose tumours contained either wild-type or mutant *TP53* (n=104). The p-value depicted on the plot is derived from a log-rank test. **C**, Kaplan-Meier plot that displays the overall survival for those patients whose tumours contained high, intermediate or low *HDMX-S/FL* ratios (n=64). The first p-value is derived from a log-rank test comparing the patients with higher, equal and lower ratios. The second p-value is derived from a log-rank test comparing the patients with higher ratios to those with low ratios, as depicted by the * symbol. **D**, predicted survival curves for patients with different *HDMX-S/FL* ratios (n=64) derived from a Cox multivariate regression analysis that was adjusted to the known independent prognostic factors of soft tissue sarcomas that included tumour stage, resection type, tumour location and tumour type. The p-value depicted on the plot is derived through the comparison of the patients with higher ratios to those with low ratios, as is depicted by the * symbol.

not significant (p=0.469, log-rank test, Figure 3.7B). However, the patients whose tumours had more *HDMX-S* than *HDMX-FL* transcripts had significantly shorter overall survival than those with equal or lower *HDMX-S* transcript levels (p=0.024 log-rank test, Figure 3.7C), with a 5.746-fold higher risk of tumour-related death (p=0.01, Figure 3.7D).

3.3 Discussion

In this chapter, the initial aim was to explore the importance of the p53 pathway during the progression of osteosarcoma, through the analysis of the *HDMX-S/FL* ratio and its association with HDMX protein levels in 22 osteosarcoma cell lines, as well as cancer progression and survival in 51 osteosarcoma patients. Increased expression of *HDMX-S* mRNA in various cancers has been reported in a number of studies (Bartel, Schulz *et al.*, 2005; Prodosmo, Giglio *et al.*, 2008; Riemenschneider, Buschges *et al.*, 1999). Interestingly, many tumours that showed increased *HDMX-S* mRNA levels had less *HDMX* full-length RNA and protein (Bartel, Schulz *et al.*, 2005; Prodosmo, Giglio *et al.*, 2008), and correlated with later tumour stage and poorer survival. For example, even in cells expressing predominantly *HDMX-S* mRNA, only full-length HDMX protein could be detected (Figure 3.4A and (Lenos and Jochemsen, 2011)). Thus, it is possible that the HDMX-S protein is very unstable or inefficiently translated and, therefore, is unlikely to play an important, dominant role in cell proliferation. Here, it is further shown that as the *HDMX-S/FL* ratio increased, HDMX full-length protein decreased in the 22 osteosarcoma cell lines and 37 breast cancer cell lines studied (Figures 3.1, 3.2

and 3.4). For example, the osteosarcoma cell lines with the highest *HDMX-S/FL* ratio expressed up to 9.5-fold less HDMX full-length protein.

In this chapter, further investigations explored the potential association of the *HDMX-S/FL* ratio with osteosarcoma progression, as it had previously been demonstrated (Bartel, Schulz *et al.*, 2005; Prodosmo, Giglio *et al.*, 2008; Riemenschneider, Buschges *et al.*, 1999). In this study, 51 high-grade osteosarcoma patients were analysed and, strikingly, high *HDMX-S/FL* ratios correlated with faster metastatic progression (Figure 3.3). Specifically, over two years, 62% of those with the highest *HDMX-S/FL* ratios had presented with metastases, compared to only 8% of those with the lowest ratios. Interestingly, a subset of the cell lines utilised in this study had previously been analysed for in vivo growth characteristics, including the capacity to metastasise (Mohseny, Machado *et al.*, 2011). One of the cell lines tested, HOS-143B, was found to produce metastases in mice, whereas the parental HOS cell line did not. Intriguingly, and in line with the observations reported here in the patient cohort, a dramatically increased *HDMX-S/FL* ratio and significantly decreased HDMX protein levels were found in HOS-143B cells compared to HOS cells (Figure 3.1B and 3.1C).

The observations described above in an osteosarcoma cell line panel and patient cohort suggest that the *HDMX-S/FL* ratio positively correlates with less HDMX protein expression, as proposed earlier (Lenos and Jochemsen, 2011), and faster metastatic progression, as well as a trend to worse overall survival. It is therefore possible that cancer cells do not retain the oncogenic activity of HDMX because they have already inhibited p53 signalling by mutations of other

key regulatory genes in the pathway and, therefore, the cell is no longer under selective pressure to sustain higher levels of HDMX. Furthermore, cells with deficient p53 activity could be under positive selection pressure to reduce HDMX levels as suggested by two recent studies, which report that full-length HDMX functions as a tumour suppressor in cells with deficient p53 function (Matijasevic, Krzywicka-Racka *et al.*, 2008; Matijasevic, Steinman *et al.*, 2008). Indeed, the observations described in this chapter, made in three cell panels comprising a total of 115 different cell lines, lend support to this model. It was observed that the cancer lines with higher *HDMX-S/FL* ratios had significantly higher frequencies of two common p53 pathway mutations, namely *TP53* gene mutation and *HDM2* over-expression (Table 3.4, Figure 3.6). An interesting prediction of this model would be that the *HDMX-S/FL* ratio could potentially serve as a more effective prognostic biomarker than *TP53* gene mutation, because alterations of other key p53 pathway genes (like *HDM2* overexpression) that result in p53 pathway attenuation could be captured simultaneously. Indeed, observations are presented above that support this hypothesis in a cohort of soft tissue sarcoma patients, where *HDMX-S/FL* ratios and *TP53* mutation status could be determined. The *HDMX-S/FL* ratio was a strikingly better prognostic indicator than *TP53* mutation. While these observations remain to be replicated in other patient cohorts and cancers, they indicate that the *HDMX-S/FL* ratio could serve as an effective biomarker for p53 attenuation in cancer cells that could be utilised in a further personalisation of therapeutic interventions in sarcomas, as well as potentially other cancers.

4 THE *HDMX-S/FL* BIOMARKER INTERACTS WITH p53 GENE MUTATIONS TO PREDICT THE METASTATIC PROGRESSION OF BREAST CANCER PATIENTS

4.1 Introduction

4.2 Results

4.2.1 High HDMX-S/FL ratios associate with p53 inhibition in breast cancer

4.2.2 The HDMX-S/FL ratio interacts with TP53 mutational status to further define individuals in their survival of breast cancer.

4.2.3 The HDMX-S/-FL ratio and TP53 mutational status predict breast cancer survival better than BC molecular subtypes

4.2.4 The HDMX-S/FL ratio interacts with TP53 mutational status to further define metastasis-free survival.

4.2.5 The HDMX-S/FL ratio associates with HDMX P2 *promoter activity*

4.3 Discussion

4.1 Introduction

The tumour suppressor p53, a central node of the cellular stress response pathway, regulates transcriptional programmes important in suppressing tumour formation and progression, and the cellular response to certain therapies. The role of p53 in activating apoptosis, cell cycle arrest and the DNA damage response is well established, associating not only with p53's tumour suppressing properties, but also the cellular response to DNA damage-inducing cancer therapies (Riley, Sontag *et al.*, 2008; Ventura, Kirsch *et al.*, 2007; Xue, Zender *et al.*, 2007). In recent years, however, the less well understood role of p53 in controlling cell migration and invasion has emerged, whereby both wild-type (wt) and mutant p53 are involved in processes of cell migration, cellular adhesion, cytoskeletal organisation and angiogenesis, which are important steps of metastatic progression (Muller, Vousden *et al.*, 2011; Roger, Gadea *et al.*, 2006).

Given p53's role in controlling the key cellular processes associated with the prevention of malignant transformation, it is not surprising that the loss of p53's function is common in many cancers. In approximately 50% of all tumours, wt p53 activity is lost by mutation of the *TP53* gene (Hainaut and Hollstein, 2000; Hollstein, Sidransky *et al.*, 1991). The majority of these mutations are point mutations leading to a single amino acid substitution. These result in the expression of a mutant p53 protein, that not only can have a dominant-negative effect over wt p53, but can also acquire oncogenic gain of functions (Muller and Vousden, 2013; Vousden and Lu, 2002). Furthermore, the function of p53 in tumours that retain wt p53 can also be compromised through

the mutation or over-expression of crucial upstream or downstream p53 pathway genes (Toledo and Wahl, 2006; Vousden and Lu, 2002).

Many attempts have been made to translate our knowledge of the p53 tumour suppressor into new therapies. One such approach was to use p53's high rate of mutation as a prognostic biomarker for overall survival, and a predictive marker for DNA damaging therapies (Bertheau, Espie *et al.*, 2008; Varna, Bousquet *et al.*, 2011). However, the effects of *TP53* mutation in isolation are too small to dramatically affect clinical decisions (Petitjean, Mathe *et al.*, 2007). Technical hurdles include the immunohistochemical (IHC) detection or sequencing of exons 5-8 as a central core of p53, used in many studies to assess *TP53* mutation status, leading to a large number of misclassified cases (Olivier, Hollstein *et al.*, 2010; Vousden and Lu, 2002). Biological limitations include the fact that there are many ways by which a cancer cell can inhibit p53's activity (Vousden and Lu, 2002).

Other biomarkers in the p53 pathway could help further define tumours with pathway attenuation together with p53 gene mutational status. One such example is the over-expression of direct p53 inhibitors such as the HDMX oncogene. HDMX, alongside its homolog HDM2, inhibits the transcriptional activity of p53 (Shvarts, Steegenga *et al.*, 1996). The over-expression or amplification of either *HDM* gene has been found in many cancers (Wade, Li *et al.*, 2013). For example, over-expression of *HDMX* has been observed in as many as 40% of cancer cell lines that mostly retain wt *TP53* (Ramos, Stad *et al.*, 2001), in up to 19% of primary breast, colon and lung tumours (Danovi, Meulmeester *et al.*, 2004), and a staggering 68% of malignant melanomas (Gembarska,

Luciani *et al.*, 2012). Furthermore, in breast tumours, it was demonstrated that the *HDMX* gene was amplified in 5% of all samples that retained wt p53, as measured by IHC and sequencing (Danovi, Meulmeester *et al.*, 2004).

In Chapter 3 it was demonstrated that a biomarker for *HDMX* expression (high *HDMX-S* alternatively spliced transcript levels compared to *HDMX* full-length transcript levels, *HDMX-S/FL* ratio) associates with common somatic genetic lesions connected with p53 inhibition, such as *TP53* mutation and *HDM2* over-expression. Moreover, in two cohorts of sarcoma patients, the *HDMX-S/FL* ratio better defined patients with worse survival rates than *TP53* mutation status. A novel role for the alternative splicing of *HDMX*, where it serves as a mechanism by which HDMX protein levels are reduced in cancer cells that already have inhibited p53 activity, was proposed. In this chapter, the possibility that the *HDMX-S/FL* ratio could help further define the progression of breast cancer in individuals is explored.

4.2 Results

4.2.1 High *HDMX-S/FL* ratios associate with p53 inhibition in breast cancer

In Chapter 3 it was shown that an increase in the splice to full-length transcript ratio of *HDMX* (*HDMX-S/FL*) associates with both lower levels of HDMX protein and an enrichment of cancer cells with an attenuated p53 pathway, either by direct *TP53* gene mutation or over-expression of *HDM2*, a key inhibitor of p53. A model was proposed that higher *HDMX-S/FL* ratios, and therefore lower HDMX protein levels, can arise in cancer cells that already have inhibited p53 signalling through alterations of other key p53 pathway genes.

In this chapter, whether or not the high levels of *HDMX* splicing associate with attenuation of p53 activity in breast cancer tumours was explored, alongside the possibility that the *HDMX-S/FL* ratio could improve the currently inconclusive prognostic value of *TP53* mutation status in breast cancer. To do so, a total of 191 breast cancer patients from 2 different breast cancer cohorts were studied, namely 113 patients from the Oslo MicroMetastasis Project (MicMa) (Naume, Zhao *et al.*, 2007; Wiedswang, Borgen *et al.*, 2003) and 78 patients from Ullevål University Hospital (ULL) (Langerod, Zhao *et al.*, 2007). *TP53* mutation status was determined in all tumours: 42 (37%) MicMa tumours and 19 (24%) ULL tumours were found to have a mutation in the p53 gene (*TP53*).

To begin exploring the possibility of associations between *TP53* mutation status and the *HDMX-S/FL* ratio in the breast cancer tumours, *HDMX-FL* and *HDMX-S* expression levels were determined by performing qRT-PCR using TaqMan gene expression assays designed to detect full-length (FL) and splice isoform S transcripts of *HDMX* (Table 2.3). The *HDMX-FL* probe detects the exon 5-6 boundary of the *HDMX* gene, which is present in *HDMX-FL* transcript and only one out of six alternative transcripts, namely *HDMX-A* (Figure 4.1). The *HDMX-S* assay was designed to recognise the exon 5-7 boundary created by the deletion of exon 6, which is specific to the *HDMX-S* transcript as depicted in the schematic drawing of the *HDMX-S* mRNA structure in Figure 4.1. The expression levels of both *HDMX-FL* and *HDMX-S* transcripts were normalized to *GAPDH* expression levels. The distribution of *HDMX-S/FL* ratios in tumours of both MicMa and ULL patients were not normal (MicMa p=1.17E-10, ULL p=4.58E-12 Shapiro-Wilk test). Specifically, they varied between 0.002 and 7.42 with a

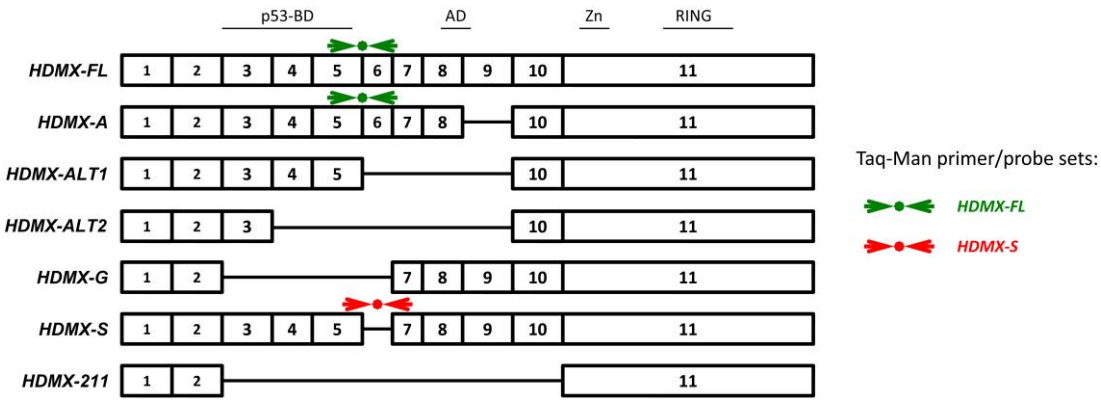


Figure 4.1 Schematic drawing of full-length *HDMX* and its alternatively spliced isoforms mRNA structure, and Taq-Man primer/probes sets, which recognise distinct isoforms.

Exons are depicted as boxes, whereas lines represent the portions of mRNA removed by splicing.

median of 1.3 and an average of 1.6 in the MicMa cohort, whereas the *HDMX-S/FL* ratio ranged from 0.13 to 8.14 with a median of 0.98 and an average of 1.62 in the ULL cohort. Tumours from both MicMa and ULL cohorts had groups of extremely high *HDMX-S/FL* ratios, as defined by one standard deviation above the mean. Specifically, 14 out of 113 MicMa tumours and 9 out of 78 ULL tumours had extremely high *HDMX-S/FL* ratios. However, none of the tumours from either cohort had an extremely low *HDMX-S/FL* ratio.

In order to begin to determine whether or not higher levels of *HDMX* splicing also associate with biomarkers for p53 pathway attenuation in breast tumours, the *HDMX-S/FL* ratios in tumours with wild-type (wt) and mutant *TP53* were compared. Interestingly, in line with the previous findings, the *HDMX-S/FL* ratios of 130 tumours with wt *TP53* were significantly lower than those of the remaining 61 tumours with mutant *TP53* (p=0.0001 Mann-Whitney test, Figure 4.2A), whereby the 130 wt *TP53* tumours contained 1.95-fold lower

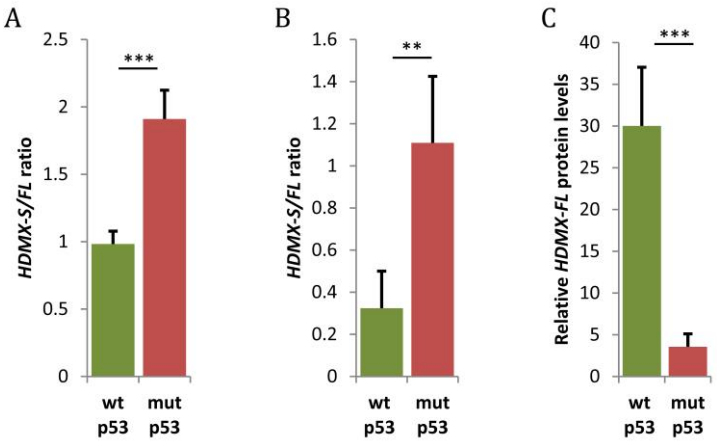


Figure 4.2 *TP53* mutational status associates with different levels of *HDMX-S/FL* ratio and HDMX-FL protein in breast cancer.

A, column graph depicting the levels of *HDMX-S/FL* ratio in 130 wt and 61 mutant *TP53* breast cancer tumours. **B**, **C**, column graphs depicting *HDMX-S/FL* ratio levels (B) and the relative levels of HDMX-FL protein (C) in 8 wt and 28 mutant *TP53* breast cancer cell lines. ** p<0.01, *** p<0.001, denote the level of statistical significance derived from the Mann-Whitney test. Error bars depict the standard error of the means.

average *HDMX-S/FL* ratios than 61 mutant *TP53* tumours.

In order to explore this further, the expression levels of *HDMX-S* and *HDMX-FL* transcripts in 36 breast cancer cell lines were measured by qRT-PCR, with specific TaqMan probes as described above. Interestingly, associations similar to those previously described were observed. Specifically, the average *HDMX-S/FL* ratio of eight wt *TP53* cell lines was 3.42-fold lower (p=0.005 Mann-Whitney test, Figure 4.2B) than that of 28 mutant *TP53* cell lines. As the protein levels of *HDMX-FL* had been determined in this cell panel (Caron de Fromentel and Soussi, 1992; Lenos, Grawenda *et al.*, 2012), the ability of the *HDMX-S/FL* ratio to serve as a biomarker for HDMX protein levels could be further explored in the context of breast cancer cells. Strikingly, HDMX-FL protein levels were

8.4-fold lower in the 28 cell lines with mutant *TP53* than in the 8 cell lines with wt *TP53* (p=0.0001 Mann-Whitney test, Figure 4.2C).

Next, the breast tumours were further utilised to explore the association of high *HDMX-S/FL* ratios with additional biomarkers of p53 pathway attenuation, namely high HDM2. To test these associations, the transcript levels of *HDM2* from both constitutive P1 and p53-responsive P2 promoters were measured, using custom-designed TaqMan probes (Table 2.3) and qRT-PCR on tumour samples from all 191 of the MicMa and ULL patients. Patients were divided into 2 groups of high and low *HDMX-S/FL* ratios, whereby the high *HDMX-S/FL* ratios group consisted of 62 patients whose tumours had *HDMX-S/FL* ratios above the mean, and the low *HDMX-S/FL* ratio group consisted of 129 patients whose tumours had *HDMX-S/FL* ratios below the mean. Strikingly, and in line with the findings described earlier, it was observed that 62 tumours with high *HDMX-S/FL* ratios were significantly enriched in *TP53* mutation or high expression of *HDM2*, regardless of whether they were transcribed from the P1 or P2 promoter. Specifically, 88% of tumours with high *HDMX-S/FL* ratios either had mutant *TP53* or high *HDM2* transcript levels, whereas only 69% of tumours with low *HDMX-S/FL* ratios had mutant *TP53* or high *HDM2* transcript levels (p=0.00095 Fisher's exact test, Figure 4.3A). These differences were even more striking when all of the tumours were divided in three groups of high, intermediate and low *HDMX-S/FL* ratios, whereby the group with high ratios consisted of tumours with extreme *HDMX-S/FL* ratios, defined by one standard deviation above the mean. Specifically, 98% of the tumours with the highest

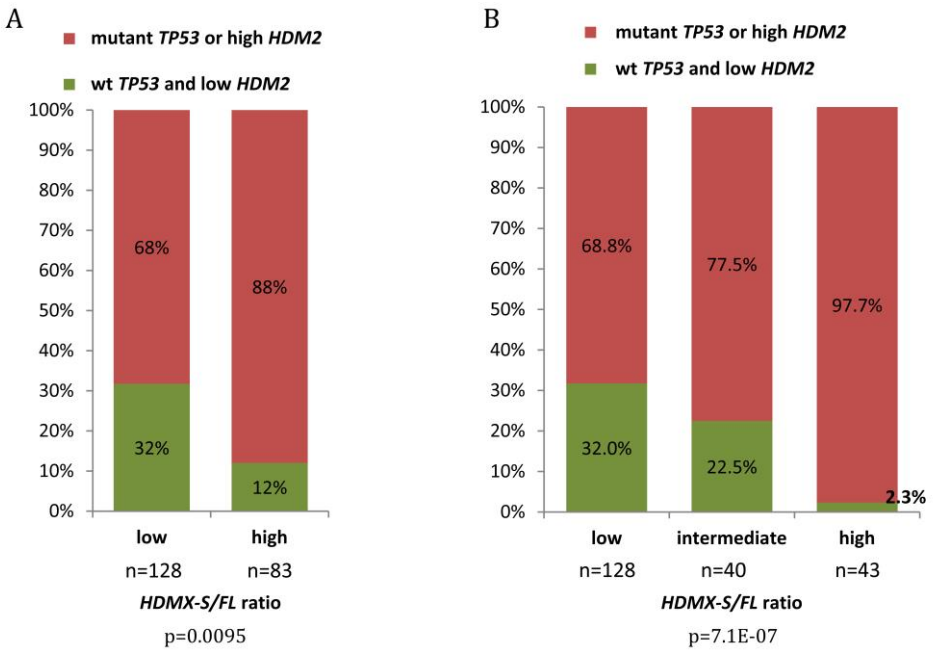


Figure 4.3 Breast tumours with high *HDMX-S/FL* ratios have significantly higher frequencies of 2 common p53 pathway mutations: p53 gene mutation and *HDM2* over-expression.

A, **B**, column graphs depicting the percentage of breast tumours with wt *TP53* and low *HDM2* from 191 breast cancer patients, divided into 2 groups (A) based on low and high levels of the *HDMX-S/FL* ratio, and 3 groups (B) based on low, intermediate, and high levels of the *HDMX-S/FL* ratio.

ratios had mutant *TP53* or high *HDM2* levels (p=7.1E-7 Fisher's exact test, Figure 4.3B).

Together, these results generated in breast tumours and cancer cells demonstrate that the high levels of *HDMX* splicing in breast cancer associate with low HDMX protein levels and two different biomarkers of p53 pathway attenuation, namely *TP53* mutation and high HDM2 levels. They therefore lend strong support to the possibility that the *HDMX-S/FL* ratio could help further define the progression of breast cancer.

4.2.2 The *HDMX-S/FL* ratio interacts with *TP53* mutational status to further define individuals in their survival of breast cancer.

To begin to explore whether the *HDMX-S/FL* ratio can interact with *TP53* mutation status to define patients with different prognoses, patients were divided into 2 groups of high and low *HDMX-S/FL* ratios, whereby the high *HDMX-S/FL* ratio group consisted of tumours with *HDMX-S/FL* ratios above the mean. Specifically, 40 patients from the MicMa cohort and 22 patients from the ULL cohort were in the high *HDMX-S/FL* group, whilst 70 patients from MicMa cohort and 56 patients from the ULL cohort were in the low *HDMX-S/FL* ratio group. Thereafter, the breast cancer survival (BCS) of patients whose tumours had wt *TP53* was compared with those whose tumours had mutant *TP53*, in both groups of low and high *HDMX-S/FL* ratios. Interestingly, a significant difference in the survival of patients with wt and mutant *TP53* tumours was only observed in the group with low *HDMX-S/FL* ratios. Specifically, the survival of the MicMa patients with low *HDMX-S/FL* ratio and mutant *TP53* tumours was significantly shorter than those with wt *TP53* (p=0.009 log-rank test, Figure 4.4A). Indeed, mutant *TP53* in a low *HDMX-S/FL* ratio group associated with a 2.822-fold higher relative risk of tumour-related death, derived from Cox multivariate regression analysis that was adjusted to known independent prognostic factors of breast cancer including pathological node status and adjuvant systemic therapy (p=0.035, Table 4.1). A similar result of shorter survival time and increased risk of tumour-related death for patients with low *HDMX-S/FL* ratio and mutant *TP53* tumours was observed in the ULL cohort (p=0.003 log-rank test, Figure 4.4B; RR=14.846 p=3.6E-4, Table 4.1). Strikingly,

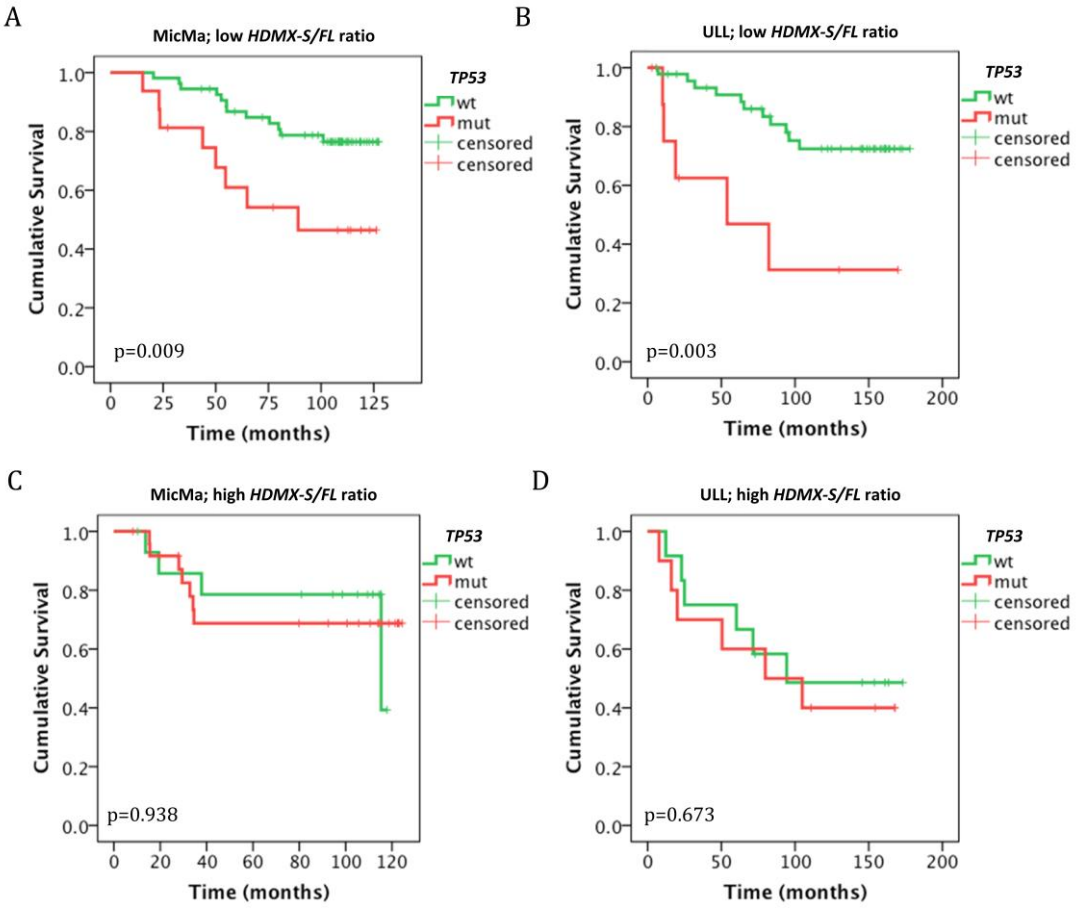


Figure 4.4 Wild-type *TP53* only associates with better clinical outcome of breast cancer patients in a low *HDMX-S/FL* ratio background in 2 cohorts.

A, Kaplan-Meier plot depicting the breast cancer survival of 70 patients from the MicMa cohort, whose tumours had low *HDMX-S/FL* ratios and either wt (n=54) or mutant (n=16) *TP53*. **B**, Kaplan-Meier plot depicting the breast cancer survival of 56 ULL cohort patients, whose tumours had low *HDMX-S/FL* ratios and either wt (n=47) or mutant (n=9) *TP53*. **C**, **D**, Kaplan-Meier plots depicting the breast cancer survival of 40 MicMa (C) and 22 ULL patients (D), whose tumours had high *HDMX-S/FL* ratios and either wt (n=15 MicMa, n=12 ULL) or mutant (n=25 MicMa, n=10 ULL) *TP53*. The p-values are derived from a log-rank test.

Table 4.1 Cox proportional regression analysis to predict the risk of tumour-related death for patients from individual MicMa and ULL cohorts.

	df	p value	RR	95% CI	
				Lower	Upper
MicMa; low *HDMX-S/FL* ratio					
TP53	1	0.035	2.822	1.077	7.393
pN	1	0.103	3.144	0.792	12.473
adjuvant systemic therapy	1	0.839	0.862	0.205	3.619
MicMa; high *HDMX-S/FL* ratio					
TP53	1	0.535	0.654	0.172	2.496
pN	1	0.064	4.312	0.92	20.208
adjuvant systemic therapy	1	0.031	0.18	0.038	0.854
ULL; low *HDMX-S/FL* ratio					
TP53	1	0.00036	14.846	3.372	65.355
pN	1	0.108	3.403	0.763	15.174
adjuvant systemic therapy	1	0.367	0.563	0.162	1.962
ULL; high *HDMX-S/FL* ratio					
TP53	1	0.851	0.877	0.224	3.438
pN	1	0.886	1.138	0.195	6.637
adjuvant systemic therapy	1	0.774	0.761	0.118	4.899

df- degrees of freedom; RR- relative risk; CI- confidence interval; pN- pathological node status

there was no difference in the survival time of patients with wt and mutant *TP53* tumours from high *HDMX-S/FL* ratio groups in either cohort (Figure 4.4C and 4.4D, Table 4.1).

Next, the overall survival time of the 191 patients from the MicMa and ULL cohorts was compared, in the same groupings of low and high *HDMX-S/FL* ratios, defined as described above for the individual cohorts. As above, in the group of low *HDMX-S/FL* ratios, the survival of patients with mutant *TP53* tumours was significantly shorter than those with wt *TP53* tumours (p=4.2E-5 log-rank test, Figure 4.5A), and associated with a 4.808-fold higher relative risk

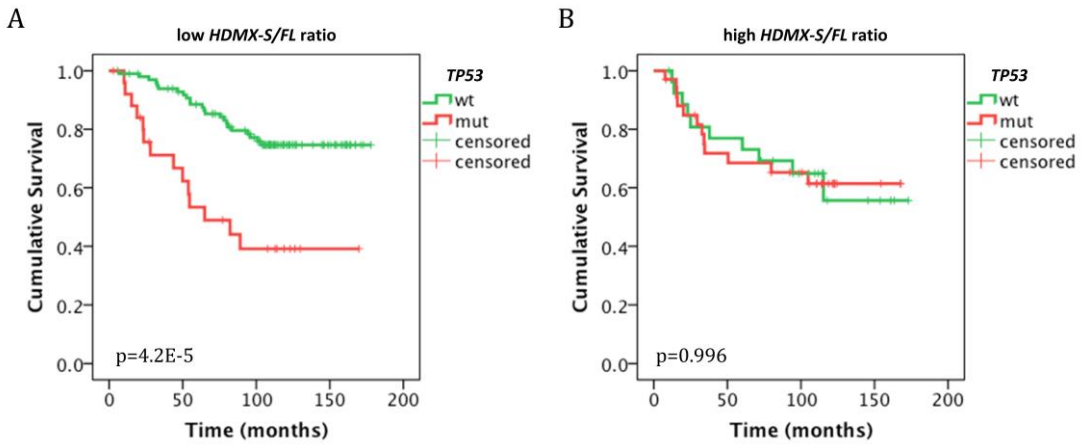


Figure 4.5 Meta-analysis of *HDMX-S/FL* ratio and *TP53* associations with breast cancer survival in the MicMa and ULL cohorts.

A, Kaplan-Meier plot depicting the breast cancer survival of 127 patients whose tumours had low *HDMX-S/FL* ratios and either wt (n=101) or mutant (n=26) *TP53*. **B**, Kaplan-Meier plot depicting the breast cancer survival of 61 patients whose tumours had high *HDMX-S/FL* ratios and either wt (n=27) or mutant (n=34) *TP53*. The p-values are derived from a log-rank test

Table 4.2 Cox proportional regression analysis to predict the risk of tumour-related death for patients from both breast cancer cohorts.

	df	p value	RR	95% CI	
				Lower	Upper
low *HDMX-S/FL* ratio					
TP53	1	0.000034	4.808	2.289	10.096
Lymph node status	1	0.037	2.786	1.065	7.287
adjuvant systemic therapy	1	0.306	0.6	0.226	1.595
high *HDMX-S/FL* ratio					
TP53	1	0.44	0.702	0.286	1.724
pN	1	0.094	2.409	0.86	6.745
adjuvant systemic therapy	1	0.021	0.292	0.102	0.833
df- degrees of freedom; RR- relative risk; CI- confidence interval; pN- pathological node status					

of tumour-related death (p=3.4E-5, Table 4.2). In contrast, there was no observed difference in the survival of patients with wt and mutant *TP53* tumours in the high *HDMX-S/FL* ratio group (Figure 4.5B and Table 4.2).

Another biomarker, estrogen receptor (ER) status, and a clinical parameter, adjuvant systemic treatment, have been suggested to interact with *TP53* mutational status to increase its prognostic value (Millar, Graham *et al.*, 2011). Thus, the possibility that these factors could affect the observed differences in the survival of patients with wt or mutant *TP53* tumours, in groups of low and high *HDMX-S/FL* ratios, was tested. Interestingly, the *HDMX-S/FL* ratio was the only factor that significantly interacted with *TP53* mutational status in the Cox proportional hazards model, to further define its prognostic value in the cohorts studied (p=0.02615, Table 4.3).

4.2.3 The *HDMX-S/FL* ratio and *TP53* mutational status predict breast cancer survival better than BC molecular subtypes

Microarray-based gene expression profiling has been very successful in developing a molecular classification system for breast cancer and prognostic multigene classifiers (Reis-Filho and Pusztai, 2011). The molecular subtype of either luminal A, luminal B, basal, ERBB2+ or normal-like was successfully determined for 172 patients using the PAM50 assay (Parker, Mullins *et al.*, 2009). As expected, low risk patients whose tumours were classified as luminal A had longer survival times than those with tumours classified as other subtypes, whereas high risk luminal B, basal and ERBB2+ subtype patients had the shortest survival time (p=0.007 log-rank test, Figure 4.6A). However, there were no differences in survival time between the high risk groups and the

Table 4.3 The interactions of *TP53* and the *HDMX-S/FL* ratio with other known prognostic factors to alter breast cancer survival[1].

	p value	
	TP53	***HDMX-S/FL* ratio**
TP53	na	0.02615
***HDMX-S/FL* ratio**	0.02615	na
Estrogen Receptor status	0.5284	0.3541
adjuvant systemic therapy	0.05789	0.0637

normal-like intermediate risk group, particularly in Cox multivariate regression analysis, whereby the only significant differences in survival time were observed between the low risk luminal A group and any of the high risk groups (Figure 4.6B).

In order to begin assessing the prognostic value of the two p53 pathway biomarkers in breast cancer, the MicMa and ULL patients were stratified into four groups based on the *TP53* mutational status and *HDMX-S/FL* ratio levels of their tumours: wt *TP53* with low *HDMX-S/FL* ratio; wt *TP53* with high *HDMX-S/FL* ratio; mutant *TP53* with low *HDMX-S/FL* ratio; and mutant *TP53* with high *HDMX-S/FL* ratio. Interestingly, 102 patients from the wt *TP53* low *HDMX-S/FL* ratio group had significantly longer survival times than patients from other groups, (p=0.001 log-rank test, Figure 4.6C) and a 5.014-fold lower relative risk of tumour-related death (p=2.23E-05, Figure 4.6D) than the 26 patients from the worst survival group, namely mutant *TP53* low *HDMX-S/FL* ratio. In five years, 11% of those patients from the wt *TP53* low *HDMX-S/FL* ratio group died

[1] Emmanouela Repapi, University of Oxford

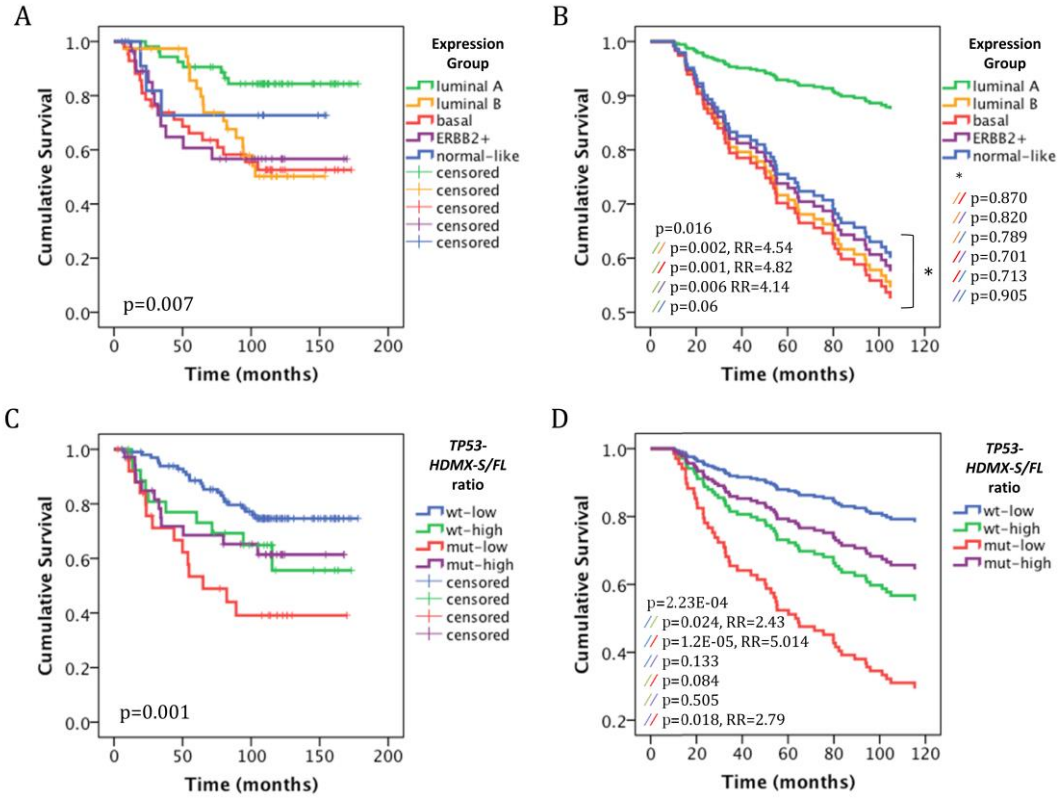


Figure 4.6 The *TP53* mutation status and *HDMX-S/FL* ratio define the breast cancer survival better than the known five molecular breast cancer subtypes.

A, a Kaplan-Meier plot depicting the breast cancer survival of 170 patients divided into five groups of different molecular subtypes, namely luminal A (n=53), luminal B (n=38), basal (n=42), ERB2+ (n=28) and normal-like (n=14). The p-value is derived from a log-rank test. **B**, predicted survival curves for patients with tumours from different molecular subtypes derived from a Cox multivariate regression analysis that was adjusted to the known independent prognostic factors of breast cancer, which included pathologic lymph node status and adjuvant therapy treatment; RR- relative risk. **C**, a Kaplan-Meier plot depicting the breast cancer survival of 188 patients divided into four groups depending on tumours' *TP53* status and *HDMX-S/FL* ratio levels, namely wt *TP53* with low *HDMX-S/FL* ratio (n=101), wt *TP53* with high *HDMX-S/FL* ratio (n=27), mutant *TP53* with low *HDMX-S/FL* ratio (n=26) and mutant *TP53* with high *HDMX-S/FL* ratio (n=34). The p-value is derived from log-rank test. **D**, predicted survival curves for patients with different *TP53* mutation status and different *HDMX-S/FL* ratios derived from a Cox multivariate regression analysis that was adjusted to the known independent prognostic factors of breast cancer, which included pathologic lymph node status and adjuvant therapy treatment; RR- relative risk.

of breast cancer, compared to 51% of those patients from the mutant *TP53* low *HDMX-S/FL* ratio group. These results suggest that *TP53-HDMX-S/FL* ratio grouping can better identify the distinct breast cancer risk groups than the molecular subtyping and can offer a novel poor survival biomarker for breast cancer.

4.2.4 The *HDMX-S/FL* ratio interacts with *TP53* mutational status to further define metastasis-free survival.

A loss of functional p53 is known to increase a tumour's ability to both metastasise and become resistant to DNA-damaging therapies (Royds and Iacopetta, 2006). To begin to assess whether the p53 pathway biomarker associations observed for BCS are a consequence of p53-dependent metastatic progression, time to metastasis survival analyses were performed. Interestingly, similar to that seen with BCS, *TP53* status associated with significant differences in metastasis-free survival time only in those patients whose tumours had low *HDMX-S/FL* ratios (p=0.003 log-rank test, Figure 4.7A), whereby patients whose tumours had mutant *TP53* were at a 3.44-fold higher relative risk of developing metastatic disease than patients whose tumours retained wt T*P53* (p=0.001 Table 4.4). There were no differences in metastasis-free survival time between patients whose tumours had either wt or mutant *TP53* in the high *HDMX-S/FL* ratio group (Figure 4.7B, Table 4.4).

Of the 191 patients from the MicMa and ULL cohorts, 103 patients had been treated with adjuvant therapies. Only 25 of these were treated with non-hormonal chemotherapeutics, thirteen of which received combination chemo- and radiotherapy, while a further 28 patients were treated with radiotherapy

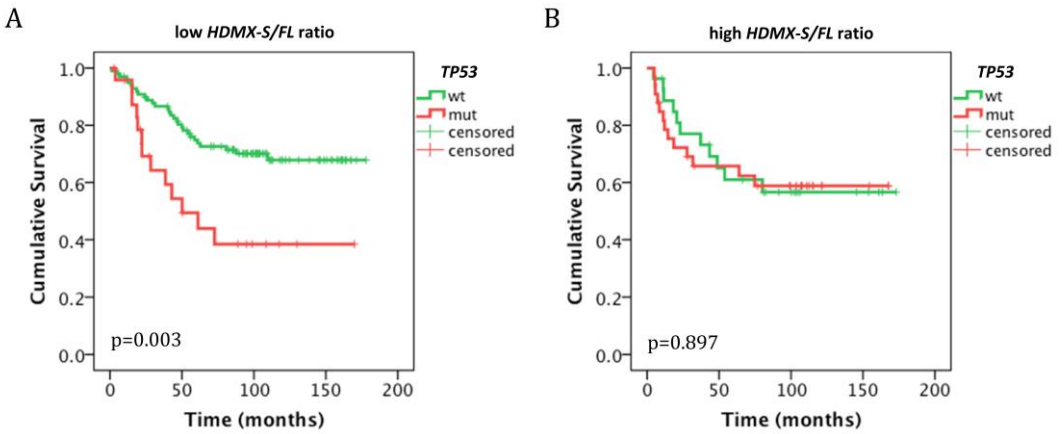


Figure 4.7 *TP53* mutation status and *HDMX-S/FL* ratio levels associate with differences in the metastatic progression of breast cancer patients.

A, Kaplan-Meier plot depicting the metastasis-free survival of 125 breast cancer patients, whose tumours had low *HDMX-S/FL* ratios and either wt (n=100) or mutant (n=25) *TP53*. **B**, Kaplan-Meier plot depicting the metastasis-free survival of 60 breast cancer patients whose tumours had high *HDMX-S/FL* ratios and either wt (n=27) or mutant (n=33) *TP53*. The p-values are derived from a log-rank test.

Table 4.4 Cox proportional regression analysis to predict the risk of metastatic progression for patients from both breast cancer cohorts.

	df	p value	RR	95% CI	
				Lower	Upper
low *HDMX-S/FL* ratio					
TP53	1	0.001	3.44	1.67	7.087
pN	1	0.043	2.564	1.029	6.39
adjuvant systemic therapy	1	0.469	0.711	0.283	1.788
high *HDMX-S/FL* ratio					
TP53	1	0.534	0.763	0.326	1.788
pN	1	0.017	3.595	1.251	10.327
adjuvant systemic therapy	1	0.006	0.232	0.081	0.663
df- degrees of freedom; RR- relative risk; CI- confidence interval; pN- pathological node status					

only. In order to assess whether p53 pathway biomarkers can have a predictive value for metastatic disease independent of adjuvant treatment or radiotherapy, time to metastasis survival analyses were performed on the 68 patients who did not receive any type of adjuvant treatment. Strikingly, similar associations to those described above were observed, whereby in the low *HDMX-S/FL* ratio group the metastatic progression of patients whose tumours had mutant *TP53* was significantly faster (p=0.011 log-rank test, Figure 4.8A), and these patients were at a 6.178-fold higher risk of developing metastatic disease than those with wt *TP53* (p=0.012, Table 4.5). Similar to the previously observed associations, there was no significant difference in survival time between patients whose tumours had either wt or mutant *TP53* in a high *HDMX-S/FL* group (p=0.606 log-rank test, Figure 4.8B, Table 4.5). These results suggest that the associations observed regarding the survival of breast cancer patients are independent of p53's role in mediating the response to DNA-damaging therapy, and are probably due to p53's role in preventing metastatic progression.

4.2.5 The *HDMX-S/FL* ratio associates with *HDMX* P2 promoter activity

Thus far, it has been demonstrated that the lower *HDMX-S/FL* ratio associates with wt *TP53* in soft tissue sarcomas and breast cancer tumours, as well as osteosarcoma cancer, breast and NCI60 panel cancer cell lines. However, the mechanism by which the activity of wt p53 affects the *HDMX-S/FL* ratio is unknown. To begin to investigate how the *HDMX-S/FL* ratio 'senses' p53 activity, the *HDMX-FL* and *HDMX–S* mRNA levels were compared in tumours of the 191 breast cancer patients with either wt *TP53* or mutant *TP53* in which

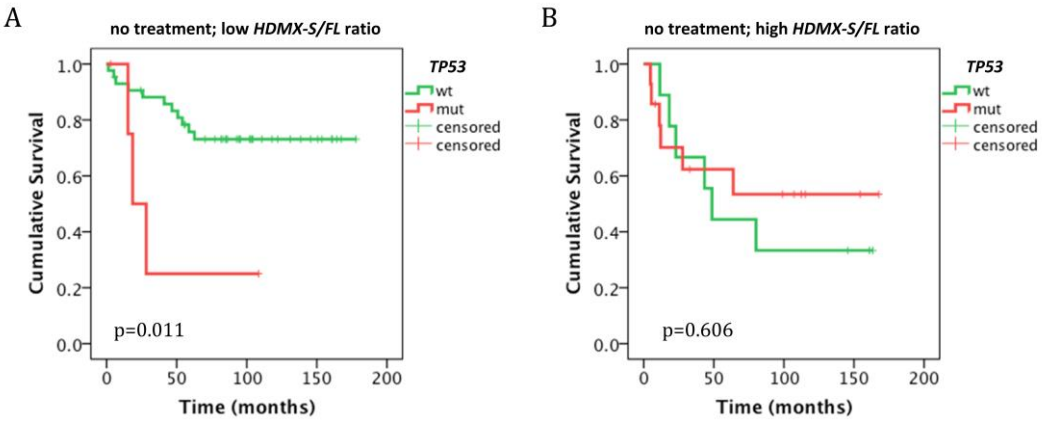


Figure 4.8 The associations of *TP53* mutation status and *HDMX-S/FL* ratio levels with metastatic progression in breast cancer are independent of treatment.

A, Kaplan-Meier plot depicting the metastasis-free survival of 45 breast cancer patients that did not receive any type of cancer treatment, and whose tumours had low *HDMX-S/FL* ratios and either wt (n=40) or mutant (n=5) *TP53*. **B**, Kaplan-Meier plot depicting the metastasis-free survival of 23 breast cancer patients that did not receive any type of cancer treatment, and whose tumours had high *HDMX-S/FL* ratios and either wt (n=9) or mutant (n=14) *TP53*. The p-values are derived from a log-rank test.

Table 4.5 Cox proportional regression analysis to predict the risk of metastatic progression for patients from both breast cancer cohorts who received no cancer treatment.

	df	p value	RR	95% CI	
				Lower	Upper
No treatment & low *HDMX-S/FL* ratio					
TP53	1	0.009	6.714	1.613	27.953
pN	1	0.885	0.856	0.103	7.111
No treatment & high *HDMX-S/FL* ratio					
TP53	1	0.376	0.589	0.183	1.902
pN	1	0.042	3.702	1.05	13.048

df- degrees of freedom; RR- relative risk; CI- confidence interval; pN- pathological node status

significant differences in *HDMX-S/FL* ratio levels had been observed earlier (Figure 4.2A). Interestingly, the mRNA levels of *HDMX-FL* were significantly higher in the 130 tumours with wt *TP53* than the 61 tumours with mutant *TP53* (p=0.0001 Mann-Whitney test, Figure 4.9A), whereas no differences in the mRNA levels of *HDMX-S* were observed in tumours with either wt or mutant *TP53* (p=0.927 Mann-Whitney test, Figure 4.9A). To investigate this further, *HDMX-FL* and *HDMX-S* mRNA levels were compared in the 36 cell lines of the breast cancer panel in which the significantly lower *HDMX-S/FL* ratio was in wt *TP53* cell lines than in mutant *TP53* cells was previously demonstrated (Figure 4.2B). Similarly to the result observed in the breast cancer tumours, the *HDMX-FL* mRNA levels of 8 wt *TP53* cell lines were significantly higher than those of 28 mutant *TP53* cell lines (p=0.02 unpaired t-test, Figure 4.8B), whereas no significant differences in levels of *HDMX-S* were observed (p=0.081 unpaired t-test, Figure 4.9B).

To further investigate the effect of active p53 on *HDMX-FL* and *HDMX-S* transcript levels and, in turn, on the *HDMX-S/FL* ratio, we treated MCF7 and ZR75-1 wt *TP53* breast cancer cells with Nutlin-3, which stabilises p53 through the inhibition of HDM2 (Vassilev, Vu *et al.*, 2004). Cells were harvested for RNA analysis 6 hours post Nutlin-3 treatment, and the mRNA levels of the p53 target p21 analysed to confirm Nutlin-3's effect on p53 activity (data not shown). The *HDMX* gene, similarly to its homolog *HDM2*, contains the p53-responsive promoter P2 (Phillips, Teunisse *et al.*, 2010). Therefore, to further confirm the success of the Nutlin-3 treatment and assess whether any changes in *HDMX* transcript levels were directly affected by p53, the *HDMX* transcripts specific to

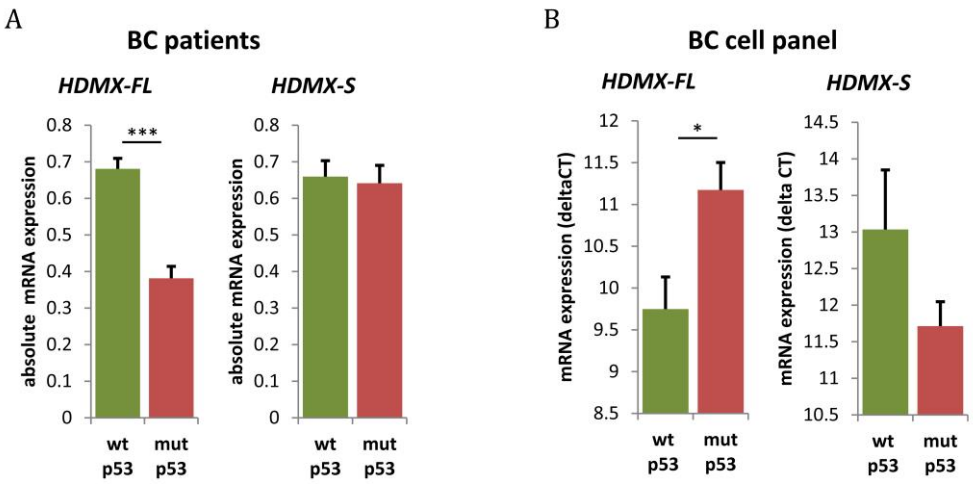


Figure 4.9 Analysis of *HDMX-S* and *HDMX-FL* expression in 191 breast cancer patients and 36 breast cancer cell lines.

A, **B**, column graphs depicting the average mRNA levels of *HDMX-S* and *HDMX-FL* in breast cancer tumours (A) and breast cancer cell lines (B). * $p<0.05$, *** $p<0.001$, denote the level of statistical significance derived from the Mann-Whitney test. Error bars depict the standard error of the means.

constitutive P1 and p53-responsive P2 promoters using custom-designed TaqMan probes were measured (Table 2.3). The *HDMX* mRNA levels from constitutively active promoter P1 in MCF7 cells were not affected by Nutlin-3 treatment ($p=0.13$ unpaired t-test, Figure 4.10A), whereas the activation of p53 by Nutlin-3 treatment resulted in a staggering 70.19-fold increase of the low abundance P2 promoter *HDMX* transcript ($p<0.0001$ unpaired t-test, Figure 4.10A). Similar results were observed in ZR75-1 cells, where Nutlin-3-treated cells had 53.52-fold higher levels of the *HDMX-P2* transcript than DMSO-treated cells ($p<0.0001$ unpaired t-test, Figure 4.10A), whereas *HDMX-P1* transcript levels were only 1.66-fold higher in Nutlin-3 treated cells than in DMSO control cells ($p= 0.0032$ unpaired t-test, Figure 4.10A).

Next, *HDMX-FL* and *HDMX-S* transcript levels were measured using specific TaqMan probes as described in Section 4.2.1, and the *HDMX-S/FL* ratio was also calculated. Strikingly, analysis of the individual *HDMX-FL* and *HDMX-S* transcripts revealed that activation of p53 results in a significant increase of *HDMX-FL* transcripts in both MCF7 and ZR75-1 cells, whereas the changes in *HDMX-S* transcript levels were only of a small magnitude. These results are in line with the results observed in breast cancer tumours and the breast cancer cell panel. Specifically, the *HDMX-FL* transcript levels in Nutlin-3-treated MCF7 cells were on average 2.83-fold higher than *HDMX-FL* transcript levels in DMSO-treated MCF7 cells ($p<0.001$ Mann-Whitney test, Figure 4.10B). Despite the significant differences, the *HDMX-S* transcript levels in Nutlin-3-treated MCF7 cells were of small magnitude (1.17-fold, $p=0.019$ unpaired t-test, Figure 4.10B). Similarly, the *HDMX-FL* levels in Nutlin-3-treated ZR75-1cells were on average 1.85-fold higher than in DMSO-treated cells ($p<0.001$ Mann-Whitney test, Figure 4.10B), whereas there were no differences in *HDMX-S* transcript levels ($p=0.93$ Mann-Whitney test, Figure 4.10B). Interestingly, the observed changes in *HDMX* transcript levels upon Nutlin-3 treatment resulted in a significantly lower *HDMX-S/FL* ratio in both MCF7 and ZR75-1 cells ($p=0.038$ Mann-Whitney test, $p=0.031$ unpaired t-test, MCF7 and ZR75-1 respectively, Figure 4.10C). Together, these results support a model where p53 activity affects the transcription of *HDMX*, which in turn results in changes in the levels of the *HDMX-S/FL* ratio.

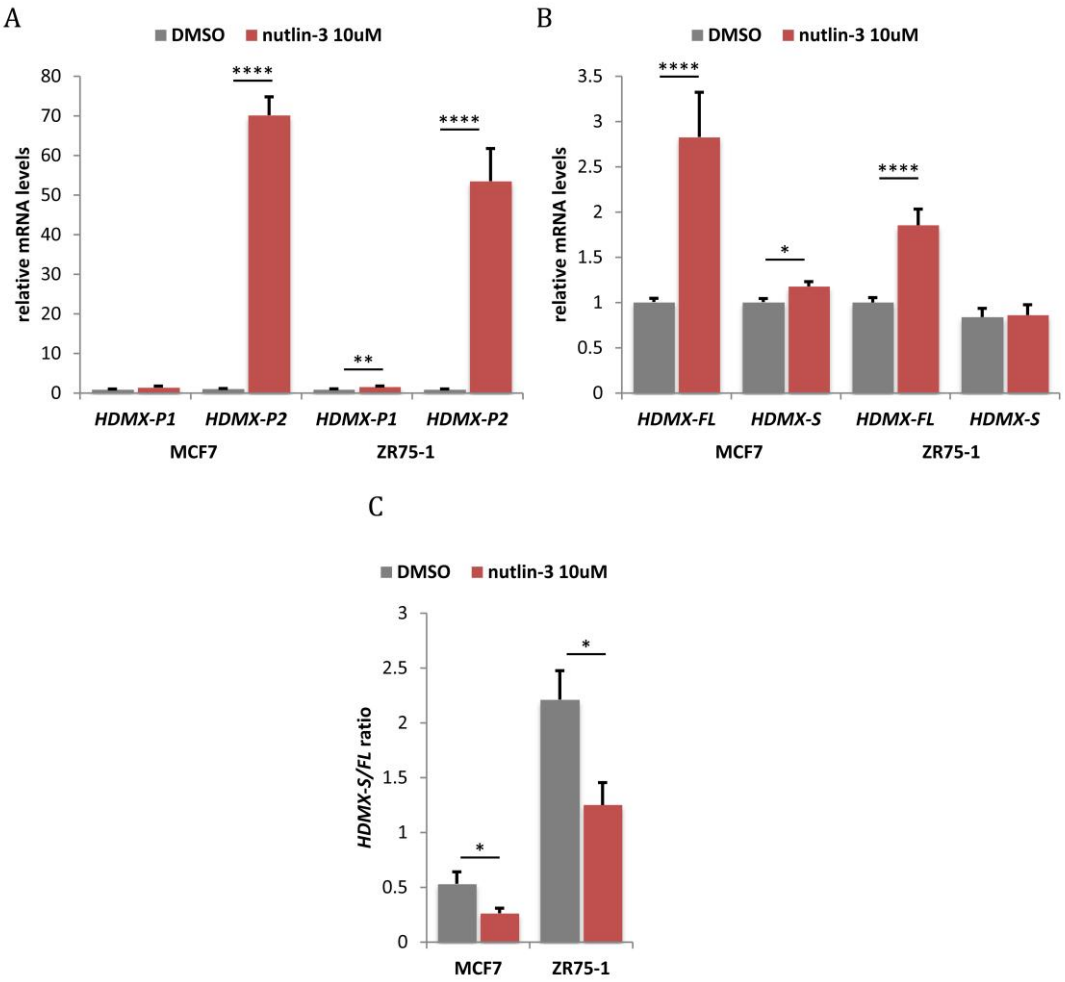


Figure 4.10 Analysis of *HDMX* RNA transcripts in Nutlin-3-treated wt *TP53* MCF7 and ZR75-1 breast cancer cells.

A, **B**, column graphs depicting the relative mRNA levels of *HDMX-P1* and *HDMX-P2* transcripts (A) and *HDMX-FL* and *HDMX-S* transcripts (B) in DMSO and Nutlin-3-treated MCF7 and ZR75-1 cells. **C**, column graph depicting the *HDMX-S/FL* ratio levels in DMSO and Nutlin-3 treated MCF7 and ZR75-1 cells. * $p<0.05$, ** $p<0.01$ **** $p<0.001$, denote the levels of statistical significance derived from the Mann-Whitney test and unpaired t-test. The error bars depict the standard error of the means from multiple experiments.

4.3 Discussion

The mutation of the *TP53* gene has been associated with the poor prognosis of multiple cancers. However, its prognostic value has been validated in only a relatively small number of breast cancer cohorts (Petitjean, Mathe *et al.*, 2007). In Chapter 3, a new biomarker was described: the *HDMX-S/FL* ratio, which associates with common somatic genetic lesions that lead to p53's inhibition (Lenos, Grawenda *et al.*, 2012). It was also demonstrated that in cancers like sarcomas, which have relatively low *TP53* mutation rates, the *HDMX-S/FL* ratio defines the progression of patients and also serves as a more effective prognostic biomarker than *TP53* mutation. In this chapter, the prognostic potential of the *HDMX-S/FL* ratio biomarker to define individuals in terms of the progression of their breast cancers was explored, and the association of the *HDMX-S/FL* ratio with p53 pathway attenuation was further investigated.

Consistent with the data from 115 cancer cell lines presented in Chapter 3, it has been demonstrated that high levels of *HDMX-S/FL* ratio associate with mutant *TP53* and high *HDM2* transcript levels in breast tumours, and drastically lower levels of HDMX full-length protein in breast cancer cells. Furthermore, the analyses of *HDMX* transcript levels in breast cancer tumours and cell lines, as well as in Nutlin-3-treated breast cancer cells, suggest that the low *HDMX-S/FL* ratio levels in wt *TP53* cells derive from a direct effect of functional p53 on the *HDMX* P2 alternative promoter, as reported previously by Phillips *et al*. (Phillips, Teunisse *et al.*, 2010). The authors of this study demonstrated that p53 activation leads to the induction of the P2 promoter on the *HDMX* gene, and the

transcription of a novel *HDMX-P2* mRNA that is more efficiently translated into a HDMX-L isoform that has reduced capacity to inhibit p53. While the HDMX-L isoform has an additional 18 amino acids at its N-terminus, the difference in mobility of HDMX-L and HDMX translated from *HDMX-P1* on SDS-polyacrylamide gels is very modest (Phillips, Teunisse *et al.*, 2010). It can therefore be speculated that the high HDMX protein levels observed in the osteosarcoma and breast cancer cell lines, with low levels of *HDMX-S/FL* ratio and wt p53 (Figures 3.2, 3.4 and 4.1), predominantly consists of the HDMX-L isoform, which is less efficient at inhibiting p53. These observations could explain why patients with wt p53 tumours and low *HDMX-S/FL* ratios, which associate with high protein levels of the p53 inhibitor HDMX, as presented in this chapter and Chapter 3, have better outcomes than those patients with low levels of HDMX as indicated by high *HDMX-S/FL* ratios. Nonetheless, the mechanism by which the *HDMX-S/FL* biomarker senses p53's activity needs to be further investigated to fully understand the potential of the *HDMX-S/FL* ratio as a biomarker for p53 pathway attenuation. In particular, an understanding of the mechanism that triggers *HDMX* alternative splicing is needed. Interestingly, a recent study on the role of PRMT5, a putative splicing regulator and transcriptional cofactor, in mammalian development demonstrated that *HDMX* pre-mRNA senses defects in the spliceosome machinery, leading to alternative splicing and elevated levels of *HDMX-S* mRNA, reduced levels of HDMX protein and transduction of the p53 signalling cascade (Bezzi, Teo *et al.*, 2013). Furthermore, the study's authors demonstrated that the degree of alternative splicing was even greater in those cells deficient in p53, and suggested that wt

p53 activation leads to a rapid elimination of cells with alternatively spliced *HDMX*. Indeed, in this study, the levels of *HDMX-S* in the Nutlin-3-treated breast cancer cells remained unchanged in contrast to elevated levels of *HDMX-FL* (Figure 4.10). How p53 is activated by alternatively spliced *HDMX*, and whether activated p53 leads to the elimination of cells with alternatively spliced *HDMX* rather than the inhibition of alternative splicing, requires further experimental investigation. Nonetheless, these observations together lend support to the model whereby the alternative splicing of *HDMX* can be a biomarker for p53 pathway attenuation (Figure 4.11). Finally, a better understanding of both the regulation of *HDMX* gene transcription and the function of different isoforms of HDMX protein and their ability to inhibit p53, especially in the context of wt and mutant p53, is essential to fully understand the functional mechanisms behind the ability of the *HDMX-S/FL* ratio to sense p53 pathway attenuation and define patients with different prognoses, while also identifying p53-specific nodes for personalised interventions to treat cancer.

In line with the results presented in Chapter 3, the observations made in two independent breast cancer cohorts suggest that the *HDMX-S/FL* ratio biomarker can serve as a marker for p53 pathway attenuation in breast tumours, and can further define the prognoses of patients with wt p53 tumours, whereby high *HDMX-S/FL* ratios identify tumours in which p53 is inhibited by other means. Indeed, when the patients studied were separated into those with wt or mutant *TP53* tumours, and survival differences between high, medium and low *HDMX-S/FL* ratio groups were compared, significant differences were only noted in wt *TP53* tumours, and those with high *HDMX-S/FL* ratios had

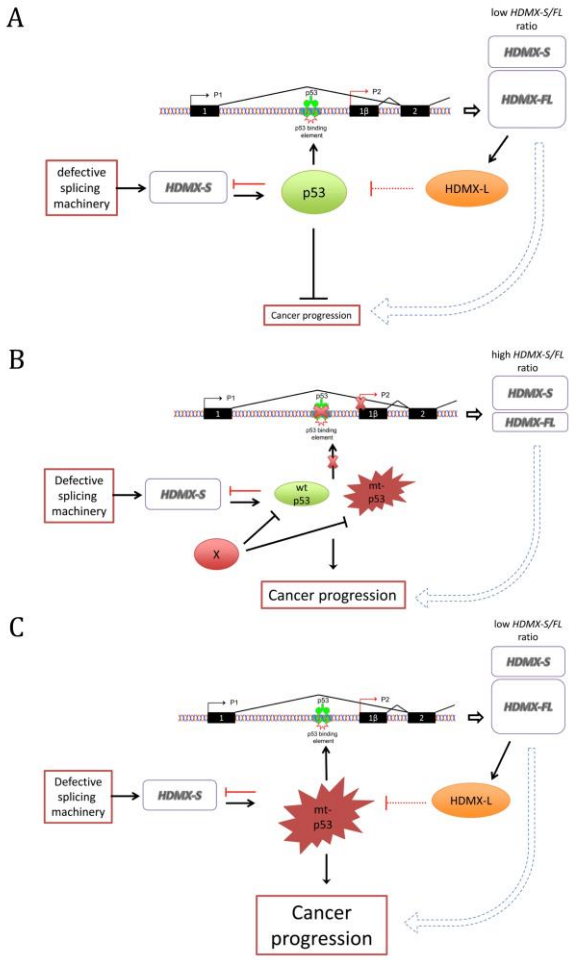


Figure 4.11 A schematic model depicting the interaction of p53 with the *HDMX* gene and its effect on *HDMX-S/FL* ratio levels and the risk of cancer progression.

A, low risk group associated with functional wt p53; wt p53 is activated as a result of defects in the splicing machinery and increased levels of alternatively spliced *HDMX*. The activation of p53 leads to p53-dependent *HDMX* transcription and clearance/inhibition of *HDMX-S*, which results in a decreased *HDMX-S/FL* ratio and higher levels of the HDMX-L protein, which is deficient in p53 inhibition. **B**, intermediate risk group associated with suppressed wt and mutant p53; wt and mutant p53 are inhibited by X, which represents any genetic alteration in the p53 pathway, e.g. high HDM2 levels that lead to the suppression of p53's function. As a result, p53-dependent transcription of the *HDMX* gene is suppressed and *HDMX-S* induced by defective splicing machinery remains at high levels. **C**, high risk group associated with active mutant p53; mutant p53 is activated as a result of defects in the splicing machinery and increased levels of alternatively spliced *HDMX*. The activation of p53 leads to p53-dependent *HDMX* transcription, which results in a decreased *HDMX-S/FL* ratio and higher levels of the HDMX-L protein, which is deficient in p53 inhibition.

shorter survival times. Over five years, 50% of those patients with wt *TP53* and a high *HDMX-S/FL* ratio died of breast cancer and 67% presented with metastases, compared to only 11% dying of breast cancer and 26% presenting with metastases in the wt *TP53* and low *HDMX-S/FL* ratio group (Figure 4.12). The attenuation of the p53 pathway has previously been demonstrated to associate not only with worse overall survival of breast cancer, but also with faster metastatic progression. Takahashi *et al.* demonstrated that p53-specific gene expression signatures define distinct groups of patients with different prognoses, whereby the mutant p53-like signature associates with faster metastatic progression (Takahashi, Moriya *et al.*, 2008). However, whether the observed association of p53 with the progression of breast cancer derived from an inhibitory role of functional p53 on cancer progression, rather than as an effect of adjuvant treatment, as p53 is an important mediator of DNA damage-inducing therapies, was not addressed in that study. In this chapter, the metastasis-free survival analyses on the subset of patients that did not receive adjuvant treatment demonstrated that the observed differences in survival time were independent of treatment, and are likely to be due to differences in the metastatic potential of breast tumours that are associated with p53 pathway attenuation. Notably, the combination of the *HDMX-S/FL* ratio biomarker and *TP53* mutation status can better define groups with different prognoses than the widely recognised microarray-based molecular subtype grouping of breast cancer, which is currently being introduced to the clinic to improve breast cancer patient management (Espinosa, Gamez-Pozo *et al.*, 2012). The gene expression profile-based molecular subtypes have the potential to predict both

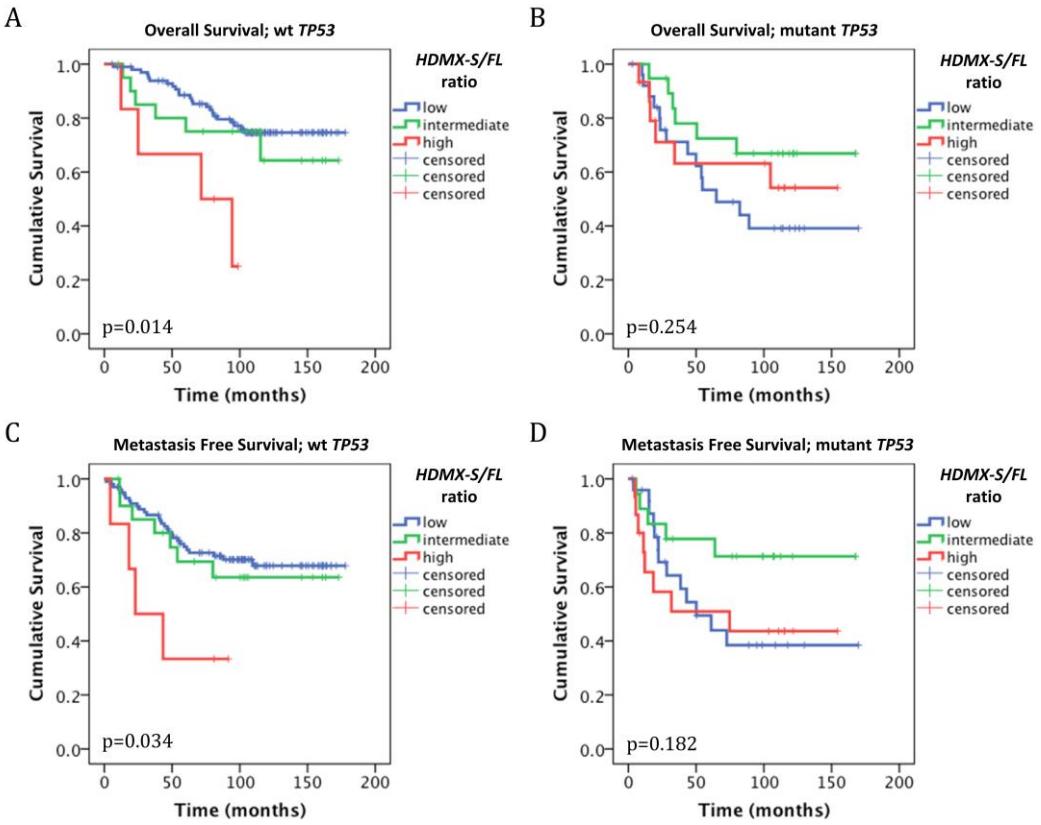


Figure 4.12 The *HDMX-S/FL* ratio further defines the prognosis of patients whose tumours have wt *TP53*.

A, **B**, Kaplan-Meier plots depicting the breast cancer survival of 128 patients with wt *TP53* tumours (A) and 60 patients with mutant *TP53* tumours (B), divided into three groups of low, intermediate and high *HDMX-S/FL* ratios. **C**, **D**, Kaplan-Meier plots depicting the metastasis-free survival of 128 patients with wt *TP53* tumours (C) and 58 patients with mutant *TP53* tumours (D), divided into three groups of low, intermediate and high *HDMX-S/FL* ratios. The p-values are derived from a log-rank test.

outcome as well as the metastatic potential of breast tumours (Langerod, Zhao *et al.*, 2007; Sorlie, Perou *et al.*, 2001). However, these signatures do not offer a direct predictive utility for personalised treatment strategies. In contrast, *TP53* mutation status and levels of *HDMX* splicing could be utilised to improve personalised interventions in breast cancer, as *TP53* mutation status and *HDMX* splicing can act as biomarkers for metastatic progression, and identify those

patients whose tumours have an attenuated p53 pathway and could therefore greatly benefit from p53 reactivating therapies. At the same time, these two biomarkers could more efficiently define those women with a functional p53 pathway and who are, therefore, at low risk of progression, for whom adjuvant treatment is unnecessary (Figure 4.11A). Based on the results presented in this chapter, as well as those in Chapter 3, it can be speculated that those women with wt *TP53* but a high *HDMX-S/FL* ratio are most likely have an attenuated p53 pathway, resulting from high HDM2 levels, and are therefore likely to be at a higher risk of metastatic progression (Figure 4.11B). Although the clinical efficacy and therapeutic advantage of the HDM2-targeted therapies that are currently in clinical trials has not yet been fully elucidated, *in vivo* animal models have demonstrated that Nutlin-3 is a potent activator of p53 activity that leads to the inhibition of tumour growth by 90%, but has few toxic effects on the animals treated (Vassilev, Vu *et al.*, 2004). Furthermore, Ventura *et al.* have demonstrated that the re-expression of p53 leads to up to 100% regression of autochthonous lymphomas and sarcomas in mice, with no p53-mediated cytotoxicity to normal organs (Ventura, Kirsch *et al.*, 2007). Thus, targeted therapy using HDM2 inhibitors could be used to inhibit or treat metastatic disease in this group of patients. On the other hand, high levels of p53 inhibitors, as marked by high *HDMX-S/FL* ratios in those patients whose tumours have mutant p53 (Figure 4.11B), indicate that higher levels of p53 inhibitors lead to the suppression of mutant p53. Indeed, it has previously been demonstrated that mutant p53, similarly to wt p53, is regulated by HDM2-mediated protein degradation, and that a lack of functional mdm2 in mice leads

to the stabilisation of mutant p53, an earlier age of tumour onset and a more aggressive phenotype (Terzian, Suh *et al.*, 2008). The results presented here, that patients with mutant p53 tumours but high levels of p53 inhibitors as marked by high *HDMX–S/FL* ratios have significantly better outcomes that those patients with mutant p53 tumours but low *HDMX-S/FL* ratios (Figure 4.6C and D), therefore lend evidence that mutant p53 can be suppressed by similar mechanisms to wt p53 in human cancers. Consequently, reactivation of wt p53 using either small molecule drugs that target mutant p53 or recombinant viruses should be used to treat patients with mutant p53 tumours, rather than targeted cancer therapies with HDM2 inhibitors. These two strategies, similar to HDM2 inhibitors, have had very promising results in the pre-clinical and clinical phases of their development and can lead to complete and durable remission (ClinicalTrials.gov; Senzer, Nemunaitis *et al.*, 2007; Vazquez, Bond *et al.*, 2008). They could, therefore, offer a very attractive alternative to genotoxic treatment strategies.

Together, these observations demonstrate that the *HDMX-S/FL* ratio can serve as a biomarker for p53 pathway attenuation, by means other than *TP53* mutation, in breast tumours. This lends further support to the role of the p53 pathway in breast cancer progression, and identifies a node of intervention for its prevention. In addition to breast cancer, the p53 pathway has been linked to the progression of other cancers like renal carcinoma, colon or ovarian cancer. However, due to inconsistencies in assessing p53 status, as well as the role of other pathway alterations in the attenuation of the p53 pathway, the role of p53 in the progression of these cancers remains inconclusive (Malats, Bustos *et al.*,

2005; Noon, Vlatkovic *et al.*, 2010; Tejpar, Bertagnolli *et al.*, 2010; Wang, Zheng *et al.*, 2004). Thus, *TP53* status and the *HDMX-S/FL* ratio potentially offer a prognostic tool that could lead to improvements in cancer management beyond that of breast cancer and sarcomas. Therefore, the observations reported in this chapter need to be extended, not only to more breast cancer cohorts, but also to other cancer types where p53 has been implicated in affecting prognostic outcome, to fully elucidate the clinical utility of the p53 pathway biomarkers.

5 SINGLE NUCLEOTIDE POLYMORPHISMS IN THE *HDMX* GENE ASSOCIATE WITH DIFFERENTIAL BREAST CANCER RISK AND PROGRESSION

5.1 Introduction

5.2 Results

5.2.1 The HDMX haplotype block is the most reproducible eQTL, and associates with differential cancer risk of the most types of cancer

5.2.2 The HDMX haplotype block associates with breast cancer survival

5.2.3 The HDMX SNP and HDMX-S/FL ratio

5.2.4 The HDMX SNP interacts with TP53 mutation and Estrogen Receptor status to define progression-free and overall survival of breast cancer patients

5.3 Discussion

5.1 Introduction

In Chapters 3 and 4 it was demonstrated that altered expression of the *HDMX* gene associates with different prognoses for sarcomas and breast cancer. A large body of evidence suggests that high frequency functional SNPs in the p53 network, some of which affect the transcription of the host gene, can lead to alterations in cancer risk, progression and survival (Bond, Hu *et al.*, 2004; Grochola, Zeron-Medina *et al.*, 2010). A large haplotype block of SNPs in the *HDMX* gene was identified in a study that screened SNPs across *HDMX* genes for signs of natural selection, which can be a characteristic of functional p53 pathway SNPs. Indeed, the identified haplotype demonstrates a deviation from standard assumptions of selective neutrality, whereby the major alleles of the haplotype block can be found in 67% of the Caucasian population. Further analysis revealed that neutral, non-selected alleles of the haplotype block associated with an earlier age of onset of familial and sporadic ovarian cancer, and an increased risk of developing breast cancer in the Ashkenazi Jewish population (Atwal, Kirchhoff *et al.*, 2009). Subsequently, the non-selected haplotype in the *HDMX* gene has also been reported to associate with an earlier age of onset of estrogen-negative breast cancer in two independent patient cohorts (Kulkarni, Vazquez *et al.*, 2009), as well as increased cancer risk, as noted by three different GWASs that included breast cancer risk in BRCA1 mutation carriers, estrogen receptor-negative breast cancer, and prostate cancer (CouchWang *et al.*, 2013; EelesOlama *et al.*, 2013; Garcia-ClosasCouch *et al.*, 2013). Moreover, alleles of the non-selected haplotype have been identified to associate with relatively higher levels of *HDMX* expression in seven different

expression quantitative trait loci (eQTL) studies, which, in total, were performed in 4 different tissue or cell types (LCLs, skin, monocytes, and B-cells) (Dimas, Deutsch *et al.*, 2009; Montgomery, Sammeth *et al.*, 2010; Nica, Parts *et al.*, 2011; Stranger, Nica *et al.*, 2007; Veyrieras, Kudaravalli *et al.*, 2008; Zeller, Wild *et al.*, 2010). Together, these observations suggest that the *HDMX* gene harbours a group of closely linked SNPs that alter gene expression, thereby resulting in differential cancer risk. Indeed, this haplotype block is a well-validated inherited biomarker of *HDMX* gene expression (Dimas, Deutsch *et al.*, 2009; Montgomery, Sammeth *et al.*, 2010; Nica, Parts *et al.*, 2011; Stranger, Nica *et al.*, 2007; Veyrieras, Kudaravalli *et al.*, 2008; Zeller, Wild *et al.*, 2010). Therefore, whether the SNPs in this haplotype block that affect cancer risk could also serve as prognostic biomarkers in cancers was investigated in this chapter, as the tumour biomarker for HDMX levels (the *HDMX S/FL* ratio, Chapters 3 and 4) had proved to be so successful.

5.2 Results

5.2.1 The *HDMX* haplotype block is the most reproducible eQTL, and associates with differential cancer risk of the most types of cancer

As mentioned above, the SNPs of the *HDMX* haplotype block were noted in multiple GWASs designed to identify cancer risk loci and expression quantitative trait loci. How many other genes in the genome also harbour SNPs that associate with altered expression levels and cancer risk in such diverse tissues and cell types was of interest. To investigate this, a collaboration was established with Douglas Bell, from The National Institute of Environmental Health Sciences (NIEHS), to take advantage of data generated from eQTL studies

that are designed to look genome wide for SNPs or groups of SNPs that associate with significant differences in transcript levels. The results of many of these studies are publicly available and, through additional collaborations, we curated eQTL data from 9 different studies that are mostly from European descents and have a sample size from 266 to 1490. These eQTL studies utilised 4 different cell types (LCLs, monocytes, B-cells, peripheral blood cells) and 4 different tissues (adipose, skin, liver and lung)(Brown, Mangravite *et al.*, 2013; Fairfax, Makino *et al.*, 2012; Fehrmann, Jansen *et al.*, 2011; Grundberg, Small *et al.*, 2012; Hao, Bosse *et al.*, 2012; Innocenti, Cooper *et al.*, 2011; Liang, Morar *et al.*, 2013; Schadt, Molony *et al.*, 2008; Zeller, Wild *et al.*, 2010). With these data, combined with the data from the genome-wide association studies (GWAS), all SNPs were sorted that reside either 10kb up- or –downstream from all currently annotated genes (5,381,122 SNPs) based on their association with differences in gene expression and cancer risk (Table 5.1). Dramatically, the three SNPs that associated with differential gene expression and cancer risk the most times to date belong to the *HDMX* haplotype block.

The reproducibility of the association of one of the HDMX SNPs (rs4245739) is particularly striking. Specifically, rs4245739 associates with differential *HDMX* transcript levels in 7 of the 12 eQTL studies, which were performed in 4 different tissue or cell types (LCLs, skin, monocytes, and B-cells). Moreover, rs4245739 is tightly linked to four SNPs from the *HDMX* haplotype that significantly associated with differential cancer risk in three different GWASs, which included breast cancer risk in BRCA1

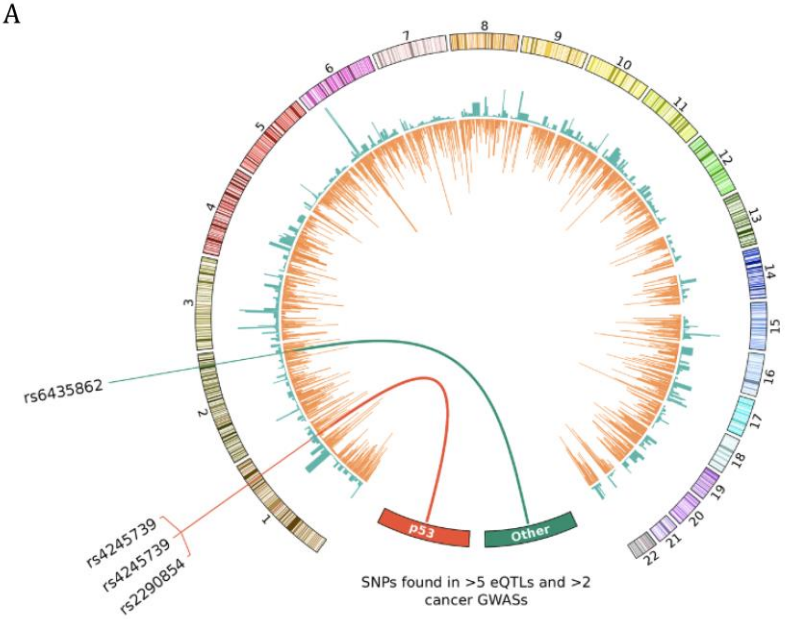
Table 5.1 Associations of 5,381,122 SNPs with cancer GWASs and eQTLs[1].

	>2 Cancers	2 Cancers	1 Cancer	No Cancers
eQTL in 4 Tissue Types	3	2	50	5,256
eQTL in 3 Tissue Types	4	8	91	11,585
eQTL in 2 Tissue Types	13	38	279	25,138
eQTL in 1 Tissue Type	68	683	3,742	254,487
Not in eQTL	243	1,494	12,396	5,065,542

mutation carriers, estrogen receptor-negative breast cancer, and prostate cancer (CouchWang *et al.*, 2013; EelesOlama *et al.*, 2013; Garcia-ClosasCouch *et al.*, 2013). Additional, two SNPs rs10900597 and rs2290854 in *HDMX* gene are also associated with *HDMX* transcript levels in 6 of the 12 eQTL studies, and are in strong LD with the 4 cancer GWAS SNPs. This highly reproducible and significant cancer-associated eQTL appears to be very rare in the genome, but enriched among 22,141 SNPs in or around (+/- 10kb) the 83 p53 pathway genes (p= 2.778e-07, Fisher's exact test, Figure 5.1). Utilising the same methodology and datasets, the 5,358,980 SNPs found in and around all the other annotated genes of the genome (n=25,534) were screened, and only one SNP rs6435862 in BARD1 gene was found to associate with differential transcript levels in 5 or more eQTL studies and 3 different cancer GWASs. Together, these data clearly demonstrate that the p53 pathway SNPs harbour a unique, highly reproducible and significant eQTL in the *HDMX* gene that reproducibly associates with differential cancer risk.

[1] Xuting Wang, The National Institute of Environmental Health Sciences

A



B

	83 p53 Genes	25,534 Other Genes
SNPs in >5 eQTLs and >2 cancerGWASs	3	1
SNPs not in >5 eQTLs and >2 cancerGWASs	22,139	5,358,980

p=2.78e-07

Figure 5.1 Highly reproducible cancer-associated eQTLs appear to be very rare in the genome, but significantly enriched among p53 pathway genes[1].

A, a Circos plot displaying the cancer GWAS SNPs and their proxies screened for their association with reproducible eQTLs. Chromosomes are arranged in a half-circle end-to-end with chromosome's cytobands in the outer ring. The location of the cancer GWAS SNPs are displayed in the blue inner ring and the eQTLs are displayed in the orange inner ring. The red line denotes the SNPs that reside in or around the 83 p53 pathway genes that were found in >5 eQTLs and >2 GWASs. Green line denotes the single SNP in the 25,534 other known genes in the genome that was also found to associate with differential transcript levels in 5 or more eQTL studies and 3 different cancer GWASs. **B**, a table indicating the significant enrichment of these SNPs in the p53 pathway and the p-value calculated by the Fisher's exact test.

[1] Xuting Wang, The National Institute of Environmental Health Sciences;
Francesc Castro-Giner, University of Oxford

5.2.2 The *HDMX* haplotype block associates with breast cancer survival

SNPs of the *HDMX* haplotype clearly associate with differential *HDMX* expression and cancer risk, whereby a total of four studies clearly showed associations in breast cancer (Atwal, Kirchhoff *et al.*, 2009; CouchWang *et al.*, 2013; Garcia-ClosasCouch *et al.*, 2013; Kulkarni, Vazquez *et al.*, 2009). However, given our results with the somatic biomarker of HDMX levels (the *HDMX S/FL* ratio), we wanted to explore whether or not this inherited HDMX biomarker would also associate with altered breast cancer progression in the same cohorts of patients, wherein the *HDMX S/FL* ratio was shown to be prognostic. To do so, a representative SNP (rs1563828) of the *HDMX* haplotype block was genotyped in 102 breast cancer patients from the MicMa cohort and 46 from the ULL breast cancer cohort, described in Chapter 4, for which genomic DNA was available for analysis. Fifty-one patients (50%) from the MicMa cohort were found to be G/G in genotype, 39 (38%) were A/G and 12 (12%) A/A, whereas in the ULL cohort 21 (46%) patients were G/G in genotype, 22 (47%) were A/G and 3 (6%) were A/A.

As mentioned above, in the eQTL studies the major alleles of the haplotype block were shown to associate with higher levels of *HDMX* expression compared to the minor alleles. Moreover, in the cancer GWAS studies, individuals with the minor alleles where shown to harbour increased cancer risk. Strikingly, the patients homozygous for the minor allele (A/A genotype) also associate with the fastest metastatic progression and shortest overall survival in both the MicMa and ULL cohorts. Specifically, the metastasis-free survival of 12 MicMa patients homozygous for the A allele of the HDMX SNP was

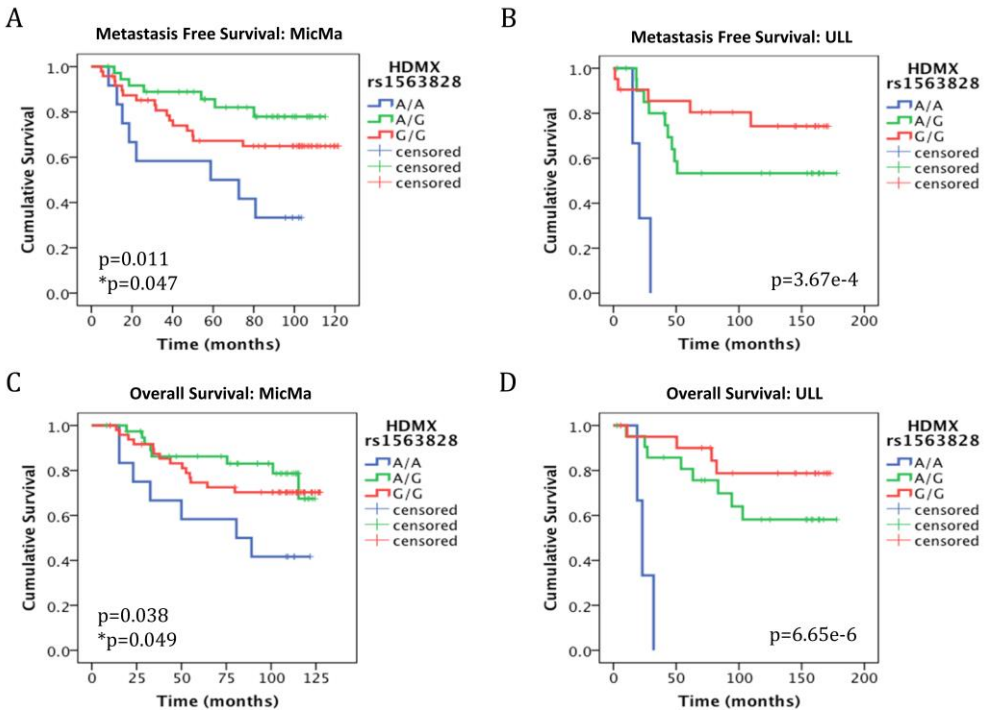


Figure 5.2 The HDMX SNP associates with altered clinical outcome of breast cancer patients.

A, Kaplan-Meier plot depicting the metastasis free survival of 97 patients from the MicMa cohort with either the A/A (n=12), A/G (n=37) or G/G (n=48) genotype of the HDMX SNP. **B**, Kaplan-Meier plot depicting the metastasis free survival of 46 patients from the ULL cohort with either the A/A (n=3), A/G (n=22) or G/G (n=21) genotype of the HDMX SNP. **C**, Kaplan-Meier plot depicting the breast cancer survival of 100 patients from the MicMa cohort with either the A/A (n=12), A/G (n=39) or G/G (n=49) genotype of the HDMX SNP. **D**, Kaplan-Meier plot depicting the breast cancer survival of 46 patients from the ULL cohort with either the A/A (n=3), A/G (n=22) or G/G (n=21) genotype of the HDMX SNP. The p-value is derived from a log-rank test. The p-value depicted by * is derived through the comparison of patients A/A and G/G in genotype.

significantly shorter than that of 90 patients who were A/G or G/G in genotype (p=0.011 log-rank test, Figure 5.2A). Likewise, the metastasis free survival of 3 ULL patients who were A/A in genotype was significantly shorter than the survival of the remaining 43 patients with either A/G or G/G genotypes (p=3.67E-4 log-rank test, Figure 5.2B). Similar significant associations were

observed with overall survival, whereby the survival of A/A genotype patients in both the MicMa and ULL cohorts was significantly shorter than that of patients A/G or G/G in genotype (p=0.038 and p=6.65E-6 MicMa and ULL respectively, Figure 5.2C and 5.2D).

The significant association of the A/A genotype with faster metastatic progression and shorter overall survival was further confirmed by analysis of all 148 patients from both the MicMa and ULL cohorts, where 72 patients were G/G in genotype (49%), 61 (41%) A/G and 15 (10%) A/A. As expected from the associations observed in the individual cohorts, the metastasis free survival of 15 patients homozygous for the A allele of the HDMX SNP was significantly shorter than that of 59 patients who were A/G in genotype and 69 patients G/G in genotype (p=0.001 log rank test, Figure 5.3A). Similarly, the overall survival of 15 patients who were A/A in genotype was significantly shorter than that of patients G/G in genotype (p=0.001 log-rank test, Figure 5.3B). The observed significant associations of the A/A genotype of the HDMX SNP with shorter metastasis-free and overall survival are further supported by Cox proportionate multivariate regression analysis, adjusted for known independent prognostic markers in breast cancer, namely pathological lymph node status (pN) and adjuvant therapy (Table 5.2). Specifically, patients A/A in HDMX SNP genotype associated with a 3.9-fold higher relative risk of progression to metastatic disease than patients G/G in genotype (p=0.0004, Table 5.2). Similarly, the A/A genotype associated with a 4.5-fold higher relative risk of tumour-related death than the G/G genotype (p=0.00027, Table 5.2).

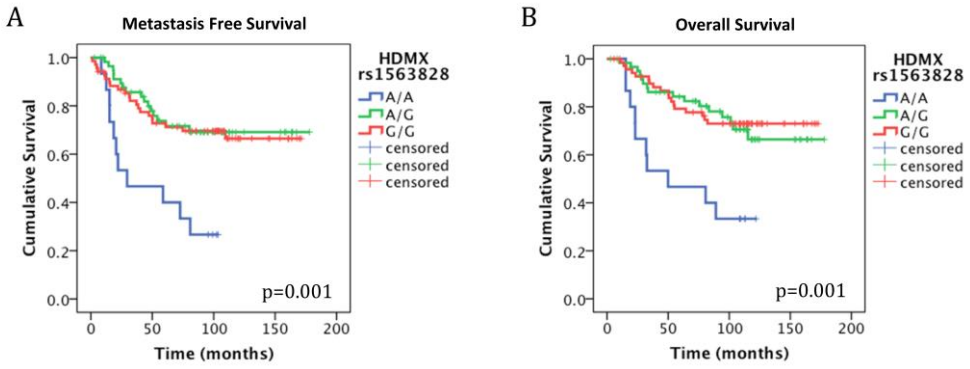


Figure 5.3 Meta-analysis of HDMX SNP associations with metastasis free survival and breast cancer survival in the MicMa and ULL cohorts.

A, Kaplan-Meier plot depicting the metastasis free survival of 143 patients A/A (n=15), A/G (n=59) or G/G (n=69) in genotype of the HDMX SNP. **B**, Kaplan-Meier plot depicting the breast cancer survival of 146 patients A/A (n=15), A/G (n=61) or G/G (n=70) genotype of the HDMX SNP. The p-value is derived from a log-rank test.

Table 5.2 Cox proportional regression analysis of patients from the MicMa and ULL cohorts.

	Metastasis Free Survival						Overall Survival					
	N	df	p value	RR	95.0% CI for RR		N	df	p value	RR	95.0% CI for RR	
					Lower	Upper					Lower	Upper
rs1563828 A/A	15	2	0.00045				15	2	0.001			
rs1563828 A/G	52	1	0.00041	0.231	0.102	0.52	54	1	0.001	0.254	0.111	0.578
rs1563828 G/G	61	1	0.00044	0.254	0.119	0.546	61	1	0.00027	0.222	0.099	0.5
pN -ve	59						60					
pN +ve	69	1	0.018	2.632	1.177	5.887	70	1	0.013	2.759	1.235	6.163
Adjuvant Therapy -ve	52						53					
Adjuvant Therapy +ve	76	1	0.2	0.595	0.269	1.315	77	1	0.088	0.505	0.23	1.108

pN- pathological lymph node status; df- degrees of freedom; RR- relative risk; CI- confidence interval

5.2.3 The HDMX SNP and *HDMX-S/FL* ratio

The eQTL studies provide strong evidence that a functional SNP from the *HDMX* haplotype block results in altered *HDMX* expression, whereas the work presented in Chapters 3 and 4 demonstrates that *HDMX* expression levels (measured as the *HDMX-S/FL* ratio) affects the progression of cancers like

sarcoma and breast cancer. Thus, whether the interaction of the HDMX SNP with the described HDMX biomarker could better define breast cancer tumours with regard to their metastatic potential was investigated. Furthermore, it was reasoned that cancer cells from individuals with the risk alleles of this haplotype block may be more likely to retain the oncogenic activity of HDMX and, therefore, harbour lower *HDMX-S/FL* ratios. To test this, the average *HDMX-S/FL* ratios for each genotype of the HDMX SNP were first compared. Interestingly, the average *HDMX-S/FL* ratio was the lowest in tumours of individuals A/A in genotype. Specifically, tumours of 15 patients A/A in HDMX SNP genotype had an average *HDMX-S/FL* ratio that was 1.3-fold lower than the average *HDMX-S/FL* ratio of tumours from 72 patients G/G in HDMX SNP genotype. However, the observed differences in the average *HDMX-S/FL* ratios in tumours with different genotypes were not significant (p=0.351 Mann-Whitney test, data not shown).

Thereafter, whether or not the *HDMX-S/FL* ratio affects the observed HDMX SNP associations with metastasis-free survival of breast cancer patients was explored. To do so, differences in the survival of patients with different genotypes of the HDMX SNP in two groups of low and high *HDMX-S/FL* ratios were assessed. Significant differences in metastasis-free and overall survival in patients with different HDMX SNP genotypes were observed only in the group of patients with low *HDMX-S/FL* ratios. However a clear trend in altered metastasis free survival and the overall survival of patients with different HDMX SNP genotypes was also seen in the group with high *HDMX-S/FL* ratios,

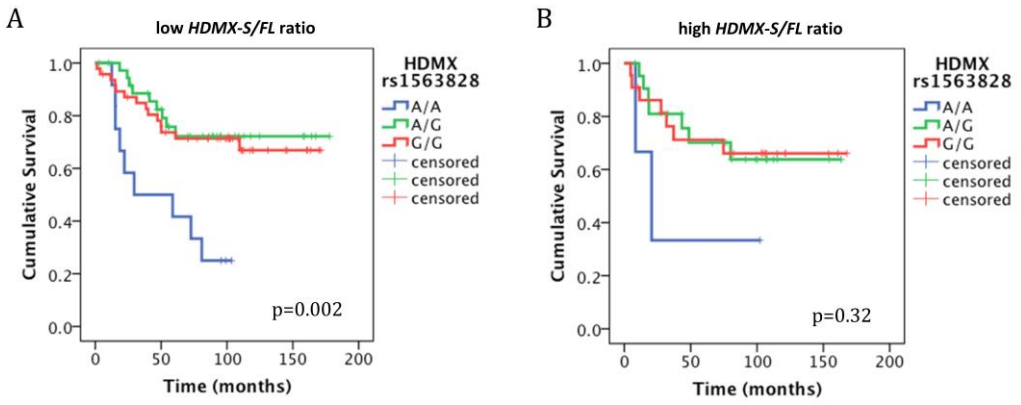


Figure 5.4 The associations of the HDMX SNP with altered clinical outcome of breast cancer patients are independent of the *HDMX-S/FL* ratio.

A, Kaplan-Meier plot depicting the metastasis free survival of 96 patients whose tumours had low *HDMX-S/FL* ratios and had A/A (n=12), A/G (n=37) or G/G (n=47) genotypes of the HDMX SNP. **B**, Kaplan-Meier plot depicting the metastasis free survival of 49 patients whose tumours had high *HDMX-S/FL* ratios and had A/A (n=3), A/G (n=22) or G/G (n=22) genotypes of the HDMX SNP. The p-value is derived from a log-rank test.

suggesting that *HDMX-S/FL* ratio does not cooperate with the HDMX SNP to define the metastatic potential of breast cancer (Figure 5.4).

5.2.4 The HDMX SNP interacts with *TP53* mutation and Estrogen Receptor status to define metastasis-free and overall survival of breast cancer patients

As mentioned above, studies in cohorts of breast and ovarian cancers, as well as two recent GWAS studies, suggest that the associations of the HDMX SNPs with cancer risk could depend on the absence of expression of the estrogen receptor (ER) (CouchWang *et al.*, 2013; Garcia-ClosasCouch *et al.*, 2013; Kulkarni, Vazquez *et al.*, 2009). ER status was determined for 146 of 148 breast cancer tumours with known HDMX SNP genotypes. Specifically, 94 (64%) tumours had positive ER status and 52 (36%) had negative ER status.

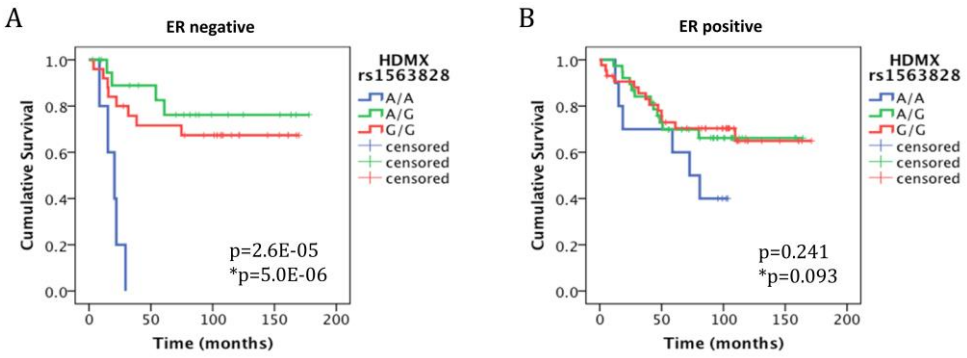


Figure 5.5 The HDMX SNP interacts with the tumour's estrogen receptor status to alter the clinical outcome of breast cancer patients.

A, Kaplan-Meier plot depicting the metastasis free survival of 51 patients whose tumours had estrogen receptor- negative status and were A/A (n=5), A/G (n=21) or G/G (n=25) in genotypes for the HDMX SNP. **B**, Kaplan-Meier plot depicting the metastasis free survival of 91 patients whose tumours had estrogen receptor- positive status and were A/A (n=10), A/G (n=38) or G/G (n=43) in genotype for the HDMX SNP. The p-value is derived from a log-rank test. The p-value depicted by * symbol is derived through the comparison of patients A/A and G/G in genotype.

Whether the ER status of the tumour interacts with the HDMX SNP to further define the progression of breast cancer patients was, therefore, investigated. To do so, the 146 patients were divided into two groups of ER-positive and ER-negative tumours. Interestingly, in line with the risk association studies, significant differences in progression free survival of patients with different HDMX SNP genotypes were only observed in the group of patients with ER-negative tumours (Figure 5.5A), whereas there were no significant differences in the progression free survival of ER-positive patients (Figure 5.5B). Specifically, the metastatic progression of patients A/A in genotype was significantly faster than that of patients who were A/G or G/G (p=2.6E-5 log-rank test, Figure 5.5A), whereby patients homozygous for the A allele of the HDMX SNP were at a 6.13-fold higher risk of metastatic disease than patients

Table 5.3 Cox proportional regression analysis of patients whose tumours had either positive or negative estrogen receptor status.

	ER positive						ER negative					
	N	df	p value	RR	95.0% CI for RR		N	df	p value	RR	95.0% CI for RR	
					Lower	Upper					Lower	Upper
rs1563828 A/A	10	2	0.087				5	2	0.01			
rs1563828 A/G	36	1	0.061	0.373	0.133	1.048	16	1	0.008	0.129	0.028	0.582
rs1563828 G/G	36	1	0.035	0.326	0.115	0.924	24	1	0.005	0.163	0.046	0.581
pN -ve	37						21					
pN +ve	45	1	0.018	3.897	1.261	12.05	24	1	0.557	1.488	0.394	5.612
Adjuvant Therapy +ve	29						22					
Adjuvant Therapy +ve	53	1	0.021	0.278	0.094	0.826	23	1	0.629	1.405	0.354	5.574
pN- pathological lymph node status; df- degrees of freedom; RR- relative risk; CI- confidence interval												

homozygous for the G allele (p=0.005, Table 5.3).

ER-negative tumours are often enriched for *TP53* mutation (Troester, Herschkowitz *et al.*, 2006). Indeed, 54% of ER-negative tumours had mutant *TP53*, in contrast to only 21% of ER-positive tumours (p<0.0001 Fishers exact test, Figure 5.6A). To explore the possibility that the observed association of the HDMX SNP and ER status with altered progression of breast cancer patients could be an effect of the interaction of the HDMX SNP with *TP53* mutation status, the survival of patients with the individual HDMX SNP genotypes were compared in two groups of wt and mutant *TP53*. Of 148 tumours, 100 (68%) had wt *TP53* and 48 (32%) had mutant *TP53*. Indeed, the above-mentioned association of the HDMX SNP with metastasis free survival was only significant in a group of patients with mutant *TP53* (Figure 5.6B) and not in that with wt *TP53* (Figure 5.6C). Specifically, the metastatic progression of patients A/A in HDMX SNP genotype was significantly faster than that of patients A/G or G/G in genotype (p=0.0002 log-rank test, Figure 5.6B), whereby the A/A genotype associated with a 4.5-fold higher risk of progression to metastatic disease than

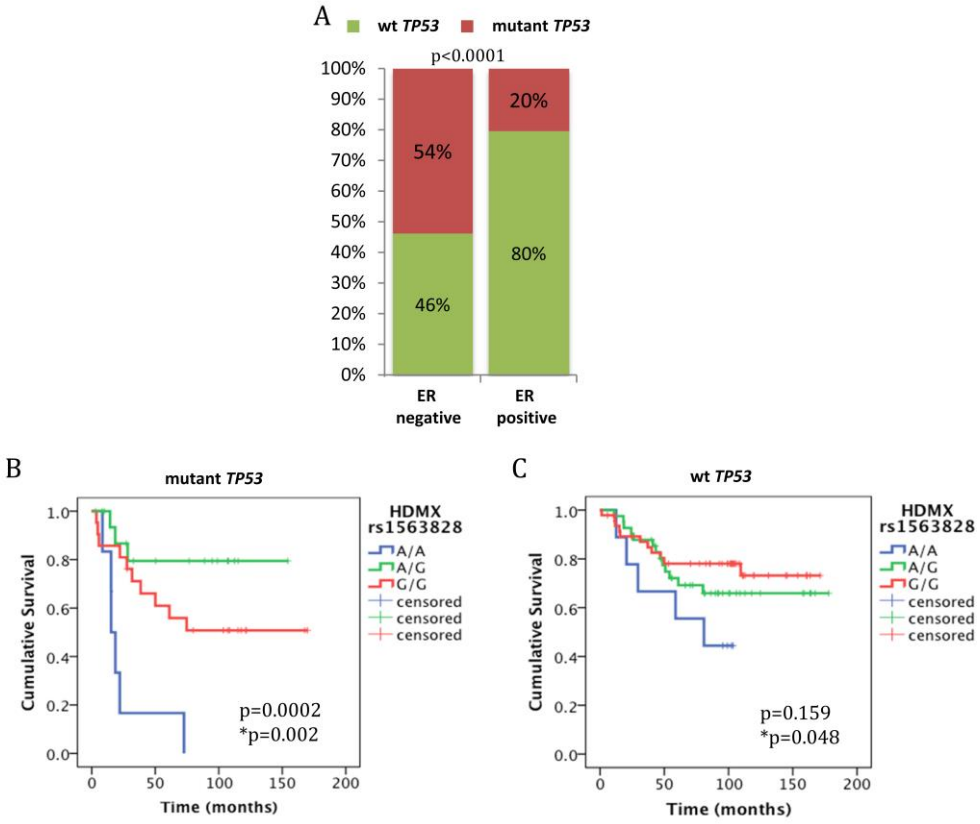


Figure 5.6 The interaction of the HDMX SNP with tumour estrogen receptor status to alter the clinical outcome of breast cancer patients can be dependent on *TP53* mutation status.

A, column graph depicting the enrichment of wt *TP53* in tumours with estrogen-positive status, the p value is derived from Fisher's exact test. **B**, Kaplan-Meier plot depicting the metastasis free survival of 45 patients whose tumours had mutant *TP53* and were A/A (n=6), A/G (n=18) or G/G (n=21) in genotype for the HDMX SNP. **C**, Kaplan-Meier plot depicting the metastasis free survival of 98 patients whose tumours had wt *TP53* and were A/A (n=9), A/G (n=41) or G/G (n=48) in genotype for the HDMX SNP. The p-value (B, C) is derived from a log-rank test. The p-value depicted by * symbol is derived through the comparison of patients A/A and G/G in genotype.

Table 5.4 Cox proportional regression analysis of the risk of metastatic progression in patients whose tumours had either wt or mutant *TP53* status.

	wt *TP53*						mutant *TP53*					
	N	df	p value	RR	95.0% CI for RR		N	df	p value	RR	95.0% CI for RR	
					Lower	Upper					Lower	Upper
rs1563828 A/A	9	2	0.156				6	2	0.002			
rs1563828 A/G	36	1	0.136	0.434	0.145	1.302	16	1	0.001	0.065	0.012	0.345
rs1563828 G/G	41	1	0.055	0.334	0.109	1.025	20	1	0.006	0.22	0.074	0.651
pN -ve	40						19					
pN +ve	46	1	0.477	1.455	0.518	4.086	23	1	0.01	7.937	1.628	38.702
Adjuvant Therapy +ve	36						16					
Adjuvant Therapy +ve	50	1	0.975	1.016	0.365	2.827	26	1	0.015	0.137	0.028	0.682
pN- pathological lymph node status; df- degrees of freedom; RR- relative risk; CI- confidence interval												

the G/G genotype (p=0.006, Table 5.4).

To further analyse the observed interaction of the HDMX SNP with the *TP53* mutation, the breast cancer patients were stratified into four groups based on their *TP53* status and homozygous genotype of the HDMX SNP, and their progression to metastatic disease was compared. As expected, the patients A/A in genotype with mutant *TP53* tumours developed metastatic disease significantly faster than patients from other groups (p=7.0E-6 log-rank test, Figure 5.7), and associated with a 11.6-fold higher risk of developing the metastatic disease than patients G/G in genotype and wt *TP53* tumours (p=1.1E-5, Table 5.5). Together, these results lend strong support to the hypothesis that an inherited polymorphism in the *HDMX* gene, which associates with altered gene expression and cancer risk, can also affect the progression of cancer and, together with somatic lesions like *TP53* mutation and ER status, can serve as a prognostic biomarker.

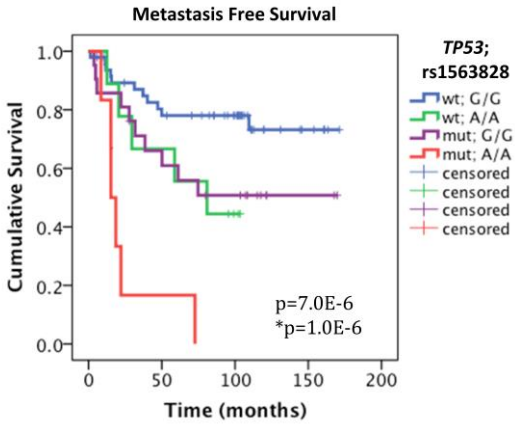


Figure 5.7 The HDMX SNP interacts with *TP53* mutation status to predict the metastatic potential of the tumour.

Kaplan-Meier plot depicting the metastasis free survival of 84 patients whose tumours had wt *TP53* status and the G/G genotype of the HDMX SNP (n=48), wt *TP53* and A/A genotype (n=9), mutant *TP53* and G/G genotype (n=21) and mutant *TP53* and A/A genotype (n=6). The p-value is derived from a log-rank test. The p-value depicted by * symbol is derived through the comparison of patients A/A in genotype with mutant *TP53* tumours and patients G/G in genotype with wt *TP53* tumours.

Table 5.5 Cox proportional regression analysis of the risk of metastatic progression in patients A/A or G/G in HDMX SNP genotype, whose tumours had either wt or mutant *TP53* status.

	N	df	p value	RR	95.0% CI for RR	
					Lower	Upper
wt *TP53*; rs1563828 G/G	41	3	0.000141			
wt *TP53*; rs1563828 A/A	9	1	0.00795	4.720415	0.066	0.816
mut *TP53*; rs1563828 G/G	20	1	0.045871	2.616	0.9	11.986
mut *TP53*; rs1563828 A/A	6	1	0.000011	11.613	0.182	2.183
pN -ve	32					
pN +ve	44	1	0.002	7.862	2.17	28.48
Adjuvant Therapy +ve	29					
Adjuvant Therapy +ve	47	1	0.035	0.274	0.082	0.911
pN- pathological lymph node status; df- degrees of freedom; RR- relative risk; CI- confidence interval						

5.3 Discussion

In this chapter, the inherited haplotype block in the *HDMX* oncogene was demonstrated to be a unique, highly reproducible eQTL that associates with cancer risk. Studies on polymorphisms in the *TP53* gene (Arg72Pro) have previously demonstrated that functional polymorphisms in the p53 pathway associate with faster progression of breast cancer patients (Toyama, Zhang *et al.*, 2007), and can also be predictive of primary chemotherapeutic resistance and shorter progression-free survival of advanced non-small cell lung cancer patients (Han, Lee *et al.*, 2008). However, despite the strong associations with cancer risk and the altered expression levels of the *HDMX* oncogene, no evidence has been presented to date about the effect of the *HDMX* haplotype block on either cancer progression or overall survival.

The data presented here demonstrate that a proxy SNP from the *HDMX* haplotype block can predict different prognoses of breast cancer in two independent patient cohorts, whereby the minor A-allele of the HDMX rs1563828 SNP, which has been shown to associate with an increased risk of breast, ovarian and prostate cancer (Atwal, Kirchhoff *et al.*, 2009; CouchWang *et al.*, 2013; Garcia-ClosasCouch *et al.*, 2013; Kulkarni, Vazquez *et al.*, 2009) and lower levels of *HDMX* gene expression (Dimas, Deutsch *et al.*, 2009; Montgomery, Sammeth *et al.*, 2010; Nica, Parts *et al.*, 2011; Stranger, Nica *et al.*, 2007; Veyrieras, Kudaravalli *et al.*, 2008; Zeller, Wild *et al.*, 2010), strongly associates with an increased risk of metastatic progression. Furthermore, it is demonstrated here that the previously observed associations of the HDMX SNP with ER status and cancer risk can be a consequence of mutant *TP53*

enrichment in ER-negative tumours. Indeed, a growing body of evidence supports a role of mutant p53 not only in tumourigenesis and tumour clearance, but also in accelerating the metastatic potential of cancer cells, whereby mutant p53 through gain of function inhibits p63, which is an important suppressor of the invasive phenotype of cancer cells (Adorno, Cordenonsi *et al.*, 2009; Melino, 2011; Muller, Caswell *et al.*, 2009). Studies on genetically engineered mice have demonstrated that mutant p53 mice develop tumours with more aggressive phenotypes that lead to more metastases, unlike p53-null mice (Lang, Iwakuma *et al.*, 2004; Olive, Tuveson *et al.*, 2004). It needs to be determined whether the observed differences in the time to metastatic progression in tumours with different *TP53* mutation status and genotypes of the HDMX SNP are independent of adjuvant treatment, or are derived from the combined effects of the p53 pathway on cancer progression and the response to DNA-damaging therapies. Nonetheless, the results presented here further support the important role of the p53 pathway in the progression of breast cancer, indicated in Chapter 4, and demonstrate that genetic alterations in the p53 pathway can be good prognostic biomarkers for the metastatic risk of breast tumours.

The results presented in Chapter 4 indicate that high levels of the p53 inhibitor HDM2 can supress pro-metastatic mutant p53 and lead to better patient outcome, which has previously been indicated in an *in vivo* mouse model (Terzian, Suh *et al.*, 2008). Based on the results presented here, and the results from eQTL studies that demonstrated that the G-allele associates with higher levels of *HDMX* mRNA, it can be speculated that high levels of HDMX have a positive effect on patient outcome, as HDMX can act as inhibitor of mutant p53

and lead to the suppression of metastatic progression, whereas tumours with the A-allele and mutant p53 have more aggressive tumours (Figure 5.8A). These results, therefore, support the idea that p53 inhibitors can supress mutant p53 and subsequently suppress metastatic progression dependent on mutant p53. In fact, 80% of all *TP53* mutations in the MicMa and ULL breast tumours were missense mutations that were located in exon 4 of the *TP53* gene, indicating that most mutant p53 tumours might associate with oncogenic gain of function. It is, therefore, highly likely that elevated levels of HDMX, similarly to HDM2, can improve patient outcome by inhibiting pro-metastatic mutant p53. These results underscore the previous findings that inhibition of mutant p53 by HDM2 can be beneficial to overall outcome, and that HDM2-targeted therapies need to be used with caution in the context of mutant p53. In contrast, therapeutic strategies currently in clinical development that aim to reactivate wt p53 with recombinant viruses or small molecule drugs, as well as new strategies in pre-clinical development that use RNA interference and HDAC inhibitors to eradicate mutant p53 (Braicu, Pileczki *et al.*, 2013; Liu, 2011; Yan, Liu *et al.*, 2013), could be particularly favourable for patients from a high risk of progression group that have mutant p53 but no protective effect from p53 inhibitors.

The associations of the HDMX SNP with breast cancer progression were most significant in mutant p53 tumours, however, the analyses presented here demonstrate that HDMX SNP also interacts with wt p53 to change the prognoses of breast cancer patients (Figure 5.7). While determination of the causal SNP in the *HDMX* haplotype block and functional analyses are needed to fully elucidate

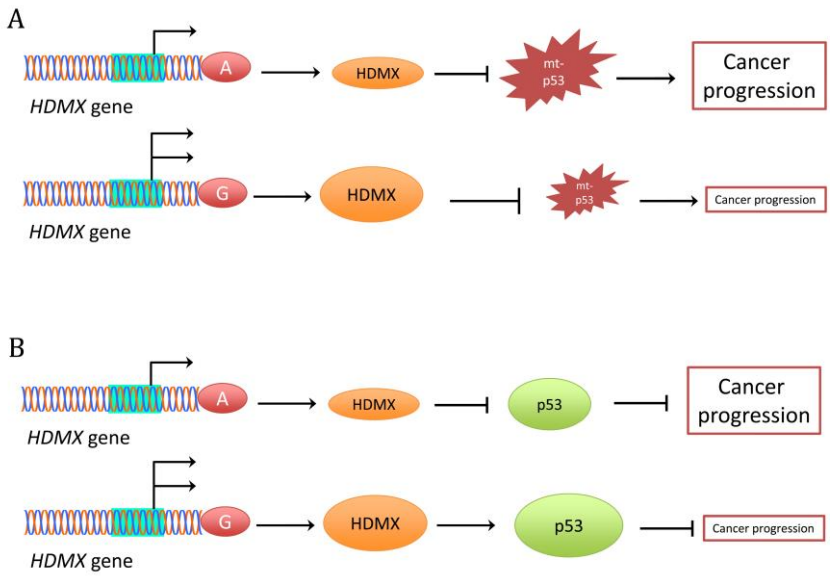


Figure 5.8 A schematic model depicting the effect of different alleles of HDMX SNP on the levels of *HDMX* gene transcription and HDMX protein levels and, subsequently, mutant p53 (A) or wt p53 (B).

the effect of the HDMX SNP on the gene expression of *HDMX*, and subsequently the protein levels of HDMX, the results presented here indicate that high levels of the HDMX associated with the G-allele of the HDMX SNP are also beneficial for patients whose tumours have wt p53, as those patients are at the lowest risk of metastatic progression (Figure 5.8B). Indeed, the literature offers support to this hypothesis. It has previously been demonstrated that, upon p53 activation, excess HDMX can compete with p53 for HDM2-dependent ubiquitination and, in turn, lead to the stabilisation of p53 (Wang and Jiang, 2012; Wang, Wade *et al.*, 2007). Moreover, Conza *et al.* demonstrated that in mouse embryonic fibroblasts (MEFs) and non-transformed human cell lines, HDMX stabilises p53 and protects it from HDM2-mediated degradation. Furthermore, upon DNA damage, HDMX promotes conformational changes of p53 towards the active state (Di Conza, Mancini *et al.*, 2012). Similarly, Mancini *et al.* demonstrated that

a distinct fraction of mitochondrial HDMX in MEFs facilitates the p53-dependent intrinsic apoptotic pathway and that a loss of HDMX confers resistance to DNA damage-induced apoptosis. Further to that, based on associations found in ovarian cancer, whereby high HDMX levels associated with a good response to cisplatin treatment, it was suggested that the observed associations of HDMX with p53 observed in MEFs are also applicable to cancer cells (Mancini, Di Conza *et al.*, 2009). It can, therefore, be speculated that the distinct isoform of HDMX that activates p53-dependent apoptosis can also be crucial for the activation of p53 to prevent metastatic progression, as wt p53 in contrast to mutant p53 has been implicated in the suppression of pro-metastatic mechanisms including EMT, invasion of the ECM and cytoskeleton reorganisation (Muller, Vousden *et al.*, 2011; Roger, Gadea *et al.*, 2006). However, to fully elucidate effect of the HDMX SNP on *HDMX* gene expression and subsequently on p53 activity, and determine whether the high levels of HDMX associated with the HDMX SNP G-allele accelerate the response to adjuvant treatment, analyses in a larger cohort of breast cancer patients are needed. It is possible that the HDMX SNP could be a biomarker for a HDMX isoform for which high levels are beneficial in suppressing metastatic progression, in both wt and mutant p53 patients, and could also be an indicator of a good response to DNA-damaging therapies.

Together, these results support the idea that functional polymorphisms in the p53 pathway can not only alter cancer incidence, but also cancer progression, and could therefore be used as prognostic biomarkers to improve patient management in the clinic. Moreover, the evidence presented here, as

well as in Chapter 4, demonstrates that p53 pathway attenuation can be a critical event not only in tumourigenesis but also in cancer progression. Therefore, new therapeutic strategies aimed at the reactivation of p53 could offer a stand alone treatment option to prevent cancer progression. Finally, analyses with two biomarkers for HDMX levels, the HDMX SNP described in this chapter and the *HDMX-S/FL* ratio described in Chapter 4, which can distinguish distinct isoforms of HDMX with clearly different effects on the function of p53, underscore the importance of HDMX in controlling the p53 pathway, as well as the need for a better understanding of how the *HDMX* gene is regulated and the functional interactions of different isoforms of HDMX with p53.

6 IDENTIFICATION AND ANALYSIS OF FUNCTIONAL SINGLE NUCLEOTIDE POLYMORPHISMS THAT AFFECT MELANOMA PROGRESSION

6.1 Introduction

6.2 Results

6.2.1 The HDMX SNP associates with the progression of melanoma patients

6.2.2 A screen for SNPs in p53 network genes identifies a SNP in the FOXO3 gene that affects melanoma progression

6.2.3 The analysis of the FOXO3 rs2802292 SNP haplotype block identifies three functional SNP candidates that could affect FOXO3 gene transcription

6.2.4 The rs2802292 SNP associates with the strongest evidence for regulatory potential affecting FOXO3 gene transcription

6.2.5 The GATA3 transcription factor binds to the causal SNP candidate rs2802292 in vitro and in vivo

6.2.6 Endogenous GATA3 regulates transcription of the FOXO3 gene

6.3 Discussion

6.1 Introduction

The incidence rates of highly metastatic malignant melanoma have been rising over the years, and have more than doubled in the UK in the last two decades (Garbe and Leiter, 2009; Giblin and Thomas, 2007). The risk of developing melanoma is determined, as in other malignancies, by genetic and environmental factors. Alterations in the CDKN2A, CDK4 and MC1R genes are associated with inherited predisposition to melanoma, however familial melanoma represents only a small percentage of all melanoma cases (Chin, 2003).

Despite an ever-increasing body of knowledge about the inherited and somatic genetic lesions that increase melanoma susceptibility and progression, there is currently no effective therapy for the treatment of metastatic melanoma. However, some progress has been made in recent years, which has lead to the development of a drug that targets a high frequency somatic mutation, namely the activation of the BRAF kinase. BRAF has activating mutations in 60% of melanomas (Chin, 2003) and its potent inhibitor, PLX4032, has shown remarkable clinical activity, with a 81% response rate achieved in a Phase I trial of melanoma patients (Bollag, Hirth *et al.*, 2010). However, as is the case with other targeted therapies, resistance is rapidly developed, and no efficacy is observed in the 40% of patients that lack activating mutations of BRAF. Together, these challenges in the treatment of metastatic melanoma result in a median survival rate of only 6 months, leading to 5 year survival rate of less than 5% (Gray-Schopfer, Wellbrock *et al.*, 2007).

Unlike other cancers where the p53 gene is frequently inactivated by mutations and/or deletions, most melanomas retain a wild-type p53 gene (Box and Terzian, 2008). Nevertheless, studies in transgenic mice lend support for p53's role as a potent tumour suppressor in melanoma. The first indirect evidence came from mice with p53/Rb impaired by transformation with the SV40 T-antigen under tyrosinase promoter control. These mice developed aggressive and highly invasive tumours that were histopathologically similar to human melanomas (Bradl, Klein-Szanto *et al.*, 1991). The role of the p53 pathway in melanoma suppression was further validated in another mouse model where it was demonstrated that melanoma-specific, tyrosinase-driven RAS activation and p53 loss cooperate in malignant transformation, leading to the development of cutaneous melanomas (Bardeesy, Bastian *et al.*, 2001). Indeed, p53 target genes have been found to be deregulated in wt *TP53* metastatic melanoma tumours and cell lines (Avery-Kiejda, Bowden *et al.*, 2011; Houben, Hesbacher *et al.*, 2011)

These data suggest that p53 signalling can suppress melanoma development, and that the p53 pathway could be silenced through other genetic lesions or alterations in the pathway other than somatic mutation or deletion of the p53 gene itself. Indeed, mutation or deletion of the genomic region CDKN2A, which encodes p14/ARF the inhibitor of the p53 negative-regulator HDM2, is associated with the majority of familial melanoma cases (Meyle and Guldberg, 2009; Nelson and Tsao, 2009). Moreover, levels of HDM2, which blocks p53's transcriptional activity and targets it for degradation, have been found to increase with melanoma progression (Polsky, Bastian *et al.*, 2001). Two other

negative regulators of p53 have recently been demonstrated to play a pivotal role in the suppression of p53's activity in malignant melanoma. Gembarska *et al.* demonstrated that a homologue of *HDM2*, *HDMX*, is over-expressed in over 60% of stage I-IV malignant melanomas, and that the inhibition of the p53-HDMX interaction leads to the sensitisation of melanomas to chemotherapeutic agents (Gembarska, Luciani *et al.*, 2012). In addition, Lu *et al*. have demonstrated that the p53 inhibitor iASPP is activated in a CDK1-dependent manner in the majority of wt *TP53* melanomas, and that the concurrent inhibition of iASPP and HDM2 leads to the restoration of wt p53 function (Lu, Breyssens *et al.*, 2013).

Nonetheless, it can be speculated that p53's function could be impaired by mechanisms that have not yet been described. As discussed in Section 1.3.2, a growing body of evidence supports the idea that functional SNPs in the p53 network can lead to altered cancer risk, progression and survival. Indeed, in Chapter 5, it is demonstrated that a SNP in the *HDMX* gene affects the metastatic progression and survival of breast cancer. It is, therefore, possible that the identification of novel functional SNPs in the p53 pathway could lead to new insights into the development of metastatic melanoma, which could help identify individuals at greater risk, as well as potential nodes for therapeutic intervention. Furthermore, SNPs in isolation are unlikely to be of use as this type of genetic polymorphism can only predict the survival of small subset of patients and, therefore, need to be looked at in terms of the proteins that affect their function. Therefore, the aim of this chapter was to find a novel SNP in the p53 network that affects cancer progression, utilising a cohort of patients with

advanced melanoma who are at high risk of metastatic disease and, thereafter, to investigate how the identified SNP can be affected by other proteins that control its function and therefore affect its utility.

6.2 Results

6.2.1 The HDMX SNP associates with the progression of melanoma patients

The work of Gembarska *et al*. (Gembarska, Luciani *et al.*, 2012) suggests that HDMX might be one of the key players involved in the inhibition of p53's function in melanomas. Therefore, we wanted investigate whether the *HDMX* gene SNP, which associates with allelic differences in *HDMX* gene expression in 7 GWAS eQTL studies and altered progression of breast cancer (Chapter 5), can affect the metastatic progression of malignant melanoma. To do so, the HDMX rs1563828 SNP was genotyped in a cohort of 105 patients diagnosed with advanced cutaneous melanoma, collected by our collaborator Mark Middleton (Department of Oncology, University of Oxford). Of the 105 patients, 57 were male and 48 were female. Detailed histopathological characteristics of these patients are detailed in Table 2.8 of Section 2.2.4. Metastatic progression data was available for 102 patients, of which 49 (48%) were G/G in genotype, 48 (47%) A/G and 5 (5%) A/A. Similarly to the associations observed in breast cancer (Chapter 5), patients who were A/A in genotype progressed to metastatic disease significantly faster than patients A/G or G/G in genotype (p=0.034 log-rank test, Figure 6.1A), whereby the A/A genotype associated with 3.67-fold higher risk of developing metastatic disease than G/G (p=0.049, Figure 6.1C). A similar, albeit non-significant trend was observed for overall survival

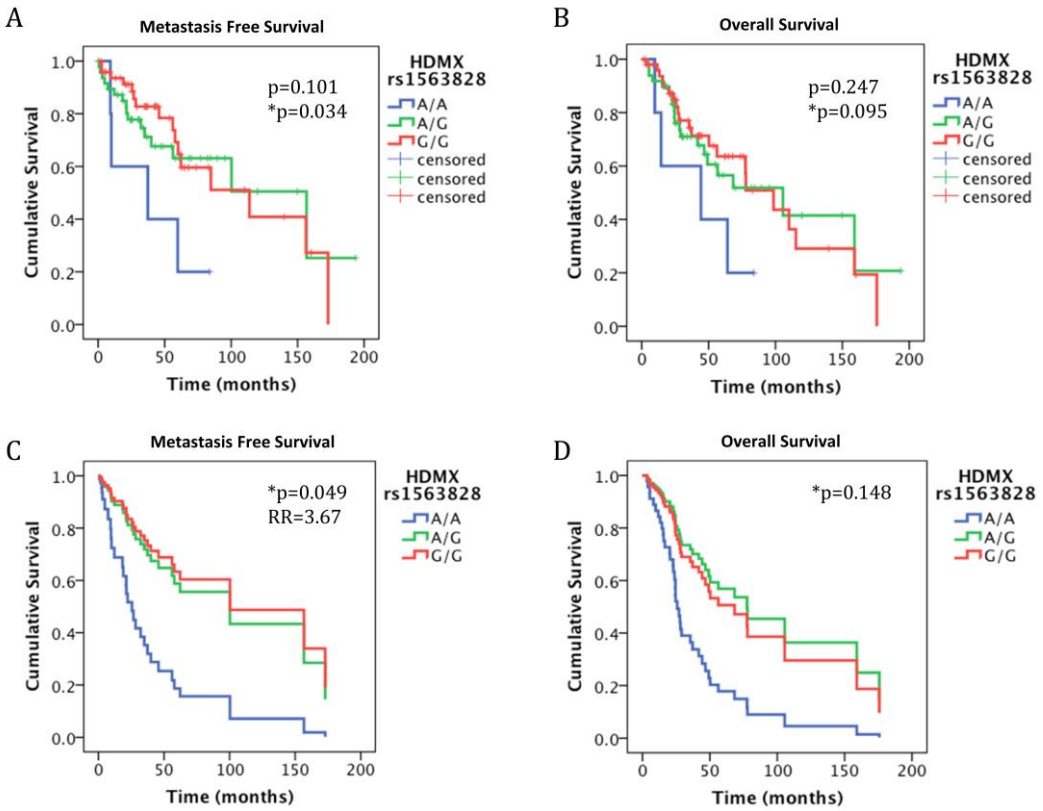


Figure 6.1 The HDMX SNP associates with altered clinical outcome of malignant melanoma patients.

A, Kaplan-Meier plot depicting the metastasis-free survival of 102 patients from a melanoma cohort in either A/A (n=5), A/G (n=48) or G/G (n=49) in genotype of the HDMX SNP. **B**, Kaplan-Meier plot depicting the overall survival of 105 patients from a melanoma cohort either A/A (n=5), A/G (n=49) or G/G (n=51) in genotype of the HDMX SNP. **C**, **D**, Predicted survival curves for patients with different HDMX SNP genotypes derived from a Cox multivariate regression analysis, that was adjusted to the known independent prognostic factors of malignant melanoma including AJCC tumour stage and anatomic location for metastasis-free survival (C) for patients G/G (n=42), G/A (n=37) and A/A (n=11) in HDMX SNP genotype, and for overall survival of melanoma (D) for patients G/G (n=42), G/A (n=39) and A/A (n=13) in HDMX SNP genotype. The Kaplan-Meier survival p-value is derived from a log-rank test. The p-value depicted by * symbol is derived through the comparison of patients A/A and G/G in genotype; RR- relative risk.

(p=0.095 log-rank test Figure 6.1B and p=0.148, Cox multivariate regression model Figure 6.1D).

This result gives support to the hypothesis that functional polymorphisms in p53 pathway genes can affect the metastatic progression of melanoma patients. Therefore, it can be speculated that polymorphisms in other p53 network genes may also affect the progression of malignant melanoma, and that their identification could help determine novel strategies to both prevent and treat metastatic melanoma.

6.2.2 A screen for SNPs in p53 network genes identifies a SNP in the *FOXO3* gene that affects melanoma progression

To identify novel SNPs in the p53 gene network that could affect melanoma progression to metastatic disease, a screening approach was developed and implemented in which 672[1] high frequency tag SNPs in 114 genes from the p53 network were focussed on, encompassing 77.2% of the genetic variability in these genes, which is present in at least 20% of the Caucasian population (Table 6.1). These SNPs were genotyped using a GoldenGate Illumina genotyping platform in 105 melanoma patients and associations of these loci with metastatic progression of melanoma in this cohort was sought.

In this screening approach, developed in collaboration with Emmanouela Repapi, it was first determined which of the 672 above-mentioned genotyped SNPs associated with significant allelic differences in time to the development of

[1] Lukasz F Grochola, University of Oxford

Table 6.1 The percentage coverage of known haplotype blocks for each gene included in the analytical pipeline of the metastasis-free survival screen[1].

Gene	Haplotype Blocks*	Genotyped in Analysis (n)	Coverage (%)
APC	4	4	100
APEX1	2	2	100
BAD	2	2	100
BAX	2	2	100
BCAR1	3	3	100
CBL	3	3	100
CCNG1	2	2	100
CDKN1A	1	1	100
CDKN2A	2	2	100
CHEK2	6	6	100
CSE1L	4	4	100
CSNK2A1	4	4	100
CTNNB1	2	2	100
DUSP16	4	4	100
DYRK2	3	3	100
E2F1	1	1	100
E4F1	1	1	100
EP300	4	4	100
ESR2	6	6	100
FRAP1	2	2	100
GADD45A	2	2	100
GTF2H1	4	4	100
GTF2H3	2	2	100
GTF2H4	1	1	100
HIPK2	1	1	100
HRAS	1	1	100
ILK	3	3	100
LRDD	2	2	100
MAP4	2	2	100
MAPK8	3	3	100
MDM2	2	2	100
MMP2	5	5	100
MTA2	1	1	100
PCNA	1	1	100
PDPK1	1	1	100

[1] Lukasz F Grochola, University of Oxford

Table 6.1 (continued)

PIAS1	4	4	100
PIK3CD	6	6	100
PIK3R2	1	1	100
PIK3R3	3	3	100
PPP1R13B	3	3	100
PTEN	1	1	100
RBBP7	2	2	100
RELA	1	1	100
SHC1	11	1	100
TDG	4	4	100
TP53BP1	2	2	100
TSC2	1	1	100
VEGFA	3	3	100
KDR	13	12	92.3
TP63	71	63	88.7
ERCC2	8	7	87.5
TCF7L1	29	25	86.2
FAS	7	6	85.7
NUMB	7	6	85.7
MAP3K5	12	10	83.3
TP73	18	15	83.3
MAPK10	21	17	81
ITGB1	5	4	80
MAP2K4	10	8	80
MAPK9	15	12	80
RAF1	5	4	80
SOS2	5	4	80
SRC	5	4	80
TNFRSF10B	10	8	80
FLT1	28	22	78.6
ESR1	23	18	78.3
FHL2	9	7	77.8
EGFR	31	24	77.4
TCF7L2	31	24	77.4
CASP3	4	3	75
JMY	4	3	75
MAPK1	4	3	75
PIK3CA	4	3	75
RCHY1	4	3	75
EGF	7	5	71.4
LEF1	7	5	71.4
IGF1R	71	50	70.4
AKT1	3	2	66.7
AKT2	3	2	66.7

Table 6.1 (continued)

ATM	3	2	66.7
ATR	3	2	66.7
ERCC3	3	2	66.7
hCG_1789827	3	2	66.7
HDAC2	6	4	66.7
MDM4	3	2	66.7
PIK3CB	3	2	66.7
RFWD2	3	2	66.7
RHEB	6	4	66.7
TP53BP2	3	2	66.7
XPC	6	4	66.7
AKT3	5	3	60
FOXO3	5	3	60
MAP2K1	5	3	60
MAP2K2	10	6	60
IGF1	7	4	57.1
NFKB1	7	4	57.1
USP7	11	6	54.5
CASP9	4	2	50
CREBBP	8	4	50
PMAIP1	2	1	50
PXN	4	2	50
RB1	2	1	50
SOS1	2	1	50
TSC1	6	3	50
PIK3R1	21	10	47.6
APAF1	5	2	40
GSK3B	9	3	33.3
PTK2	9	3	33.3
REL	3	1	33.3
RELB	3	1	33.3
P2RY5	1	0	0
Total	**766**	**591**	**77.2**

* HapMap Phase II data; MAF ≥ 20%

visceral metastases. 22 SNPs that showed significant allelic differences in metastasis-free survival using the Kaplan-Meier (KM) survival test were identified (Phase I, see Table 6.2 and Figure 6.2). Unfortunately, screening 672 SNPs in 105 patients can lead to an abundance of false positives. Therefore, additional steps were incorporated that we anticipated would reduce the number of false positives identified. To do this, further statistical tests and data

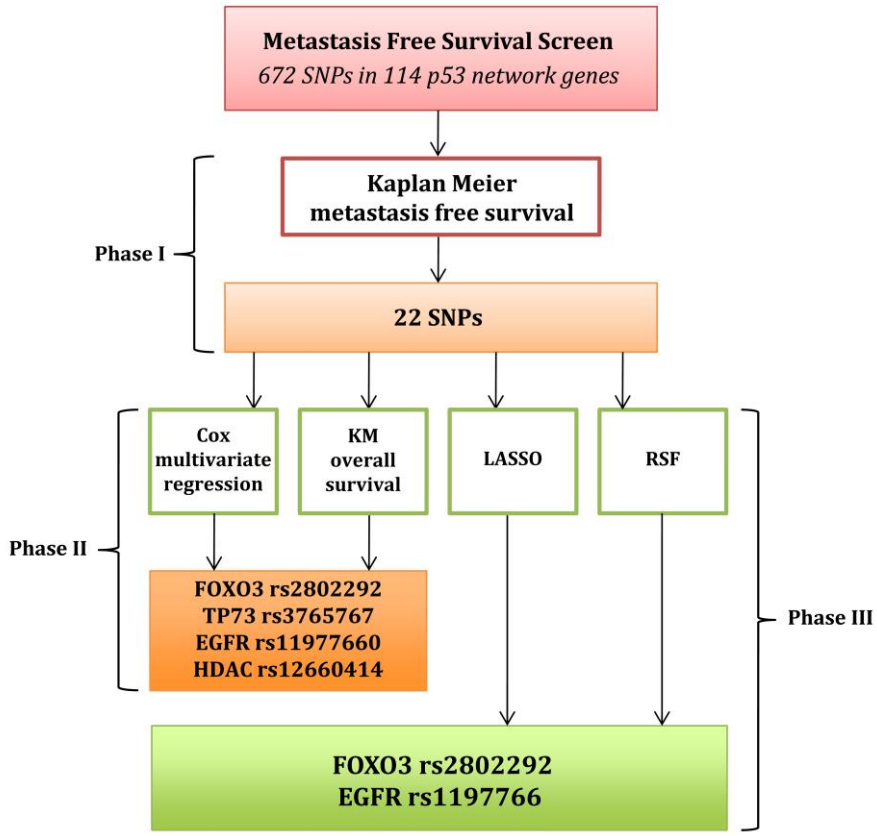


Figure 6.2 Flowchart depicting the metastasis-free survival screen of melanoma patients.

mining techniques were applied to the 22 SNPs. Specifically, Cox multivariate regression analysis was used for metastasis-free survival, adjusted for the known independent prognostic factors for melanoma such as AJCC tumour stage and location. Furthermore, a KM survival test for overall survival was applied to each of the 22 SNPs, with the reasoning that any locus affecting metastasis should associate with significant allelic differences in overall survival, given that this cohort had been followed on average for 49 months since diagnosis. Lastly, two data mining techniques, namely Random Survival Forest (RSF) (Ishwaran and Kogalur, 2010) and the Least Absolute Shrinkage and Selection Operator (LASSO) (Tibshirani, 1997), which are designed to improve predictions in high

Table 6.2 List of 22 SNPs identified in Phase I of the metastasis-free survival screen of melanoma, with corresponding p values from Phase I and Phase II of the screen, as well as scores from Phase III.

	Gene symbol	SNP	Phase I	Phase II		Phase III	
			Metastasis-Free Survival		Overall Survival	Metastasis-Free Survival	
			Kaplan Meier p value	Cox regression p value	Kaplan Meier p value	Lasso count	RSF count
1	*FOXO3*	rs2802292	0.003	0.0273	0.0298	15	38
2	*TP73*	rs3765767	0.0047	0.0001	0.0118		
3	*MAPK10*	rs11097091	0.005	0.1458	0.0185		
4	*EGFR*	rs11977660	0.008	0.0036	0.0043	21	69
5	*MAP4*	rs5012971	0.0179	0.0698	0.83	19	40
6	*TCF7L2*	rs4073288	0.0181	0.0667	0.192	20	43
7	*MAPK10*	rs6531917	0.0212	0.0506	0.0391		
8	*CSE1L*	rs2075678	0.0222	0.0115	0.1758	17	34
9	*IGF1R*	rs867431	0.0246	0.1101	0.0574		
10	*PIK3R3*	rs785520	0.0265	0.2598	0.0118		
11	*ESR1*	rs2347867	0.0268	0.3381	0.0187	4	35
12	*P2RY5*	rs9568036	0.0313	0.0689	0.0555	13	30
13	*TP63*	rs10155001	0.0319	0.0057	0.0868	4	30
14	*TP53BP2*	rs1890120	0.0338	0.11	0.6068	13	32
15	*MAPK9*	rs3095944	0.0378	0.0647	0.1121	16	49
16	*MAPK10*	rs13112959	0.0386	0.2253	0.0615		
17	*E4F1*	rs27382	0.0404	0.1446	0.0756	16	31
18	*IGF1R*	rs1879612	0.0405	0.4475	0.1607	9	30
19	*HDAC2*	rs12660414	0.0436	0.0282	0.0374	25	30
20	*TP63*	rs1881993	0.0437	0.0076	0.12	20	31
21	*TP63*	rs9817981	0.0462	0.0719	0.2285	13	31
22	*EGFR*	rs12535226	0.0477	0.059	0.1714	23	31

dimensional data where the number of analysed variables exceeds the sample size, were applied to the metastasis-free survival data for SNPs where the number of missing genotype calls did not exceed 10%.

Of the 22 SNPs studied, four SNPs, including three SNPs that ranked in the top 4 of KM metastasis-free survival, exhibited significant allelic differences both in the Cox regression analysis for metastasis-free survival and the KM analyses for overall survival (Phase II see Table 6.2 and Figures 6.2 and 6.3). Furthermore, LASSO and RSF counts were available for three of these SNPs and,

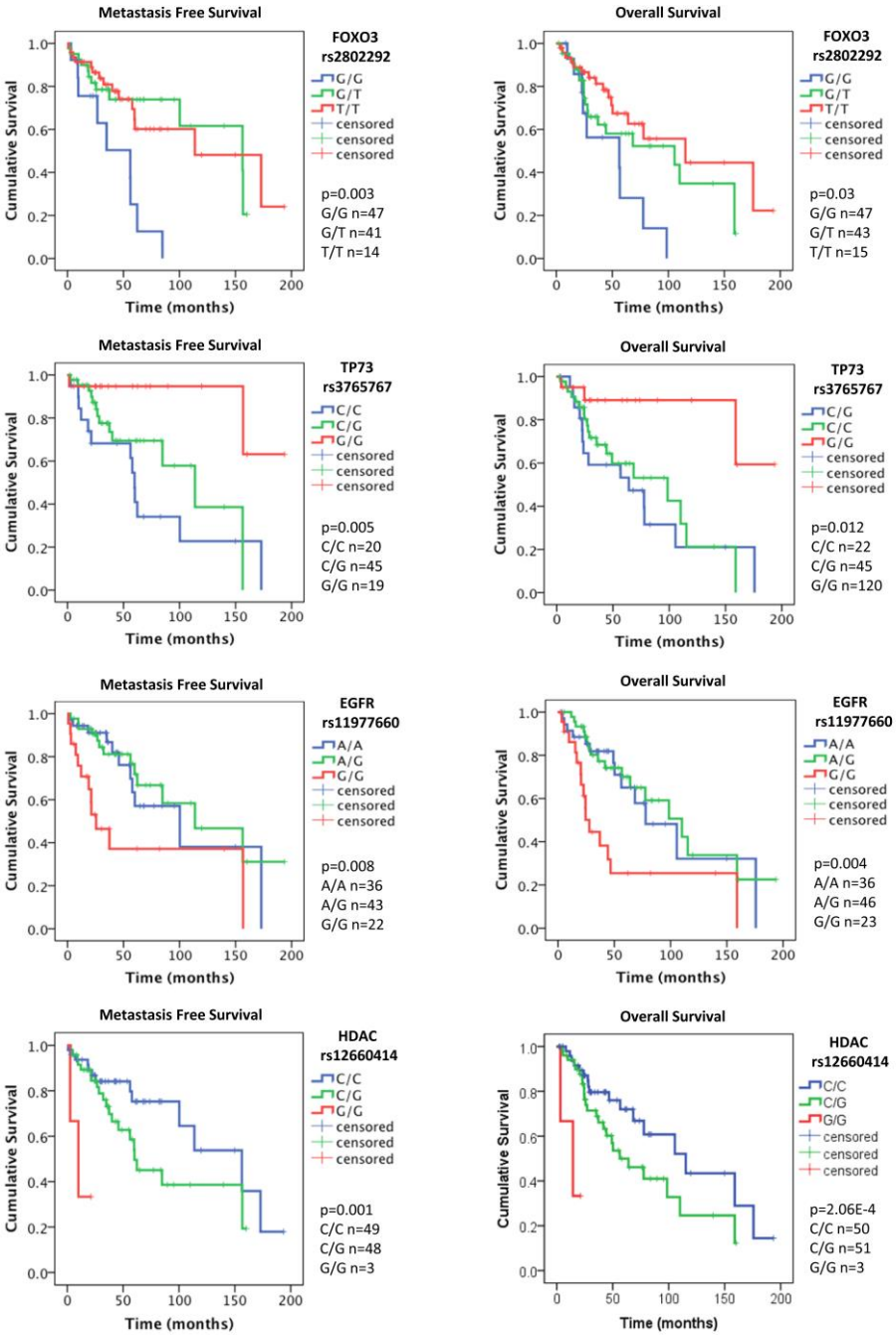


Figure 6.3 Kaplan-Meier plots depicting the allelic differences in metastasis-free survival and overall survival of top four SNPs from Phase II of the metastasis-free survival screen.

interestingly, the two top ranking SNPs had high counts for both the RSF and LASSO (Phase III, Table 6.2 and Figure 6.2). Specifically, the EGFR SNP rs11977660 was ranked in the top 5 for both LASSO and RSF, and the FOXO3 SNP rs2802292 was ranked in the top 10 and top 5 in the LASSO and RSF respectively.

Notably, the top hit FOXO3 SNP rs2802292 is part of a well-studied haplotype block in the Forkhead Box O3 gene, that has already been shown to demonstrate allelic differences in other human phenotypes such as longevity (Anselmi, Malovini *et al.*, 2009; Flachsbart, Caliebe *et al.*, 2009; Soerensen, Dato *et al.*, 2010; Willcox, Donlon *et al.*, 2008; Zeng, Cheng *et al.*, 2010). In cancer, FOXO3, a known tumour suppressor, plays a role in tumour cell invasion (Gan, Liu *et al.*, 2009; Shiota, Song *et al.*, 2010; Storz, Doppler *et al.*, 2009), the metastatic progression of melanoma (Segura, Hanniford *et al.*, 2009; Zanella, Renner *et al.*, 2010), and survival (Hilmi, Larribere *et al.*, 2008). The FOXO3 SNP showed the most significant allelic differences in KM metastasis-free survival (p=0.003 log-rank test), significant differences in the Cox multivariate regression analysis for metastasis-free survival (p= 0.022), and in the KM overall survival analysis (p=0.03), as well as obtaining high counts for both LASSO (15) and RSF (38) for metastasis-free survival. Specifically, we observed that patients homozygous for the minor G-allele associate with poorer metastasis-free survival (p=0.001 log-rank test, Figure 6.3; p=0.007, Cox multivariate regression, RR= 4.137 Figure 6.4A) than those carrying the major T-allele, which results in similar trends in overall survival (p=0.018 log-rank test, Figure 6.3; RR=3.36, p=0.022, Figure 6.4B). These results suggest that this

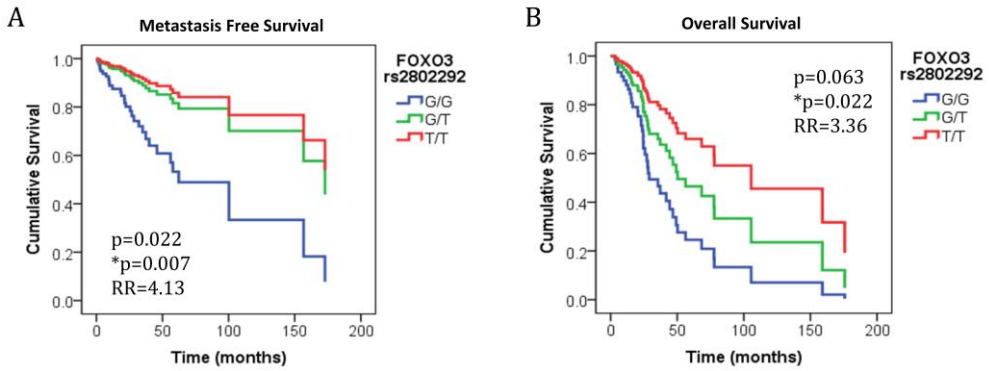


Figure 6.4 The G-allele of the FOXO3 rs2802292 SNP, the top hit from the metastasis-free survival of melanoma screen, associates with significantly higher risk of earlier development of visceral metastases and tumour-related death.

A, **B**, predicted survival curves for patients with different FOXO3 SNP genotypes derived from a Cox multivariate regression analysis that was adjusted to the known independent prognostic factors of malignant melanoma, including AJCC tumour stage and anatomic location for metastasis-free survival of melanoma (A) for patients G/G (n=42), G/T (n=37) and T/T (n=11) in FOXO3 SNP genotype, and for overall survival of melanoma (B) for patients G/G (n=42), G/T (n=39) and T/T (n=13) in FOXO3 SNP genotype. The p-value marked by * symbolis derived through the comparison of patients G/G and T/T in genotype; RR- relative risk.

approach could identify SNPs in p53 network genes that affect metastatic progression.

6.2.3 The analysis of the FOXO3 rs2802292 SNP haplotype block identifies three functional SNP candidates that could affect *FOXO3* gene transcription

Based on the results of the screen to identify SNPs that associate with the metastatic progression of melanoma two SNPs, FOXO3 SNP rs2802292 and EGFR SNP rs11977660, which associated with significant allelic differences in all survival analyses applied and high scores in RSF and LASSO, were selected for further analyses to begin to identify the causal SNPs that underlie the

observed clinical associations with melanoma. SNPs closely linked to FOXO3 SNP rs2802292 and EGFR SNP rs11977660 were determined using the data generated by the HapMap (Consortium, 2003) and 1000 genomes projects (Abecasis, Auton *et al.*, 2012) in the European (CEU) population. Using a threshold of R-squared greater than 0.8, an additional nine SNPs that were closely linked to the FOXO3 SNP rs2802292, located either directly upstream of the transcriptional start site or in the 1st/2nd intron of the *FOXO3* gene were identified (Figure 6.5, Table 6.3), whereas there was no SNPs in close LD with EGFR SNP rs11977660, which is located in intron 1 of the *EGFR* gene.

To concentrate on identifying and characterising the causal SNP, processes that could be significantly affected by single base pair changes such as transcription, splicing and microRNA regulation were focused on. First, SNPs located in regulatory regions of the gene, based on a survey of the literature and genetic databases were prioritised. Next, it was explored whether these SNPs reside in regions that contain epigenetic signatures, namely histone post-translational modifications such as the mono- and tri-methylation of histone 3 in lysine 4 (H3K4Me1 is often found near regulatory elements, and H3K4Me3 is often found near promoters), and the acetylation of histone 3 in lysine 27 (H3K27Ac is often found near active regulatory elements); DNaseI hypersensitivity, and ChIP-Seq for known transcription factors. To do this, publicly available data was utilised from the international collaborative project, the Encyclopedia of DNA Elements (ENCODE) (BirneyStamatoyannopoulos *et al.*, 2007). Out of ten SNPs from the *FOXO3* haplotype, three SNPs (rs2802292, rs2802288 and rs2764261) were found to be in regions with strong signals for

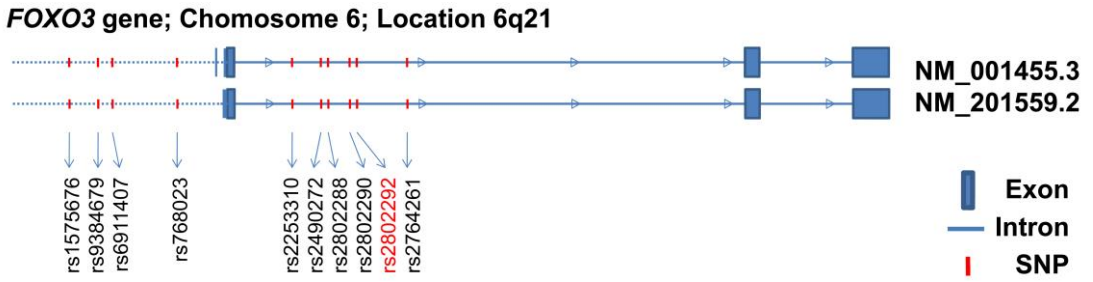


Figure 6.5 Schematic representation of the *FOXO3* gene and the approximate genic position of the identified linked SNPs from the rs2802292 SNP haplotype.
The *FOXO3* gene encodes two transcript variants. While the longer transcript has an additional exon at the 5'-end, both transcripts encode the same protein

at least three markers of DNA regulatory elements in multiple cell lines. Moreover, the first introns of many genes often harbour transcriptional enhancer elements (Ernst, Kheradpour *et al.*, 2011; Visel, Blow *et al.*, 2009), and these three SNPs all reside in intron 1/2 of the *FOXO3* gene (Figure 6.5). This analysis suggests that these SNPs could affect *FOXO3*'s transcriptional regulation and, therefore, result in allelic differences in cellular FOXO3 levels and activity. Conversely, no evidence was found that the EGFR SNP rs11977660 is a causal SNP, suggesting that other SNPs, yet unidentified, could underlie the observed clinical associations with melanoma. Therefore, based on the above-described analyses, which identified the causal SNP candidates in the *FOXO3* haplotype, as well as the results of previous association studies with this haplotype SNPs on other human traits, the FOXO3 SNP was selected for further functional analyses.

To explore whether the FOXO3 SNP associates with allelic differences in *FOXO3* mRNA levels in cancer cells, *FOXO3* transcript levels were measured in a panel of 36 melanoma cell lines using qRT-PCR and a *FOXO3*-specific TaqMan

Table 6.3 List of SNPs from the haplotype centred on SNP rs2802292 and their association with potential regulatory regions in the *FOXO3* gene.

SNP	Distance	R-Squared	D-Prime	ENCODE regulatory region (functional element) GRCh37/hg19	*FOXO3* gene localization
rs2802292	0	1	1	H3K27Ac in HSMM, Huvec, NHEK, NHLF	intron 1/2
				H3K4Me1 in GM12878, H1-hESC, HSMM, Huvec, K562, NHEK, NHLF	
				H3K4Me3 in HSMM, NHEK, NHLF	
				DNase Clusters in H1-hESC, H7-hESC	
rs2802288	12303	1	1	H3K4Me1 in K562	Intron1/ 2
				DNase Clusters in BE2_C, HSMMtube, K562, SK-N-SH_RA	
				ChIP-Seq: CEBPB in K562; Gata1 in PDBE; Gata2 in K562, SHY5Y; Pol2 in PBDE; K562 Tal-1 in K562	
rs2490272	13132	1	1	none	intron 1/2
rs2253310	19925	1	1	H3K4Me1 in NHLF	intron 1/2
rs768023	32516	1	1	H3K4Me1 in NHEK	5' of the gene
rs6911407	41487	1	1	none	5' of the gene
rs9384679	44099	1	1	DNAse clusters in GM12892, GM18507, GM19239, HGF, PANC-1, Urothelia	5' of the gene
				ChIP-Seq: CTCF in K562	
rs2802290	2838	0.932	1	H3K4Me1 in NHLF	intron 1/2
				DNAse clusters in AoAF, HAEpiC, HCM, HPAF, HVMF, NHDF-neo	
rs1575676	47254	0.931	1	ChIP-Seq: SETDB1 in U2OS	5' of the gene
rs2764261	19324	0.896	0.963	H3K27Ac in K562	intron 1/2
				H3K4Me1 in K562	
				H3K4Me3 in K562	
				DNase Clusters in AoAF, HA-h, HA-sp, HCF, HCM, HMVEC-LBl, HRCEpiC, K562, NHLF	
				ChIP-seq: Gata2 in K562 Gata1 in PBDE	

probe (Table 2.3). Interestingly, the five melanoma cell lines homozygous for the G-allele of FOXO3 SNP rs2802292 associated with higher levels of *FOXO3* mRNA than the 21 cell lines homozygous for the T-allele, although the difference was not significant (p=0.505 unpaired t-test, Figure 6.6A). To determine whether the observed trend in the allelic differences in *FOXO3* mRNA levels could be observed in a bigger panel of cancer cell lines, *FOXO3* mRNA levels were measured and analysed in the NCI60 panel, which consists of 59 cancer cell lines from 9 different tissue types. It was found that six cancer-derived cell lines homozygous for the G-allele of FOXO3 SNP rs2802292 associated with significantly higher levels of the *FOXO3* transcript, by 26% on

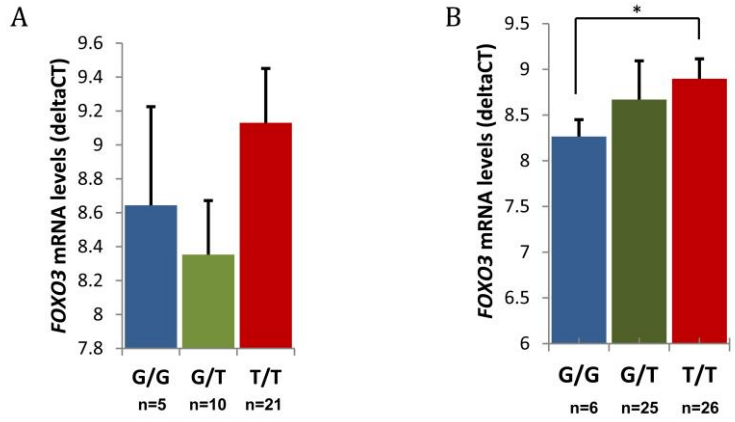


Figure 6.6 The G-allele of FOXO3 SNP rs2802292 associates with higher *FOXO3* mRNA levels.

A, panel of 36 melanoma cell lines demonstrates a non-significant trend for higher *FOXO3* mRNA levels in those cells that harbour the G-allele. **B**, NCI60 panel cells with the G/G-genotype harbour significantly higher levels of *FOXO3* mRNA than those with T/T-genotype. *p<0.05 denotes the level of statistical significance derived from an unpaired t-test comparing T/T and G/G genotype cells with either high or low *FOXO3* mRNA levels. Error bars depict the standard error of the means.

average, than the 26 lines homozygous for the T-allele (p= 0.0416 unpaired t-test, Figure 6.6B).

6.2.4 The rs2802292 SNP associates with the strongest evidence for regulatory potential affecting *FOXO3* gene transcription

To begin to explore the possibility that the causal FOXO3 SNP could be affecting the binding of transcription factors that could underlie the allelic differences in mRNA steady state levels, a protein/DNA-binding assay called the electro-mobility shift assay (EMSA) was performed. For each of the three candidate SNPs, a set of two ^{32}P-labelled oligonucleotide probes were used that were analogous to each allele (Figure 6.7A). Nuclear protein extracts came from two cell lines that were derived from melanoma metastases (IGR37 and SK-

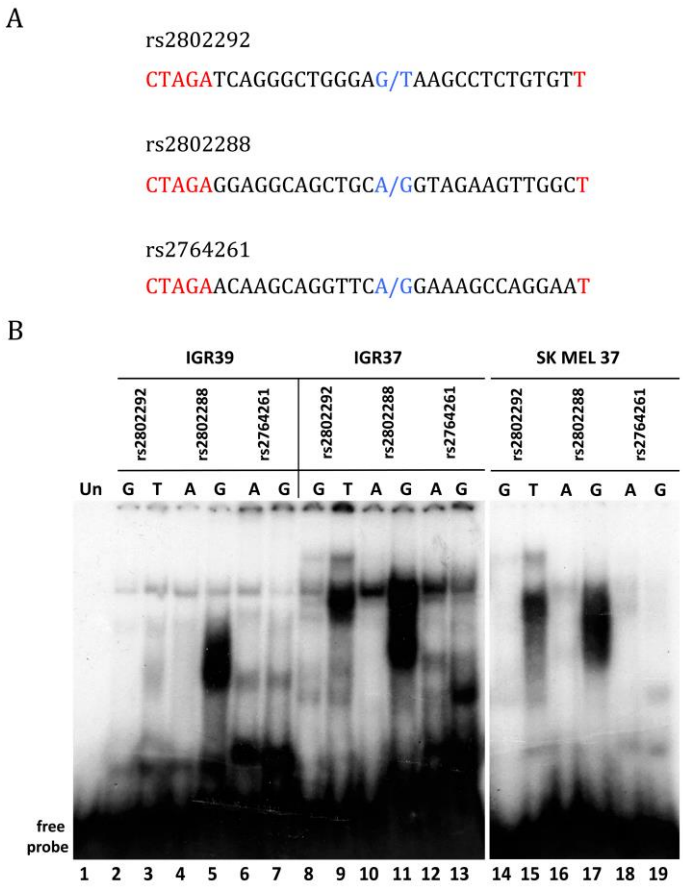


Figure 6.7 Electromobility shift assays (EMSAs) of three functional candidate SNPs.

A, the top strand oligonucleotide sequences used in EMSA experiments, SNP alleles are depicted in blue, whereas red colour denotes overhangs added for ^{32}P-labelling purposes. **B**, EMSA radiographs show different affinities of nuclear proteins, derived from a primary melanoma-derived cell line (IGR39, lanes 2-7) and two metastatic melanoma-derived cell lines (IGR37, lanes 8-13 and SK MEL 37, lanes 14-19), to oligonucleotide probes containing allele-specific sequences of three functional SNP candidates, rs2802292 (G/T lanes 2-3, 8-9, 14-15), rs2802288 (A/G lanes 4-5, 10-11, 16-17) and rs2764261 (A/G lanes 6-7, 12-13, 18-19). Lane 1 depicts a control reaction with no protein extract.

MEL-37), and one cell line derived from the primary malignant melanoma lesion (IGR39) derived from the same individual as the IGR37 cell line. Interestingly, the addition of the nuclear protein extracts from the cell lines derived from

melanoma metastases, IGR37 and SK-MEL-37, produced a significantly different pattern of band-shifts for oligonucleotide probe-sets of rs2802292 and rs2802288 SNPs. The T-allele-containing probes of the rs2802292 SNP and the G-allele-containing probes of the rs2802288 SNP formed significantly more protein complexes, both in number and intensity, with a similar pattern for nuclear extracts from each cell line (Figure 6.7B compare lanes 8-9; 14-15 and 10-11; 16-17). Intriguingly, the addition of rs2802292 SNP probes to the nuclear protein extract from the primary melanoma tumour derived cell line (IGR39) produced a pattern of band shifts with very low intensity (Figure 6.7B, lanes 2 and 3). These results, where significant allelic differences in the pattern of band-shifts were observed in the metastatic but not the primary melanoma-derived cell lines, suggest that the rs2802292 SNP has the strongest potential as a causal SNP that could lead to the observed allelic differences in the time to metastatic progression of melanoma patients.

To extend these observations to more cell lines, EMSA was performed using oligonucleotide probes for rs2802292 SNP and nuclear protein extracts from four further metastatic melanoma-derived cell lines (LOXIMVI, SK-MEL-23, 1205Lu, MDA-MB-435) and one cell line derived from the a primary melanoma tumour (WM115). Similarly to the observations made with the IGR37 and SK-MEL-37 melanoma cell lines (Figure 6.7B), the addition of probes containing the T-allele of the rs2802292 SNP to nuclear protein extracts from two of the metastatic melanoma-derived cell lines (LOXIMVI and SK MEL 23), and also the primary melanoma-derived cell line WM115 resulted in significantly more protein complexes being formed both in number and intensity (Figure 6.8 lanes

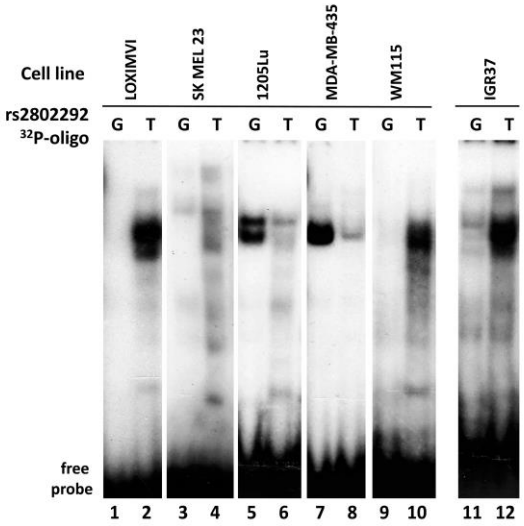


Figure 6.8 Electromobility shift assays show significant allele-specific differences in the affinity of nuclear proteins, derived from six metastatic melanoma-derived cell lines (LOXIMVI, SK-MEL-23, 1205Lu, MDA-MB-435) and one primary melanoma-derived cell line (WM115,) to oligonucleotide probes containing either the G- or T-allele of rs2802292 SNP.

The radiograph of the IGR37 cell line (lanes 11-12) is included for comparison purposes. The T-allele-containing probes, which formed more protein complexes both in number and intensity with nuclear protein extracts derived from IGR37 and SK MEL 37 cell, formed a similar pattern of protein complexes in another two metastasis-derived cell lines and one primary melanoma-derived cell line (compare lanes 1-2, 3-4, 9-10 with IGR37 11-12). The G-allele-containing probes formed more intense protein complexes with nuclear protein extracts derived from two metastatic melanoma-derived cell lines (compare lanes 5-6 and 7-8).

1-2, 3-4 and 9-10, compare with IGR37 lanes 11-12). Nonetheless, the addition of nuclear protein extracts from two other melanoma cell lines, 1205Lu and MD-MB-435, associated with significantly more protein complexes being formed with the G-allele and not the T-allele (Figure 6.8, lanes 5-6 and 7-8), suggesting that both alleles of the SNP could have the potential to exert a function depending on the biological background of the cell.

Finally, to explore whether the genomic regions surrounding any of the three FOXO3 SNPs constitute transcriptional enhancer regions, luciferase expression vectors were constructed under the control of a minimal thymidine kinase promoter (pGL3-TK) with a 54bp genomic sequence containing one of the alleles of each SNP (Figure 6.9A). IGR37 and IGR39 melanoma cells were transfected with each of the SNP specific insert-containing luciferase vectors, as well as control vector without the 54bp inserts, which was later used to normalise the luciferase signal across all SNP vectors. Interestingly, in both cell lines similar associations with luciferase gene activity were observed for each of the three SNPs. However, significant allelic differences in activation of the luciferase gene were observed for rs2802292 SNP in metastatic melanoma-derived IGR37 cells ($p=0.033$ Mann-Whitney test, Figure 6.9B), whereas the allelic differences in activation of the luciferase gene by rs2802292 SNP in primary melanoma-derived IGR39 cells, which does not associate with significant differences in binding of nuclear protein in EMSA, were not significant ($p=0.065$ Mann-Whitney test, Figure 6.9C).

To further investigate the allelic differences in luciferase activity associated with the rs2802292 SNP, pGL3-TK vectors with either the G- or T-allele of the rs2802292 SNP were transfected into three different melanoma cell lines, in which significant allele-specific patterns of band-shifts were verified by EMSA (Figure 6.8). Strikingly, the transfection of luciferase vector carrying the G-allele insert associated with a significantly higher luciferase signal than the vector carrying the T-allele in all four cell lines (Figure 6.10, Table 6.4). Specifically, the luciferase signal associated with the G-allele was on average

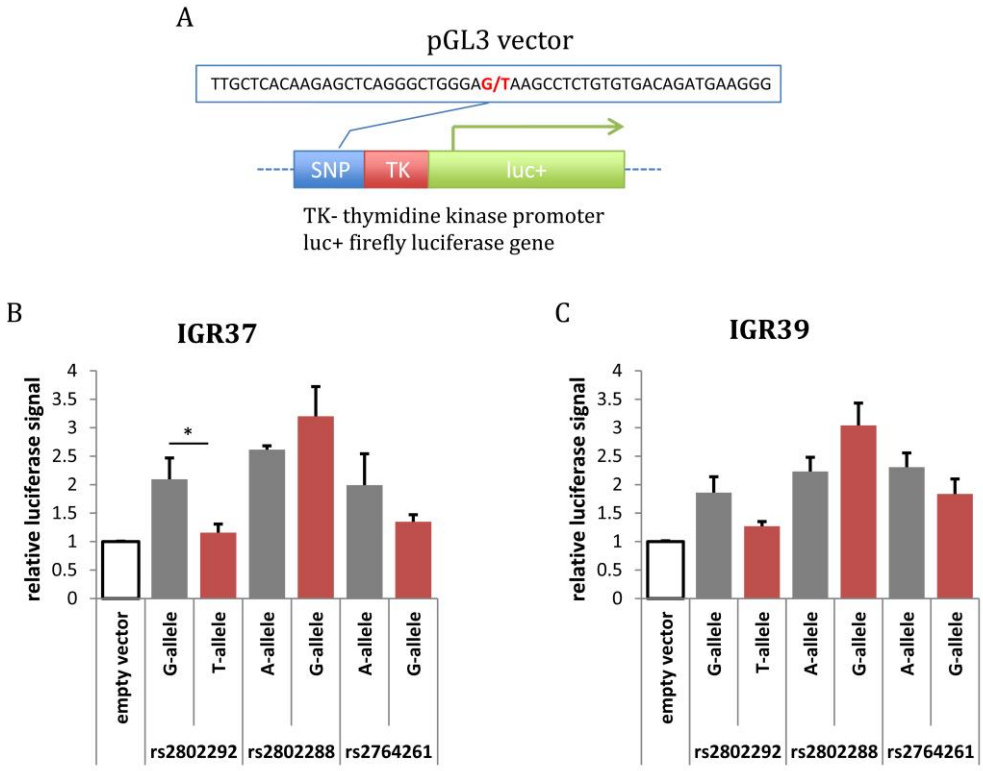


Figure 6.9 The rs2802292 SNP associates with significant allelic differences in the modulation of luciferase gene expression in luciferase reporter assay experiments.

A, a schematic drawing depicting the pGL3 vector map with a 54bp SNP-specific sequence upstream of the TK promoter. **B**, **C**, relative firefly luciferase gene expression from pGL3 vectors with SNP rs2802292, rs2802288 and rs2764261 allele-specific sequences in IGR37 (B) and IGR39 (C) melanoma cell lines. * $p<0.05$ denotes the level of statistical significance derived from a Mann-Whitney test. Error bars depict the standard error of the means from multiple experiments.

2.07-fold higher than that associated with the T-allele ($p<0.0001$ Mann-Whitney test, Figure 6.10, Table 6.4). The difference between the luciferase signals from the two alleles of the rs2802292 SNP ranged from 2.56-fold in MDA-MB-435 cells ($p=0.0011$ Mann-Whitney test, Table 6.4), to 1.77-fold in 1205Lu cells ($p=0.007$ Mann-Whitney test, Table 6.4).

6.2.5 The GATA3 transcription factor binds to the causal SNP candidate rs2802292 *in vitro* and *in vivo*

To begin to investigate whether the different alleles of the SNPs from the *FOXO3* haplotype could alter a transcription factor-binding site, a computational algorithm was run using the Explain 3.0 algorithm[1] with the TRANSFAC 2009.3 database (Matys, Fricke *et al.*, 2003). Interestingly, only the FOXO3 SNP rs2802292 (G/T), which associated with significant allelic differences in binding of nuclear protein extracts in EMSA and in luciferase reporter gene modulation, was predicted to have allelic differences in transcription factor binding. It was predicted that the GATA-family transcription factors, specifically GATA2 and GATA3, could only bind to the T-allele of the rs2802292 SNP (Figure 6.11), that associated with a significantly stronger pattern of protein band-shifts in EMSAs in four different metastatic melanoma-derived cell lines than the G-allele (Figures 6.7 and 6.8).

To test the Explain 3.0 algorithm prediction, the breast cancer cell line MCF7 was selected, which expresses *GATA2* and high levels of *GATA3* according to the BioGPS[2] database. First, EMSA was performed using nuclear protein extract from MCF7 cells and oligonucleotide probes with either a G or T base in the rs2802292 SNP, to assess and verify the allelic specificity of nuclear extract proteins binding to the T-allele. Strikingly, the pattern and intensity of the DNA-protein complexes formed with either G- or T-allele probes was very similar to those observed in melanoma cell lines, where the T-allele associated with more

[1] Biobase; http://www.biobase-international.com
[2] http://biogps.org

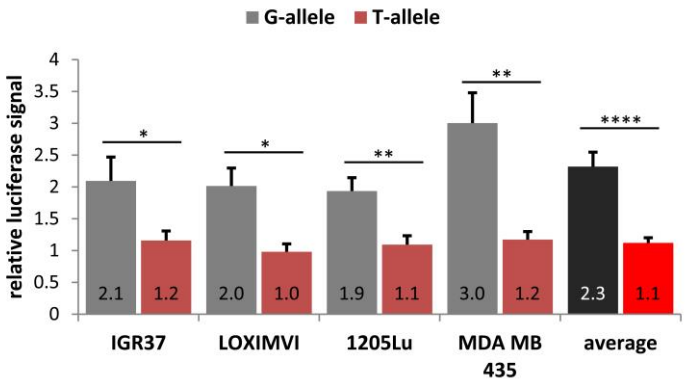


Figure 6.10 The G-allele-vector associates with a significantly higher luciferase signal than the T-allele-vector in four different metastatic melanoma-derived cell lines.

The firefly luciferase gene expression vector pGL3, with SNP rs2802292 allele-specific sequences upstream of the TK promoter, demonstrated significant allelic differences in luciferase gene activation. * $p<0.05$, ** $p<0.01$, **** $p<0.0001$ denote the level of statistical significance derived from a Mann-Whitney test. Error bars depict the standard error of the means from multiple experiments.

Table 6.4 The fold difference in luciferase signal between the G-and T-allele of the rs2802292 SNP in five different cell lines.

cell line	G-allele/T-allele luciferase signal ratio	p-value Mann-Whitney test
IGR37	1.81	0.033
LOXIMVI	2.05	0.028
1205Lu	1.77	0.007
MDA MB 435	2.56	0.0011
average (4 cell lines)	2.07	p<0.0001
MCF7	2.65	0.0003
average (5 cell lines)	2.18	p<0.0001



Figure 6.11 The transcription factor (TF) binding computational algorithm predicts a high-affinity binding site of transcription factors from the Gata family to the sequence containing the T-allele of rs2802292 SNP (top panel).
The algorithm's prediction also depicts the binding of TFs such as Tal1 and E2A, and other E-box TFs, that often acts as co-factors of Gata proteins. The bottom panel depicts positional weight matrices of predicted Gata family binding sites.

protein binding (Figure 6.12A, compare lanes 2-3 with IGR37 lanes 8-9). To assess the allelic specificity of this binding, a large excess (approximately 10x) of cold oligonucleotide probes, with either G-or T-alleles, were added to the reaction mix prior the addition of ^{32}P-labelled probes. The addition of both G- and T-allele cold competitors to the reaction mix containing ^{32}P-labelled G-allele probes resulted in competition of all DNA-protein complexes (Figure 6.12A lanes 4-5), suggesting that these complexes are not allele specific and might also be formed within a region of the probe that is distant from the allele. Nonetheless, we observed that the T-allele specific binding was not affected by the presence of the G-allele oligonucleotide competitor (Figure 6.12A, compare lanes 6-7 DNA/protein complex marked with an arrow), suggesting that this DNA/protein complex might contain either GATA3 or GATA2 protein, which

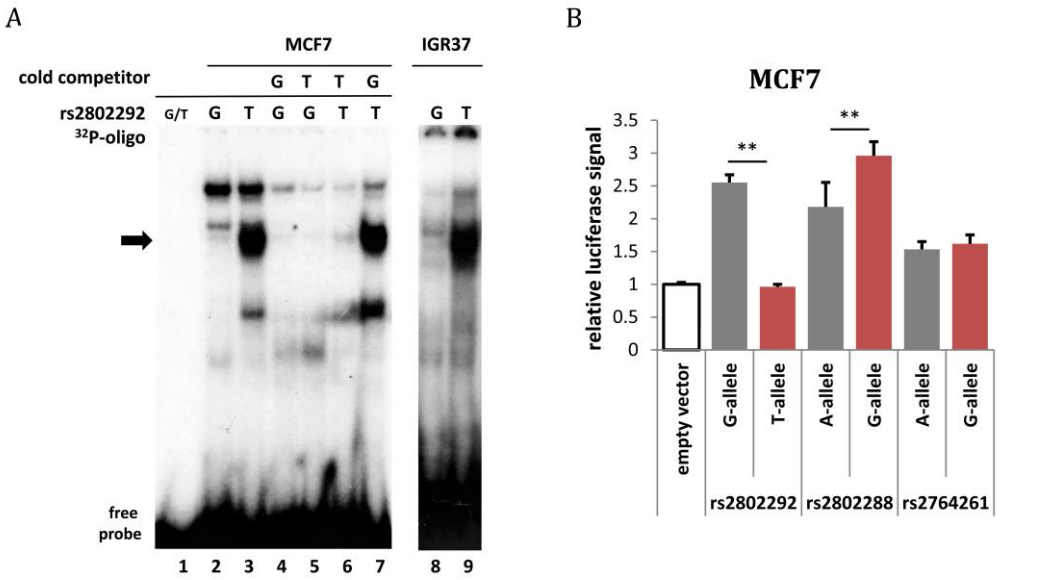


Figure 6.12 The rs2802292 SNP associates with significant allelic differences in the binding of nuclear proteins and luciferase reporter gene signal in MCF7 cells. **A**, electromobility shift assay demonstrates the high binding affinity of the nuclear protein derived from MCF7 cells to the T-allele of rs2802292 SNP (lane 3, DNA/protein complex marked with arrow) with competition from a cold T-allele competitor (lane 6), but not a G-allele cold competitor (lane 7), whereas the G-allele shows no specificity in nuclear protein binding (lanes 4-5). Lane 1 depicts a control reaction with no protein extract. A radiograph of EMSA with IGR37 nuclear protein extract is included for comparison of allele-specific DNA/protein complexes (lanes 8 and 9). **B**, relative firefly luciferase gene expression from pGL3 vectors with SNP rs2802292, rs2802288 and rs2764261 allele-specific sequences in MCF7 cell lines. ** $p<0.01$ denotes the level of statistical significance derived from a Mann-Whitney test. Error bars depict the standard error of the means from multiple experiments.

was predicted to bind to the T-allele by the Explain 3.0 algorithm.

Next, to assess whether the rs2802292 SNP also associated with significant allelic differences in modulating the expression of the luciferase reporter gene in MCF7 cells, as observed in melanoma cells, pGL3-TK vector transfection was performed with the three candidate SNPs that were previously tested in melanoma cells. As in the melanoma cells, the luciferase signal from

the G-allele vector was on average 2.65-fold higher than that from the T-allele (p=0.0003 Mann-Whitney test, Figure 6.12B, Table 6.4). The rs2802288 SNP also associated with a higher signal of luciferase than empty vector control, and the difference between the luciferase signal of both alleles was significant, although of small magnitude (1.34-fold p=0.0013 Man-Whitney test, Figure 6.12B), whereas no allelic differences in luciferase gene activation were observed for the rs2764261 SNP.

Finally, to begin to test whether any of the predicted Gata proteins could bind to the T-allele of the rs2802292 FOXO3 SNP, EMSA was performed with GATA3- and GATA2-specific antibodies and nuclear protein extract from MCF7 cells. Interestingly, the addition of the GATA3 but not the GATA2 antibody resulted in a super-shift of the T-containing DNA-protein complex (Figure 6.13 compare lanes 3, 4 and 5). Next, to test the affinity of the GATA3 antibody to the DNA-protein complexes formed by both the T- and G-allele, EMSA was performed with increasing amounts of GATA3 antibody added to the binding reaction containing either the T- or G-allele, and protein extract from MCF7 cells. An increasing signal of a GATA3 super-shift across the whole range of GATA3 antibody in the T-allele binding reaction was observed (Figure 6.14A compare lanes 8-12). The signal from the G-allele binding reaction was significantly lower than that of the T-allele signal, and only detectable at a much longer exposure time (Figure 6.14B lanes 3-7), whereby it was observed that only high concentrations of GATA3 antibody showed some affinity to one of the protein complexes formed with the G-allele. However, this protein complex differed from the high GATA3 affinity complex formed with the T-allele (Figure

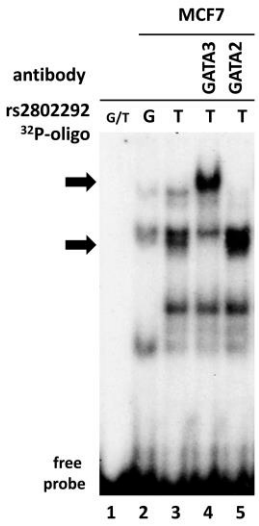


Figure 6.13 The GATA3 transcription factor binds to the T-allele of FOXO3 SNP rs2802292 in MCF7 cells.

An electromobility shift assay with nuclear protein extract derived from MCF7 cells demonstrates that the GATA3 antibody binds to one of the T-allele DNA/protein complexes (lane 3, bottom arrow) forming a super-shift (lane 4, top arrow). No super-shifts are formed with the GATA2 antibody (lane 5). Lane 1 depicts a control reaction with no protein extract.

6.14B lanes 6-8).

To extend this result to the melanoma phenotype, GATA2 and GATA3 super-shift EMSA experiments were performed using nuclear protein extracts from the melanoma cell lines IGR37 and SK-MEL-37. However, the addition of either antibody did not result in a super-shift (data not shown). Nonetheless, the addition of GATA3 specific antibody to the reaction mix containing the T-allele oligonucleotide and nuclear protein extract from the LOXIMI cell line, which associated with the T-allele specific nuclear protein complex, resulted in inhibition of the DNA-protein complex (Figure 6.15, compare lanes 3 and 4), lending further support to the theory that GATA3 controls *FOXO3* gene expression in an allele-specific manner.

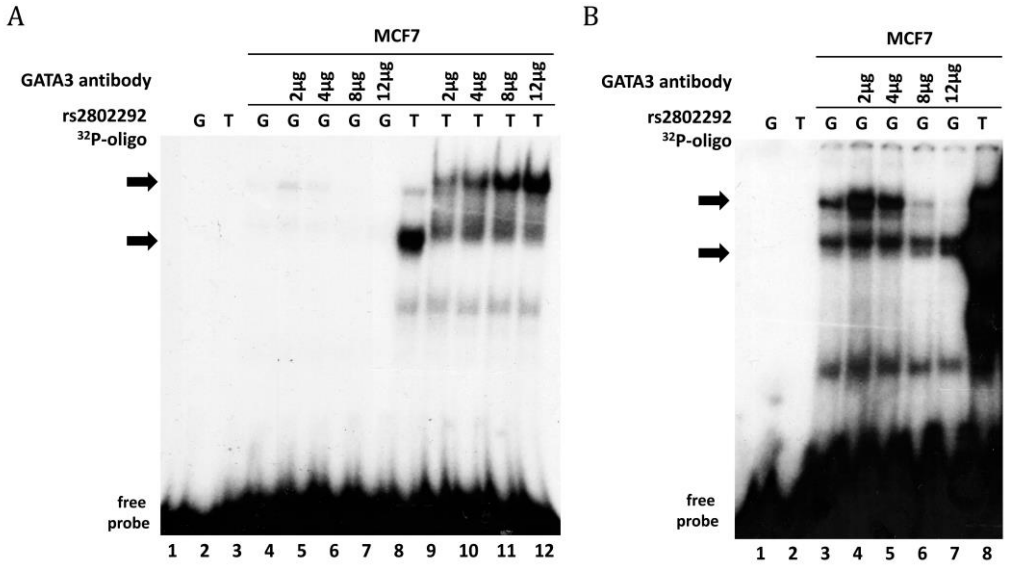


Figure 6.14 The GATA3 transcription factor binds to the T-allele of FOXO3 SNP rs2802292 with high affinity.

A, radiograph of an EMSA with nuclear extract derived from MCF7 cells, depicting the binding of GATA3 antibody to a DNA/protein complex-containing sequence with the T-allele of rs2802292 SNP (lane 8, bottom arrow) across a wide antibody amount range (2-12µg) (lanes 9-12, top arrow), while very weak binding to the G-allele-containing oligonucleotides occurs (lanes 3-7). **B**, long exposure EMSA radiograph depicts some affinity of large amounts of the GATA3 antibody (8-12µg)(lanes 6 and 7) to the DNA/protein complex-containing sequence with the G-allele of rs2802292 SNP (lane 3, top arrow), which also differs from the T-allele major DNA/protein complex (indicated by bottom arrow). Lane 1 depicts a control reaction with no protein extract.

To test whether the in vitro binding of the GATA3 protein can also be observed in vivo under normal cell culture conditions, a chromatin immuno-precipitation (ChIP) experiment was performed with a GATA3-specific antibody and mouse-IgG as a negative control, on lysates containing chromatin cross-linked with protein from logarithmically grown MCF7 cells that are heterozygous for the rs2802292 SNP. First, to determine whether GATA3 binds to the rs2802292 SNP, PCR was performed on GATA3 immuno-precipitated chromatin with primers specific to the genomic DNA region containing the

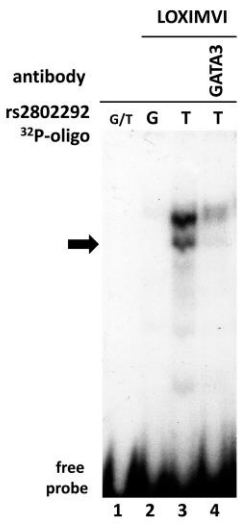


Figure 6.15 The GATA3 transcription factor binds to the T-allele of FOXO3 SNP rs2802292 in LOXIMVI melanoma cells.

An EMSA with nuclear protein extract derived from melanoma LOXIMVI cells demonstrates that the GATA3 antibody competes for the formation of one of the T-allele DNA/protein complexes (compare lane 3 and 4). Lane 1 depicts a control reaction with no protein extract.

rs2802292 SNP. Markedly, genomic DNA containing FOXO3 SNP rs2802292 was detected in the GATA3-IP, but not the negative control mIgG-IP (Figure 6.16A). Next, to determine whether GATA3 preferentially binds to the T-allele of the SNP, the allelic imbalance of the GATA3-IP was assessed by qRT-PCR with an allele specific Taq-Man probe. The signal from GATA3-IP chromatin was compared to input chromatin. Specifically, a standard curve of the differences in fluorescence for both alleles was generated over varying input DNA concentrations, and utilised to calculate the fold-difference in fluorescence for both alleles found in the GATA3-IP chromatin. Strikingly, in line with the computational algorithm prediction and EMSA experiments described earlier, it was found that GATA3 preferentially binds to the T-allele of the rs2802292 SNP. Specifically, GATA3-IP chromatin was enriched in the T-allele by 32%

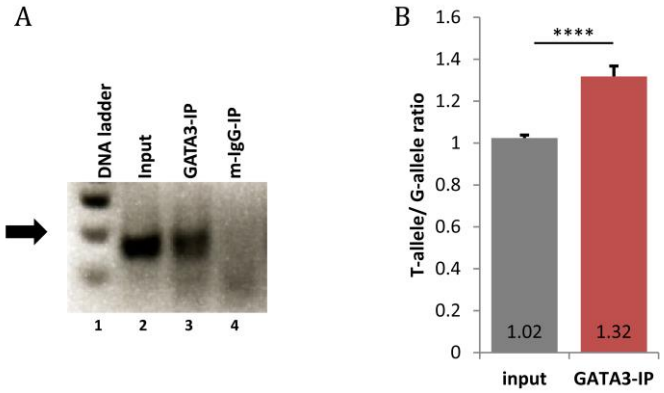


Figure 6.16 GATA3 binds to the T-allele of SNP rs2802292 with significantly higher affinity than to the G-allele in a chromatin immunoprecipitation assay in logarithmically growing MCF7 cells.

A, agarose gel-resolved products of a PCR with either positive control input chromatin (lane 2), chromatin immunoprecipitated with GATA3 antibody (lane 3) or negative control chromatin immunoprecipitated with mouse-IgG, and primers designed to amplify the genomic region containing the rs2802292 SNP demonstrates the specificity of GATA3 protein binding to the genomic region containing rs2802292 SNP. **B**, bar graph depicting the ratios of T-allele over G-allele signals from the allele-specific qRT-PCR with either input chromatin or chromatin immunoprecipitated with GATA3 antibody (GATA3-IP) that was normalized to the fluorescence signal for both alleles over varying input chromatin dilutions. **** $p<0.0001$ denotes the level of statistical significance derived from an unpaired t-test. Error bars depict the standard error of the means from multiple experiments.

($p=0.0001$ unpaired t-test, Figure 6.16B). Together, these data support a model where GATA3 binds the T-allele of the rs2802292 SNP to affect *FOXO3*'s transcriptional regulation and, thus, results in allelic differences in cellular FOXO3 levels and activity.

6.2.6 Endogenous GATA3 regulates transcription of the *FOXO3* gene

To explore whether endogenous GATA3 can affect the transcription of the *FOXO3* gene, GATA3 was depleted in the MCF7 cell line using a *GATA3*-specific pool of four different siRNAs. Interestingly, upon *GATA3* knock-down (kd),

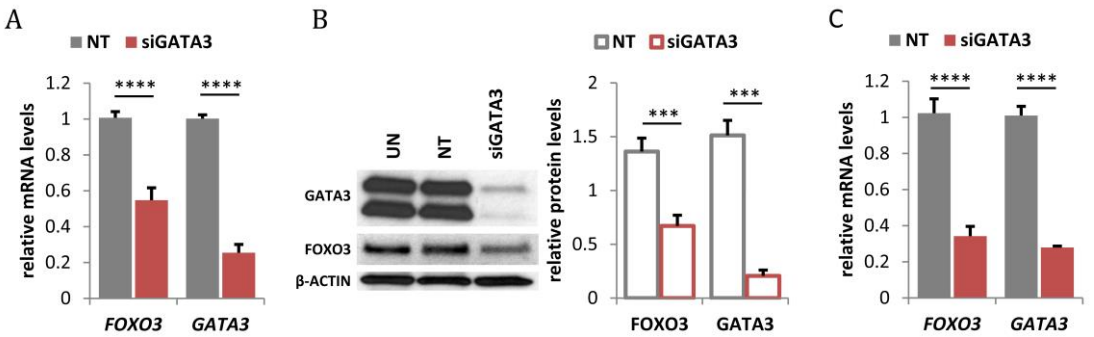


Figure 6.17 Depletion of GATA3 results in a significant decrease of *FOXO3* mRNA and protein levels.

A, bar graph depicting the relative *FOXO3* and *GATA3* mRNA levels in MCF7 cells, 24h post transfection, with either control non-targeting (NT) siRNA or *GATA3*-specific siRNA (siGATA3). **B**, Western blot depicting the protein levels of GATA3, FOXO3 and loading-control β-ACTIN in untreated MCF7 cells and cells 48h post transfection, with either control non-targeting siRNA or *GATA3*-specific siRNA, and a bar graph depicting quantification of the above Western blot. **C**, bar graph depicting the relative *FOXO3* and *GATA3* mRNA levels in melanoma Colo853 cells 24h post transfection, with either control non-targeting siRNA or *GATA3*-specific siRNA. *** $p<0.001$, **** $p<0.0001$ denote the level of statistical significance derived from a Mann-Whitney test. Error bars depict the standard error of the means from multiple experiments.

which resulted in a significant reduction of both *GATA3* mRNA (4-fold $p<0.0001$ Mann-Whitney test, Figure 6.17A) and GATA3 protein (4.76-fold $p=0.0079$ Mann-Whitney test, Figure 6.17B), *FOXO3* mRNA levels were significantly reduced. Specifically, *FOXO3* mRNA levels in MCF7 cells 24h post *GATA3* kd were, on average, 1.8-fold lower than in cells transfected with non-targeting (NT) control siRNA ($p<0.0001$ Mann-Whitney test, Figure 6.17A). Moreover, depletion of the GATA3 protein also resulted in a significant reduction of FOXO3 protein at 48h (1.49-fold $p=0.0006$ Mann Whitney test, Figure 6.17B). Next, it was explored whether GATA3 has an effect on *FOXO3* transcription in melanoma cells. GATA3 was successfully depleted in the Colo853 melanoma cell

line, which is homozygous for the T-allele of the rs2802292 SNP. Strikingly, the depletion of *GATA3*, which associated with a 3.57-fold reduction of *GATA3* mRNA levels (p=0.0001 Mann-Whitney test, Figure 6.17C), resulted in a 2.94-fold reduction of *FOXO3* mRNA (p=0.0001 Mann-Whitney test, Figure 6.17C). Together, these results lend further support to the model that GATA3 regulates the transcription of the *FOXO3* gene.

6.3 Discussion

In Chapter 5, it was demonstrated that inherited polymorphisms in the p53 pathway gene *HDMX* associate with the metastatic progression of breast cancer. In this chapter, it has been shown that the HDMX SNP can also define different prognoses of patients with highly invasive malignant melanoma, whereby the A-allele of the HDMX SNP, which associates with faster metastatic progression of breast cancer, also associates with faster metastatic progression of malignant melanoma. Together, these results provide strong support for the idea that functional polymorphisms in the p53 pathway can alter cancer progression in many cancer types, not just breast tumours, and can serve as biomarkers for p53 pathway activity.

The screening approach used in this chapter identified a novel functional SNP in the p53 pathway that affects the metastatic progression of malignant melanoma. A SNP in the *FOXO3* gene, a well-established tumour suppressor that controls cell death and cell cycle arrest, associated with significant differences in the time to metastatic melanoma progression of over a hundred malignant melanoma patients. Although it is necessary for these screen results to be validated in larger cohorts of melanoma patients, with sufficient clinical

information and follow-up times of the patients to fully evaluate the FOXO SNP's prognostic potential, SNPs from the same *FOXO3* haplotype block have previously been associated with longer lifespan, whereby centenarians from six worldwide cohorts were found to be significantly enriched for the G-allele of the FOXO3 SNP with ORs ranging from 1.16 to 2.75 (Anselmi, Malovini *et al.*, 2009; Flachsbart, Caliebe *et al.*, 2009; Soerensen, Dato *et al.*, 2010; Willcox, Donlon *et al.*, 2008; Zeng, Cheng *et al.*, 2010). This lends strong support to the theory that the FOXO3 SNP is a functional polymorphism that can affect *FOXO3* gene function. FOXO3 is a downstream effector of IGF-1 signalling, which has strong implications not only on aging, but also on cancer. Indeed, components of the IGF1 pathway, particularly PI3K-AKT, have been the subject of extensive research to develop therapeutic targets with which to treat cancer, many of which are already in clinical use (Rodon, Dienstmann *et al.*, 2013). Therefore, the FOXO3 SNP could potentially serve as an indictor of activity of the PI3K-AKT-FOXO3 axis, and act not only as a prognostic biomarker for metastatic progression, but also as a predictive biomarker for PI3K-specific therapeutic strategies.

The gene expression results in the melanoma samples and NCI60 cell panels, as well as the luciferase reporter assay results, indicate that the G-allele associates with higher levels of transcriptional activity in cancer cells, which results in high levels of *FOXO3* mRNA. These results are in line with a recent study of the role of the FOXO3 SNP rs2802292 (G/T) in insulin sensitivity, where it was observed that G-allele carriers associate with increased *FOXO3* mRNA levels in skeletal muscle compared to T-allele carriers, by 32% on

average (Banasik, Ribel-Madsen *et al.*, 2010). Based on the association studies on long-lived centenarians and the role of FOXO3 in longevity, whereby the activation of *FOXO3* and its orthologues in worms, flies and mice has been demonstrated to be critical for extended lifespan (Kamrava, Gius *et al.*, 2011; Ziv and Hu, 2011), it can also be speculated that the G-allele of the FOXO3 SNP associates with high levels of FOXO3 across different healthy tissues. In contrast to the beneficial effect of the G-allele on longer lifespan, melanoma patients homozygous for the G-allele of the FOXO3 SNP were demonstrated to progress to metastatic disease significantly faster than those homozygous for the T-allele. It can, therefore, be speculated that while high *FOXO3* gene expression associated with the G-allele is beneficial for longer lifespan and disease prevention including cancer in healthy individuals, it might become unfavourable once cancer occurs and may subsequently lead to faster metastatic progression (Figure 6.18A). Indeed, evidence is emerging that high levels of FOXO3 can lead to cancer progression and a more aggressive phenotype of breast tumours (Chen, Gomes *et al.*, 2010; Storz, Doppler *et al.*, 2009). Additionally, Tenbaum *et al*. recently demonstrated that, in the presence of high β-catenin nuclear content, the activation of FOXO3 upon inhibition of the PI3K-AKT signalling axis promotes metastatic progression in colon cancer (Tenbaum, Ordonez-Moran *et al.*, 2012).

Interestingly, the work described in this chapter suggests that the causal SNP from the *FOXO3* haplotype block resides in an intronic region of the *FOXO3* gene that serves as a regulatory element controlled by the GATA3 transcription factor, whereby GATA3 binds to the genomic region containing the T-allele

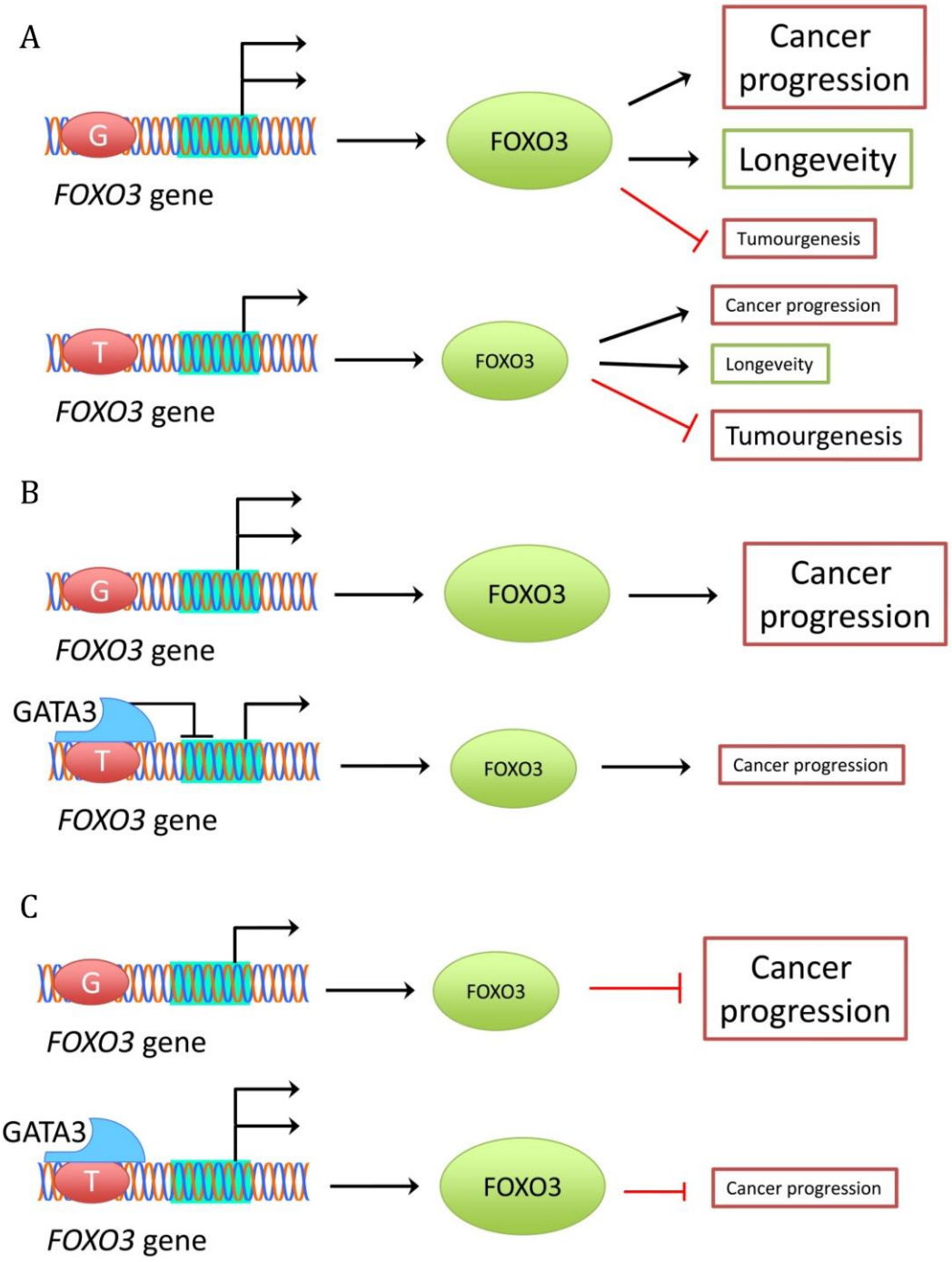


Figure 6.18 Schematic models depicting the possible effects of different alleles of the FOXO3 SNP on the levels of *FOXO3* gene transcription, FOXO3 protein and cellular phenotypes, based on the literature and cancer cell panel experiments (A), and functional analyses of the causal SNP in support of the negative regulation of the *FOXO3* gene by GATA3 binding to the T-allele (B) and in support of positive regulation of the *FOXO3* gene by GATA3 binding to the T-allele (C).

of the FOXO3 SNP in an allele specific manner. Although further experimental evidence is needed, it can be speculated that the observed allelic differences in the luciferase gene activity, and the *FOXO3* mRNA levels in the NCI60 cell lines and the skeletal muscles (Banasik, Ribel-Madsen *et al.*, 2010) result from the GATA3 binding to the T-allele of the FOXO3 SNP, which in turn results in lower levels of FOXO3 and less aggressive phonotype of the cancer cells (Figure 6.18B). However, the experiments with a depletion of the endogenous GATA3 in MCF7 and Colo853 cell lines suggest that GATA3 could, in fact, facilitate the enhanced transcription of the *FOXO3* gene from the T-allele of the FOXO3 SNP, and therefore, high FOXO3 levels in cancer cells protect against metastatic progression (Figure 6.18C). Interestingly, unlike other GATA family members that are predominantly expressed in haematopoietic cells, GATA3 can be found in the skin as well as breast tissues, and has been strongly implicated in breast cancer, where it was demonstrated that GATA3 suppresses metastasis its low levels associate with an invasive phenotype and poor clinical outcome (Chou, Lin *et al.*, 2013; Chou, Provot *et al.*, 2010). Furthermore, loss of GATA3 in PTEN-deficient prostate cancer associates with accelerated invasiveness (Nguyen, Tremblay *et al.*, 2013). Intriguingly, the microarray study on 40 metastatic melanoma samples and 42 primary cutaneous cancers, which included 16 primary melanomas, also demonstrates that the expression of *GATA3* is significantly lower in invasive metastatic melanoma (Riker, Enkemann *et al.*, 2008). This suggests that, similarly to breast cancer, GATA3 could play a role in the suppression of the metastatic progression of malignant melanoma, possibly through the suppression of the pro-metastasis FOXO3 (Figure 6.18B). If true, the

GATA3 signalling axis could offer a new node for interventions to prevent and treat metastatic melanoma, as supported by studies in breast cancer (Chou, Lin *et al.*, 2013). In melanoma, however, FOXO3 has been implicated in the suppression of an invasive phenotype, and its levels diminish in melanoma metastases compared to primary melanomas (Segura, Hanniford *et al.*, 2009; Zanella, Renner *et al.*, 2010), which gives support to the model where the T-allele of the FOXO3 SNP associates with the higher levels of the *FOXO3* expression upregulated by the GATA3 (Figure 6.18C).

Therefore, to determine whether the T-allele associates with either high or low levels of FOXO3, and how FOXO3 regulates metastatic progression, it is necessary for the FOXO3 SNP associations to be investigated in the context of GATA3 levels in bigger melanoma cell panels, and particularly in invasive melanoma tumours. Moreover, given the important roles of GATA3 in breast cancer, it would also be particularly interesting to elucidate the association of the FOXO3 SNP with an invasive phenotype of breast tumours. Together, these analyses could provide further indications of how FOXO3 affects metastatic progression, and how the *FOXO3* gene is regulated in context of GATA3 and different genotypes of the FOXO3 SNP, which could eventually lead to the identification of attractive new therapeutic targets with which to treat metastatic disease.

7 GENERAL DISCUSSION

The p53 pathway plays an important role in the suppression of tumourigenesis (Kruse and Gu, 2009; Vogelstein, Lane *et al.*, 2000), but also has an impact on later stages of the disease where it controls multiple processes that are associated with metastatic progression (Muller, Vousden *et al.*, 2011; Roger, Gadea *et al.*, 2006). Consequently, components of the p53 pathway are attractive candidates for molecular biomarkers that would assist in the identification of patients with different prognoses. The identification of new biomarkers that could define the activity of the p53 pathway would facilitate a significant leap in cancer prognostication. Additionally, functional p53 is an important effector of DNA damaging cancer therapies and facilitates tumour clearance. Therefore, p53 pathway biomarkers could also further define the p53 pathway with regards to targeted therapies, and serve as good predictors of appropriate targeted therapies including those directed at the reactivation of the p53 pathway itself.

The aim of this study was to contribute to the understanding of the effects that alterations in the p53 pathway can have on cancer progression, and explore the potential of these molecular alterations as independent prognostic biomarkers for aggressive phenotypes of primary tumours. To achieve this, cohorts of osteosarcoma, soft tissue sarcoma, breast carcinoma and malignant melanoma, as well as cell panels of osteosarcoma, breast cancer, the NCI60 and malignant melanoma, were utilised to seek and characterise associations of p53 pathway molecular alterations with metastasis-free survival and the overall survival of cancer patients. Firstly, the role of alternatively spliced transcripts of

the p53 inhibitor HDMX (measured as *HDMX-S/FL* ratio) in cancer progression was explored, and the *HDMX-S/FL* ratio was identified as an independent prognostic biomarker of p53 pathway attenuation and progression of osteosarcoma, soft tissue sarcoma and breast cancer. Secondly, the associations of p53 pathway attenuation and breast cancer progression with an inherited polymorphism in the *HDMX* gene, which associates with cancer risk and highly reproducible differences in the transcript levels of the *HDMX* gene, were identified. Lastly, a screen based on the Kaplan Meier metastasis-free survival of melanoma patients was developed and applied to identify novel SNPs in the p53 network that affect metastatic progression. The SNP in the *FOXO3* gene was identified as the strongest candidate, and the functional mechanism behind this SNP investigated to understand the biological role of the causal polymorphism. These analyses have provided further evidence that p53 pathway attenuation is strongly associated with a high risk of metastatic disease, and that somatic and inherited alterations in p53 pathway genes could further define the prognoses of both wt and mutant *TP53* patients, allowing further definition of patient risk groups. Notably, p53 pathway biomarkers could serve as prognostic and predictive biomarkers. Moreover, inherited polymorphisms and genetic alterations in p53 pathway genes interact with each other and affect the metastatic potential of tumours.

The *TP53* gene is one of the most frequently mutated genes in human cancer, and associates with the adverse prognosis of many cancers (Petitjean, Achatz *et al.*, 2007). Factors like *TP53* mutation detection and classification methods, the type of *TP53* mutation concerned, clinicopathologic status of the

tumours, and study size have all contribute to the inconclusive assessment of mutant *TP53*'s prognostic value (Olivier, Langerod *et al.*, 2006). Advances have been made in methods of detecting *TP53* mutations (Boyd and Vlatkovic, 2008). However, in tumours that retain wt *TP53*, other mechanisms upstream and downstream of p53 lead to the pathway's attenuation (Toledo and Wahl, 2006; Vousden and Lu, 2002), therefore *TP53* mutation alone is not sufficient for use as a prognostic biomarker for cancer progression in the clinic. More effective detection of p53 pathway attenuation through biomarkers that would sense the attenuation of the p53 pathway in wt *TP53* tumours, and a deeper understanding of distinct alterations of p53 pathway components that are frequently associated with poor outcome, is needed. The role of HDMX, and its alternatively spliced transcripts frequently found in tumours, in the inhibition of p53 has not yet been solved. In Chapters 3 and 4, the associations of the *HDMX* splice variant with p53 pathway attenuation were explored. It was demonstrated that high levels of the alternatively spliced transcript *HDMX-S*, compared to *HDMX* full-length transcript levels (*HDMX-S/FL* ratio), associate with common somatic genetic lesions associated with p53 inhibition, such as *TP53* mutation and *HDM2* over-expression in cell panels of osteosarcoma, breast cancer and NCI60. A meta-analysis based on 106 cancer cell lines from all three cell panels demonstrated that 97% of the cells with the highest *HDMX-S/FL* ratios had attenuated p53 pathways, either by *TP53* mutation or *HDM2* overexpression, whereas the rate of these alterations in cell lines with low *HDMX-S/FL* ratios was significantly lower (66%, p=0.001). Importantly, very similar associations were observed in tumour samples of 191 breast cancer

patients, where *TP53* mutation or *HDM2* overexpression were observed in 98% of tumours with the highest *HDMX-S/FL* ratios, and only 68% of tumours with lowest *HDMX-S/FL* ratios (p=7.1E-07). Similarly, 32% of STS sarcoma tumours with high *HDMX-S/FL* ratios had mutated *TP53* in contrast to only 6% of tumours with low *HDMX-S/FL* ratios (p=0.0337).

Additionally, the results presented in Chapter 4 suggest that the *HDMX-S/FL* ratio is a measure of p53 activity and can, therefore, offer a specific marker of p53 activity. The analyses performed in BC tumours and cell lines demonstrate that wt p53 associates with significantly higher levels of full-length *HDMX* mRNA, whereas *HDMX-S* mRNA levels are similar to those found in mutant *TP53* tumours and cell lines, indicating that the *HDMX-S/FL* ratio could be a net measure of p53-specific transcription of the *HDMX* gene from a p53-responsive P2 promoter that has been previously described (Phillips, Teunisse *et al.*, 2010). Indeed, activation of wt p53 in MCF7 and ZR75-1 breast cancer cell lines provided support for this hypothesis, whereby Nutlin-3 treatment resulted in a significant increase of *HDMX-FL* (MCF7, 2.83-fold, p<0.0001; ZR75-1, 1.85-fold, p<0.0001) and HDMX-P2 transcripts (MCF7, 70.19-fold, p<0.0001; ZR75-1, 53.52-fold, p<0.0001), whilst the levels of the *HDMX-S* transcript remained mostly unchanged. To fully evaluate this model, the mechanism and function of *HDMX* alternative splicing needs to be fully elucidated. Additionally, the observations made in breast cancer cell lines need to be validated in cancer cells of different tissue origin, especially those that associate with increased levels of *HDMX-S* in poor prognosis tumours like soft tissue sarcomas and papillary thyroid carcinomas (Bartel, Schulz *et al.*, 2005; Prodosmo, Giglio *et al.*, 2008).

Nonetheless, these results support the rationale that the ratio of gene expression levels of the *HDMX-S* transcript over *HDMX-FL* can serve as an effective biomarker for the attenuation of the p53 pathway.

In order to fully elucidate the role of p53 pathway attenuation in cancer progression, and evaluate the prognostic value of p53 pathway biomarkers, clinically relevant endpoints like overall survival and metastasis-free survival were utilised. First, in Chapter 3, survival analyses in 51 osteosarcoma patients and 64 soft tissue sarcoma patients demonstrated that the *HDMX-S/FL* ratio can identify distinct groups of patients with different prognoses in tumours that associate with relatively low (20% or less) rates of *TP53* gene mutation (Olivier, Goldgar *et al.*, 2003; Park, Jung *et al.*, 2004; Wunder, Gokgoz *et al.*, 2005; Yokoyama, Schneider-Stock *et al.*, 1998). p53 pathway attenuation, determined by *HDMX-S/FL* ratio levels, was sufficient to identify osteosarcoma patients at higher risk of metastatic progression (p=0.005). Additionally, in soft tissue sarcomas, high *HDMX-S/FL* ratios better defined a group of patients with adverse prognosis (p=0.008) than *TP53* mutation (p=0.469). Next, in Chapter 4, biomarkers for p53 pathway attenuation, *HDMX-S/FL* ratio and *TP53* mutation were evaluated in two breast cancer cohorts comprising a total of 191 breast cancer patients. Among all tumour types, to date *TP53* mutation status has been most consistent as a prognostic biomarker in breast cancer tumours, although it has been largely unreliable (Olivier, Langerod *et al.*, 2006; Petitjean, Achatz *et al.*, 2007). Consequently, the *HDMX-S/FL* ratio biomarker described in sarcoma cohorts was a good candidate for evaluation as a biomarker of p53 pathway attenuation complimentary to the *TP53* gene mutation. Indeed, evidence from

p53-specific gene expression profiling studies suggests that gene expression signatures could allow the better definition of p53 pathway status, and vastly improve *TP53* status utility (Miller, Smeds *et al.*, 2005; Takahashi, Moriya *et al.*, 2008; Troester, Herschkowitz *et al.*, 2006). The survival analyses in 191 breast cancer patients demonstrated that the *HDMX-S/FL* ratio further defines the prognoses of patients with wt *TP53*, whereby patients with high *HDMX-S/FL* ratios had significantly shorter metastasis-free (0.003) and overall survival (p=4.2E-05). The *HDMX-S/FL* ratio interacts with *TP53* mutation status to define patients with significantly different prognoses, identifying 3 distinct groups of low (wt *TP53* and low *HDMX-S/FL* ratio tumours), intermediate (high *HDMX-S/FL* ratio and either wt or mutant *TP53* tumours) and high (mutant *TP53* and low *HDMX-S/FL* ratio tumours) risk (p=0.0.001).

The p53-specific microarray-based gene expression signature has previously been demonstrated to define different prognoses of patients with wt *TP53* (Miller, Smeds *et al.*, 2005). This and other similar p53-specific gene expression signatures had very few overlapping genes. Moreover, very few of these classifier genes were known p53 targets (Miller, Smeds *et al.*, 2005; Takahashi, Moriya *et al.*, 2008; Troester, Herschkowitz *et al.*, 2006). Notably, these gene classifiers were identified using similar methods that lead to the description of five distinct molecular subtypes of breast cancer (Sorlie, Perou *et al.*, 2001). p53 pathway biomarkers, namely *TP53* mutation in combination with *HDMX-S/FL* ratio, define breast cancer survival better than these five molecular subtypes. It can, therefore, be speculated that simpler but more specific gene expression and mutation signatures can be much better prognostic biomarkers

than microarray-based gene expression, which still faces technical barriers, and it is estimated that transcript detection overlap between different platforms is as low as 30-40% (Cookson, Liang *et al.*, 2009).

A large body of evidence suggests that inherited polymorphisms in p53 pathway genes can modulate the activity of the p53 pathway (Grochola, Zeron-Medina *et al.*, 2010). Germ-line biomarkers offer more attractive alternatives for clinical use than biomarkers derived from tumour material, as the material for analysis is not only more stable but also more readily accessible. Genetic screening using phenotype-specific SNP panels for retinal degradation has already been clinically validated and offers low-cost, high quality molecular diagnoses (Katsanis and Katsanis, 2013). It is likely that high frequency inherited polymorphisms in p53 pathway genes could affect p53-dependent progression to metastatic disease, and be used in combination with other p53 pathway biomarkers to define patient populations at different risk of metastatic progression.

It has been reasoned that p53 pathway SNPs that associate with significant differences in the transcript levels of the gene harbouring the SNP, and have also been demonstrated to associate with cancer risk, would also have an effect on metastatic progression. The *HDMX* gene harbours a group of closely linked SNPs that are the most well validated eQTL loci known to date (Dimas, Deutsch *et al.*, 2009; Montgomery, Sammeth *et al.*, 2010; Nica, Parts *et al.*, 2011; Stranger, Nica *et al.*, 2007; Veyrieras, Kudaravalli *et al.*, 2008; Zeller, Wild *et al.*, 2010), and also associate with differential cancer risk (CouchWang *et al.*, 2013; EelesOlama *et al.*, 2013; Garcia-ClosasCouch *et al.*, 2013; Kulkarni, Vazquez *et al.*,

2009). The analyses in cohorts of 191 breast cancer patients (Chapter 5) and 102 malignant melanoma patients (Chapter 6) presented in this thesis demonstrate that the SNP proxy of the *HDMX* haplotype block, which strongly associates with allelic differences in *HDMX* transcript levels in 4 different tissue or cell types, can predict different prognoses of breast cancer (p=0.001) and malignant melanoma (p=0.034) patients. This is consistent with experimental *in vitro* and *in vivo* evidence from studies on HDM2 SNP309, that demonstrate that even small changes in *HDM2* gene transcription levels imposed by SNP309 are sufficient to affect p53 function, tumour formation and overall survival (Bond, Hu *et al.*, 2004; Post, Quintas-Cardama *et al.*, 2010).

However, despite the growing body of evidence that SNPs can predict the clinical outcome of cancer patients, SNPs in isolation are not of use as this type of genetic polymorphism can only predict the survival of a small subset of patients. Moreover, SNP frequencies differ between populations, which further limits their use as single prognostic biomarkers. To identify a more robust set of prognostic biomarkers, we need to understand how inherited polymorphisms interact with frequent somatic epigenetic and genetic alterations. *HDMX* is a good model system to study this, because the HDMX molecule interacts with two proteins that are frequently altered in cancers, namely p53 and the estrogen receptor (ER) (Kulkarni, Vazquez *et al.*, 2009; Perry, 2010). Indeed, in Chapter 5 it was demonstrated that the predictive value of HDMX SNP is vastly improved by interaction with ER status and *TP53* status. The A/A genotype of HDMX SNP, which associates with lower levels of *HDMX* mRNA, associated with very high risk of metastatic progression for breast cancer patients whose

tumours were ER-negative (p=5.0E-06) or had mutant *TP53* (p=0.0002). Although whether or not the observed effect in differential survival is a direct effect of *TP53* mutation or ER-negative status needs to be investigated in bigger cohorts, the survival analyses of patients with different *TP53* status and different alleles of the HDMX SNP presented here clearly demonstrates that the combination of somatic and inherited genetic variations can contribute to clearer prognostications of breast cancer patients.

Nonetheless, the combination of *TP53* status with HDMX SNP genotypes allows the identification of 3 distinct groups of patients with low (wt *TP53* and G/G HDMX SNP), intermediate (wt *TP53* and A/A HDMX SNP or mutant *TP53* and G/G HDMX SNP) and high (mutant *TP53* and A/A HDMX SNP) risks of metastatic progression (p=1.6E-06). Further analyses of interactions of p53 network genes and their molecular alterations, particularly including other validated p53 pathway genes like HDM2 SNP309 and p53-codon 72 SNP, which have been already demonstrated to associate with differential survival, could offer further specificity and allow the development of a robust set of p53-specific biomarkers with significant clinical validity.

eQTLs studies associate with some limitations in the detection of SNPs that associate with different transcript levels of the host gene. It is estimated that only 60% of gene transcripts can be found in all of the cell lines and tissues analysed so far (Cookson, Liang *et al.*, 2009). Moreover, some transcript signatures might be only tissue- or cancer-specific. Therefore, in Chapter 6, a screening approach was developed and implemented to identify novel p53 pathway SNPs that could affect cancer progression, but at the same identify

genes that are strong effectors or modulators of the p53 pathway. Survival analyses for 672 high frequency tag SNPs from 114 p53 network genes were performed in a cohort of 105 malignant melanoma patients. SNPs in the *FOXO3* (p=0.003), *TP73* (p=0.005), *EGFR* (p=0.008) and *HDAC2* (p=0.04) genes were identified as good candidates for biomarkers of metastatic progression. Validation of these SNPs in larger cohorts of melanoma and other cancer types that are controlled by the p53 pathway is necessary. However, the results of the screen give strong support to the hypothesis that functional SNPs in the p53 pathway can affect metastatic progression.

To fully assess functional inherited polymorphisms as biomarkers for metastatic progression, further elucidation of the molecular mechanisms underlying the observed SNP-dependent phenotypes is needed. The identification and analysis of a causal SNP in the *HDMX* haplotype block has been carried out by others in the group (Lukasz F. Grochola and Juliet Hewitt). In this study, functional analyses of the FOXO3 SNP identified in the metastasis-free survival screen were undertaken. Utility of the publicly available SNP catalogues (HapMap and 1000 Genomes) and databases of functional elements of the genome (ENCODE) have enabled the identification of 3 causal SNP candidates within the *FOXO3* haplotype block. The most recent release of the ENCODE database offers up to 80% genome coverage (Bernstein, Birney *et al.*, 2012), however, current SNP catalogues do not offer full genome coverage and might not include all SNPs with high LD. Only further high-resolution genotyping will allow more adequate determination of SNP haplotype blocks and the identification of causal SNPs. However, the functional analyses

described in Chapter 6 suggest that the causal SNP from the *FOXO3* haplotype block, similarly to the HDMX SNP, affects *FOXO3* gene transcription. Moreover, the experimental evidence presented suggests that the causal SNP is regulated by the protein GATA3, the loss of which is associated with ER-positive breast cancer and low levels of GATA3 protein expression have been described as an independent predictor of breast cancer progression (Mehra, Varambally *et al.*, 2005). Analyses of the FOXO3 SNP in the breast cancer cohorts are needed to determine the implicated interactions of the SNP with GATA3, ER status and cancer progression. Nonetheless, the results presented in Chapters 5 and 6 demonstrate that somatic mutations frequently associated with cancer are likely to modulate the effect of functional polymorphisms in the p53 pathway, and need to be taken into strong consideration when fully evaluating the prognostic value of functional p53 pathway SNPs.

Importantly, in Chapter 4, the analysis of two p53 pathway biomarkers (*HDMX-S/FL* ratio and *TP53* mutation) in a group of breast cancer patients that did not receive any adjuvant treatment demonstrated that the observed associations of p53 pathway attenuation with accelerated metastatic progression are independent of adjuvant treatment. This result indicates that the p53 pathway is critical not only in tumour prevention, but also metastatic progression and that, as suggested by Bernards and Weinberg, genes implicated in tumourigenesis are also important in processes that drive the metastatic potential of primary tumour cells (Bernards and Weinberg, 2002). Utilisation of p53 pathway biomarkers could have strong implications in the clinic. Firstly, p53 pathway biomarkers could allow the recognition of distinct groups of

patients with early stage disease, who lack the standard pathological markers for the aggressive phenotype but are, in fact, at very high risk of metastatic disease. Indeed, it has been proposed that *TP53* mutation in low-grade dysplasia with a high rate of *TP53* can indicate a high risk of malignant transformation into poor prognosis in oesophageal and endometrial cancers *(Jia, Liu et al., 2008).* Thus, it is possible that screening for p53 attenuation in early stage tumours could reduce the number of patients with metastatic disease, which could have a very significant clinical and also economic impact, as the disease burden imposed by breast cancer alone is tremendous. The direct cost of treating breast cancer patients in the year 2010 accounted for 13% of the total cost of cancer treatment in the United States, but the statistics reveal even more drastic numbers whereby the yearly cost of treatment of advanced stage breast cancer exceeds that of low stage cancers by over 500% (Zimmerman and Mehr, 2012). Secondly, p53 pathway biomarkers could improve the prognostication of low risk patients.

The utilisation of multiple pathological and molecular biomarkers, particularly hormone receptor status, has improved breast cancer management by enabling the more effective identification of low- and high-risk patient groups (Espinosa, Gamez-Pozo *et al.*, 2012; Reis-Filho and Pusztai, 2011). Nonetheless, the vast majority of patients are placed in the intermediate-risk group and, therefore, treatment decisions for these patients remain a great challenge, resulting in the overtreatment of many cancer patients (Espinosa, Gamez-Pozo *et al.*, 2012; Weigelt, Peterse *et al.*, 2005). Further elucidation of p53 pathway biomarkers is needed in larger cancer patient cohorts to fully

understand how they interact with each other to predict the aggressive phenotype of primary tumours. However, it is likely that p53 pathway biomarkers could contribute to better prognostication, and decrease the over-diagnosis and overtreatment of patients with non-aggressive lesions. Finally, p53 pathway biomarkers could serve as predictive biomarkers and be applied in personalised treatment strategies to treat primary and metastatic lesions.

Different strategies to reactivate the p53 pathway are currently under clinical development (Lehmann, Bykov *et al.*, 2012; Pearson, Jia *et al.*, 2004; Ray-Coquard, Blay *et al.*, 2012; Senzer, Nemunaitis *et al.*, 2007; Vazquez, Bond *et al.*, 2008; Yuan, Liao *et al.*, 2011). For instance, the reactivation of the p53 pathway using HDM2-specific inhibitors in tumours with wt *TP53* and low *HDMX-S/FL* ratio, or small molecules that refold mutant p53 in tumours with mutant *TP53* and the A/A genotype of HDMX SNP, could be used as stand-alone treatments or in combination with other cancer therapeutics to treat primary and metastatic lesions. The survival analyses suggest that biomarkers for high levels of p53 inhibitors, HDM2 and HDMX can indicate better prognosis for patients with mutant p53, whereby high levels of HDMX assessed by HDMX SNP G/G genotype and high levels of HDM2 assessed by high *HDMX-S/FL* ratio demonstrate a better prognosis of patients with mutant p53, suggesting that the inhibitory effect of HDMX and HDM2 on mutant p53 leads to the suppression of pro-metastatic activities. Restoration of wt p53 function in tumours with mutant p53 could offer an effective treatment for breast cancer patients with ER-negative tumours, particularly those that belong to the triple negative breast cancer (TNBC) group, for whom current treatment options are very limited and

no specific targeted therapies are available to date (Bayraktar and Gluck, 2013). *In vivo* experiments in mice give a strong support to the idea that p53 attenuation is important in tumour maintenance, and that reactivation of the p53 pathway results in tumour clearance (Ventura, Kirsch *et al.*, 2007; Xue, Zender *et al.*, 2007). p53's reactivation with the recombinant adenovirus Advexin has been demonstrated to induce regression of the metastatic lesion of a patient with refractory, progressive Li-Fraumeni syndrome (Senzer, Nemunaitis *et al.*, 2007). Additionally, p53 pathway reactivation could be used as a preventative treatment in high risk groups identified by p53 pathway biomarkers. A similar strategy has already been evaluated where Tamoxifen, which is used to treat ER-positive primary and metastatic cancers, has been used as an effective therapy to prevent breast cancer in high-risk groups (Cuzick, Sestak *et al.*, 2013; Powles, Ashley *et al.*, 2007).

Taken together, the work presented in this thesis provides strong support for the role of the p53 pathway in the metastatic progression of cancer, and suggests that molecular biomarkers that can detect changes in the activity of p53 pathway genes could offer a robust set of biomarkers for cancer progression applicable to different types of cancer. Further elucidation of other genes from the wider p53 pathway is needed to better understand the tight molecular network that controls the mechanisms that lead to metastatic progression. In addition, further validation of p53 pathway biomarkers is needed in more cancer cohorts, including all cancer types where the p53 pathway has been strongly implicated in either tumourigenesis or metastatic progression, to fully evaluate the clinical utility of p53 pathway biomarkers.

Nonetheless, p53-specific biomarkers could lead to the improvement of prognostication of cancer patients, and could also be used as predictive biomarkers for therapies aimed at the reactivation of p53 that are likely to be very effective in preventing and treating metastatic disease, when given to the right group of patients.

8 REFERENCES

Abecasis, GR, Auton, A, Brooks, LD, DePristo, MA, Durbin, RM, Handsaker, RE, (…) McVean, GA (2012). An integrated map of genetic variation from 1,092 human genomes. Nature *491*, 56-65.

Adorno, M, Cordenonsi, M, Montagner, M, Dupont, S, Wong, C, Hann, B, (…) Piccolo, S (2009). A Mutant-p53/Smad complex opposes p63 to empower TGFbeta-induced metastasis. Cell *137*, 87-98.

Ambrosini, G, Sambol, EB, Carvajal, D, Vassilev, LT, Singer, S, and Schwartz, GK (2007). Mouse double minute antagonist Nutlin-3a enhances chemotherapy-induced apoptosis in cancer cells with mutant p53 by activating E2F1. Oncogene *26*, 3473-3481.

Anselmi, CV, Malovini, A, Roncarati, R, Novelli, V, Villa, F, Condorelli, G, (…) Puca, AA (2009). Association of theFOXO3ALocus with Extreme Longevity in a Southern Italian Centenarian Study. Rejuvenation Research *12*, 95-104.

Asomaning, K, Reid, AE, Zhou, W, Heist, RS, Zhai, R, Su, L, (…) Liu, G (2008). MDM2 promoter polymorphism and pancreatic cancer risk and prognosis. Clin Cancer Res *14*, 4010-4015.

Atwal, GS, Kirchhoff, T, Bond, EE, Montagna, M, Menin, C, Bertorelle, R, (…) Bond, GL (2009). Altered tumor formation and evolutionary selection of genetic variants in the human MDM4 oncogene. Proc Natl Acad Sci U S A *106*, 10236-10241.

Avery-Kiejda, KA, Bowden, NA, Croft, AJ, Scurr, LL, Kairupan, CF, Ashton, KA, (…) Hersey, P (2011). P53 in human melanoma fails to regulate target genes associated with apoptosis and the cell cycle and may contribute to proliferation. BMC Cancer *11*, 203.

Badciong, JC, and Haas, AL (2002). MdmX is a RING finger ubiquitin ligase capable of synergistically enhancing Mdm2 ubiquitination. J Biol Chem *277*, 49668-49675.

Banasik, K, Ribel-Madsen, R, Gjesing, AP, Wegner, L, Andersson, A, Poulsen, P, (…) Vaag, A (2010). The FOXO3A rs2802292 G-Allele Associates with Improved Peripheral and Hepatic Insulin Sensitivity and Increased Skeletal Muscle-FOXO3A mRNA Expression in Twins. Journal of Clinical Endocrinology & Metabolism *96*, E119-E124.

Bardeesy, N, Bastian, BC, Hezel, A, Pinkel, D, DePinho, RA, and Chin, L (2001). Dual inactivation of RB and p53 pathways in RAS-induced melanomas. Mol Cell Biol *21*, 2144-2153.

Bartel, F, Schulz, J, Bohnke, A, Blumke, K, Kappler, M, Bache, M, (…) Hauptmann, S (2005). Significance of HDMX-S (or MDM4) mRNA splice variant

overexpression and HDMX gene amplification on primary soft tissue sarcoma prognosis. Int J Cancer *117*, 469-475.

Bayraktar, S, and Gluck, S (2013). Molecularly targeted therapies for metastatic triple-negative breast cancer. Breast Cancer Res Treat *138*, 21-35.

Bernards, R, and Weinberg, RA (2002). A progression puzzle. Nature *418*, 823.

Bernstein, BE, Birney, E, Dunham, I, Green, ED, Gunter, C, and Snyder, M (2012). An integrated encyclopedia of DNA elements in the human genome. Nature *489*, 57-74.

Bertheau, P, Espie, M, Turpin, E, Lehmann, J, Plassa, LF, Varna, M, (…) de The, H (2008). TP53 status and response to chemotherapy in breast cancer. Pathobiology *75*, 132-139.

Bezzi, M, Teo, SX, Muller, J, Mok, WC, Sahu, SK, Vardy, LA, (…) Guccione, E (2013). Regulation of constitutive and alternative splicing by PRMT5 reveals a role for Mdm4 pre-mRNA in sensing defects in the spliceosomal machinery. Genes Dev *27*, 1903-1916.

Bidard, FC, Pierga, JY, Soria, JC, and Thiery, JP (2013). Translating metastasis-related biomarkers to the clinic--progress and pitfalls. Nat Rev Clin Oncol *10*, 169-179.

Biomarkers and surrogate endpoints: preferred definitions and conceptual framework. (2001). Clin Pharmacol Ther *69*, 89-95.

Birch, JM, Hartley, AL, Tricker, KJ, Prosser, J, Condie, A, Kelsey, AM, (…) et al. (1994). Prevalence and diversity of constitutional mutations in the p53 gene among 21 Li-Fraumeni families. Cancer Res *54*, 1298-1304.

Birney, E, Stamatoyannopoulos, JA, Dutta, A, Guigo, R, Gingeras, TR, Margulies, EH, (…) de Jong, PJ (2007). Identification and analysis of functional elements in 1% of the human genome by the ENCODE pilot project. Nature *447*, 799-816.

Bollag, G, Hirth, P, Tsai, J, Zhang, J, Ibrahim, PN, Cho, H, (…) Nolop, K (2010). Clinical efficacy of a RAF inhibitor needs broad target blockade in BRAF-mutant melanoma. Nature *467*, 596-599.

Bond, GL, Hu, W, Bond, EE, Robins, H, Lutzker, SG, Arva, NC, (…) Levine, AJ (2004). A Single Nucleotide Polymorphism in the MDM2 Promoter Attenuates the p53 Tumor Suppressor Pathway and Accelerates Tumor Formation in Humans. Cell *119*, 591-602.

Bond, GL, and Levine, AJ (2007). A single nucleotide polymorphism in the p53 pathway interacts with gender, environmental stresses and tumor genetics to influence cancer in humans. Oncogene *26*, 1317-1323.

Bougeard, G, Baert-Desurmont, S, Tournier, I, Vasseur, S, Martin, C, Brugieres, L, (…) Frebourg, T (2006). Impact of the MDM2 SNP309 and p53 Arg72Pro polymorphism on age of tumour onset in Li-Fraumeni syndrome. J Med Genet *43*, 531-533.

Box, NF, and Terzian, T (2008). The role of p53 in pigmentation, tanning and melanoma. Pigment Cell Melanoma Res *21*, 525-533.

Boyd, MT, and Vlatkovic, N (2008). p53: a molecular marker for the detection of cancer. Expert Opin Med Diagn *2*, 1013-1024.

Bradl, M, Klein-Szanto, A, Porter, S, and Mintz, B (1991). Malignant melanoma in transgenic mice. Proc Natl Acad Sci U S A *88*, 164-168.

Braicu, C, Pileczki, V, Irimie, A, and Berindan-Neagoe, I (2013). p53siRNA therapy reduces cell proliferation, migration and induces apoptosis in triple negative breast cancer cells. Mol Cell Biochem *381*, 61-68.

Brown, CD, Mangravite, LM, and Engelhardt, BE (2013). Integrative Modeling of eQTLs and Cis-Regulatory Elements Suggests Mechanisms Underlying Cell Type Specificity of eQTLs. PLoS genetics *9*, e1003649.

Brown, JM, and Attardi, LD (2005). The role of apoptosis in cancer development and treatment response. Nat Rev Cancer *5*, 231-237.

Buddingh, EP, Anninga, JK, Versteegh, MI, Taminiau, AH, Egeler, RM, van Rijswijk, CS, (…) Gelderblom, H (2010). Prognostic factors in pulmonary metastasized high-grade osteosarcoma. Pediatr Blood Cancer *54*, 216-221.

Burrell, RA, McGranahan, N, Bartek, J, and Swanton, C (2013). The causes and consequences of genetic heterogeneity in cancer evolution. Nature *501*, 338-345.

Caron de Fromentel, C, and Soussi, T (1992). TP53 tumor suppressor gene: a model for investigating human mutagenesis. Genes Chromosomes Cancer *4*, 1-15.

Cattelani, S, Ferrari-Amorotti, G, Galavotti, S, Defferrari, R, Tanno, B, Cialfi, S, (…) Calabretta, B (2012). The p53 codon 72 Pro/Pro genotype identifies poor-prognosis neuroblastoma patients: correlation with reduced apoptosis and enhanced senescence by the p53-72P isoform. Neoplasia *14*, 634-643.

Cesario, A, Marcus, FB, and SpringerLink (Online service) (2011). Cancer systems biology, bioinformatics and medicine research and clinical applications (Dordrecht ; New York: Springer,), pp. 1 online resource (xxviii, 484 p.).

Chen, J, Gomes, AR, Monteiro, LJ, Wong, SY, Wu, LH, Ng, TT, (…) Khoo, US (2010). Constitutively nuclear FOXO3a localization predicts poor survival and promotes Akt phosphorylation in breast cancer. PLoS One *5*, e12293.

Chin, L (2003). The genetics of malignant melanoma: lessons from mouse and man. Nature Reviews Cancer *3*, 559-570.

Chou, J, Lin, JH, Brenot, A, Kim, JW, Provot, S, and Werb, Z (2013). GATA3 suppresses metastasis and modulates the tumour microenvironment by regulating microRNA-29b expression. Nat Cell Biol *15*, 201-213.

Chou, J, Provot, S, and Werb, Z (2010). GATA3 in development and cancer differentiation: cells GATA have it! J Cell Physiol *222*, 42-49.

Cleton-Jansen, AM, Anninga, JK, Briaire-de, BI, Romeo, S, Oosting, J, Egeler, RM, (…) Hogendoorn, PC (2009). Profiling of high-grade central osteosarcoma and its putative progenitor cells identifies tumourigenic pathways. BrJCancer *101*, 1909-1918.

ClinicalTrials.gov; Available from: http://www.clinicaltrials.gov

Consortium, TIH (2003). The International HapMap Project. Nature *426*, 789-796.

Cookson, W, Liang, L, Abecasis, G, Moffatt, M, and Lathrop, M (2009). Mapping complex disease traits with global gene expression. Nat Rev Genet *10*, 184-194.

Cotter, TG (2009). Apoptosis and cancer: the genesis of a research field. Nat Rev Cancer *9*, 501-507.

Couch, FJ, Wang, X, McGuffog, L, Lee, A, Olswold, C, Kuchenbaecker, KB, (…) Antoniou, AC (2013). Genome-wide association study in BRCA1 mutation carriers identifies novel loci associated with breast and ovarian cancer risk. PLoS Genet *9*, e1003212.

Courtois-Cox, S, Jones, SL, and Cichowski, K (2008). Many roads lead to oncogene-induced senescence. Oncogene *27*, 2801-2809.

Coutant, C, Rouzier, R, Qi, Y, Lehmann-Che, J, Bianchini, G, Iwamoto, T, (…) Pusztai, L (2011). Distinct p53 gene signatures are needed to predict prognosis and response to chemotherapy in ER-positive and ER-negative breast cancers. Clin Cancer Res *17*, 2591-2601.

Cuzick, J, Sestak, I, Bonanni, B, Costantino, JP, Cummings, S, DeCensi, A, (…) Wickerham, DL (2013). Selective oestrogen receptor modulators in prevention of breast cancer: an updated meta-analysis of individual participant data. Lancet *381*, 1827-1834.

da Costa, CE, Szuhai, K, van Eijk, R, Hoogeboom, M, Sciot, R, Mertens, F, (…) Annels, NE (2009). No genomic aberrations in Langerhans cell histiocytosis as assessed by diverse molecular technologies. Genes Chromosomes Cancer *48*, 239-249.

Danovi, D, Meulmeester, E, Pasini, D, Migliorini, D, Capra, M, Frenk, R, (…) Marine, JC (2004). Amplification of Mdmx (or Mdm4) directly contributes to tumor formation by inhibiting p53 tumor suppressor activity. Mol Cell Biol *24*, 5835-5843.

De Craene, B, and Berx, G (2013). Regulatory networks defining EMT during cancer initiation and progression. Nat Rev Cancer *13*, 97-110.

Di Conza, G, Mancini, F, Buttarelli, M, Pontecorvi, A, Trimarchi, F, and Moretti, F (2012). MDM4 enhances p53 stability by promoting an active conformation of the protein upon DNA damage. Cell Cycle *11*, 749-760.

Dimas, AS, Deutsch, S, Stranger, BE, Montgomery, SB, Borel, C, Attar-Cohen, H, (…) Antonarakis, SE (2009). Common regulatory variation impacts gene expression in a cell type-dependent manner. Science *325*, 1246-1250.

Eeles, RA, Olama, AA, Benlloch, S, Saunders, EJ, Leongamornlert, DA, Tymrakiewicz, M, (…) Easton, DF (2013). Identification of 23 new prostate cancer susceptibility loci using the iCOGS custom genotyping array. Nat Genet *45*, 385-391, 391e381-382.

el-Deiry, WS, Kern, SE, Pietenpol, JA, Kinzler, KW, and Vogelstein, B (1992). Definition of a consensus binding site for p53. Nat Genet *1*, 45-49.

Elstrodt, F, Hollestelle, A, Nagel, JH, Gorin, M, Wasielewski, M, van den Ouweland, A, (…) Schutte, M (2006). BRCA1 mutation analysis of 41 human breast cancer cell lines reveals three new deleterious mutants. Cancer Res *66*, 41-45.

Ernst, J, Kheradpour, P, Mikkelsen, TS, Shoresh, N, Ward, LD, Epstein, CB, (…) Bernstein, BE (2011). Mapping and analysis of chromatin state dynamics in nine human cell types. Nature *473*, 43-49.

Espinosa, E, Gamez-Pozo, A, Sanchez-Navarro, I, Pinto, A, Castaneda, CA, Ciruelos, E, (…) Vara, JA (2012). The present and future of gene profiling in breast cancer. Cancer Metastasis Rev *31*, 41-46.

Fairfax, BP, Makino, S, Radhakrishnan, J, Plant, K, Leslie, S, Dilthey, A, (…) Knight, JC (2012). Genetics of gene expression in primary immune cells identifies cell type-specific master regulators and roles of HLA alleles. Nature genetics *44*, 502-510.

Fehrmann, RS, Jansen, RC, Veldink, JH, Westra, HJ, Arends, D, Bonder, MJ, (…) Franke, L (2011). Trans-eQTLs reveal that independent genetic variants associated with a complex phenotype converge on intermediate genes, with a major role for the HLA. PLoS genetics *7*, e1002197.

Firoz, EF, Warycha, M, Zakrzewski, J, Pollens, D, Wang, G, Shapiro, R, (…) Polsky, D (2009). Association of MDM2 SNP309, age of onset, and gender in cutaneous melanoma. Clin Cancer Res *15*, 2573-2580.

Flachsbart, F, Caliebe, A, Kleindorp, R, Blanche, H, von Eller-Eberstein, H, Nikolaus, S, (…) Nebel, A (2009). Association of FOXO3A variation with human longevity confirmed in German centenarians. Proceedings of the National Academy of Sciences *106*, 2700-2705.

Funk, WD, Pak, DT, Karas, RH, Wright, WE, and Shay, JW (1992). A transcriptionally active DNA-binding site for human p53 protein complexes. Mol Cell Biol *12*, 2866-2871.

Gadea, G, Lapasset, L, Gauthier-Rouviere, C, and Roux, P (2002). Regulation of Cdc42-mediated morphological effects: a novel function for p53. EMBO J *21*, 2373-2382.

Gan, L, Liu, P, Lu, H, Chen, S, Yang, J, McCarthy, JB, (…) Huang, H (2009). Cyclin D1 promotes anchorage-independent cell survival by inhibiting FOXO-mediated anoikis. Cell Death and Differentiation *16*, 1408-1417.

Garbe, C, and Leiter, U (2009). Melanoma epidemiology and trends. Clinics in Dermatology *27*, 3-9.

Garcia-Closas, M, Couch, FJ, Lindstrom, S, Michailidou, K, Schmidt, MK, Brook, MN, (…) Kraft, P (2013). Genome-wide association studies identify four ER negative-specific breast cancer risk loci. Nat Genet *45*, 392-398, 398e391-392.

Gelderblom, H, Jinks, RC, Sydes, M, Bramwell, VH, van, GM, Grimer, RJ, (…) Whelan, J (2011). Survival after recurrent osteosarcoma: data from 3 European Osteosarcoma Intergroup (EOI) randomized controlled trials. EurJCancer *47*, 895-902.

Gembarska, A, Luciani, F, Fedele, C, Russell, EA, Dewaele, M, Villar, S, (…) Marine, JC (2012). MDM4 is a key therapeutic target in cutaneous melanoma. Nat Med.

Georgescu, MM (2010). PTEN Tumor Suppressor Network in PI3K-Akt Pathway Control. Genes Cancer *1*, 1170-1177.

Giblin, AV, and Thomas, JM (2007). Incidence, mortality and survival in cutaneous melanoma. Journal of Plastic, Reconstructive & Aesthetic Surgery *60*, 32-40.

Goh, AM, Coffill, CR, and Lane, DP (2011). The role of mutant p53 in human cancer. J Pathol *223*, 116-126.

Gray-Schopfer, V, Wellbrock, C, and Marais, R (2007). Melanoma biology and new targeted therapy. Nature *445*, 851-857.

Greaves, M, and Maley, CC (2012). Clonal evolution in cancer. Nature *481*, 306-313.

Grochola, LF, Zeron-Medina, J, Meriaux, S, and Bond, GL (2010). Single-nucleotide polymorphisms in the p53 signaling pathway. Cold Spring Harb Perspect Biol *2*, a001032.

Grundberg, E, Small, KS, Hedman, AK, Nica, AC, Buil, A, Keildson, S, (…) Spector, TD (2012). Mapping cis- and trans-regulatory effects across multiple tissues in twins. Nature genetics *44*, 1084-1089.

Gryshchenko, I, Hofbauer, S, Stoecher, M, Daniel, PT, Steurer, M, Gaiger, A, (…) Tinhofer, I (2008). MDM2 SNP309 is associated with poor outcome in B-cell chronic lymphocytic leukemia. J Clin Oncol *26*, 2252-2257.

Haber, DA, and Settleman, J (2007). Cancer: drivers and passengers. Nature *446*, 145-146.

Hainaut, P, and Hollstein, M (2000). p53 and human cancer: the first ten thousand mutations. Adv Cancer Res *77*, 81-137.

Han, JY, Lee, GK, Jang, DH, Lee, SY, and Lee, JS (2008). Association of p53 codon 72 polymorphism and MDM2 SNP309 with clinical outcome of advanced nonsmall cell lung cancer. Cancer *113*, 799-807.

Hao, K, Bosse, Y, Nickle, DC, Pare, PD, Postma, DS, Laviolette, M, (…) Sin, DD (2012). Lung eQTLs to help reveal the molecular underpinnings of asthma. PLoS genetics *8*, e1003029.

Haupt, Y, Maya, R, Kazaz, A, and Oren, M (1997). Mdm2 promotes the rapid degradation of p53. Nature *387*, 296-299.

Hilmi, C, Larribere, L, Deckert, M, Rocchi, S, Giuliano, S, Bille, K, (…) Bertolotto, C (2008). Involvement of FKHRL1 in melanoma cell survival and death. Pigment Cell & Melanoma Research *21*, 139-146.

Hirata, H, Hinoda, Y, Kikuno, N, Kawamoto, K, Suehiro, Y, Tanaka, Y, and Dahiya, R (2007). MDM2 SNP309 polymorphism as risk factor for susceptibility and poor prognosis in renal cell carcinoma. Clin Cancer Res *13*, 4123-4129.

Hollstein, M, Sidransky, D, Vogelstein, B, and Harris, CC (1991). p53 mutations in human cancers. Science *253*, 49-53.

Houben, R, Hesbacher, S, Schmid, CP, Kauczok, CS, Flohr, U, Haferkamp, S, (…) Becker, JC (2011). High-level expression of wild-type p53 in melanoma cells is frequently associated with inactivity in p53 reporter gene assays. PLoS One *6*, e22096.

Hu, W, Feng, Z, Ma, L, Wagner, J, Rice, JJ, Stolovitzky, G, and Levine, AJ (2007). A single nucleotide polymorphism in the MDM2 gene disrupts the oscillation of p53 and MDM2 levels in cells. Cancer Res *67*, 2757-2765.

Huang, L, Yan, Z, Liao, X, Li, Y, Yang, J, Wang, ZG, (…) Yuan, ZM (2011). The p53 inhibitors MDM2/MDMX complex is required for control of p53 activity in vivo. Proc Natl Acad Sci U S A *108*, 12001-12006.

Innocenti, F, Cooper, GM, Stanaway, IB, Gamazon, ER, Smith, JD, Mirkov, S, (…) Brown, CD (2011). Identification, replication, and functional fine-mapping of expression quantitative trait loci in primary human liver tissue. PLoS genetics *7*, e1002078.

Ishwaran, H, and Kogalur, UB (2010). Consistency of Random Survival Forests. Stat Probab Lett *80*, 1056-1064.

Itahana, K, Mao, H, Jin, A, Itahana, Y, Clegg, HV, Lindstrom, MS, (…) Zhang, Y (2007). Targeted inactivation of Mdm2 RING finger E3 ubiquitin ligase activity in the mouse reveals mechanistic insights into p53 regulation. Cancer Cell *12*, 355-366.

Ito, M, Barys, L, O'Reilly, T, Young, S, Gorbatcheva, B, Monahan, J, (…) Lisztwan, J (2011). Comprehensive mapping of p53 pathway alterations reveals an apparent role for both SNP309 and MDM2 amplification in sarcomagenesis. ClinCancer Res *17*, 416-426.

Jia, L, Liu, Y, Yi, X, Miron, A, Crum, CP, Kong, B, and Zheng, W (2008). Endometrial glandular dysplasia with frequent p53 gene mutation: a genetic evidence supporting its precancer nature for endometrial serous carcinoma. Clin Cancer Res *14*, 2263-2269.

Jones, SN, Roe, AE, Donehower, LA, and Bradley, A (1995). Rescue of embryonic lethality in Mdm2-deficient mice by absence of p53. Nature *378*, 206-208.

Kamrava, M, Gius, D, Casagrande, G, and Kohn, E (2011). Will targeting insulin growth factor help us or hurt us?: An oncologist's perspective. Ageing Res Rev *10*, 62-70.

Katsanis, SH, and Katsanis, N (2013). Molecular genetic testing and the future of clinical genomics. Nat Rev Genet *14*, 415-426.

Kawai, H, Wiederschain, D, and Yuan, ZM (2003). Critical contribution of the MDM2 acidic domain to p53 ubiquitination. MolCell Biol *23*, 4939-4947.

Kern, SE (2012). Why your new cancer biomarker may never work: recurrent patterns and remarkable diversity in biomarker failures. Cancer Res *72*, 6097-6101.

Kim, NH, Kim, HS, Li, XY, Lee, I, Choi, HS, Kang, SE, (…) Yook, JI (2011). A p53/miRNA-34 axis regulates Snail1-dependent cancer cell epithelial-mesenchymal transition. J Cell Biol *195*, 417-433.

Kruse, JP, and Gu, W (2009). Modes of p53 regulation. Cell *137*, 609-622.

Kulkarni, DA, Vazquez, A, Haffty, BG, Bandera, EV, Hu, W, Sun, YY, (…) Hirshfield, KM (2009). A polymorphic variant in human MDM4 associates with accelerated age of onset of estrogen receptor negative breast cancer. Carcinogenesis *30*, 1910-1915.

Lam, S, Lodder, K, Teunisse, AF, Rabelink, MJ, Schutte, M, and Jochemsen, AG (2010). Role of Mdm4 in drug sensitivity of breast cancer cells. Oncogene *29*, 2415-2426.

Lane, D, and Levine, A (2010). p53 Research: the past thirty years and the next thirty years. Cold Spring Harb Perspect Biol *2*, a000893.

Lang, GA, Iwakuma, T, Suh, YA, Liu, G, Rao, VA, Parant, JM, (…) Lozano, G (2004). Gain of function of a p53 hot spot mutation in a mouse model of Li-Fraumeni syndrome. Cell *119*, 861-872.

Langerod, A, Zhao, H, Borgan, O, Nesland, JM, Bukholm, IR, Ikdahl, T, (…) Jeffrey, SS (2007). TP53 mutation status and gene expression profiles are powerful prognostic markers of breast cancer. Breast Cancer Res *9*, R30.

Lau, LM, Nugent, JK, Zhao, X, and Irwin, MS (2008). HDM2 antagonist Nutlin-3 disrupts p73-HDM2 binding and enhances p73 function. Oncogene *27*, 997-1003.

Laurie, NA, Donovan, SL, Shih, CS, Zhang, J, Mills, N, Fuller, C, (…) Dyer, MA (2006). Inactivation of the p53 pathway in retinoblastoma. Nature *444*, 61-66.

Lehmann, S, Bykov, VJ, Ali, D, Andren, O, Cherif, H, Tidefelt, U, (…) Andersson, PO (2012). Targeting p53 in vivo: a first-in-human study with p53-targeting compound APR-246 in refractory hematologic malignancies and prostate cancer. J Clin Oncol *30*, 3633-3639.

Lenos, K, Grawenda, AM, Lodder, K, Kuijjer, ML, Teunisse, AF, Repapi, E, (…) Jochemsen, AG (2012). Alternate splicing of the p53 inhibitor HDMX offers a superior prognostic biomarker than p53 mutation in human cancer. Cancer Res *72*, 4074-4084.

Lenos, K, and Jochemsen, AG (2011). Functions of MDMX in the modulation of the p53-response. J Biomed Biotechnol *2011*, 876173.

Lewis, IJ, Nooij, MA, Whelan, J, Sydes, MR, Grimer, R, Hogendoorn, PC, (…) Taminiau, AH (2007). Improvement in histologic response but not survival in osteosarcoma patients treated with intensified chemotherapy: a randomized

phase III trial of the European Osteosarcoma Intergroup. JNatlCancer Inst *99*, 112-128.

Li, FP, Fraumeni, JF, Jr., Mulvihill, JJ, Blattner, WA, Dreyfus, MG, Tucker, MA, and Miller, RW (1988). A cancer family syndrome in twenty-four kindreds. Cancer Res *48*, 5358-5362.

Liang, L, Morar, N, Dixon, AL, Lathrop, GM, Abecasis, GR, Moffatt, MF, and Cookson, WO (2013). A cross-platform analysis of 14,177 expression quantitative trait loci derived from lymphoblastoid cell lines. Genome research *23*, 716-726.

Lim, SO, Kim, H, and Jung, G (2010). p53 inhibits tumor cell invasion via the degradation of snail protein in hepatocellular carcinoma. FEBS Lett *584*, 2231-2236.

Linares, LK, Hengstermann, A, Ciechanover, A, Muller, S, and Scheffner, M (2003). HdmX stimulates Hdm2-mediated ubiquitination and degradation of p53. Proc Natl Acad Sci U S A *100*, 12009-12014.

Liu, YY (2011). Resuscitating wild-type p53 expression by disrupting ceramide glycosylation: a novel approach to target mutant p53 tumors. Cancer Res *71*, 6295-6299.

Lu, M, Breyssens, H, Salter, V, Zhong, S, Hu, Y, Baer, C, (…) Lu, X (2013). Restoring p53 function in human melanoma cells by inhibiting MDM2 and cyclin B1/CDK1-phosphorylated nuclear iASPP. Cancer Cell *23*, 618-633.

Lundgren, K, Montes de Oca Luna, R, McNeill, YB, Emerick, EP, Spencer, B, Barfield, CR, (…) Finlay, CA (1997). Targeted expression of MDM2 uncouples S phase from mitosis and inhibits mammary gland development independent of p53. Genes Dev *11*, 714-725.

Malats, N, Bustos, A, Nascimento, CM, Fernandez, F, Rivas, M, Puente, D, (…) Real, FX (2005). P53 as a prognostic marker for bladder cancer: a meta-analysis and review. Lancet Oncol *6*, 678-686.

Malkin, D (2011). Li-fraumeni syndrome. Genes Cancer *2*, 475-484.

Mancini, F, Di Conza, G, Pellegrino, M, Rinaldo, C, Prodosmo, A, Giglio, S, (…) Moretti, F (2009). MDM4 (MDMX) localizes at the mitochondria and facilitates the p53-mediated intrinsic-apoptotic pathway. EMBO J *28*, 1926-1939.

Marcel, V, Palmero, EI, Falagan-Lotsch, P, Martel-Planche, G, Ashton-Prolla, P, Olivier, M, (…) Achatz, MI (2009). TP53 PIN3 and MDM2 SNP309 polymorphisms as genetic modifiers in the Li-Fraumeni syndrome: impact on age at first diagnosis. J Med Genet *46*, 766-772.

Marine, JC, and Jochemsen, AG (2005). Mdmx as an essential regulator of p53 activity. BiochemBiophysResCommun *331*, 750-760.

Matijasevic, Z, Krzywicka-Racka, A, Sluder, G, and Jones, SN (2008). MdmX regulates transformation and chromosomal stability in p53-deficient cells. Cell Cycle *7*, 2967-2973.

Matijasevic, Z, Steinman, HA, Hoover, K, and Jones, SN (2008). MdmX promotes bipolar mitosis to suppress transformation and tumorigenesis in p53-deficient cells and mice. Mol Cell Biol *28*, 1265-1273.

Matys, V, Fricke, E, Geffers, R, Gossling, E, Haubrock, M, Hehl, R, (…) Wingender, E (2003). TRANSFAC: transcriptional regulation, from patterns to profiles. Nucleic Acids Res *31*, 374-378.

McLendon, R, Friedman, A, and Bigner, D (2008). Comprehensive genomic characterization defines human glioblastoma genes and core pathways. Nature *455*, 1061-1068.

Mehlen, P, and Puisieux, A (2006). Metastasis: a question of life or death. Nat Rev Cancer *6*, 449-458.

Mehra, R, Varambally, S, Ding, L, Shen, R, Sabel, MS, Ghosh, D, (…) Kleer, CG (2005). Identification of GATA3 as a breast cancer prognostic marker by global gene expression meta-analysis. Cancer Res *65*, 11259-11264.

Mejia, JE, and Larin, Z (2000). The assembly of large BACs by in vivo recombination. Genomics *70*, 165-170.

Melino, G (2011). p63 is a suppressor of tumorigenesis and metastasis interacting with mutant p53. Cell Death Differ *18*, 1487-1499.

Merlo, LM, Pepper, JW, Reid, BJ, and Maley, CC (2006). Cancer as an evolutionary and ecological process. Nat Rev Cancer *6*, 924-935.

Meulmeester, E, Frenk, R, Stad, R, de, GP, Marine, JC, Vousden, KH, and Jochemsen, AG (2003). Critical role for a central part of Mdm2 in the ubiquitylation of p53. MolCell Biol *23*, 4929-4938.

Meulmeester, E, Pereg, Y, Shiloh, Y, and Jochemsen, AG (2005). ATM-mediated phosphorylations inhibit Mdmx/Mdm2 stabilization by HAUSP in favor of p53 activation. Cell Cycle *4*, 1166-1170.

Meyle, KD, and Guldberg, P (2009). Genetic risk factors for melanoma. Human Genetics *126*, 499-510.

Millar, EK, Graham, PH, McNeil, CM, Browne, L, O'Toole, SA, Boulghourjian, A, (…) Sutherland, RL (2011). Prediction of outcome of early ER+ breast cancer is improved using a biomarker panel, which includes Ki-67 and p53. Br J Cancer *105*, 272-280.

Miller, LD, Smeds, J, George, J, Vega, VB, Vergara, L, Ploner, A, (…) Bergh, J (2005). An expression signature for p53 status in human breast cancer predicts mutation status, transcriptional effects, and patient survival. Proc Natl Acad Sci U S A *102*, 13550-13555.

Mohseny, AB, Machado, I, Cai, Y, Schaefer, KL, Serra, M, Hogendoorn, PC, (…) Cleton-Jansen, AM (2011). Functional characterization of osteosarcoma cell lines provides representative models to study the human disease. Lab Invest *91*, 1195-1205.

Momand, J, Jung, D, Wilczynski, S, and Niland, J (1998). The MDM2 gene amplification database. Nucleic Acids Res *26*, 3453-3459.

Momand, J, Wu, HH, and Dasgupta, G (2000). MDM2--master regulator of the p53 tumor suppressor protein. Gene *242*, 15-29.

Montes de Oca Luna, R, Wagner, DS, and Lozano, G (1995). Rescue of early embryonic lethality in mdm2-deficient mice by deletion of p53. Nature *378*, 203-206.

Montgomery, SB, Sammeth, M, Gutierrez-Arcelus, M, Lach, RP, Ingle, C, Nisbett, J, (…) Dermitzakis, ET (2010). Transcriptome genetics using second generation sequencing in a Caucasian population. Nature *464*, 773-777.

Muller, PA, Caswell, PT, Doyle, B, Iwanicki, MP, Tan, EH, Karim, S, (…) Vousden, KH (2009). Mutant p53 drives invasion by promoting integrin recycling. Cell *139*, 1327-1341.

Muller, PA, and Vousden, KH (2013). p53 mutations in cancer. Nat Cell Biol *15*, 2-8.

Muller, PA, Vousden, KH, and Norman, JC (2011). p53 and its mutants in tumor cell migration and invasion. J Cell Biol *192*, 209-218.

Naume, B, Zhao, X, Synnestvedt, M, Borgen, E, Russnes, HG, Lingjaerde, OC, (…) Sorlie, T (2007). Presence of bone marrow micrometastasis is associated with different recurrence risk within molecular subtypes of breast cancer. Mol Oncol *1*, 160-171.

Neilsen, PM, Noll, JE, Suetani, RJ, Schulz, RB, Al-Ejeh, F, Evdokiou, A, (…) Callen, DF (2011). Mutant p53 uses p63 as a molecular chaperone to alter gene expression and induce a pro-invasive secretome. Oncotarget *2*, 1203-1217.

Nelson, A, and Tsao, H (2009). Melanoma and genetics☆. Clin Dermatol *27*, 46-52.

Nguyen, AH, Tremblay, M, Haigh, K, Koumakpayi, IH, Paquet, M, Pandolfi, PP, (…) Bouchard, M (2013). Gata3 antagonizes cancer progression in Pten-deficient prostates. Hum Mol Genet *22*, 2400-2410.

Nica, AC, Parts, L, Glass, D, Nisbet, J, Barrett, A, Sekowska, M, (…) Spector, TD (2011). The architecture of gene regulatory variation across multiple human tissues: the MuTHER study. PLoS Genet *7*, e1002003.

Nieto, MA (2011). The ins and outs of the epithelial to mesenchymal transition in health and disease. Annu Rev Cell Dev Biol *27*, 347-376.

Noon, AP, Vlatkovic, N, Polanski, R, Maguire, M, Shawki, H, Parsons, K, and Boyd, MT (2010). p53 and MDM2 in renal cell carcinoma: biomarkers for disease progression and future therapeutic targets? Cancer *116*, 780-790.

Ohmiya, N, Taguchi, A, Mabuchi, N, Itoh, A, Hirooka, Y, Niwa, Y, and Goto, H (2006). MDM2 promoter polymorphism is associated with both an increased susceptibility to gastric carcinoma and poor prognosis. J Clin Oncol *24*, 4434-4440.

Okamoto, K, Taya, Y, and Nakagama, H (2009). Mdmx enhances p53 ubiquitination by altering the substrate preference of the Mdm2 ubiquitin ligase. FEBS Lett *583*, 2710-2714.

Olive, KP, Tuveson, DA, Ruhe, ZC, Yin, B, Willis, NA, Bronson, RT, (…) Jacks, T (2004). Mutant p53 gain of function in two mouse models of Li-Fraumeni syndrome. Cell *119*, 847-860.

Olivier, M, Goldgar, DE, Sodha, N, Ohgaki, H, Kleihues, P, Hainaut, P, and Eeles, RA (2003). Li-Fraumeni and related syndromes: correlation between tumor type, family structure, and TP53 genotype. Cancer Res *63*, 6643-6650.

Olivier, M, Hollstein, M, and Hainaut, P (2010). TP53 mutations in human cancers: origins, consequences, and clinical use. Cold Spring Harb Perspect Biol *2*, a001008.

Olivier, M, Langerod, A, Carrieri, P, Bergh, J, Klaar, S, Eyfjord, J, (…) Borresen-Dale, AL (2006). The clinical value of somatic TP53 gene mutations in 1,794 patients with breast cancer. Clin Cancer Res *12*, 1157-1167.

Olivier, M, Petitjean, A, Marcel, V, Petre, A, Mounawar, M, Plymoth, A, (…) Hainaut, P (2009). Recent advances in p53 research: an interdisciplinary perspective. Cancer Gene Ther *16*, 1-12.

Onel, K, and Cordon-Cardo, C (2004). MDM2 and prognosis. Mol Cancer Res *2*, 1-8.

Oshima, K, Naoi, Y, Kishi, K, Nakamura, Y, Iwamoto, T, Shimazu, K, (…) Noguchi, S (2011). Gene expression signature of TP53 but not its mutation status predicts response to sequential paclitaxel and 5-FU/epirubicin/cyclophosphamide in human breast cancer. Cancer Lett *307*, 149-157.

Ottaviano, L, Schaefer, KL, Gajewski, M, Huckenbeck, W, Baldus, S, Rogel, U, (…) Poremba, C (2010). Molecular characterization of commonly used cell lines for bone tumor research: a trans-European EuroBoNet effort. Genes ChromosomesCancer *49*, 40-51.

Palmero, EI, Achatz, MI, Ashton-Prolla, P, Olivier, M, and Hainaut, P (2010). Tumor protein 53 mutations and inherited cancer: beyond Li-Fraumeni syndrome. Curr Opin Oncol *22*, 64-69.

Pant, V, Xiong, S, Iwakuma, T, Quintas-Cardama, A, and Lozano, G (2011). Heterodimerization of Mdm2 and Mdm4 is critical for regulating p53 activity during embryogenesis but dispensable for p53 and Mdm2 stability. Proc Natl Acad Sci U S A *108*, 11995-12000.

Parant, J, Chavez-Reyes, A, Little, NA, Yan, W, Reinke, V, Jochemsen, AG, and Lozano, G (2001). Rescue of embryonic lethality in Mdm4-null mice by loss of Trp53 suggests a nonoverlapping pathway with MDM2 to regulate p53. Nat Genet *29*, 92-95.

Park, HR, Jung, WW, Bertoni, F, Bacchini, P, Park, JH, Kim, YW, and Park, YK (2004). Molecular analysis of p53, MDM2 and H-ras genes in low-grade central osteosarcoma. PatholResPract *200*, 439-445.

Parker, JS, Mullins, M, Cheang, MC, Leung, S, Voduc, D, Vickery, T, (…) Bernard, PS (2009). Supervised risk predictor of breast cancer based on intrinsic subtypes. J Clin Oncol *27*, 1160-1167.

Pearson, S, Jia, H, and Kandachi, K (2004). China approves first gene therapy. Nat Biotechnol *22*, 3-4.

Perfumo, C, Parodi, S, Mazzocco, K, Defferrari, R, Inga, A, Haupt, R, (…) Tonini, GP (2008). Impact of MDM2 SNP309 genotype on progression and survival of stage 4 neuroblastoma. Eur J Cancer *44*, 2634-2639.

Perou, CM, Sorlie, T, Eisen, MB, van de Rijn, M, Jeffrey, SS, Rees, CA, (…) Botstein, D (2000). Molecular portraits of human breast tumours. Nature *406*, 747-752.

Perry, ME (2010). The regulation of the p53-mediated stress response by MDM2 and MDM4. Cold Spring Harb Perspect Biol *2*, a000968.

Petitjean, A, Achatz, MI, Borresen-Dale, AL, Hainaut, P, and Olivier, M (2007). TP53 mutations in human cancers: functional selection and impact on cancer prognosis and outcomes. Oncogene *26*, 2157-2165.

Petitjean, A, Mathe, E, Kato, S, Ishioka, C, Tavtigian, SV, Hainaut, P, and Olivier, M (2007). Impact of mutant p53 functional properties on TP53 mutation patterns and tumor phenotype: lessons from recent developments in the IARC TP53 database. Hum Mutat *28*, 622-629.

Phillips, A, Teunisse, A, Lam, S, Lodder, K, Darley, M, Emaduddin, M, (…) Jochemsen, AG (2010). HDMX-L is expressed from a functional p53-responsive promoter in the first intron of the HDMX gene and participates in an autoregulatory feedback loop to control p53 activity. J Biol Chem *285*, 29111-29127.

Pishas, KI, Al-Ejeh, F, Zinonos, I, Kumar, R, Evdokiou, A, Brown, MP, (…) Neilsen, PM (2011). Nutlin-3a is a potential therapeutic for ewing sarcoma. ClinCancer Res *17*, 494-504.

Polsky, D, Bastian, BC, Hazan, C, Melzer, K, Pack, J, Houghton, A, (…) Osman, I (2001). HDM2 protein overexpression, but not gene amplification, is related to tumorigenesis of cutaneous melanoma. Cancer Res *61*, 7642-7646.

Post, SM, Quintas-Cardama, A, Pant, V, Iwakuma, T, Hamir, A, Jackson, JG, (…) Lozano, G (2010). A high-frequency regulatory polymorphism in the p53 pathway accelerates tumor development. Cancer Cell *18*, 220-230.

Powell, B, Soong, R, Iacopetta, B, Seshadri, R, and Smith, DR (2000). Prognostic significance of mutations to different structural and functional regions of the p53 gene in breast cancer. Clin Cancer Res *6*, 443-451.

Powles, TJ, Ashley, S, Tidy, A, Smith, IE, and Dowsett, M (2007). Twenty-year follow-up of the Royal Marsden randomized, double-blinded tamoxifen breast cancer prevention trial. J Natl Cancer Inst *99*, 283-290.

Prodosmo, A, Giglio, S, Moretti, S, Mancini, F, Barbi, F, Avenia, N, (…) Moretti, F (2008). Analysis of human MDM4 variants in papillary thyroid carcinomas reveals new potential markers of cancer properties. JMolMed(Berl) *86*, 585-596.

Rallapalli, R, Strachan, G, Tuan, RS, and Hall, DJ (2003). Identification of a domain within MDMX-S that is responsible for its high affinity interaction with p53 and high-level expression in mammalian cells. JCell Biochem *89*, 563-575.

Ramos, YF, Stad, R, Attema, J, Peltenburg, LT, van der Eb, AJ, and Jochemsen, AG (2001). Aberrant expression of HDMX proteins in tumor cells correlates with wild-type p53. Cancer Res *61*, 1839-1842.

Ray-Coquard, I, Blay, JY, Italiano, A, Le Cesne, A, Penel, N, Zhi, J, (…) Bui, BN (2012). Effect of the MDM2 antagonist RG7112 on the P53 pathway in patients with MDM2-amplified, well-differentiated or dedifferentiated liposarcoma: an exploratory proof-of-mechanism study. Lancet Oncol *13*, 1133-1140.

Raymond, AK, Ayala, AG, and Knuutila, S (2002). Conventional Osteosarcoma. In World Health Organization Classification of Tumours Pathology and Genetics of Tumours of Soft Tissue and Bone, C.D.M. Fletcher, K.K. Unni, and F. Mertens, eds. (Lyon: IARC Press.), pp. 264-270.

Reis-Filho, JS, and Pusztai, L (2011). Gene expression profiling in breast cancer: classification, prognostication, and prediction. The Lancet *378*, 1812-1823.

Riemenschneider, MJ, Buschges, R, Wolter, M, Reifenberger, J, Bostrom, J, Kraus, JA, (…) Reifenberger, G (1999). Amplification and overexpression of the MDM4 (MDMX) gene from 1q32 in a subset of malignant gliomas without TP53 mutation or MDM2 amplification. Cancer Res *59*, 6091-6096.

Riemenschneider, MJ, Knobbe, CB, and Reifenberger, G (2003). Refined mapping of 1q32 amplicons in malignant gliomas confirms MDM4 as the main amplification target. IntJCancer *104*, 752-757.

Riker, AI, Enkemann, SA, Fodstad, O, Liu, S, Ren, S, Morris, C, (…) Matta, J (2008). The gene expression profiles of primary and metastatic melanoma yields a transition point of tumor progression and metastasis. BMC Med Genomics *1*, 13.

Riley, T, Sontag, E, Chen, P, and Levine, A (2008). Transcriptional control of human p53-regulated genes. Nat Rev Mol Cell Biol *9*, 402-412.

Rinn, JL, and Huarte, M (2011). To repress or not to repress: this is the guardian's question. Trends Cell Biol *21*, 344-353.

Robles, AI, and Harris, CC (2010). Clinical outcomes and correlates of TP53 mutations and cancer. Cold Spring Harb Perspect Biol *2*, a001016.

Rodon, J, Dienstmann, R, Serra, V, and Tabernero, J (2013). Development of PI3K inhibitors: lessons learned from early clinical trials. Nat Rev Clin Oncol *10*, 143-153.

Roger, L, Gadea, G, and Roux, P (2006). Control of cell migration: a tumour suppressor function for p53? Biol Cell *98*, 141-152.

Royds, JA, and Iacopetta, B (2006). p53 and disease: when the guardian angel fails. Cell Death Differ *13*, 1017-1026.

Ruijs, MW, Schmidt, MK, Nevanlinna, H, Tommiska, J, Aittomaki, K, Pruntel, R, (…) Van't Veer, LJ (2007). The single-nucleotide polymorphism 309 in the MDM2 gene contributes to the Li-Fraumeni syndrome and related phenotypes. Eur J Hum Genet *15*, 110-114.

Sakamuro, D, Sabbatini, P, White, E, and Prendergast, GC (1997). The polyproline region of p53 is required to activate apoptosis but not growth arrest. Oncogene *15*, 887-898.

Sankpal, NV, Willman, MW, Fleming, TP, Mayfield, JD, and Gillanders, WE (2009). Transcriptional repression of epithelial cell adhesion molecule contributes to p53 control of breast cancer invasion. Cancer Res *69*, 753-757.

Sawyers, CL (2008). The cancer biomarker problem. Nature *452*, 548-552.

Schadt, EE, Molony, C, Chudin, E, Hao, K, Yang, X, Lum, PY, (…) Ulrich, R (2008). Mapping the genetic architecture of gene expression in human liver. PLoS Biol *6*, e107.

Segura, MF, Hanniford, D, Menendez, S, Reavie, L, Zou, X, Alvarez-Diaz, S, (…) Hernando, E (2009). Aberrant miR-182 expression promotes melanoma metastasis by repressing FOXO3 and microphthalmia-associated transcription factor. Proc Natl Acad Sci U S A *106*, 1814-1819.

Senzer, N, Nemunaitis, J, Nemunaitis, M, Lamont, J, Gore, M, Gabra, H, (…) Chada, S (2007). p53 therapy in a patient with Li-Fraumeni syndrome. Mol Cancer Ther *6*, 1478-1482.

Shibagaki, I, Tanaka, H, Shimada, Y, Wagata, T, Ikenaga, M, Imamura, M, and Ishizaki, K (1995). p53 mutation, murine double minute 2 amplification, and human papillomavirus infection are frequently involved but not associated with each other in esophageal squamous cell carcinoma. Clin Cancer Res *1*, 769-773.

Shiota, M, Song, Y, Yokomizo, A, Kiyoshima, K, Tada, Y, Uchino, H, (…) Naito, S (2010). Foxo3a Suppression of Urothelial Cancer Invasiveness through Twist1, Y-Box-Binding Protein 1, and E-Cadherin Regulation. Clinical Cancer Research *16*, 5654-5663.

Shoemaker, RH (2006). The NCI60 human tumour cell line anticancer drug screen. Nat Rev Cancer *6*, 813-823.

Shvarts, A, Steegenga, WT, Riteco, N, van Laar, T, Dekker, P, Bazuine, M, (…) Jochemsen, AG (1996). MDMX: a novel p53-binding protein with some functional properties of MDM2. EMBO J *15*, 5349-5357.

Sigal, A, and Rotter, V (2000). Oncogenic mutations of the p53 tumor suppressor: the demons of the guardian of the genome. Cancer Res *60*, 6788-6793.

Simpson, AJ (2009). Sequence-based advances in the definition of cancer-associated gene mutations. Curr Opin Oncol *21*, 47-52.

Skaug, V, Ryberg, D, Kure, EH, Arab, MO, Stangeland, L, Myking, AO, and Haugen, A (2000). p53 mutations in defined structural and functional domains are related to poor clinical outcome in non-small cell lung cancer patients. Clin Cancer Res *6*, 1031-1037.

Soerensen, M, Dato, S, Christensen, K, McGue, M, Stevnsner, T, Bohr, VA, and Christiansen, L (2010). Replication of an association of variation in the FOXO3A gene with human longevity using both case-control and longitudinal data. Aging Cell *9*, 1010-1017.

Sorlie, T, Perou, CM, Tibshirani, R, Aas, T, Geisler, S, Johnsen, H, (…) Borresen-Dale, AL (2001). Gene expression patterns of breast carcinomas distinguish

tumor subclasses with clinical implications. Proc Natl Acad Sci U S A *98*, 10869-10874.

Steeg, PS, and Theodorescu, D (2008). Metastasis: a therapeutic target for cancer. Nat Clin Pract Oncol *5*, 206-219.

Storz, P, Doppler, H, Copland, JA, Simpson, KJ, and Toker, A (2009). FOXO3a promotes tumor cell invasion through the induction of matrix metalloproteinases. Mol Cell Biol *29*, 4906-4917.

Stranger, BE, Nica, AC, Forrest, MS, Dimas, A, Bird, CP, Beazley, C, (…) Dermitzakis, ET (2007). Population genomics of human gene expression. Nat Genet *39*, 1217-1224.

Su, X, Chakravarti, D, Cho, MS, Liu, L, Gi, YJ, Lin, YL, (…) Flores, ER (2010). TAp63 suppresses metastasis through coordinate regulation of Dicer and miRNAs. Nature *467*, 986-990.

Takahashi, S, Moriya, T, Ishida, T, Shibata, H, Sasano, H, Ohuchi, N, and Ishioka, C (2008). Prediction of breast cancer prognosis by gene expression profile of TP53 status. Cancer Sci *99*, 324-332.

Tejpar, S, Bertagnolli, M, Bosman, F, Lenz, HJ, Garraway, L, Waldman, F, (…) Roth, A (2010). Prognostic and predictive biomarkers in resected colon cancer: current status and future perspectives for integrating genomics into biomarker discovery. Oncologist *15*, 390-404.

Tenbaum, SP, Ordonez-Moran, P, Puig, I, Chicote, I, Arques, O, Landolfi, S, (…) Palmer, HG (2012). beta-catenin confers resistance to PI3K and AKT inhibitors and subverts FOXO3a to promote metastasis in colon cancer. Nat Med *18*, 892-901.

Terzian, T, Suh, YA, Iwakuma, T, Post, SM, Neumann, M, Lang, GA, (…) Lozano, G (2008). The inherent instability of mutant p53 is alleviated by Mdm2 or p16INK4a loss. Genes Dev *22*, 1337-1344.

Tibshirani, R (1997). The lasso method for variable selection in the Cox model. Stat Med *16*, 385-395.

Toledo, F, and Wahl, GM (2006). Regulating the p53 pathway: in vitro hypotheses, in vivo veritas. Nat Rev Cancer *6*, 909-923.

Tovar, C, Graves, B, Packman, K, Filipovic, Z, Higgins, B, Xia, M, (…) Vassilev, LT (2013). MDM2 small-molecule antagonist RG7112 activates p53 signaling and regresses human tumors in preclinical cancer models. Cancer Res *73*, 2587-2597.

Toyama, T, Zhang, Z, Nishio, M, Hamaguchi, M, Kondo, N, Iwase, H, (…) Fujii, Y (2007). Association of TP53 codon 72 polymorphism and the outcome of adjuvant therapy in breast cancer patients. Breast Cancer Res *9*, R34.

Troester, MA, Herschkowitz, JI, Oh, DS, He, X, Hoadley, KA, Barbier, CS, and Perou, CM (2006). Gene expression patterns associated with p53 status in breast cancer. BMC Cancer *6*, 276.

Varley, JM (2003). Germline TP53 mutations and Li-Fraumeni syndrome. Hum Mutat *21*, 313-320.

Varna, M, Bousquet, G, Plassa, LF, Bertheau, P, and Janin, A (2011). TP53 status and response to treatment in breast cancers. J Biomed Biotechnol *2011*, 284584.

Vassilev, LT, Vu, BT, Graves, B, Carvajal, D, Podlaski, F, Filipovic, Z, (…) Liu, EA (2004). In vivo activation of the p53 pathway by small-molecule antagonists of MDM2. Science *303*, 844-848.

Vazquez, A, Bond, EE, Levine, AJ, and Bond, GL (2008). The genetics of the p53 pathway, apoptosis and cancer therapy. Nat Rev Drug Discov *7*, 979-987.

Vazquez, A, Grochola, LF, Bond, EE, Levine, AJ, Taubert, H, Muller, TH, (…) Bond, GL (2010). Chemosensitivity profiles identify polymorphisms in the p53 network genes 14-3-3tau and CD44 that affect sarcoma incidence and survival. Cancer Res *70*, 172-180.

Ventura, A, Kirsch, DG, McLaughlin, ME, Tuveson, DA, Grimm, J, Lintault, L, (…) Jacks, T (2007). Restoration of p53 function leads to tumour regression in vivo. Nature *445*, 661-665.

Veyrieras, JB, Kudaravalli, S, Kim, SY, Dermitzakis, ET, Gilad, Y, Stephens, M, and Pritchard, JK (2008). High-resolution mapping of expression-QTLs yields insight into human gene regulation. PLoS Genet *4*, e1000214.

Visel, A, Blow, MJ, Li, Z, Zhang, T, Akiyama, JA, Holt, A, (…) Pennacchio, LA (2009). ChIP-seq accurately predicts tissue-specific activity of enhancers. Nature *457*, 854-858.

Vogelstein, B, Lane, D, and Levine, AJ (2000). Surfing the p53 network. Nature *408*, 307-310.

Vogelstein, B, Papadopoulos, N, Velculescu, VE, Zhou, S, Diaz, LA, Jr., and Kinzler, KW (2013). Cancer genome landscapes. Science *339*, 1546-1558.

Vousden, KH, and Lu, X (2002). Live or let die: the cell's response to p53. Nat Rev Cancer *2*, 594-604.

Vousden, KH, and Prives, C (2005). P53 and prognosis: new insights and further complexity. Cell *120*, 7-10.

Wade, M, Li, YC, and Wahl, GM (2013). MDM2, MDMX and p53 in oncogenesis and cancer therapy. Nat Rev Cancer *13*, 83-96.

Wang, JL, Zheng, BY, Li, XD, Angstrom, T, Lindstrom, MS, and Wallin, KL (2004). Predictive significance of the alterations of p16INK4A, p14ARF, p53, and proliferating cell nuclear antigen expression in the progression of cervical cancer. Clin Cancer Res *10*, 2407-2414.

Wang, SP, Wang, WL, Chang, YL, Wu, CT, Chao, YC, Kao, SH, (…) Yang, PC (2009). p53 controls cancer cell invasion by inducing the MDM2-mediated degradation of Slug. Nat Cell Biol *11*, 694-704.

Wang, X, and Jiang, X (2012). Mdm2 and MdmX partner to regulate p53. FEBS Lett *586*, 1390-1396.

Wang, YV, Wade, M, Wong, E, Li, YC, Rodewald, LW, and Wahl, GM (2007). Quantitative analyses reveal the importance of regulated Hdmx degradation for p53 activation. Proc Natl Acad Sci U S A *104*, 12365-12370.

Wasielewski, M, Elstrodt, F, Klijn, JG, Berns, EM, and Schutte, M (2006). Thirteen new p53 gene mutants identified among 41 human breast cancer cell lines. Breast Cancer Res Treat *99*, 97-101.

Weigelt, B, Peterse, JL, and van 't Veer, LJ (2005). Breast cancer metastasis: markers and models. Nat Rev Cancer *5*, 591-602.

Whibley, C, Pharoah, PD, and Hollstein, M (2009). p53 polymorphisms: cancer implications. Nat Rev Cancer *9*, 95-107.

Wiedswang, G, Borgen, E, Karesen, R, and Naume, B (2003). Detection of isolated tumor cells in BM from breast-cancer patients: significance of anterior and posterior iliac crest aspirations and the number of mononuclear cells analyzed. Cytotherapy *5*, 40-45.

Willcox, BJ, Donlon, TA, He, Q, Chen, R, Grove, JS, Yano, K, (…) Curb, JD (2008). FOXO3A genotype is strongly associated with human longevity. Proceedings of the National Academy of Sciences *105*, 13987-13992.

Wu, C, Macleod, I, and Su, AI (2013). BioGPS and MyGene.info: organizing online, gene-centric information. Nucleic Acids Res *41*, D561-565.

Wunder, JS, Gokgoz, N, Parkes, R, Bull, SB, Eskandarian, S, Davis, AM, (…) Andrulis, IL (2005). TP53 mutations and outcome in osteosarcoma: a prospective, multicenter study. JClinOncol *23*, 1483-1490.

Xiong, S, Pant, V, Suh, YA, Van Pelt, CS, Wang, Y, Valentin-Vega, YA, (…) Lozano, G (2010). Spontaneous tumorigenesis in mice overexpressing the p53-negative regulator Mdm4. Cancer Res *70*, 7148-7154.

Xu, Y, Yao, L, Ouyang, T, Li, J, Wang, T, Fan, Z, (…) Xie, Y (2005). p53 Codon 72 polymorphism predicts the pathologic response to neoadjuvant chemotherapy in patients with breast cancer. Clin Cancer Res *11*, 7328-7333.

Xue, W, Zender, L, Miething, C, Dickins, RA, Hernando, E, Krizhanovsky, V, (…) Lowe, SW (2007). Senescence and tumour clearance is triggered by p53 restoration in murine liver carcinomas. Nature *445*, 656-660.

Yan, W, Liu, S, Xu, E, Zhang, J, Zhang, Y, Chen, X, and Chen, X (2013). Histone deacetylase inhibitors suppress mutant p53 transcription via histone deacetylase 8. Oncogene *32*, 599-609.

Yilmaz, M, and Christofori, G (2010). Mechanisms of motility in metastasizing cells. Mol Cancer Res *8*, 629-642.

Yokoyama, R, Schneider-Stock, R, Radig, K, Wex, T, and Roessner, A (1998). Clinicopathologic implications of MDM2, p53 and K-ras gene alterations in osteosarcomas: MDM2 amplification and p53 mutations found in progressive tumors. PatholResPract *194*, 615-621.

Yuan, Y, Liao, YM, Hsueh, CT, and Mirshahidi, HR (2011). Novel targeted therapeutics: inhibitors of MDM2, ALK and PARP. J Hematol Oncol *4*, 16.

Zandi, R, Selivanova, G, Christensen, CL, Gerds, TA, Willumsen, BM, and Poulsen, HS (2011). PRIMA-1Met/APR-246 induces apoptosis and tumor growth delay in small cell lung cancer expressing mutant p53. Clin Cancer Res *17*, 2830-2841.

Zanella, F, Renner, O, Garcia, B, Callejas, S, Dopazo, A, Peregrina, S, (…) Link, W (2010). Human TRIB2 is a repressor of FOXO that contributes to the malignant phenotype of melanoma cells. Oncogene *29*, 2973-2982.

Zauberman, A, Flusberg, D, Haupt, Y, Barak, Y, and Oren, M (1995). A functional p53-responsive intronic promoter is contained within the human mdm2 gene. Nucleic Acids Res *23*, 2584-2592.

Zeller, T, Wild, P, Szymczak, S, Rotival, M, Schillert, A, Castagne, R, (…) Cambien, F (2010). Genetics and beyond--the transcriptome of human monocytes and disease susceptibility. PLoS One *5*, e10693.

Zeng, Y, Cheng, L, Chen, H, Cao, H, Hauser, ER, Liu, Y, (…) Vaupel, JW (2010). Effects of FOXO Genotypes on Longevity: A Biodemographic Analysis. The Journals of Gerontology Series A: Biological Sciences and Medical Sciences *65A*, 1285-1299.

Zhao, S, and Fernald, RD (2005). Comprehensive algorithm for quantitative real-time polymerase chain reaction. J Comput Biol *12*, 1047-1064.

Zimmerman, MP, and Mehr, SR (2012). Breast cancer: will treatment costs outpace effectiveness? Am J Manag Care *18*, SP200-202.

Ziv, E, and Hu, D (2011). Genetic variation in insulin/IGF-1 signaling pathways and longevity. Ageing Res Rev *10*, 201-204.